

PMEL Tsunami Forecast Series: Vol. #
**A Tsunami Forecast Model for Honolulu,
Hawaii**

(Draft 3.0)

L. Tang
C.D. Chamberlin

NOAA Center for Tsunami Research
Pacific Marine Environmental Laboratory
Seattle, WA
December 2012

noaa

NATIONAL OCEANIC AND
ATMOSPHERIC ADMINISTRATION



Office of Oceanic and
Atmospheric Research

Contents

Abstract.....	3
1 Introduction.....	4
2 Forecast Method.....	5
2.1 Construction of a Propagation Scenario Based on Deep-Ocean Tsunameter Measurements and Pre-computed Tsunami Source Functions	5
2.2 Coastal Predictions by Running High-Resolution Forecast Models in Real-Time.....	7
3 Model Setups	8
3.1 Forecast area and tsunami data.....	8
3.2 Bathymetry and topography	9
3.3 Grid setups	10
4 Results and Discussion	10
4.1 Validation and error estimate.....	10
4.2 Assessment of potential impact for Honolulu from simulated magnitude 7.5, 8.2, 8.7 and 9.3 Tsunamis	12
5 Summaries.....	13
Acknowledgements.....	14
References.....	15
Appendix A.....	26
Figures.....	29

Tables

Table 1 Tsunami source functions in the Pacific, Atlantic and Indian Oceans	19
Table 2 Tsunami sources for fourteen historical tsunamis	20
Table 3 Data sources used for grid development.....	22
Table 4 MOST setup for the Honolulu reference and forecast model.....	23
Table 5 Observed and modeled maximum wave crest at the Honolulu tide gage for 18 past tsunamis.....	24
Table 6 Sources of the 18 Mw 9.3 synthetic tsunamis and maximum wave crest at the Honolulu tide gage computed by the reference and forecast models.	24
Table 7 Simulated tsunamis for hazard assessment study for Honolulu.	25

PMEL Tsunami Forecast Series: Vol. #

A Tsunami Forecast Model for Honolulu, Hawaii

Liujuan Tang and Chris D. Chamberlin

Abstract

This study describes the development, validation, and testing of a tsunami forecast model for operational use for the coastal community of Honolulu, Hawaii. Based on the Method of Splitting Tsunamis (MOST) model, the forecast model is capable of simulating four hours of tsunami wave dynamics at a resolution of 2-arc-sec (~60 m) within 10-minute computational time using a single 3.6 GHz processor. A reference inundation model of higher resolution of 2/3 arc-sec (~20 m) was also developed in parallel, to provide modeling references for the forecast model. Both models were tested for 36 scenarios, including eighteen past tsunamis and a set of eighteen simulated magnitude 9.3 tsunamis.

Based on historical tsunami water level records at Honolulu tide station, the error of the maximum wave amplitude computed by the Honolulu forecast model is less than 30 cm. The accuracy for events with deep-ocean tsunameter measurements is greater than 70% when the observed maximum water elevation is greater than 0.5 m at the gage. The error of the modeled arrival time of the first peak is within $\pm 3\%$ of the observed travel time. Wavelet analyses indicate the peak wave period at the station mainly falls into one of four local resonant periods, near 11, 22 33 or 44 minutes (± 2 min). Which peak period was excited is relevant to the geographic location of the tsunami source. The good agreement between the model computations and observations provide a quantitative validation of the forecast model, while the numerical consistency between the model results for the maximum amplitude and velocity show reliable robustness and stability testing of the model.

The validated Honolulu forecast model was further applied to hazard assessment from 1427 scenarios of simulated magnitudes 7.5, 8.2, 8.7 and 9.3 tsunamis based on subduction zone earthquakes in the Pacific. The results show an impressive local variability of tsunami amplitudes even for far-field tsunamis, and indicate the complexity of forecasting tsunami amplitudes at a coastal location. It is essential to use high-resolution models in order to provide accuracy that is useful for coastal tsunami forecast for practical guidance.

The study highlights large tsunamis originated from Aleutian, Japan, Kamchatka, Izu, Northern Tonga (Samoa), Southern Chile, East Philippines and Canada, subduction zones, all of which can potentially generate large waves and cause flooding in Honolulu.

1 Introduction

The National Oceanic and Atmospheric Administration (NOAA) Center for Tsunami Research at NOAA's Pacific Marine Environmental Laboratory (PMEL) has developed a tsunami forecasting system for operational use by NOAA's two Tsunami Warning Centers located in Hawaii and Alaska (Titov *et al.*, 2005; Titov, 2009). The forecast system combines real-time deep-ocean tsunami measurements from tsunameters (Deep-ocean Assessment and Reporting of Tsunami (DART)) stations (González *et al.*, 2005; Meinig *et al.*, 2005, Bernard *et al.*, 2006, Bernard and Titov, 2007) with the Method of Splitting Tsunami (MOST) model, a suite of finite difference numerical codes based on the nonlinear shallow water wave equations (Titov and Synolakis, 1998; Titov and González, 1997; Synolakis *et al.*, 2008; Titov *et al.*, 2011) to produce real-time forecasts of tsunami arrival time, heights, periods and inundation. To achieve accurate and detailed forecast of tsunami impact for specific sites, high-resolution tsunami forecast models are under development for United States coastal communities at risk (Tang *et al.*, 2008^a; 2009; 2010; Arcas and Uslu, 2010; Righi and Arcas, 2010; Uslu *et al.* 2010; Wei and Arcas, 2010). The resolution of these models has to be high enough to resolve the dynamics of a tsunami inside a particular harbor, including influences of major harbor structures such as breakwaters. These models have been integrated as crucial components into the forecast system.

Presently, as shown in Figure 1, a system of 55 tsunameter stations, are deployed in the Pacific, Atlantic, Indian Oceans, Caribbean Sea, the Gulf of Mexico and South China Sea (40 U.S.-, 8 Australian-, 1 Chilean-, 1 China-, 2 Indian-, 1 Indonesian-, 1 Thailand- and 1 Russian-owned) [Spillane *et al.*, 2008]. The pre-computed propagation models currently have 1,725 scenarios covering the major tsunami-genetic subduction zones in the oceans (Table 1). High-resolution forecast inundation models are now set up for 75 U.S. coastal communities (e.g. Figs. 1 and 2). The fully implemented system will use real-time data from the tsunameter network to provide high-resolution tsunami forecasts for at least 75 communities in the U.S. by 2013, with additional models envisioned later for smaller communities. Since its first testing in the 17 November 2003 Rat Island tsunami, the forecast system has produced experimental real-time forecasts for more than 20 tsunamis in the Pacific and Indian oceans (Titov *et al.*, 2005; Wei *et al.*, 2008; Titov, 2009; Titov and Tang, 2011; Tang *et al.*, 2012; http://nctr.pmel.noaa.gov/database_devel.html). The forecast method has also been tested with data from nine additional events that produced deep-ocean tsunameter data and near-field tsunamis (http://nctr.pmel.noaa.gov/database_devel.html; Titov *et al.*, 2005; Tang *et al.*, 2008b; Wei *et al.*, 2012).

The recent 2011 Japan tsunami caused severe flooding and damages in the main Hawaiian Islands. As the capital city that has the highest population density, Honolulu is in need for a forecast flooding model. The report describes the development, testing and applications of the Honolulu forecast model. The objective is to provide NOAA's Tsunami Warning Centers the ability to assess danger posed to Honolulu following tsunami generation in the Pacific Ocean Basin, and to provide accurate and timely forecasts to enable the community to respond appropriately. A secondary objective is to

explore the potential tsunami impact, of earthquakes from major subduction zones in Pacific, to the site.

The report is organized as follows. Section 2 briefly introduces NOAA's tsunami forecast method. Section 3 describes the model development and setups. Section 4 presents the results and discussion. A tsunami hazard assessment study utilizing the validated forecast model is also included. Summary and conclusions are provided in section 5.

2 Forecast Method

NOAA's real-time tsunami forecasting scheme is a process comprised of two steps: (1) construction of a propagation scenario via inversion of deep ocean tsunameter measurements with pre-computed tsunami source functions; and (2) coastal predictions by running high-resolution forecast models in real time (*Titov et al.* 1999; 2005; Titov 2009; Tang *et al.*, 2009; 2012). The DART-constrained tsunami source, the corresponding offshore scenario from the tsunami source function database, and high-resolution forecast models cover the entire evolution of earthquake-generated tsunamis, generation, propagation and coastal inundation, providing a complete tsunami forecast capability.

2.1 Construction of a Propagation Scenario Based on Deep-Ocean Tsunameter Measurements and Pre-computed Tsunami Source Functions

Several real-time data sources, including seismic data, coastal tide gage and deep-ocean data have been used for tsunami warning and forecasting (*Satake et al.*, 2008; Whitmore, 2003; Titov, 2009). NOAA's strategy for the real-time forecasting is to use deep-ocean measurements at tsunameter stations as the primary data source due to several key features. (1) tsunameters provide a direct measure of tsunami waves, unlike seismic data, which are an indirect measure of tsunamis. (2) The deep ocean tsunami measurements are in general the earliest tsunami information available, since tsunamis propagate much faster in deep ocean than in shallow coastal area where coastal tide gages are located. (3) Compared to coastal tide gages, tsunameter data with a high signal to noise ratio can be obtained without interference from harbor and local shelf effects. (4) Wave dynamics of tsunami propagation in deep ocean is assumed to be linear (*Kanoğlu and Synolakis*, 2006; Liu, 2009). This linear process allows application of efficient inversion schemes.

Time series of tsunami observations in deep-ocean can be decomposed into a linear combination of a set of tsunami source functions in the time domain by a linear Least Squares method (*Percival et al.*, 2011). We call coefficients obtained through this inversion process *tsunami source coefficients*. During real-time tsunami forecasting, seismic waves propagate much faster than tsunami waves so the initial seismic magnitude can be estimated before the tsunameter data are available. Since time is of the essence,

the initial tsunami forecast is based on the seismic magnitude only. The tsunameter inverted source will update the forecast when it is available.

Titov *et al.* (1999; 2001) conducted sensitivity studies on far-field deep-water tsunamis to different parameters of elastic deformation model described in *Gusiakov* (1978) and *Okada* (1985). The results showed source magnitude and location essentially define far-field tsunami signals for a wide range of subduction zone earthquakes. Other parameters have secondary influence and can be pre-defined during forecast. Based on these results, tsunami source function databases for Pacific, Atlantic, and Indian Oceans have been built using pre-defined source parameters, length = 100 km, width = 50 km, slip = 1 m, rake = 90 or -90 and rigidity = 4.5×10^{10} N/m². Other parameters are location-specific; details of the databases are described in *Gica et al.* (2008). Each tsunami source function is equivalent to a tsunami from a typical $M_w = 7.5$ earthquake with defined source parameters. Figure 1 shows the locations of tsunami source functions.

The tsunami source functions in the database are computed with a time step of 10 seconds and a spatial resolution of 4-arc-minute (approximately 7.4 km along the N-S direction). The outputs, offshore wave height and depth-average velocities of the entire domain, are then compressed and saved every 1 minute in time and 16-arc-minute in space (Tolkova, 2007). The current propagation scenarios do not include inundation and a vertical wall is placed at 20 m water depth [*Gica et al.*, 2008]. The friction term is set to zero. When tsunami waves propagate into shallow water, where under the steady-state assumption, there are not any energy losses or inputs, the decrease in transport speed must be compensated by an increase in energy density in order to maintain a constant energy flux. The low spatial resolution and simplified boundary conditions of the propagation model result in inaccurate near-shore dynamics. As a consequence, the numerical dissipation (due to the low spatial resolution) will cause energy decay in the propagation modeling (Tang *et al.*, 2012). Based on consideration of energy conservation, we have developed high-resolution, site-specific inundation forecast models built on the MOST model to simulate the near shore wave dynamics.

Energy released from an earthquake and then how portions of the earthquake energy are transferred into water column are complex dynamic processes at the stage of tsunami generation. However, the goal of tsunameter inversion is not to quantify the quantities such as energy at the initial stage of tsunami generation. Instead, we try to quantify the amount of wave energy that propagates outside the source area in the form of surface long gravity waves, which can be well measured by the tsunameter stations. It is also the propagated energy that results in the coastal impacts. Our estimates of the tsunami source (the propagation scenario) focus on the characteristics of tsunami propagation which are directly constrained by the deep ocean tsunami data. Regardless of the details of earthquake processes for tsunami generation at the initial stage, the inversion can ensure the propagation scenario gives the best approximation to the tsunami measurements, and therefore, the best estimation of the total energy transferred to the tsunami waves. The database can provide offshore forecasts of tsunami amplitudes and all other wave parameters immediately once the inversion is complete. The tsunami source, which combines real-time tsunami measurements with tsunami source functions, provides an accurate offshore tsunami scenario without additional time-consuming model runs.

2.2 Coastal Predictions by Using High-Resolution Forecast Models in Real-Time.

High-resolution forecast models are designed for the final stage of the evolution of tsunami waves: coastal runup and inundation. Once the tsunameter-constrained tsunami source is obtained (as a linear combination of tsunami source functions), the pre-computed time series of offshore wave height and depth-averaged velocity from the model propagation scenario are applied as the dynamic boundary conditions for the forecast models. This saves the simulation time of basin-wide tsunami propagation. Tsunami inundation and nearshore currents are highly nonlinear processes, therefore a linear combination would not provide accurate solutions. A high-resolution model is also required to resolve shorter tsunami wavelengths nearshore with accurate bathymetric/topographic data. The forecast models are constructed with the Method of Splitting Tsunami (MOST) model, a finite difference tsunami inundation model based on nonlinear shallow-water wave equations(Titov and Synolakis, 1998; Titov and González, 1997; Synolakis *et al.*, 2008; Titov *et al.*, 2011). Each forecast model contains three telescoping computational grids with increasing resolution, covering regional, intermediate and nearshore areas. Runup and inundation are computed at the coastline. For example, Figure 2 shows forecast model setup for several tsunami forecast models in Hawaii, detailing the telescoping grids used:

- (a) One regional grid of 2-arc-minute (~3600m) resolution covers the main Hawaiian Islands (Fig. 2.a).
- (b) Then the Hawaiian Islands are divided into four intermediate grids of 12- to 18-arc-second (~ 360 –540m) for four natural geographic areas (Figs. 2.b 1-4):
 - (b1) Ni'ihau, Ka'ula Rock, and Kauai (Kauai complex),
 - (b2) Oahu,
 - (b3) Molokai, Maui, Lanai, and Kaho'olawe (the Maui Complex),
 - (b4) Hawaii.
- (c) Each intermediate grid contains 2-arc-second (~60 m) nearshore grids (Figs. 2.c 1-4).

The highest resolution grid includes the population center and coastal water level stations for forecast verification. The grids are derived from the best available bathymetric/topographic data at the time of development, and will be updated as new survey data become available. Forecast models have been developed for 13 coastal communities in Hawaii (Figure 2).

The forecast models are optimized for speed and accuracy. By reducing the computational areas and grid resolutions, each model is optimized to provide 4-hour event forecasting results in 10 minutes of computational time using one single processor, while still providing good accuracy for forecasting. To ensure forecast accuracy at every step of the process, the model outputs are validated with historical tsunami records and compared to numerical results from a reference inundation model with higher resolutions and larger computational domains. In order to provide warning guidance for long duration during a tsunami event, each forecast model has been tested to output up to 24-hour simulation since tsunami generation.

3 Model Setups

3.1 Forecast area and tsunami data

The main Hawaiian Islands are the younger and southern portion of the Hawaii Archipelago. From northeast to southwest, the islands form four natural geographic groups by shared channels and inter-island shelf, including (1) Ni'ihau, Ka'ula Rock, and Kauai, (Kauai complex) (2) Oahu, (3) Molokai, Maui, Lanai, and Kaho'olawe, (the Maui Complex), and (4) Hawaii. Honolulu is located in the middle of Oahu's south shore (Figure 3). It is the capital and the most populous place in the State (Figs. 4 and 5)

The island of Oahu lies between Kauai, to the northwest, separated by the 115 km (72 mile) wide Kauai Channel, and Molokai, to the southeast, by the 42 km (26 mile) wide Kaiwi Channel. The island has very angular shoreline, with a narrow insular shelf surrounding most of the island (Shepard *et al*, 1950). On the southern side, the shelf terminates at a shallow depth around 50 m with a very steep slope beyond out to 300 m. Then the seafloor slopes more gently down to the 500 m depth of the Kaiwi Channel. On the southeast side of the Kaiwi Channel, Penguin Bank is the most extensive shallow shelf area in the Hawaiian Islands. The 50-m isobath reaches over 42 km (26 miles) eastward from the west end of Molokai (Fig. 3).

Hawaii has a long history of distant-source tsunamis. According to NDGC tsunami database (http://www.ngdc.noaa.gov/hazard/tsu_db.shtml), 105 tsunamis were observed at Honolulu during the period of 1819 to 2012 (194 years). Eight of them produced over 1 m maximum water height. The 1837 tsunami marked the highest maximum water level of 2.5 m at Honolulu. It should be noted at the Ewa Beach, the 1957 and 1960 tsunamis show 2.7 m maximum water height. The 16 tsunamis for the past 12 years (2001-2012) yield 1.3 tsunami per year.

The Honolulu tide station in Honolulu Harbor was established 1 Jan 1905 at Pier 4. The present installation was in January 1989 (<http://tidesandcurrents.noaa.gov/>). The coordinates of the gage are at 202.13574 °E and 21.30306 °N. The mean high water level (MHW) is 1.6 m and the mean sea level (MSL) is 1.412 m. The mean range of tide (MN) is 0.389 m.

Honolulu tide station has provided the most complete tsunami water level data, including the eighteen tsunamis as summarized in Table 2. It is also the only station in Hawaii that recorded all of the 5 destructive tsunamis, the 1946 Unimak, 1952 Kamchatka, 1957 Andreanof, 1960 Chile and 1964 Alaska tsunamis (Green, 1946; Zerbe, 1953; Berkman and Symons, 1964; Spaeth and Berkman, 1967). Run-up records are available at 7 locations as in Figure 6 (Walker, 2004; Pararas-Carayannis, 1969). The 1960 tsunami caused the most significant run-up, 3 m (9 ft) at Waikiki. There is no credible inundation data available for the area.

The Honolulu coastline has changed substantially from 1940 to 1966 with the construction of the Ala Wai Marina, Magic Island, and landfills in the port area around the Sand Island. The 3.66 km (12,000-foot) Reef Runway of Honolulu International Airport in the shallow reef-lagoon between Honolulu Harbor and Pearl Harbor was built between 1973 and 1977. Tang *et al.* (2006) have shown that changes in the Honolulu coastline since 1940 have little effect on the waveforms in and Honolulu Harbor for the 1946 tsunami. In this study, we focus on the DEM developed in 2007.

3.2 Bathymetry and topography

Tsunami inundation modeling requires accurate bathymetry in coastal area as well as high-resolution topography and bathymetry in the nearshore area. Digital elevation models (DEMs) were developed at medium resolution of 6 arc-second (180 m) covering all of the major Hawaiian Islands, and high resolution of 1/3 arc-second (10 m) covering the south Oahu area (Fig. 7). Both grids include topographic and bathymetric elevations. After compilation, the grids were resampled to produce the final modeling grids.

The source grids were compiled from several data sources. Figure 7b and Table 3 shows the spatial extent of each data source used for the 1/3 arc-second (10 m) DEM. In general, the data sources listed first superseded the sources listed later when they overlapped (Table 3). The superseded datasets were used for comparison and verification.

High-resolution, recent topographic LIDAR data were available for the area of interest around Honolulu. SHOALS bathymetric LIDAR data were used in nearshore areas around several islands, providing excellent coverage of reef and shoreline regions.

High-resolution gridded datasets derived from multibeam surveys are available for many parts of the archipelago, and were used wherever available. In deep water where high-resolution multibeam data were not available, the grid was developed by interpolation of a combination of USGS GLORIA surveys and the Smith & Sandwell 2-minute (about 3.6 km in Hawaii) global seafloor dataset. These datasets were edited to remove individual points substantially different from nearby data.

Raw data sources were imported to ESRI ArcGIS-compatible file formats. Data values were converted, where necessary, to the WGS84 horizontal geodetic datum. In the point datasets, single sounding points that differed substantially from neighboring data were removed. Gridded datasets were checked for extreme values by examination of contour lines and, where available, by comparison between multiple data sources.

All selected input datasets were converted to the mean high water (MHW) vertical datum, when necessary, using offsets on the National Ocean Service tidal benchmark datasheet for the Honolulu tide station.

To compile the multiple data sources into a single grid, subsets of the source data were created in the priority order described above. A triangulated irregular network (TIN) was created from the vector point. Also added to the TIN were points taken from the edges of

the gridded data regions to ensure a smooth interpolated transition between areas with different data sources. This TIN was linearly interpolated using ArcGIS 3D Analyst to produce intermediate 1/3 arc-second (10 m) and 6 arc-second (180 m) raster grids. The gridded datasets were then bilinearly resampled to these resolutions and overlaid on the intermediate grids.

The authors consider the above DEMs to be a good representation of the local topography/bathymetry. As new digital elevation models become available, forecast models will be updated and report updates will be posted at http://nctr.pmel.noaa.gov/forecast_reports/

3.3 Grid setups

By sub-sampling from the DEMs described in section 2.2, two sets of computational grids were derived, the Honolulu reference inundation model and the forecast model (Figs. 8 and 9). Each set consists of three levels of telescoped grids A, B and C, with increasing resolution. The A-grids encompass the major Hawaii Islands and the B-grids cover the Island of Oahu, Penguin Bank and West Molokai. Run-up and inundation simulations were calculated in C-grids over the study area. Due to the large coverage and deep water enclosed by the reference C-grid, a 2/3 arc-sec (20 m) resolution was chosen to save computational time. The same 2-arc-sec (60 m) resolution was used for the forecast C-grid as the developed Hilo and Kahului forecast models (Tang et al., 2010; 2013). In Figs. 8 and 9, the solid boxes in red indicate boundaries of the nested grids. Grid details at each level and input parameters are summarized in Table 4.

For further comparison, two virtual gages were placed at 2-m depth contour in the forecast area (Fig. 9c). Gage 1 was located at the Ala Moana Beach. Gage 2 represents Waikiki.

4 Results and Discussion

4.1 Validation and error estimate

Both the Honolulu reference and forecast models were tested with the 18 historical tsunamis summarized in Table 2. Figure 10 shows the modeled amplitude time series at the Honolulu tide gage computed by both models. The computed maximum water elevation above MHW and maximum current are plotted in Figure 12 for C-grids. The maximum amplitudes recorded at the Honolulu tide station is relatively small, compared to records at Hilo and Kahului tide stations (Tang et al., 2010; 2013). The 1960 Chile generated the largest amplitude of 1.0 m at the Honolulu station. It is also the largest tsunami at Honolulu nearshore among the 18 past events. The 2011 Japan, the 1957 Aleutian, the 1946 Unimak and 1952 Kamchatka tsunamis produced the second largest amplitude of 0.64-0.69 m. Table 5 summarizes the observed and modeled maximum amplitude (η_{\max}) at the Honolulu station for the 18 tsunamis for both the reference and forecast models. The error of the maximum wave amplitude computed by the Honolulu

forecast model is less than 30 cm. The forecast model produced large discrepancy of 28, 25 and 24 cm in η_{\max} for the 1952, 1957 and 1960 tsunamis. It should be noted that the tsunami sources of the 1952 and 1957 event are very preliminary, while the 1960 source was taken directly from the seismic source (Kanomori and Cipar, 1974). Those sources are subject to debate and adjustment. If we exclude the three events, the accuracy is greater than 70% when the observed maximum wave height is greater than 0.5 m. This accuracy is lower than the 80% accuracy at Kahului (Tang *et al.*, 2013). One reason is the tsunami amplitudes are smaller at Honolulu gage than those at Kahului gage. The error of the modeled arrival time of the first peak is within $\pm 3\%$ of the travel time.

Figure 11 compares the waveforms computed by the Honolulu reference and forecast at two locations, gage 1 at Ala Moana beach and gage 2 at Waikiki. The forecast model in general reproduces similar results as those computed by the reference model.

Recorded historical tsunamis provide only a limited number of events, from limited locations. More comprehensive test cases of destructive tsunamis with different directionalities are needed to check the stability and robustness for the forecast model. A similar set of eighteen simulated magnitude 9.3 tsunamis as in Tang *et al.* (2008^a, 2010) was selected here for further testing (Table 6). Results computed by the forecast model are compared with those from the high-resolution reference model in Table 6 and Figure 13. Both models were numerically stable for all of the scenarios. Waveforms computed by the forecast model agree well with those of the reference model. Both models produced similar maximum water elevation and inundation in the study area (Figs. 12 and 15). The offshore amplitudes up to 20 m water depth are relatively small. However, the amplitude increases dramatically due to shoaling when the tsunami waves enter a nearshore area shallower than 20 m and even more so because of local shelf resonances and other coastal effects. This emphasizes the importance of using high-resolution inundation models, which resolve the local coast and harbor geometries, in order to achieve accurate tsunami amplitude forecasts for coastal communities.

Tsunami waves in the study area vary significantly for the 18 magnitude 9.3 scenarios. These results show the complexity and high nonlinearity of tsunami waves nearshore, which again demonstrate the value of high-resolution forecast model for providing accurate site-specific forecast details. The No. 3 scenario in the middle of Aleutian subduction generates severe inundation at Honolulu. The computed maximum water elevation reaches 2.7, 3.4 and 4.5 m at the Honolulu tide station, virtual gages 1 at Ala Moana and 2 at Wakiki respectively.

Wavelet analyses were performed for the 36 scenarios to explore peak resonant periods for the site. Figs. 16 and 17 show the amplitude spectrograms for the past and simulated tsunamis respectively. The spectrograms show wide range of resonant periods from 11 to 64 minutes. The two most common peak periods are 11 and 22 (± 2) minutes (Fig. 18). In addition, long resonant periods, such as 33, 44 and 64 minutes, can have similar amplitude as short period waves. Figs. 16 and 17 show reasonable agreements in peak period for the reference and forecast models.

4.2 Assessment of potential impact for Honolulu from simulated magnitude 7.5, 8.2, 8.7 and 9.3 Tsunamis

Located in the middle of Pacific, Honolulu is potentially vulnerable to a variety of Pacific-wide tsunamis. What magnitude from which location on a subduction zone can a tsunami have devastating impact on the community? Assessment of the potential impact can provide useful and important information in advance of a real event. The validated Honolulu forecast model, which was optimized for speed and accuracy, along with the forecast propagation database, provide powerful tools to address this problem.

1427 scenarios in four different magnitudes, 7.5, 8.2, 8.7 and 9.3 as in Tang et al. (2009) were tested. The details of the simulated tsunami sources and results are summarized in Figure 19 and Table 7. The maximum water elevation, η_{\max} , at Honolulu tide station from magnitude 7.5 tsunamis computed by the forecast model is plotted in bars in Fig.19b. Color represents the first arrival at the station, which is the time of water level reaching 20% height of the first significant peak or trough. Bars in Figure 19a indicate the maximum elevation at deep water offshore Honolulu from the same sources, which are taken from the propagation database. Figures 19 c, d and e show η_{\max} at Honolulu tide station from magnitudes 8.2, 8.7 and 9.3 tsunamis respectively. The color represents the difference in time between the arrival of the maximum elevation, t_{\max} , and first arrival, t_1 .

Tsunami waves in the study area generated by the same magnitude tsunamis from the major subduction zones in the Pacific vary significantly. Tsunami sources on Aleutian-Alaska-Canada-Cascadia and Kamchatka subduction zones can generate relatively large waves in Honolulu (Figure 19). Historically, earthquakes at the Aleutian Alaska and South America Subduction Zones produced significantly larger tsunami waves, such as the 1946 Unimak and 1960 Chile earthquakes.

To further investigate the transformations of tsunami amplitudes from offshore to the tide gauges, we have looked at the ratios of these amplitudes. The ratio of the offshore and nearshore η_{\max} for all computed scenarios are plotted and the linear regression analyses performed in Figure 20. To better illustrate the data trends, both the logarithmic and Cartesian coordinates were plotted with the same datasets. The logarithmic scales give a full picture of the wide range of values, while the Cartesian coordinates better illustrate the actual spread and trends of the data. In Figure 20b, the solid black lines are the best fit to the data and the dashed black lines are prediction bounds based on a 95% confidence level. The results show:

1. The relationship between tide-gauge maximum amplitude and offshore maximum amplitude appears to be complex and non-linear in nature.
2. Larger amplitudes offshore do not necessarily produce larger amplitudes at tide gauges, and larger tsunami magnitudes may not produce larger waves either offshore, or at tide gauges.
3. The simple relationships obtained through regression analysis (Figure 20a) are

insufficient to provide warning guidance during an event. The 95% confidence interval is too wide to provide any certainty for the forecast accuracy.

Tang *et al.* (2009) also show that the trends of offshore/tide gauge amplitudes are site-specific. Different sites show different regression analysis curves. These results indicate that high-resolution tsunami models are essential for providing useful accuracy for coastal amplitude forecast. If high-resolution tsunami nearshore dynamics are not included in the forecast procedures, the accuracy and the uncertainty of the amplitude forecast appear to be too high for practical guidance.

5 Summary and Conclusions

An operational forecast model was developed for Honolulu, Hawaii. The computational grids for the models were derived from the best available bathymetric and topographic data sources. The model was tested with eighteen historical tsunamis and different scenarios of simulated 7.5, 8.2, 8.7 and 9.3 tsunamis based on subduction zone earthquakes in the Pacific.

Good agreements were obtained between the model computations and observations. The numerical consistency between the model results for the maximum amplitude and velocity provides reliable robustness and stability testing of the forecast model. The error of the maximum wave amplitude computed by the Honolulu forecast model is less than 30 cm for the 18 past tsunamis. For recent tsunamis, which were well recorded by deep-ocean tsunamieters, the accuracy is greater than 70% when the observed maximum wave amplitude is greater than 0.5 m. The error of the modeled arrival time of the first peak is within $\pm 3\%$ of the travel time. Wavelet analyses indicate the peak wave period at the station mainly falls into one of four local resonant periods, near 11, 22 33 or 44 minutes (± 2 min). Those are relevant to the geographic location of the tsunami sources.

The validated Honolulu forecast model were further applied to hazard assessment from 1884 scenarios of simulated magnitudes 7.5, 8.2, 8.7 and 9.3 tsunamis based on subduction zone earthquakes in the Pacific. The results show an impressive local variability of tsunami amplitudes even for far-field tsunamis, and indicate the complexity of forecasting tsunami amplitudes at a coastal location. It is essential to use high-resolution models in order to provide accuracy that is useful for coastal tsunami forecast for practical guidance.

The study shows tsunamis originated from Aleutian, Japan, Kamchatka, Izu, Northern Tonga (Samoa), Southern Chile, East Philippines and Canada, subduction zones, can potentially generate large waves and cause flooding in Honolulu.

Acknowledgements

We thank Diego Arcas for detail review and comments; Jean Newman for assistance with the propagation database and preparing the cover page; Elena Tolkova for MOST 4; Christopher Moore for MOST versioning; Sandra Bigley for comments and editing; and Burak Uslu for providing tables and graphics for the propagation database. Collaborative contributions of the National Weather Service, the National Geophysical Data Center, and the National Data Buoy Center were invaluable.

This research is funded by the NOAA Center for Tsunami Research (NCTR) xxxx. This publication is partially funded by the Joint Institute for the Study of the Atmosphere and Ocean (JISAO) under NOAA Cooperative Agreement No. NAXxxxx, Contribution #xxxx.

References

- Arcas, D., and B. Uslu (2010): A Tsunami Forecast Model for Crescent City, California. NOAA OAR Special Report, PMEL Tsunami Forecast Series: Vol. 2, 112 pp, Gov. Print. Off., Seattle, Wash.
- Berkman, S.C., and J.M. Symons (1964): The tsunami of May 22, 1960 as recorded at tide stations. Coastal and Geodetic Survey, U.S. Department of Commerce, 79 pp.
- Bernard, E.N., H.O. Mofjeld, V.V. Titov, C.E. Synolakis, and F.I. González (2006): Tsunami: Scientific frontiers, mitigation, forecasting, and policy implications. Proc. Roy. Soc. Lon. A, 364(1845), doi: 10.1098/rsta.2006.1809, 1989–2007.
- Bernard, E., and V.V. Titov (2007): Improving tsunami forecast skill using deep ocean observations, Mar. Technol. Soc. J., 40(3), 23–26.
- Green, C.K. (1946): Seismic sea wave of April 1, 1946, as recorded on tide gages. Eos Trans. AGU, 27, 489–500.
- Gica, E., M.C. Spillane, V.V. Titov, C.D. Chamberlin, and J.C. Newman (2008), Development of the forecast propagation database for NOAA's Short-Term Inundation Forecast for Tsunamis (SIFT), *NOAA Tech. Memo. OAR PMEL-139*, 89 pp.
- Gusiakov, V.K. (1978): Static displacement on the surface of an elastic space. Ill-posed problems of mathematical physics and interpretation of geophysical data, Novosibirsk, VC SOAN SSSR, 23–51 (in Russian).
- González, F.I., E.N. Bernard, C. Meinig, M.C. Eble, H.O. Mofjeld, and S. Stalin (2005), The NTHMP tsunami network, *Natural Hazards*, 35, 25–39.
- Kanamori, H. and J.J. Cipar (1974): Focal process of the great Chilean earthquake, May 22, 1960. *Physics of the Earth and Planetary Interiors*, 9, 128–136.
- Liu, P. L.-F. (2009): Tsunami modeling—Propagation, in The Sea, vol. 15, edited by E. Bernard and A. Robinson, chap. 9, pp. 295–319, Harvard Univ. Press, Cambridge, Mass.
- López, A.M. and E.A. Okal (2006); A seismological reassessment of the source of the 1946 Aleutian 'tsunami' earthquake. *Geophysical Journal International*, Volume 165, Issue 3, Page 835-849, Jun 2006, doi: 10.1111/j.1365-246X.2006.02899.x
- Kanamori, H. and J.J. Cipar (1974): Focal process of the great Chilean earthquake, May 22, 1960. *Physics of the Earth and Planetary Interiors*, 9, 128–136.
- Meinig, C., S.E. Stalin, A.I. Nakamura, F. González, and H.G. Milburn (2005): Technology Developments in Real-Time Tsunami Measuring, Monitoring and

Forecasting. In Oceans 2005 MTS/IEEE, 19–23 September 2005, Washington, D.C.

National Geophysical Data Center, Global Tsunami Database (2000 BC to present):

http://www.ngdc.noaa.gov/seg/hazard/tsu_db.shtml

- Okada, Y., 1985; Surface deformation due to shear and tensile faults in a half-space. *Bull. Seismol. Soc. Am.*, 75, 1135–1154.
- Pararas-Carayannis, G.(1969): *Catalog of Tsunamis in The Hawaii Islands*, World Data Center A Tsunami – Coast and Geodetic Survey, 94 pp.
- Percival, D.B., D.W. Denbo, M.C. Eble, E. Gica, H.O. Mofjeld, M.C. Spillane, L. Tang, and V.V. Titov (2011): Extraction of tsunami source coefficients via inversion of DART® buoy data. *Nat. Hazards*, 58(1), doi: 10.1007/s11069-010-9688-1, 567–590.
- Righi, D., and D. Arcas (2010): A Tsunami Forecast Model for Newport, Oregon. NOAA OAR Special Report, PMEL Tsunami Forecast Series: Vol. 5, 80 pp.
- Satake, K., Y. Hasegawa, Y. Nishimae and Y. Igarashi (2008), Recent Tsunamis That Affected the Japanese Coasts and Evaluation of JMA's Tsunami Warnings. OS42B-03, AGU Fall Meeting, San Francisco.
- Shepard, F.P., G.A. Macdonald, and D.C. Cox (1950): The tsunami of April 1, 1946. *Bull. Scripps Inst. Oceanogr. Univ. Calif.*, 5, 391–528.
- Smith, W. H. F., and D. T. Sandwell (1997), Global seafloor topography from satellite altimetry and ship depth soundings, *Science*, 277, 1957–1962.
- Spaeth, M.G. and S.C. Berkman, (1967), *The tsunami of March 28, 1964, as recorded at tide stations*, U.S. Coastal and Geodetic Survey Publication. Rockville, Maryland: U.S. Coast and Geodetic Survey, 59 pp.
- Spillane, M.C., E. Gica, V.V. Titov, and H.O. Mofjeld (2008): Tsunameter network design for the U.S. DART® arrays in the Pacific and Atlantic Oceans, Tech. Memo, OAR PMEL-143, 165pp., Gov. Print. Off., Seattle, Wash.
- Synolakis, C.E., E.N. Bernard, V.V. Titov, U. Kânoğlu, and F.I. González (2008): Validation and verification of tsunami numerical models. *Pure Appl. Geophys.*, 165(11–12), 2197–2228.
- Tang, L., C. Chamberlin, E. Tolkova, M. Spillane, V.V. Titov, E.N. Bernard, and H.O. Mofjeld (2006): Assessment of potential tsunami impact for Pearl Harbor, Hawaii. NOAA Tech. Memo. OAR PMEL-131.
- Tang, L., C. Chamberlin and V.V. Titov, (2008a), Developing tsunami forecast inundation models for Hawaii: procedures and testing, *NOAA Tech. Memo., OAR PMEL -141*, 46 pp.
- Tang, L., V. V. Titov, Y. Wei, H. O. Mofjeld, M. Spillane, D. Arcas, E. N. Bernard, C. Chamberlin, E. Gica, and J. Newman (2008b), Tsunami forecast analysis for the

- May 2006 Tonga tsunami, *J. Geophys. Res.*, 113, C12015, doi:10.1029/2008JC004922.
- Tang, L., V. V. Titov, and C. D. Chamberlin (2009): Development, Testing, and Applications of Site-specific Tsunami Inundation Models for Real-time Forecasting. *J. Geophys. Res.*, 114, C12025, doi:10.1029/2009JC005476..
- Tang, L., V.V. Titov and C.D. Chamberlin (2010): A Tsunami Forecast Model for Hilo, Hawaii. NOAA OAR Special Report, PMEL Tsunami Forecast Series: Vol. 1, 44 pp.
- Tang, L., V. V. Titov, E. Bernard, Y. Wei, C. Chamberlin, J. C. Newman, H. Mofjeld, D. Arcas, M. Eble, C. Moore, B. Uslu, C. Pells, M. C. Spillane, L. M. Wright, and E. Gica (2012): Direct energy estimation of the 2011 Japan tsunami using deep-ocean pressure measurements. *J. Geophys. Res.*, 117, C08008, doi:10.1029/2011JC007635.
- Titov, V.V., and F.I. González (1997), Implementation and testing of the Method of Splitting Tsunami (MOST) model, *NOAA Tech. Memo. ERL PMEL-112*, 11 pp.
- Titov, V.V., and C.S. Synolakis (1998), Numerical modeling of tidal wave runup. *J. Waterw. Port Coast. Ocean Eng.*, ASCE, 124(4), 157–171.
- Titov, V.V., H.O. Mofjeld, F.I. Gonzalez and J.C. Newman (1999): Offshore forecasting of Alaska-Aleutian subduction zone tsunamis in Hawaii. NOAA Technical Memorandum. ERL PMEL-114, January 1999, 22 pp.
- Titov, V.V., H.O. Mofjeld, F.I. González, and J.C. Newman (2001), Offshore forecasting of Alaskan tsunamis in Hawaii, In *Tsunami Research at the End of a Critical Decade*, edited by G.T. Hebenstreit, Kluwer Academic Publishers, Amsterdam, 75–90.
- Titov, V.V., F.I. González, E.N. Bernard, M.C., Eble, H.O. Mofjeld, J.C. Newman, and A.J. Venturato (2005), Real-time tsunami forecasting: challenges and solutions, *Natural Hazards*, 35(1), 41–58.
- Titov, V.V. (2009): Tsunami forecasting. Chapter 12 in *The Sea*, Volume 15: Tsunamis, Harvard University Press, Cambridge, MA and London, England, 371–400.
- Titov, V. V., and L. Tang (2011): Estimating tsunami magnitude in real time using tttsunameter data, paper presented at XXV IUGG General Assembly, Melbourne, Victoria, Australia, 28 Jun to 7 Jul.
- Titov, V. V., C. W. Moore, D. J. M. Greenslade, C. Pattiaratchi, R. Badal, C. E. Synolakis, and U. Kanoğlu (2011): A new tool for inundation modeling: Community Modeling Interface for Tsunamis (ComMIT). *Pure Appl. Geophys.*, 168, 2121–2131, doi:10.1007/s00024-011-0292-4.
- Tolkova, E. (2007): Compression of MOST Propagation Database. NOAA Tech. Memo. OAR PMEL-134, NTIS: PB2007-108218, 9 pp., Gov. Print. Off., Seattle, Wash.

- Uslu, B., D. Arcas, V.V. Titov, and A.J. Venturato (2010): A Tsunami Forecast Model for San Francisco, California. NOAA OAR Special Report, PMEL Tsunami Forecast Series: Vol. 3, 88 pp.
- Walker, D.A. (2004): Regional Tsunami evacuations for the state of Hawaii: a feasibility study on historical runup data. *Science of Tsunami Hazards*, 22(1), 3-22.
- Wei, Y., E. Bernard, L. Tang, R. Weiss, V. Titov, C. Moore, M. Spillane, M. Hopkins, and U. Kânoğlu (2008): Real-time experimental forecast of the Peruvian tsunami of August 2007 for U.S. coastlines. *Geophys. Res. Lett.*, 35, L04609, doi: 10.1029/2007GL032250.
- Wei, Y., and D. Arcas (2010): A tsunami forecast model for Kodiak, Alaska. NOAA OAR Spec. Rep./PMEL Tsunami Forecast Ser. 4, 96 pp., Gov. Print. Off., Seattle, Wash.
- Wei, Y., C. Chamberlin, V.V. Titov, L. Tang, and E.N. Bernard (2012): Modeling of 2011 Japan Tsunami - lessons for near-field forecast. *Pure Appl. Geophys.*, doi: 10.1007/s00024-012-0519-z.
- Whitmore, P.M. (2003): Tsunami amplitude prediction during events: A test based on previous tsunamis. In *Science of Tsunami Hazards*, 21, 135–143.
- Zerbe, W.B. (1953): The tsunami of November 4, 1952, as recorded at tide stations. C&GS Special Publication #300, U.S. Dept. of Commerce, C&GS, 62pp.

Table 1 Tsunami source functions in the Pacific, Atlantic and Indian Oceans.

Source Zone			Tsunami source functions	
No.	Abbr.	Name	Line/zone	Numbers
1	ACSZ	Aleutian-Alaska-Canada-Cascadia	BAZYXW	184
2	CSSZ	Central-South American	BAZYX	382
3	EPSZ	East Philippines	BA	44
4	KISZ	Kamchatka-Kuril-Japan Trench-Izu Bonin-Marianas-Yap	BAZYXW	229
5	MOSZ	Manus Ocean Convergence Boundary	BA	34
6	NVSZ	New Britain-Solomons-Vanuatu	BA	74
7	NGSZ	North New Guinea	BA	30
8	NTSZ	New Zealand-Kermadec-Tonga	BA	81
9	NZSZ	South New Zealand	BA	14
10	RNSZ	New Ryukus-Kyushu-Nankai	BA	44
11	KISZ	Kamchatskii-Bering Source Zone	BAZ	13
			Subtotal:	1129
12	ATSZ	Atlantic	BA	214
13	SSSZ	South Sandwich	BAZ	33
			Subtotal:	247
14	IOSZ	Adaman-Nicobar-Sumatra-Java	BAZY	307
15	MKSZ	Makran	BA	20
16	WPSZ	West Philippines	BA	22
			Subtotal:	349

Total: **1725**

Table 2 Tsunami sources for fourteen historical tsunamis.

Event	Earthquake / Seismic			Model		
	USGS Date Time (UTC) Epicenter	CMT Date Time (UTC) Centroid	Magnitude Mw (CMT)	Tsunami Magnitude ¹	Subduction Zone	Tsunami Source
1946 Unimak	01 Apr 12:28:56 52.75°N 163.50°W	n/a	² 8.5	8.5	Aleutian-Alaska-Cascadia (ACSZ)	$7.5 \times b23 + 19.7 \times b24 + 3.7 \times b25$
1952 Kamchatka	04 Nov 16:58:26.0 ³ 52.76°N 160.06°E	n/a	³ 9.0	8.7	Kamchatka-Kuril-Japan-Izu-Mariana-Yap (KISZ)	Tang <i>et al.</i> (2006)
1957 Andreanov	09 Mar 14:22:31 51.56°N 175.39°W	n/a	³ 8.6	8.7	Aleutian-Alaska-Cascadia (ACSZ)	$31.4 \times a15 + 10.6 \times a16 + 12.2 \times a17$
1960 Chile	22 May 19:11:14 ³ 38.29°S 73.05°W	n/a	⁴ 9.5	n/a	Central-South America (CSSZ)	Kanamori & Ciper (1974)
1964 Alaska	28 Mar 03:36:00 ³ 61.02°N 147.65°W	n/a	³ 9.2	8.9	Aleutian-Alaska-Cascadia (ACSZ)	$15.4 \times a34 + 19.4 \times a35 + 48.3 \times z34 + 18.3 \times b34 + 15.1 \times b35$
1994 East Kuril	04 Oct 13:22:58 43.73°N 147.321°E	04 Oct 13:23:28.5 43.60°N 147.63°E	8.3	8.2	Kamchatka-Kuril-Japan-Izu-Mariana-Yap (KISZ)	$1.3 \times a20 + 3.2 \times z19 + 5.9 \times b20$
1996 Andreanov	10 Jun 04:03:35 51.56°N 175.39°W	10 Jun 04:04:03.4 51.10°N 177.410°W	7.9	8.0	Aleutian-Alaska-Cascadia (ACSZ)	$5.55 \times b15$
2003 Hokkaido	25 Sep 19:50:06 41.775°N 143.904°E	25 Sep 19:50:38.2 42.21°N 143.84°E	8.3	8.0	Kamchatka-Kuril-Japan-Izu-Mariana-Yap (KISZ)	$3.6m \times (100 \times 100\text{km})$ 109#rake, 20#dip, 230#strike, 25 m depth
2003 Rat Island	17 Nov 06:43:07 51.13°N 178.74°E	17 Nov 06:43:31.0 51.14°N 177.86°E	7.7	7.9	Aleutian-Alaska-Cascadia (ACSZ)	$2.7 \times b11 + 0.9 \times a12$
2006 Tonga	03 May 15:26:39 20.13°S 174.161°W	03 May 15:27:03.7 20.39°S 173.47°W	8.0	8.0	New Zealand-Kermadec-Tonga (NTSZ)	$6.6 \times b29$ (Tang <i>et al.</i> , 2008)
2006 Kuril	15 Nov 11:14:16 46.607°N 153.230°E	15 Nov 11:15:08 46.71°N 154.33°E	8.3	8.1	Kamchatka-Kuril-Japan-Izu-Mariana-Yap (KISZ)	$3.2 \times a12 + 6.0 \times z12$
2007 Kuril	13 Jan 04:23:20 46.272°N 154.455°E	13 Jan 04:23:48.1 46.17°N 154.80°E	8.1	7.8	Kamchatka-Kuril-Japan-Izu-Mariana-Yap (KISZ)	$-3.2 \times b13$
2007 Solomon	01 Apr 20:39:56 8.481°S 156.978°E	01 Apr 20:40:38.9 7.76°S 156.34°E	8.1	8.2	New Britain-Solomons-Vanuatu (NVSZ)	$12.0 \times b10$
2007 Peru	15 Aug 23:40:57 13.354°S 76.509°W	15 Aug 23:41:57.9 13.73°S 77.04°W	8.0	8.3	Central-South America (CSSZ)	$3.6 \times a62 + 5.7 \times z63 + 5.3 \times b62$
2009 Samoa	29 Sep 17:48:10 15.509°S 172.034°W	29 Sep 17:48:26.8 15.13°S 171.97°W	8.1	8.2	New Zealand-Kermadec-Tonga (NTSZ)	$a34 \times 6.4 + 3.2 \times c35$

¹ Preliminary source – derived from tsunami source functions and deep-ocean observations² López and Okal (2006)³ United States Geological Survey (USGS)⁴ Kanamori and Ciper (1974)⁵ Tsunami source was obtained in real time and applied to the forecast

2010 Chile	27 Feb 06:34:14 35.909°S 72.733°W	27 Feb 06:35:15.4 35.95°S 73.15°W	8.8	8.8	Central-South America (CSSZ)	$a87 \times 9.68 + z88 \times 24.5 + a88 \times 15.35 + a91 \times 13.19 + z92 \times 24.82$
2011 Japan	11 March 05:46:23 38.322°N 142.369°E	11 March 05:47:32.8 37.52°S 143.05 E	9.1	8.8	Kamchatka-Kuril-Japan-Izu-Mariana-Yap (KISZ)	$^54.66 \times b24 + 12.23 \times b25 + 26.31 \times a26 + 21.27 \times b26 + 22.75 \times a27 + 4.98 \times b27$
2012 Queen Charlotte Islands	28 October 03:04:09 52.742°N 132.131°W	28 October 03:04:39.2 52.47°N 132.13°W	7.7	8.8	Aleutian-Alaska-Cascadia (ACSZ)	$^52.80 \times 50a + 4.41 \times 51a$

Table 3 Data sources used for grid development

Data provider	Data type	Survey dates	Description
Joint Airborne Lidar Bathymetry Technical Center of Excellence	Points	1999-2000	Nearshore bathymetry and topography from SHOALS airborne LIDAR. 1-5 meter horizontal resolution.
Monterey Bay Aquarium Research Institute (MBARI)	Grid	1998	Multibeam bathymetric surveys. 10-30 meter horizontal resolution.
USGS Pacific Seafloor Mapping Project	Grid	1998	Multibeam bathymetric surveys. 8 meter resolution
Japan Agency for Marine-Earth Science and Technology (JAMSTEC)	Grid	1998-2002	Multibeam bathymetric surveys. 150 meter horizontal resolution. Multibeam tracklines at varying resolutions.
United States Navy	Point	2000	Multibeam surveys, south and west sides of Oahu
United States Army Corps of Engineers, Honolulu District	Point	2000-2005	Digital echosounder surveys in USACE harbor project areas
National Geophysical Data Center	Point	1968-1992	Bathymetric survey data. Multiple technologies, including lead line, digital echosounder, and multibeam
National Ocean Service	Point	1979-1989, 2005	Older bathymetric data points digitized from NOS nautical charts. Recent points imported from Electronic Navigational Charts (ENCs).
Smith & Sandwell 1997	Point	1997	2-minute resolution bathymetry derived from satellite altimetry and ship tracklines.
USGS GLORIA	Point	1986-1988	Sidescan sonar bathymetric surveys in deep-water regions of Hawaii's EEZ.
NOAA Coastal Services Center	Grid	2005	IfSAR (radar altimetry) topographic survey. Gridded to 5-meter horizontal resolution.
USGS National Elevation Dataset	Grid	Varies	10-meter resolution topographic data derived from USGS DEMs

Source details for the datasets incorporated into the model grids:

- Joint Airborne Lidar Bathymetry Technical Center of Expertise (JALBTCX), US Army Corps of Engineers, Mobile District. Online reference: http://shoals.sam.usace.army.mil/hawaii/pages/Hawaii_Data.htm.
- Monterey Bay Aquarium Research Institute (MBARI) Hawaii Multibeam Survey, Version 1. Online reference: <http://www.mbari.org/data/mapping/hawaii/>.
- USGS Pacific Seafloor Mapping Project. Online reference: <http://walrus.wr.usgs.gov/pacmaps/data.html>.
- Japan Agency for Marine-Earth Science and Technology (JAMSTEC) 1998-1999 multibeam bathymetric surveys. Published in: Takahashi, E., et al., eds. (2002): *Hawaiian Volcanoes: Deep Underwater Perspectives*. American Geophysical Union Monograph 128. JAMSTEC trackline data was recorded by the R/V *Mirai* during transits near in 1999 and 2002. Online reference: http://www.jamstec.go.jp/mirai/index_eng.html.
- United States Army Corps of Engineers (USACE), Honolulu District. Online reference: <http://www.poh.usace.army.mil/>.
- NOAA National Geophysical Data Center (NGDC). Online reference: http://www.ngdc.noaa.gov/mgg/gdas/gd_sys.html.
- NOAA National Ocean Service (NOS). Sounding points were digitized from NOS nautical charts 19347, 19358, 19359, 19364, 19366, 19342, 19381, and 19324. Sounding data from electronic chart (ENC) 19357 was used. This data was included in relatively shallow regions where other data sources were sparse or unavailable, or for quality control of other sources.

- Smith, W. H. F., and D. T. Sandwell, Global seafloor topography from satellite altimetry and ship depth soundings, *Science*, v. 277, p. 1957-1962, 26 Sept., 1997. Online reference: http://topex.ucsd.edu/WWW_html/mar_topo.html.
- USGS Geological Long-Range Inclined Asdic (GLORIA) surveys. Online data reference: <http://walrus.wr.usgs.gov/infobank/>
- NOAA Coastal Services Center. <http://www.csc.noaa.gov/>. The IfSAR topographic data was collected and processed for CSC by Intermap Technologies Inc. The data is subject to a restrictive license agreement and is not publicly available.
- USGS National Elevation Dataset. Online reference: <http://seamless.usgs.gov/>

Table 4 MOST setup for the Honolulu reference and forecast model.

Grid	Region	Reference Inundation Model (RIM)			Stand-by Inundation Model (SIM)		
		Coverage	Cell	Time	Coverage	Cell	Time
		Lon. [$^{\circ}$ E]	Size	Step	Lon. [$^{\circ}$ E]	Size	Step
		Lat. [$^{\circ}$ N]	["]	[sec]	Lat. [$^{\circ}$ N]	["]	[sec]
A	Hawaii	199 - 205.98 18 - 23	36 (699 x 500)	2.4	199 - 205.9667 18.0317 - 22.9967	120 (210 x 150)	12.8
B	Oahu	201.503 – 203.163 20.458 - 21.867	6 (997 x 846)	0.48	201.5033 – 202.7683 20.7217 - 21.8667	18 (254 x 230)	2.4
C	Honolulu	201.931 – 202.223 21.229 - 21.400	2/3 (1582 x 925)	0.24	202.077 – 202.215 21.247 – 21.337	2 (249 x 163)	0.8
Minimum offshore depth [m]		10			1		
Water depth for dry land [m]		0.3			0.3		
Manning coefficient, C_m		0.03			0.03		
CPU time for a 4-hour simulation		\sim 16 hours			< 10 minutes		

Computations were performed on a single Intel Xeon processor at 3.6 GHz, Dell PowerEdge 1850.

Table 5 Observed and modeled maximum wave crest at the Honolulu tide gage for 18 past tsunamis.

No.	Event	Observation			Reference model			Forecast Model			
		ID	η_{\max}	t_{\max}	η_{\max}	t_{\max}	Error	(%)	η_{\max}	t_{\max}	Error
(m)	(hour)	(m)	(hour)	(m)	(%)	(m)	(hour)	(m)	(%)		
1	19460401	0.67	5.100	0.83	5.041	0.16	24	0.76	6.062	0.09	14
2	19521104	0.64	7.619	0.40	9.579	-0.24	-37	0.36	7.889	-0.28	-43
3	19570309	0.69	6.947	0.79	5.853	0.11	15	0.94	6.269	0.25	37
4	19600522	0.98	16.830	1.18	17.907	0.20	21	1.22	17.902	0.24	25
5	19640328	0.43	9.120	0.55	5.379	0.12	28	0.47	5.373	0.04	10
6	19941004	0.11	12.529	0.18	8.905	0.07	67	0.13	8.405	0.02	17
7	19960610	0.07	5.117	0.09	5.214	0.03	36	0.08	6.280	0.01	17
8	20010623	0.09	28.652	0.09	16.293	-0.00	0	0.09	15.454	0.01	0
9	20030925	0.05	9.500	0.06	13.005	0.01	24	0.04	7.745	-0.01	0
10	20031117	0.04	5.950	0.08	8.611	0.04	94	0.07	6.536	0.03	73
11	20060503	0.13	7.772	0.21	7.750	0.08	59	0.19	7.821	0.06	45
12	20061115	0.16	8.179	0.13	12.756	-0.03	-16	0.13	8.427	-0.02	-15
13	20070113	0.06	12.437	0.09	9.840	0.02	40	0.08	8.219	0.02	28
14	20070815	0.06	13.418	0.07	14.189	0.01	24	0.06	14.227	0.01	0
15	20090929	0.17	6.764	0.21	6.833	0.04	25	0.19	7.184	0.02	14
16	20100227	0.28	28.663	0.21	17.333	-0.07	-24	0.17	16.962	-0.10	-38
17	20110311	0.69	7.710	0.89	8.199	0.20	30	0.86	8.219	0.17	24
18	20121027	0.20	6.081	0.27	6.755	0.07	37	0.24	6.142	0.04	20

Table 6 Sources of the 18 Mw 9.3 synthetic tsunamis and maximum wave crest at the Honolulu tide gage computed by the reference and forecast models.

No.	¹ Subd.	Source	alpha	Ref.	model	Forecast Model		Error	Location	
						Zone	η_{\max}	t_{\max}	(m)	(%)
							(m)	(hour)		
1	KISZ AB	22T31	29	2.27	7.623	2.29	7.621	0.02	1	Japan
2	KISZ AB	1T10	29	2.22	7.913	2.25	7.802	0.02	1	Kamchatka
3	ACSZ AB	16T25	29	2.72	4.643	2.70	4.638	-0.02	-1	Central Aleutian
4	ACSZ AB	22T31	29	1.81	5.370	1.82	5.371	0.01	1	Unimak
5	ACSZ AB	50T59	29	2.66	6.693	2.60	6.675	-0.07	-2	Canada
6	ACSZ AB	56T65	29	1.21	6.130	1.59	6.663	0.38	32	Cascadia
7	CASZ AB	1T10	29	0.44	9.150	0.41	11.476	-0.03	-6	Central American
8	CESZ AB	1T10	29	0.43	14.023	0.33	12.627	-0.10	-22	Columbia-Ecuador
9	SASZ AB	40T49	29	1.73	17.300	1.79	17.244	0.06	4	Chile
10	SCSZ AB	3T12	29	1.03	16.747	1.02	17.916	-0.01	-1	Southern Chile
11	NTSZ AB	20T29	29	0.47	9.433	0.47	8.516	0.00	0	Tonga
12	NTSZ AB	30T39	29	1.17	5.733	1.34	5.764	0.17	14	Northern Tonga
13	NVSZ AB	28T37	29	1.17	8.477	1.44	8.485	0.27	23	Vanuatu
14	MOSZ AB	1T10	29	1.55	10.723	1.37	11.365	-0.17	-11	Manus
15	NGSZ AB	3T12	29	0.56	11.323	0.71	14.161	0.15	27	New Guinea
16	EPSZ AB	6T15	29	2.41	12.247	2.80	12.236	0.39	16	East Philippines
17	RNSZ AB	12T21	29	0.94	11.500	1.19	11.423	0.25	26	Nankai
18	KISZ AB	32T41	29	1.74	9.803	1.60	9.255	-0.14	-8	Izu

1: The subduction zone names and numbers of the tsunami source functions used here were from propagation database 1.0 in 2006.

Table 7 Simulated tsunamis for hazard assessment study for Honolulu.

M_w	Numbers of TSFs	Tsunami source coef.	Lines	Numbers of tests	Range of η_{\max}		Ratio max/min
					min	max	
1	7.5	1	BA	810	0.01 cm	0.77 cm	77
2	7.5	1	B	405	0.23 cm	9.28 cm	40
3	8.2	1	B	392	0.08 cm	0.63 m	83
4	8.7	6 (3 pairs)	BA	345	3.1 cm	1.12 m	36
5	9.3	20 (10 pairs)	BA	285	17 cm	2.91 m	17

1: at water depth 4440 m offshore Honolulu from the pre-computed propagation database;

2 to 5: at Honolulu tide station computed by the Honolulu forecast model (at approximately 6.3 m water depth).

Appendix A.

The following appendix lists the input files for Honolulu developed in 2009.

A1. Reference model *.in file for Honolulu , Hawaii for MOST version 4.0

```
# ----- MOST Run 1 -----
# 0. Preparations
echo '#-----#'
echo '#      Preprocess MOST input      #'
echo '#-----#'
set main_dir="/home/tg23/data/tang/sims/honolulu/"
set path_w="$main_dir/honov4_H20030925_8h/"

set path_src="/home/tg23/data/tang/src_nc/src_sim_test/kona/H20030925_kona_"
set np="8"

set path_e="/grid/tg23/data/tolkova/public_html/v4/v4code/RttdMost_mp"

if( -d $path_w ) then
echo $path_w 'exist'
echo ' Removing files '
cd $path_w
rm -r *
else
echo Creating directory $path_w
mkdir $path_w
cd $path_w
endif

ln -sf /home/tg23/data/tang/bathy/honolulu/hono_rb3/R*.nc .

# -----
# 1. Generate INPUT for MOST
# ~~~~~~A~~~~~
cat > most3_facts_nc.in << EOF
0.001  Minimum amplitude of input offshore wave (m):
20      Input minimum depth for offshore (m)
0.1     Input "dry land" depth for inundation (m)
0.0009   Input friction coefficient (n**2)
2       Number of grids
2       Interpolation domain for outer boundary
2       inner boundary
RA_hawaii_36s_20070806.nc
RB_oahu_6s2_20070806.nc
1       Runup flag
4       Input time step (sec)
7200    Input amount of steps
0       Continue after input stops
8       Input number of steps between snapshots
1       saving inner boundaries every n-th timestep
1       ...Saving grid every n-th node, n=
0       1=initial deformation
EOF
```

EOF

```

cp most3_facts_nc.inA most3_facts_nc.in
setenv OMP_NUM_THREADS $np
$spath_e A $spath_src most3_facts_nc.in
# ~~~~~

# ~~~~B~~~~~
cat > most3_facts_nc.inB<<EOF
0.001 Minimum amplitude of input offshore wave (m):
20 Input minimum depth for offshore (m)
0.1 Input "dry land" depth for inundation (m)
0.0009 Input friction coefficient (n**2)
2 Number of grids
2 Interpolation domain for outer boundary
2 inner boundary
RB_ohau_6s2_20070806.nc
RC_hono_10ms_20070221.nc
1 Runup flag
0.72 Input time step (sec)
144000 Input amount of steps
0 Continue after input stops
42 Input number of steps between snapshots
1 saving inner boundaries every n-th timestep
1 ...Saving grid every n-th node, n=
0 1=initial deformation
EOF
cp most3_facts_nc.inB most3_facts_nc.in
setenv OMP_NUM_THREADS $np
$spath_e B A most3_facts_nc.in

```

~~~~C~~~~~

```

cat > most3_facts_nc.inC<< EOF
0.001 Minimum amplitude of input offshore wave (m):
-300 Input minimum depth for offshore (m)
0.2 Input "dry land" depth for inundation (m)
0.0009 Input friction coefficient (n**2)
1 Number of grids
2
2
RC_hono_10ms_20070221.nc
2 runup
0.12 Input time step (sec)
2440000 Input amount of steps
0 continue after input stop
250 Input number of steps between snapshots
1 ...Saving inner boundary
1 ...Saving grid every n-th node, n=
0
EOF
cp most3_facts_nc.inC most3_facts_nc.in
setenv OMP_NUM_THREADS $np
$spath_e C B most3_facts_nc.in

```

A2. Forecast model *.in file for Honolulu, Hawaii for MOST version 2.0

```

#!/bin/sh
# ----- MOST Run 1 -----
# 0. Preparations
echo '#-----#'
echo '#      Preprocess MOST input      #''
echo '#-----#'
set main_dir="/home/tg23/data/tang/sims/honolulu/"
set path_w="$main_dir/honov2_H20121027_fsrc_ob6_24h/"

```

```

set path_e="/usr/local/most"

if ( -d $path_w ) then
echo $path_w 'exist'
echo ' Removing files '
cd $path_w
rm -r *
else
echo Creating directory $path_w
mkdir $path_w
cd $path_w
endif
mkdir M_run2d
ln -sf /home/tg23/data/tang/bathy/honolulu/hono_ob6//* .
# -----
# 1. Generate INPUT for MOST
cat > most3_facts_nc.in << EOF
0.0001 Minimum amplitude of input offshore wave (m):
1 Input minimum depth for offshore (m)
0.3 Input "dry land" depth for inundation (m)
0.0009 Input friction coefficient (n**2)
1 runup flag for grids A and B (1=yes,0=no)
300.0 blowup limit
0.8 Input time step (sec)
90000 Input amount of steps
16 Compute "A" arrays every n-th time step, n=
3 Compute "B" arrays every n-th time step, n=
48 Input number of steps between snapshots
1 ...Starting from
1 ...Saving grid every n-th node, n=
hawaii_2min_20070806.asc.s.c
ohau_18s_20070806.c
hono_2s_20070221.c3c
/home/tg23/data/tang/src_nc/event/20121027/
./
1 1 1
1 Timeseries locations:
3 106 62 honolulu 202.1357408603007      21.3030554745305 depth m: 6.55      HON      Honolulu, HI
EOF
cp most3_facts_nc.in M_run2d/
# -----
# 2. run MOST

$path_e/most3_facts_nc M S1_honolulu_ ./ &

```

Figures

Figure 1 (a) Overview of the tsunami Forecast System. System components include tsunameter (DART) network (triangles), pre-computed tsunami source function (unfilled black rectangles) and high-resolution forecast models (red squares). Filled color shows the offshore forecast of the computed maximum sea surface elevation in m for the March 11, 2011 tsunami. Contours indicate the travel time in hours. (b) Eighteen past tsunamis and (c) eighteen simulated magnitude 9.3 tsunamis tested in this study.....	32
Figure 2 Forecast model setups for 13 coastalt sites in Hawaii: (a) 2-arc-min (~3600m) regional, (b) 12-18-arc-sec (~360-540m) intermediate and (c) 2-arc-sec (~60m) nearshore grids for Nawiliwili, Honolulu, Kahului and Hilo. ●, coastal tide stations. +, offshore locations.	33
Figure 3 A chart of Oahu, Hawaii (NOAA Chart 19013). Soundings in fathoms at Mean Lower Low Water. Contour and summit elevation values are in feet above Mean Sea Level.	34
Figure 4 An aerial photo of Honolulu (image courtesy of Google map).	35
Figure 5 Population density, Oahu. (Source: 2010Census).	36
Figure 6 Run-ups in feet at Honolulu coast for the 1946, 1952,1957 and 1960 tsunamis (Image from Walker, 2004).	37
Figure 7 Bathymetric and topographic data source overview. (a) 6" sec (~180m) Hawaii DEM ; (b) 1/3" (~10m) DEM for south Oahu.	38
Figure 8 Grid setup for the Honolulu Reference model with resolution of (a) 36, (b) 6 and (c) 2/3 arc sec (20 m). ●, Honolulu tide station	39
Figure 9 Grid setup for the Honolulu forecast model with resolution of (a) 120, (b) 18 and (c) 2 arc sec. ●, Honolulu tide station.....	40
Figure 10 Tsunami time-series of observed and modeled amplitudes for past tsunamis. The green and red lines were computed by the Honolulu reference and forecast models respectively. The model time series were shifted Δt min behind.....	44
Figure 11 Tsunami time-series of modeled amplitudes at two virtual gages at 2 m water depth for past tsunamis. (a) Gage 1 locates at Ala Moana and (b) Gage 2 is at Waikiki.....	46
Figure 12 Maximum water elevation and current computed by the Honolulu reference and forecast models for past tsunamis.	55
Figure 13 Modeled tsunami time-series for simulated magnitude 9.3 tsunamis.	57
Figure 14 Tsunami time-series of modeled amplitudes at two virtual gages at 2 m water depth for 18 simulated magnitude 9.3 tsunamis. (a) Gage 1 locates at Ala Moana and (b) Gage 2 is at Waikiki.	59
Figure 15 Maximum water elevation and current computed by the Honolulu reference and forecast models for the simulated magnitude 9.3 tsunamis.	68
Figure 16 (a) Modeled η time series at Honolulu tide station for the 18 past tsunamis. (b) Wavelet-derived amplitude spectrogram for the observations. Real part of the spectrograms for (c) observations, (d) the reference and (e) the forecast models.	77
Figure 17 (a) Modeled η time series at Honolulu tide station for the 18 simulated $M_w=9.3$ tsunamis. (b) Wavelet-derived amplitude spectrogram for the reference model. (c and d) Real part of the spectrograms computed by the reference and forecast models.	86
Figure 18 (a) Forecast accuracy and uncertainty in the η_{max} at Honolulu tide station computed from the forecast model for the 36 scenarios. (b) Uncertainty v.s. peak period. Filled markers, 18 past tsunamis; open markers, 18 simulated $M_w = 9.3$ tsunamis.	87
Figure 19 Maximum water elevation at (a) Honolulu offshore from the propagation database and (b,c, d and e) at Honolulu tide station computed by the Honolulu forecast model for simulated magnitude 7.5, 8.2, 8.7 and 9.3 tsunamis. Colors in (b) represent the first arrival at the station. Colors in (c),	87

(d) and (e) represent the difference in time between the arrival of the maximum elevation and the first arrival. 90

Figure 20 Computed maximum water elevation at offshore deep water (4440 m) and Honolulu tide station (~7 m) in (a) logarithmic and (b) Cartesian coordinates. Colors represent tsunami magnitudes. Solid line is the fit by regression analysis in logarithmic scale. Dashed lines are the prediction bounds based on 95% confident level. R, square of the correlation; rmse, root 91

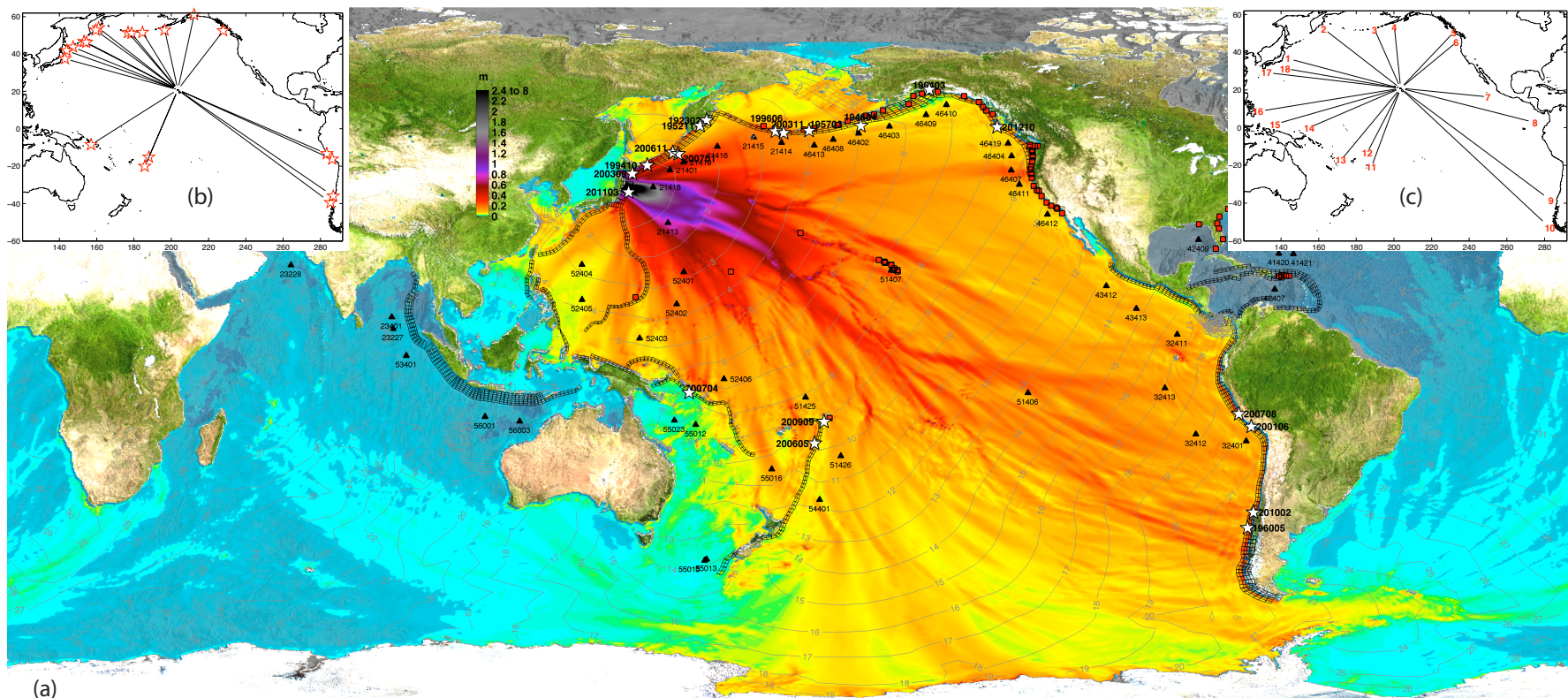


Figure 1 (a) Overview of the tsunami Forecast System. System components include tsunameter (DART) network (triangles), pre-computed tsunami source function (unfilled black rectangles) and high-resolution forecast models (red squares). Filled color shows the offshore forecast of the computed maximum sea surface elevation in m for the March 11, 2011 tsunami. Contours indicate the travel time in hours. (b) Eighteen past tsunamis and (c) eighteen simulated magnitude 9.3 tsunamis tested in this study.

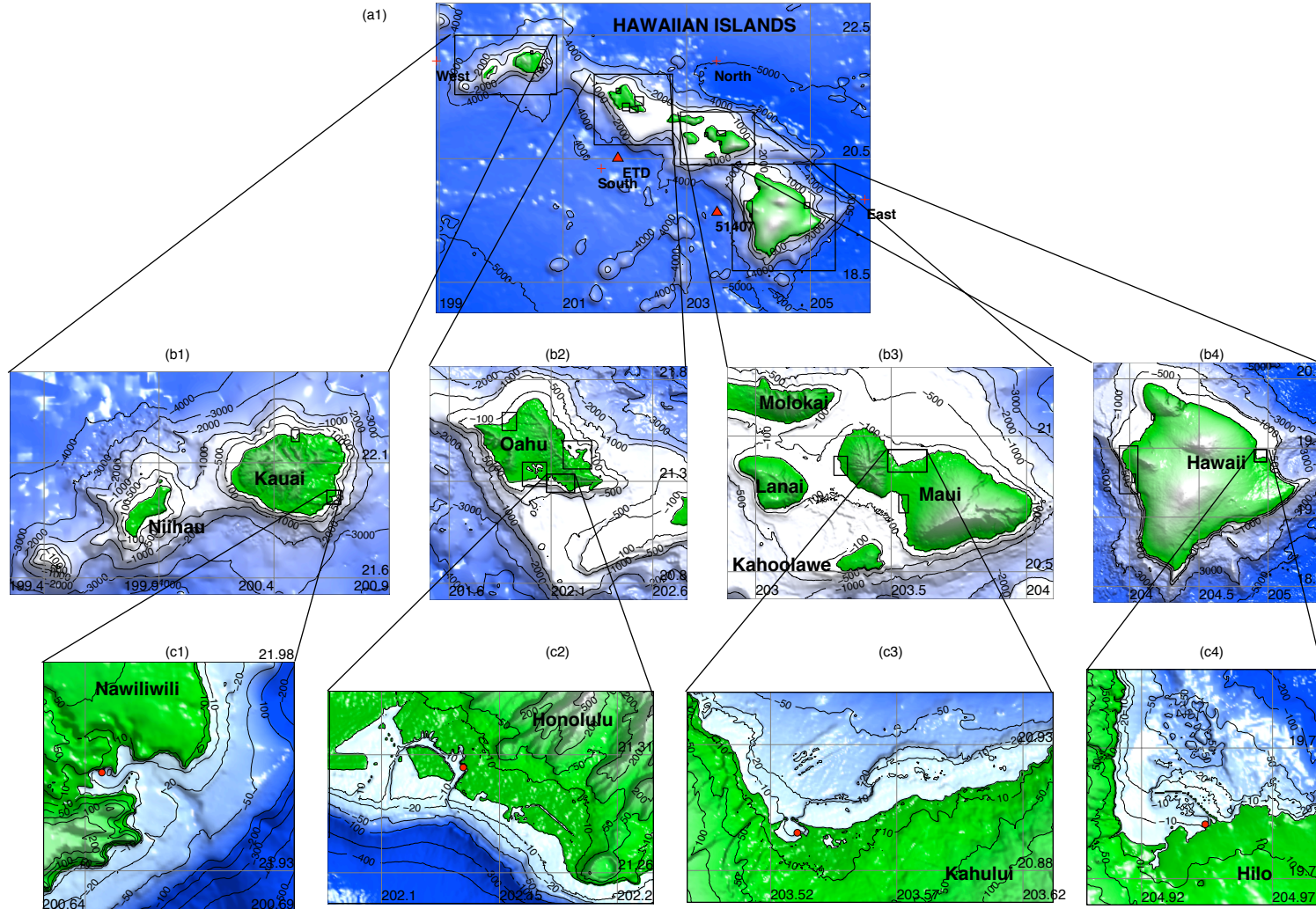


Figure 2 Forecast model setups for 13 coastal sites in Hawaii: (a) 2-arc-min (~3600m) regional, (b) 12-18-arc-sec (~360-540m) intermediate and (c) 2-arc-sec (~60m) nearshore grids for Nawiliwili, Honolulu, Kahului and Hilo. •, coastal tide stations. +, offshore locations.

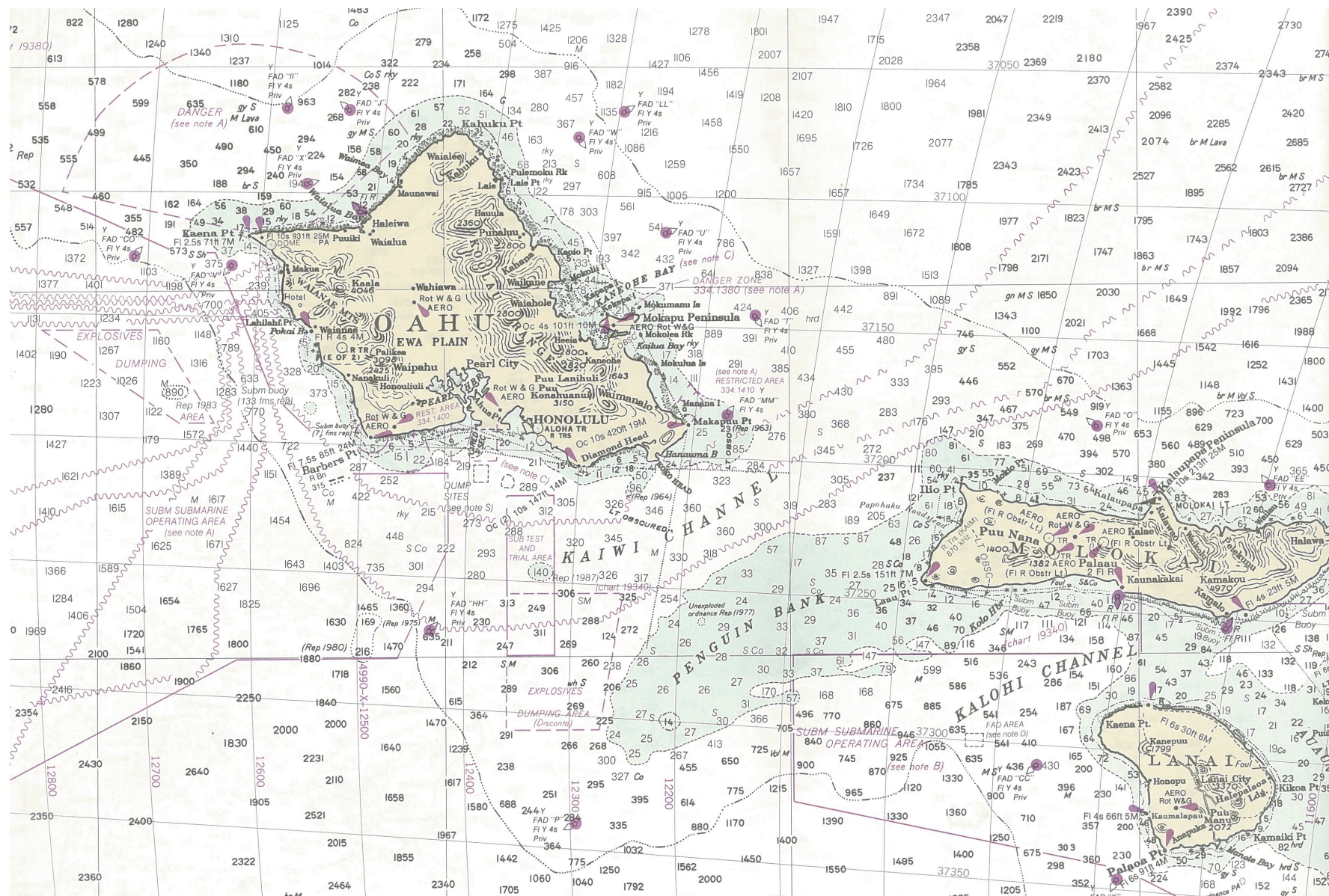


Figure 3 A chart of Oahu, Hawaii (NOAA Chart 19013). Soundings in fathoms at Mean Lower Low Water. Contour and summit elevation values are in feet above Mean Sea Level.

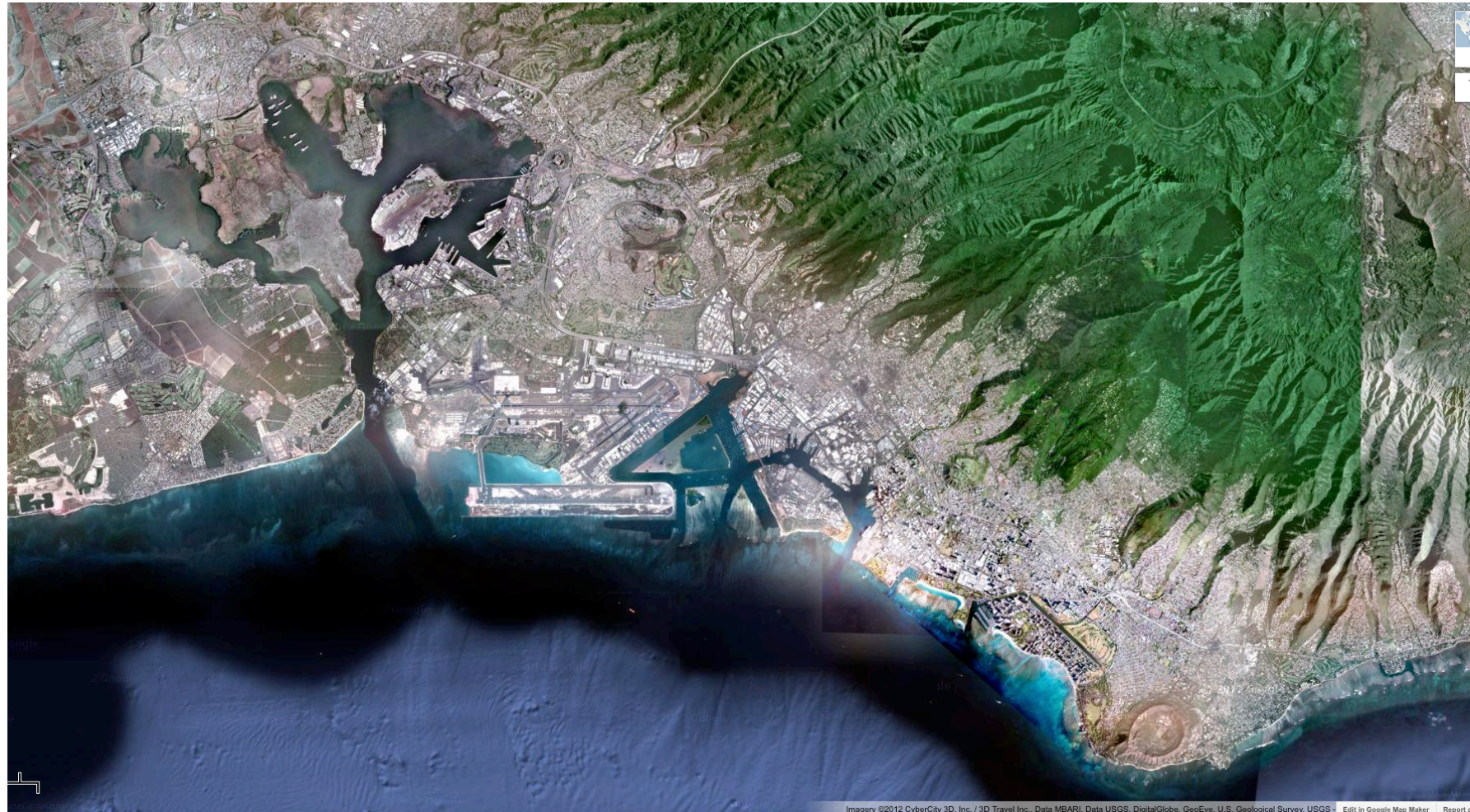


Figure 4 An aerial photo of Honolulu (image courtesy of Google map).

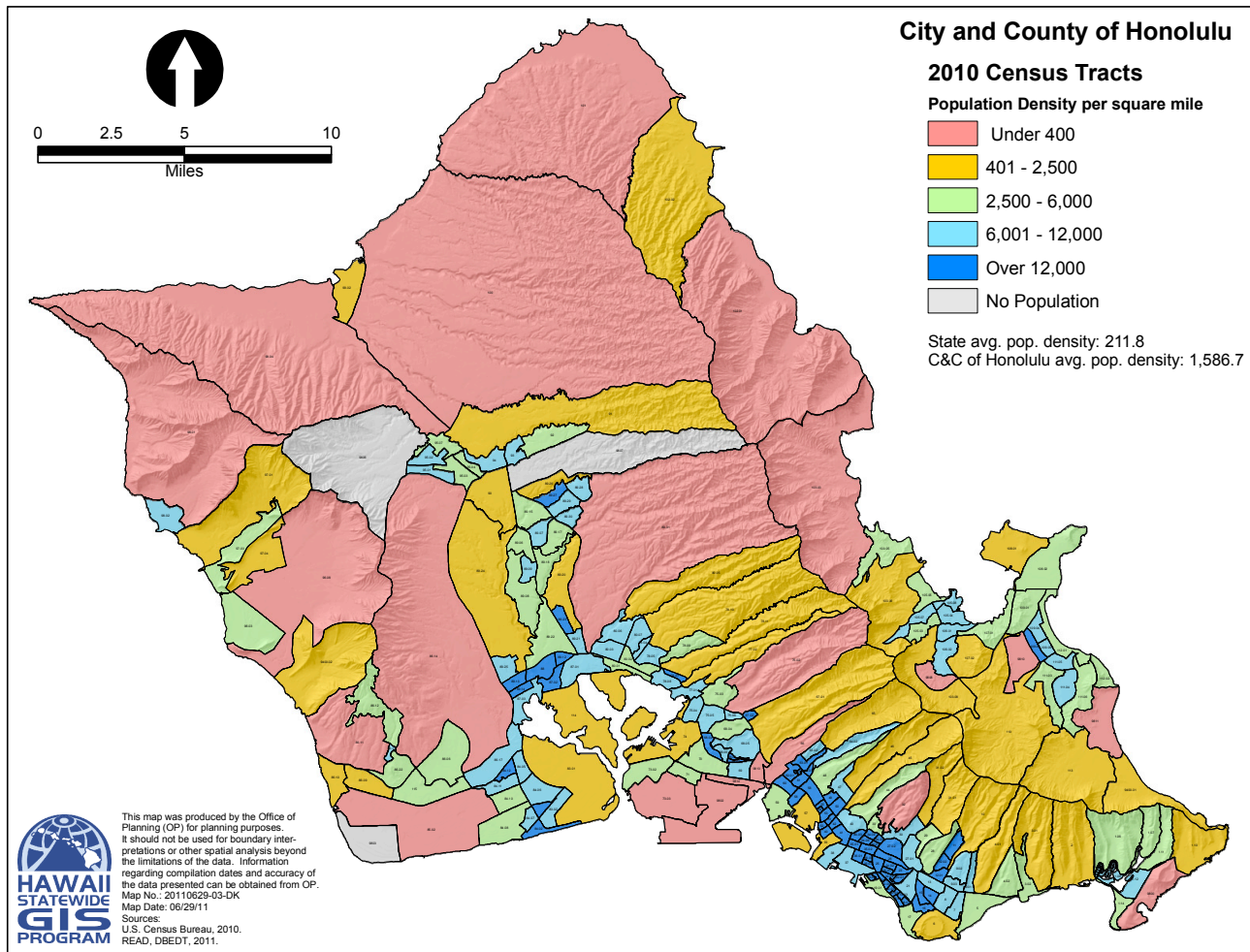


Figure 5 Population density, Oahu. (Source: 2010Census)

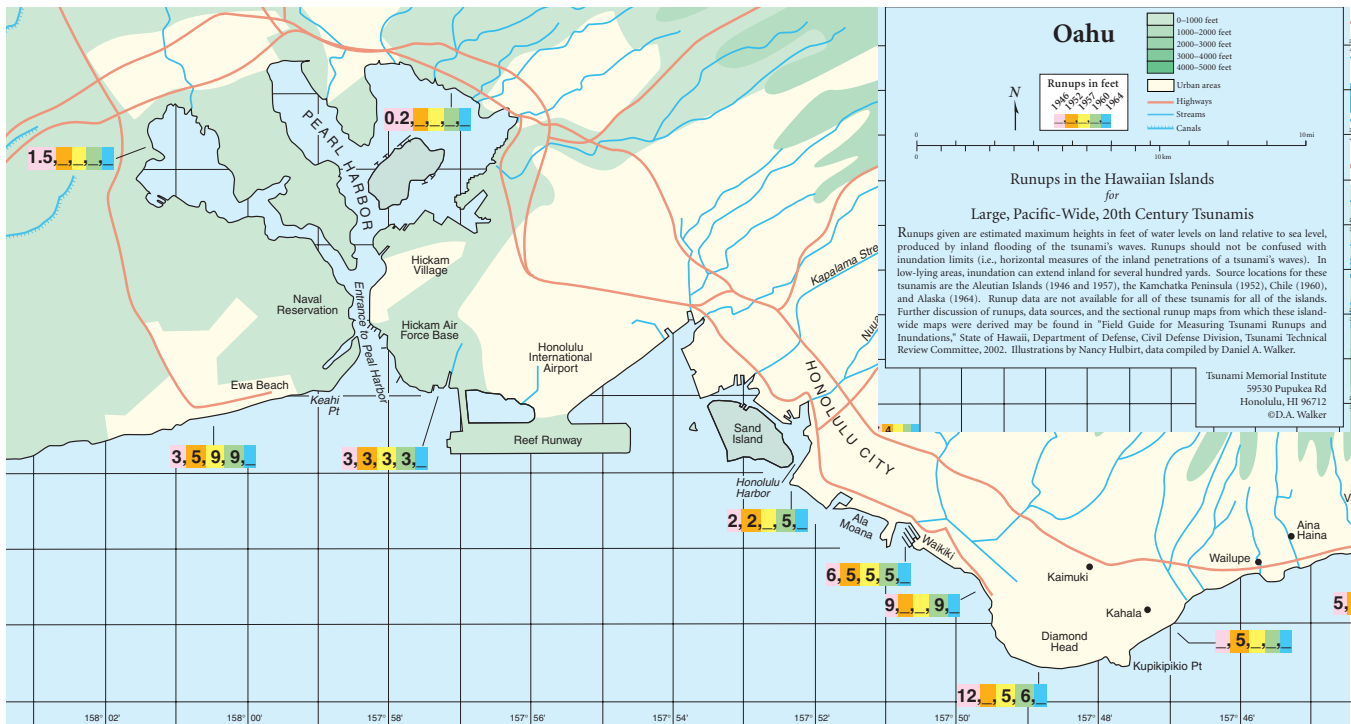


Figure 6 Run-ups in feet at Honolulu coast for the 1946, 1952, 1957 and 1960 tsunamis (Image from Walker, 2004).

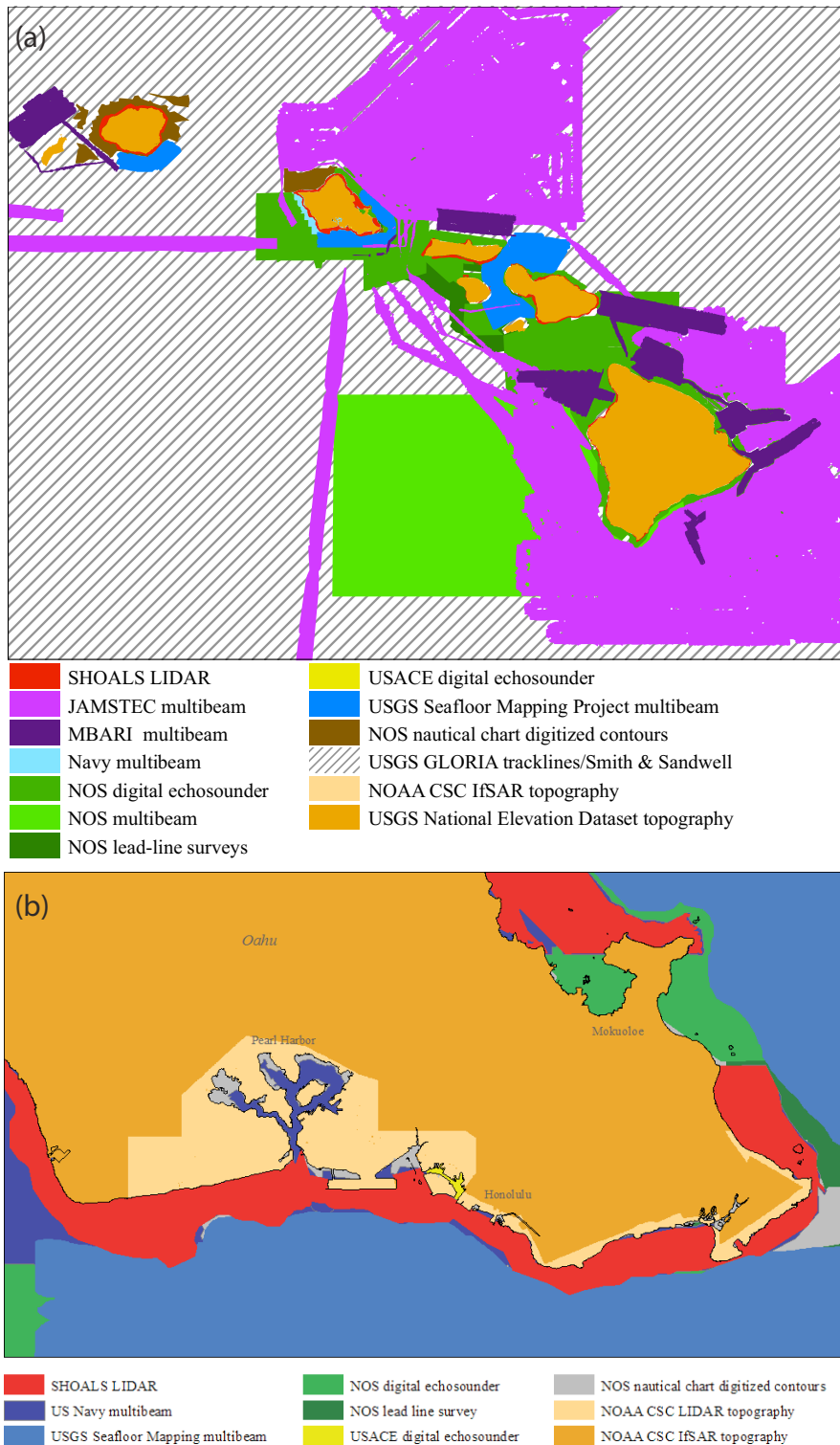


Figure 7 Bathymetric and topographic data source overview. (a) 6'' sec (~180m) Hawaii DEM ; (b) 1/3'' (~10m) DEM for south Oahu.

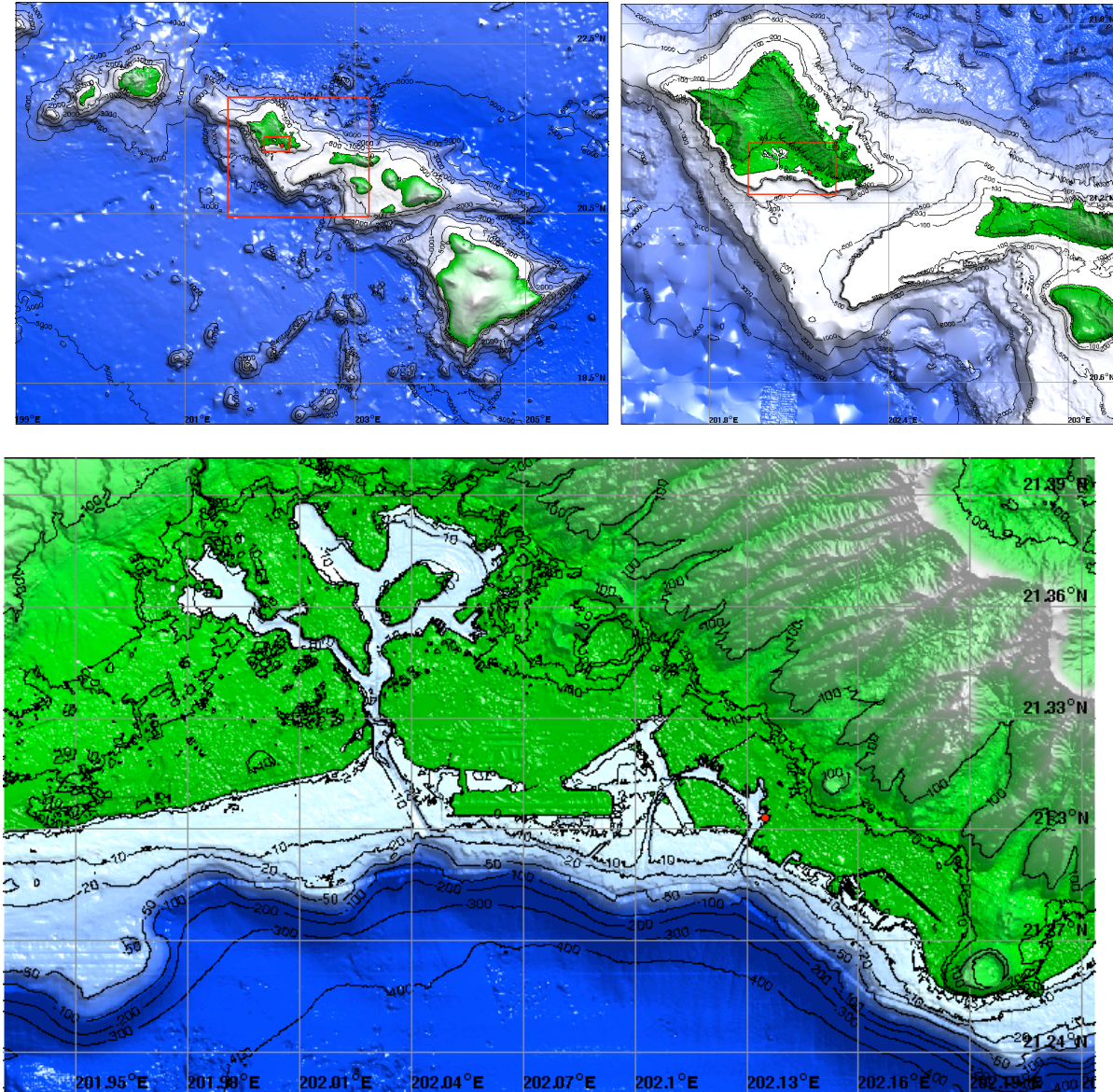


Figure 8 Grid setup for the Honolulu Reference model with resolution of (a) 36, (b) 6 and (c) 2/3 arc sec (20 m). •, Honolulu tide station.

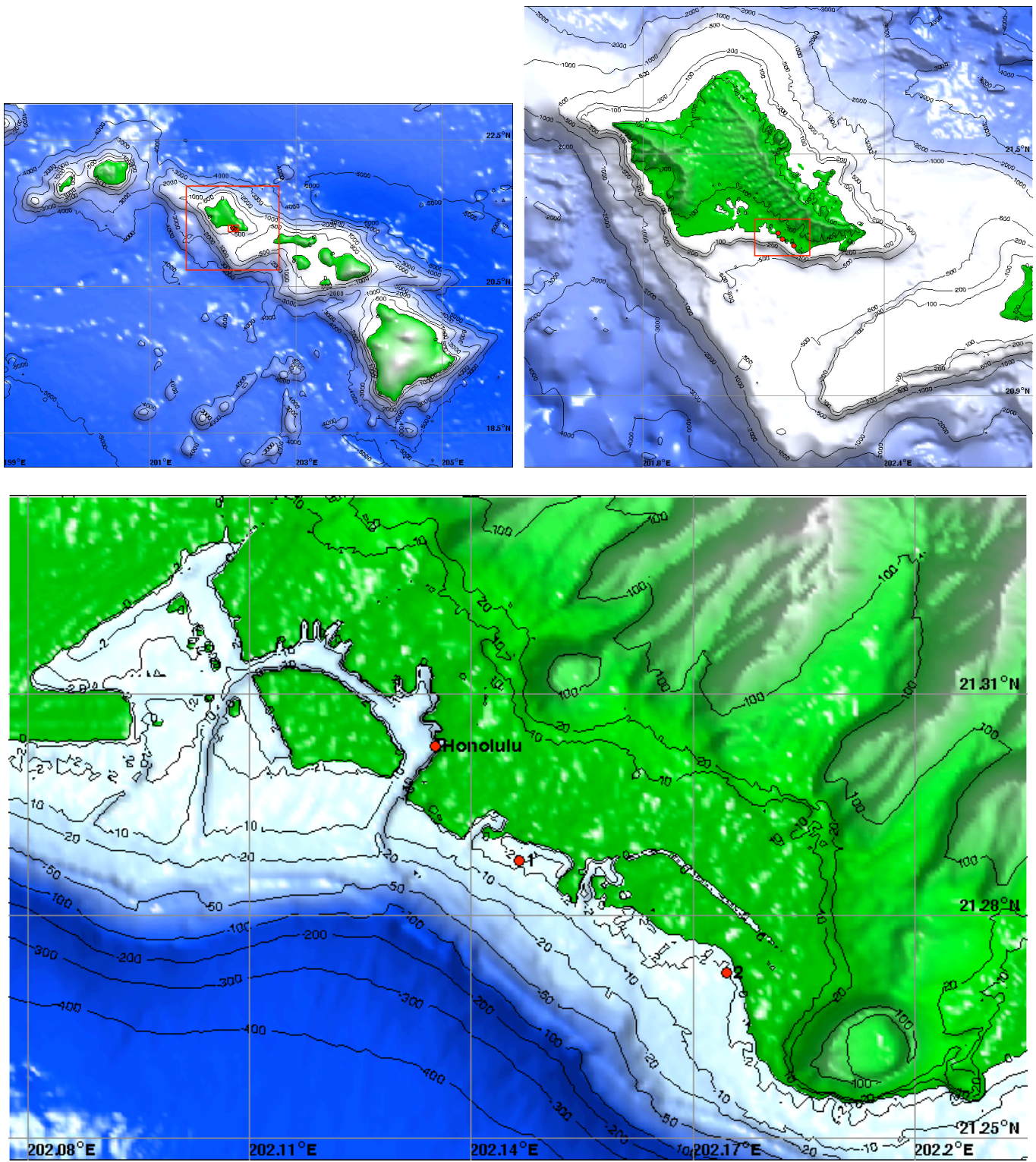
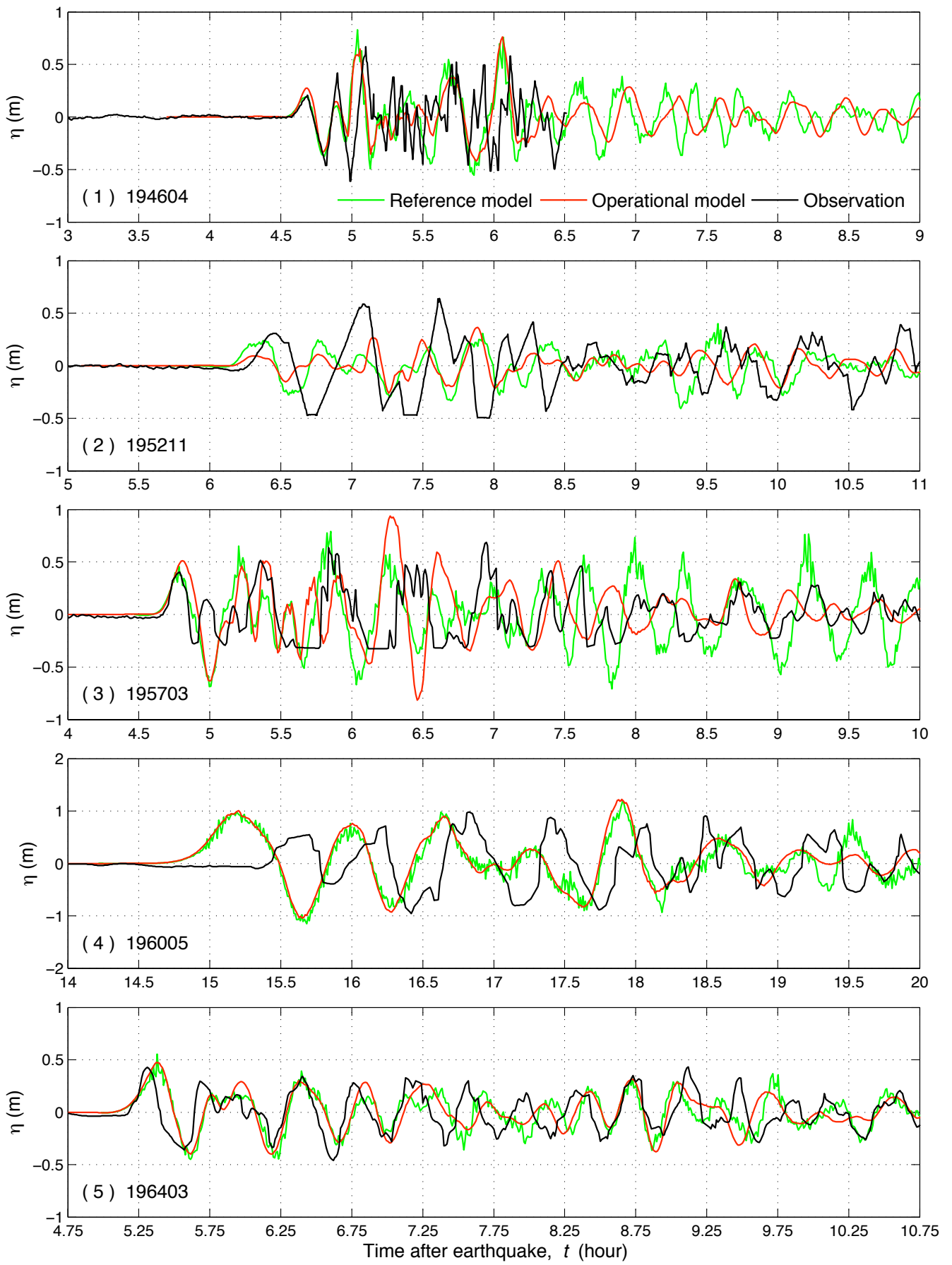
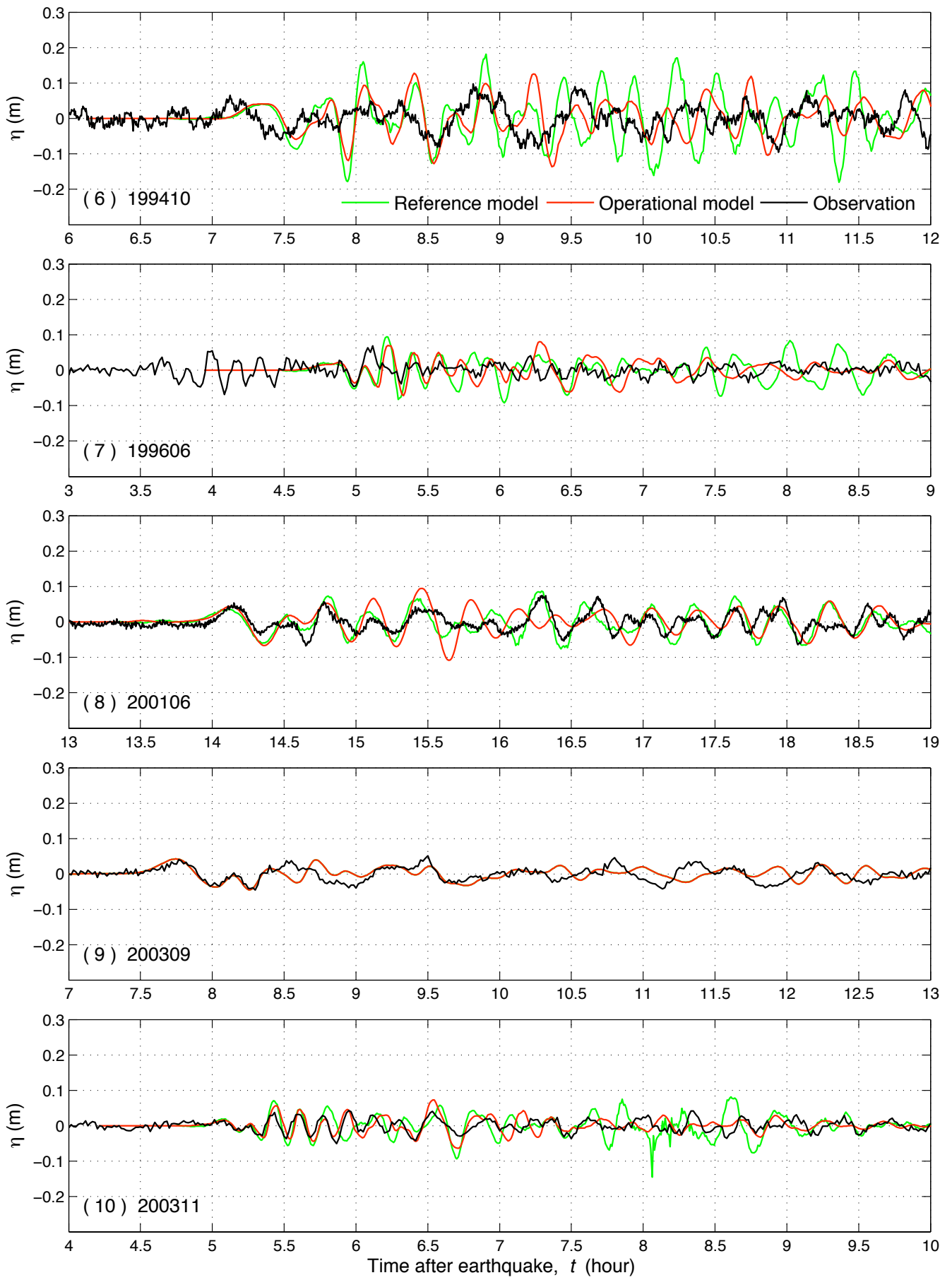
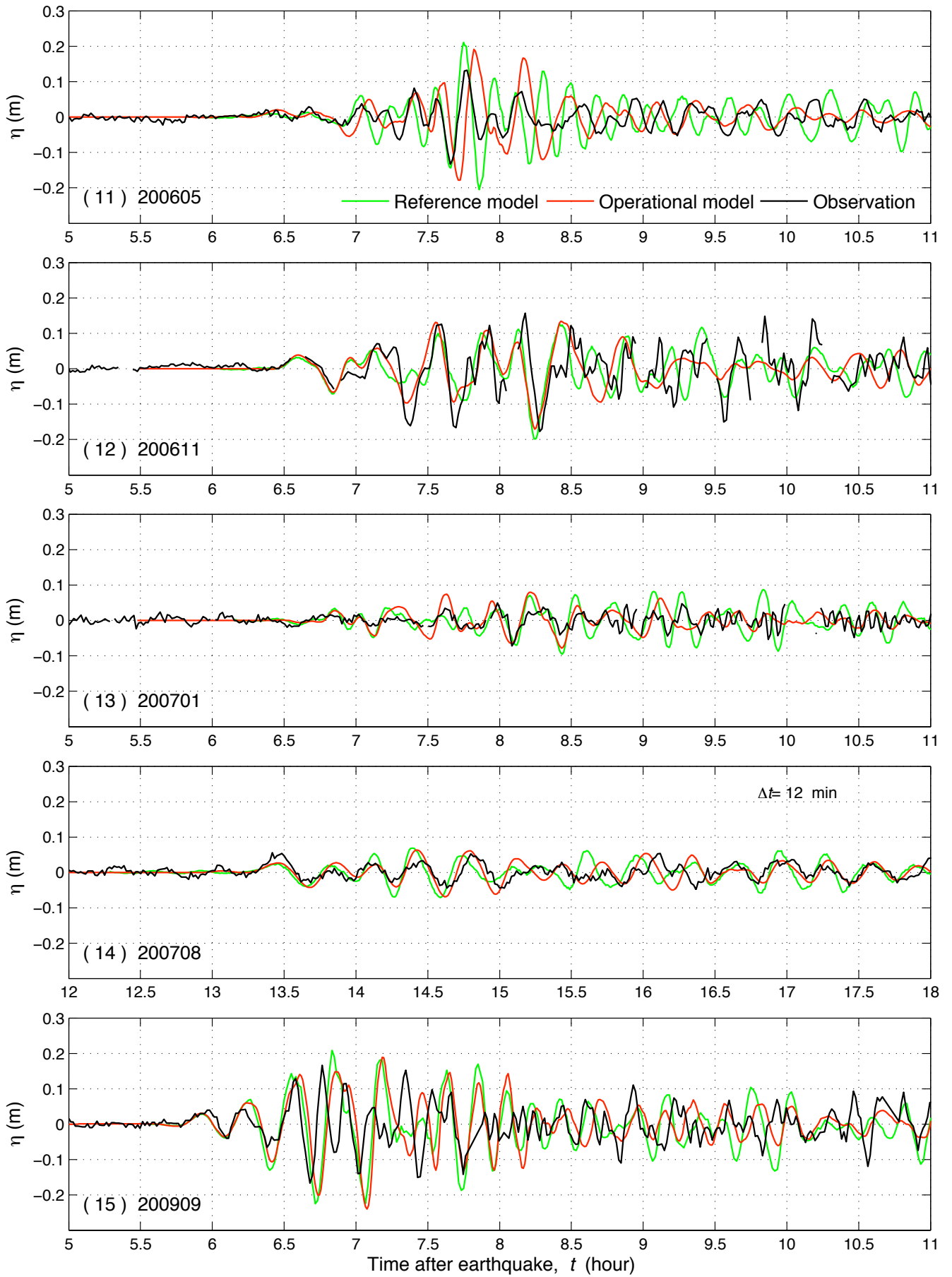


Figure 9 Grid setup for the Honolulu forecast model with resolution of (a) 120, (b) 18 and (c) 2 arc sec.
 ●, Honolulu tide station







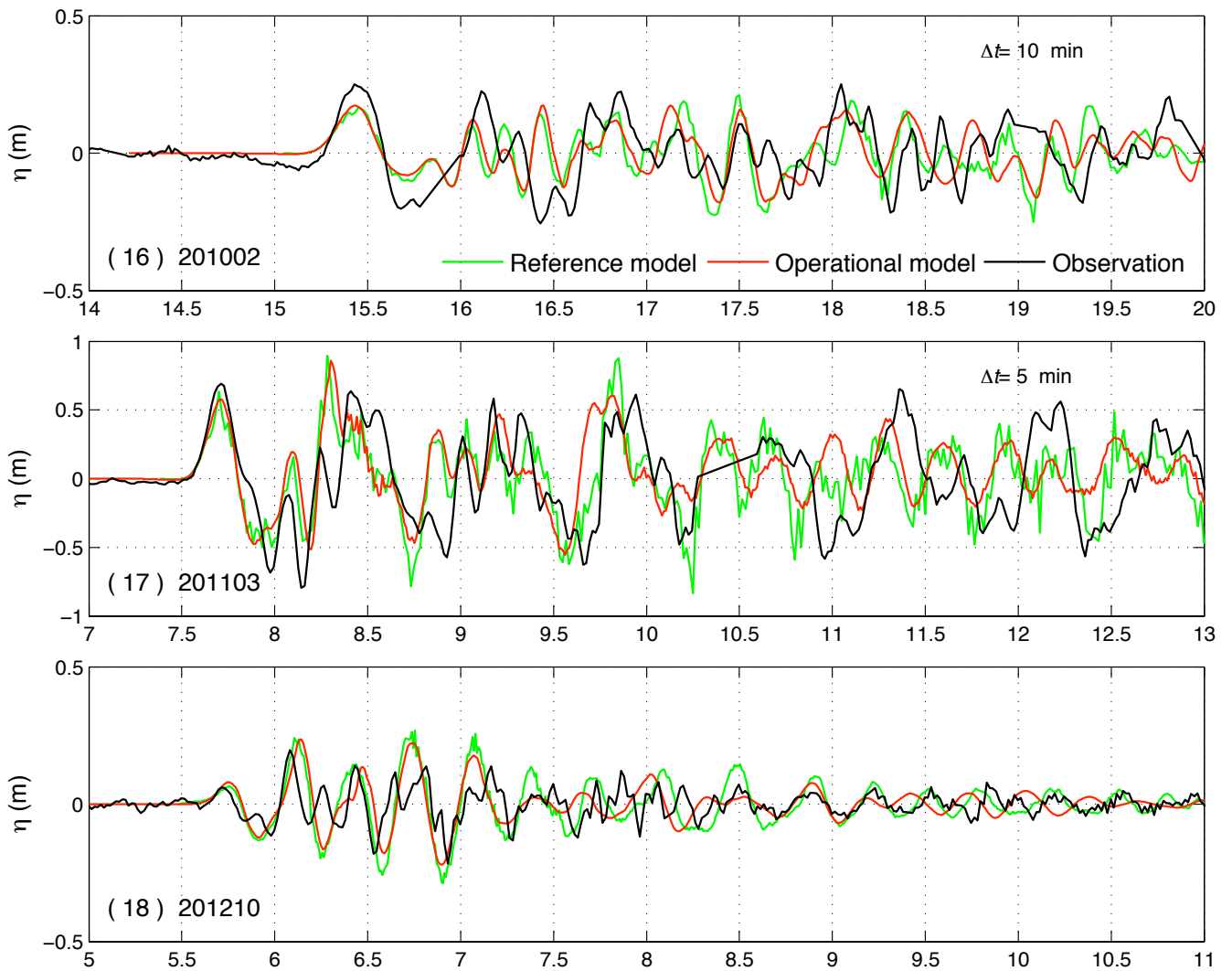
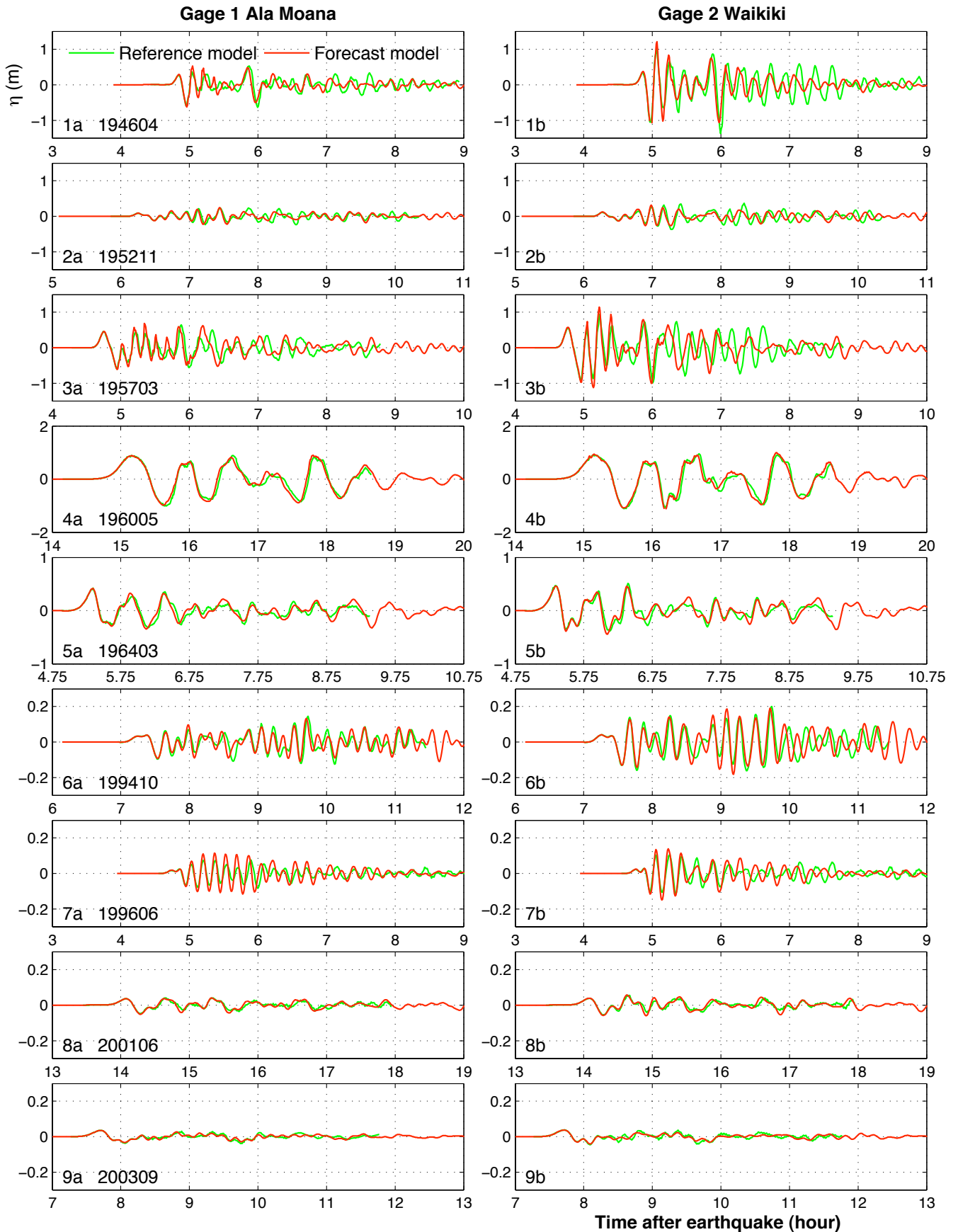


Figure 10 Tsunami time-series of observed and modeled amplitudes for past tsunamis. The green and red lines were computed by the Honolulu reference and forecast models respectively. The model time series were shifted Δt min behind.



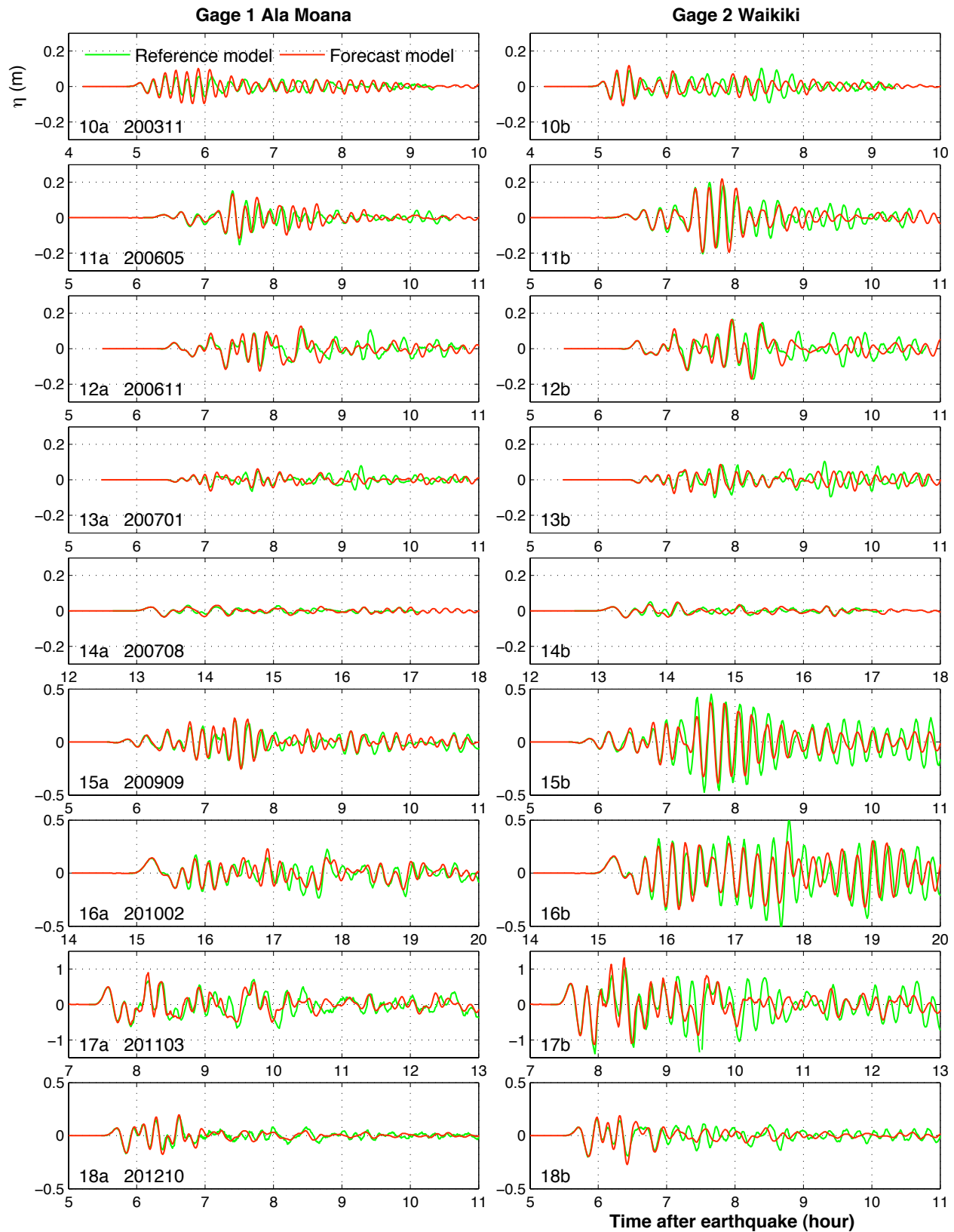
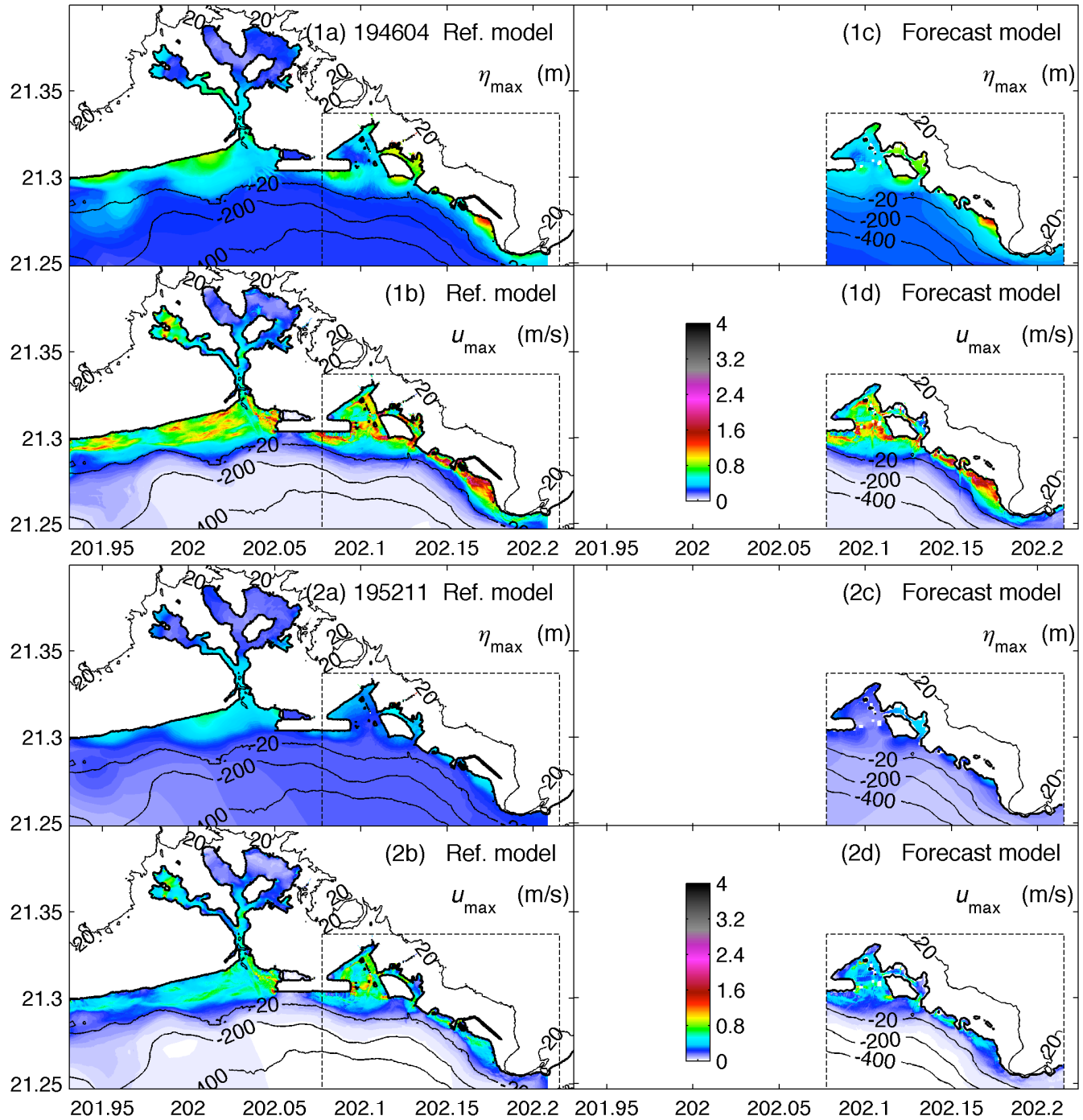
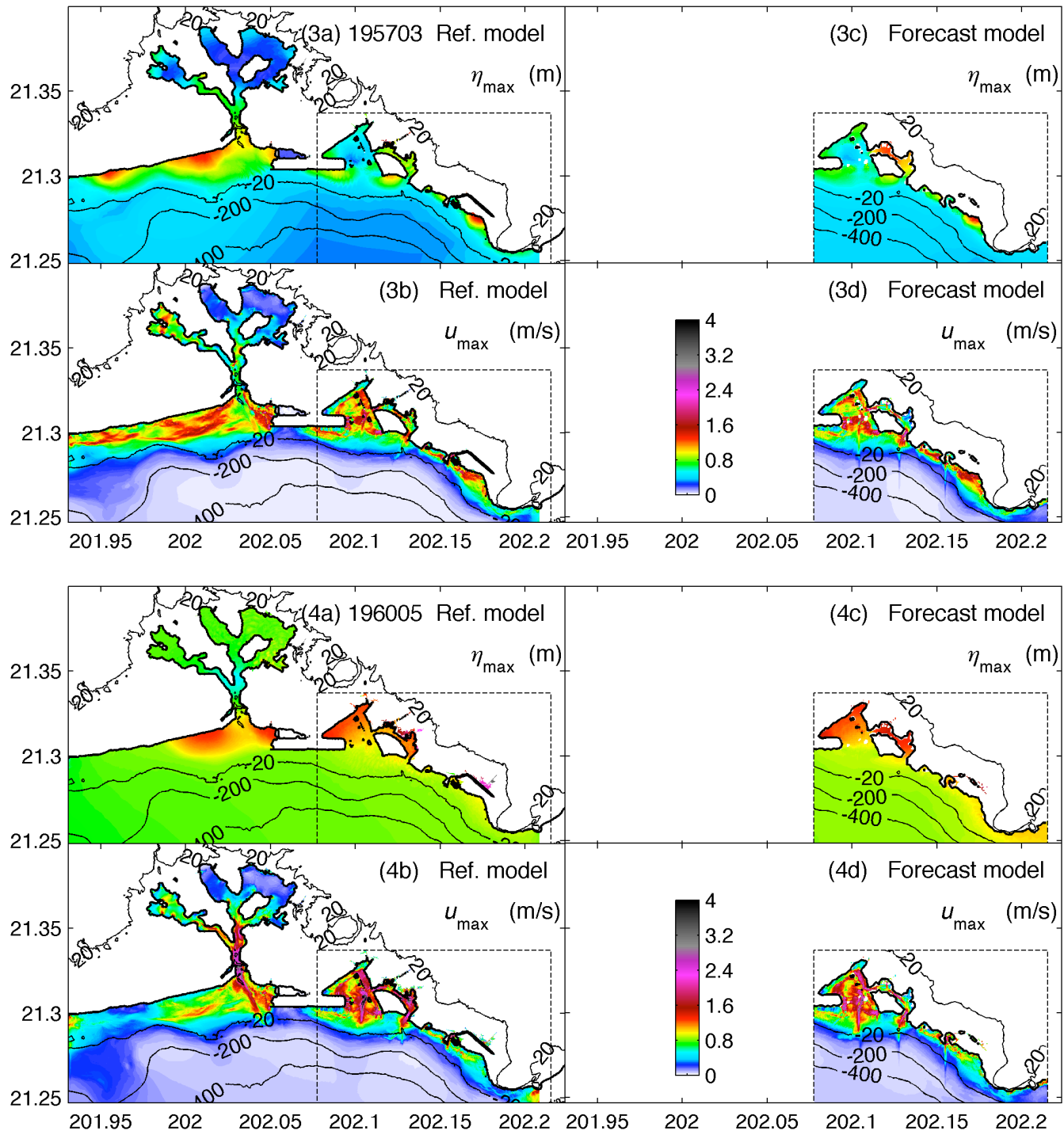
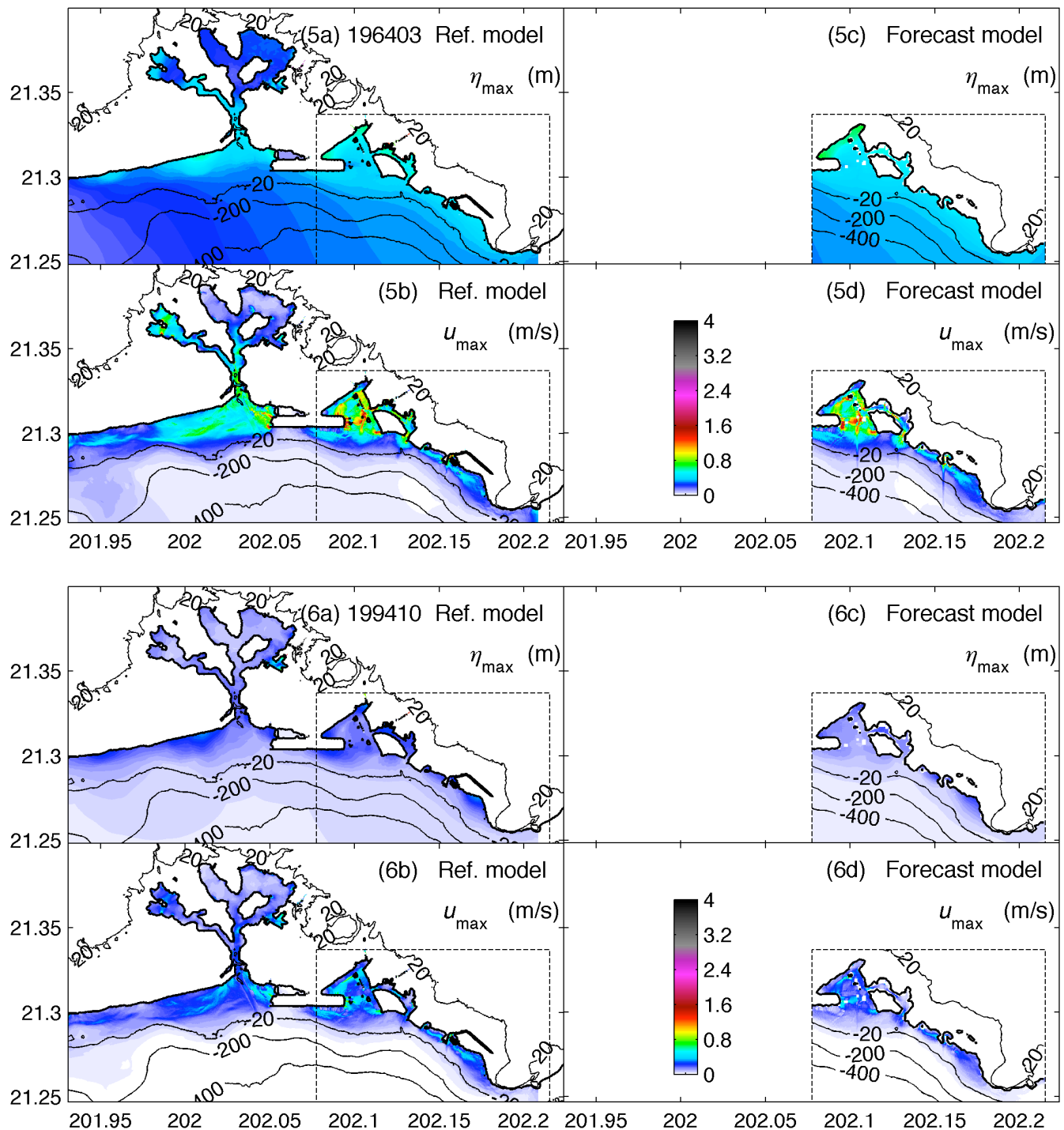
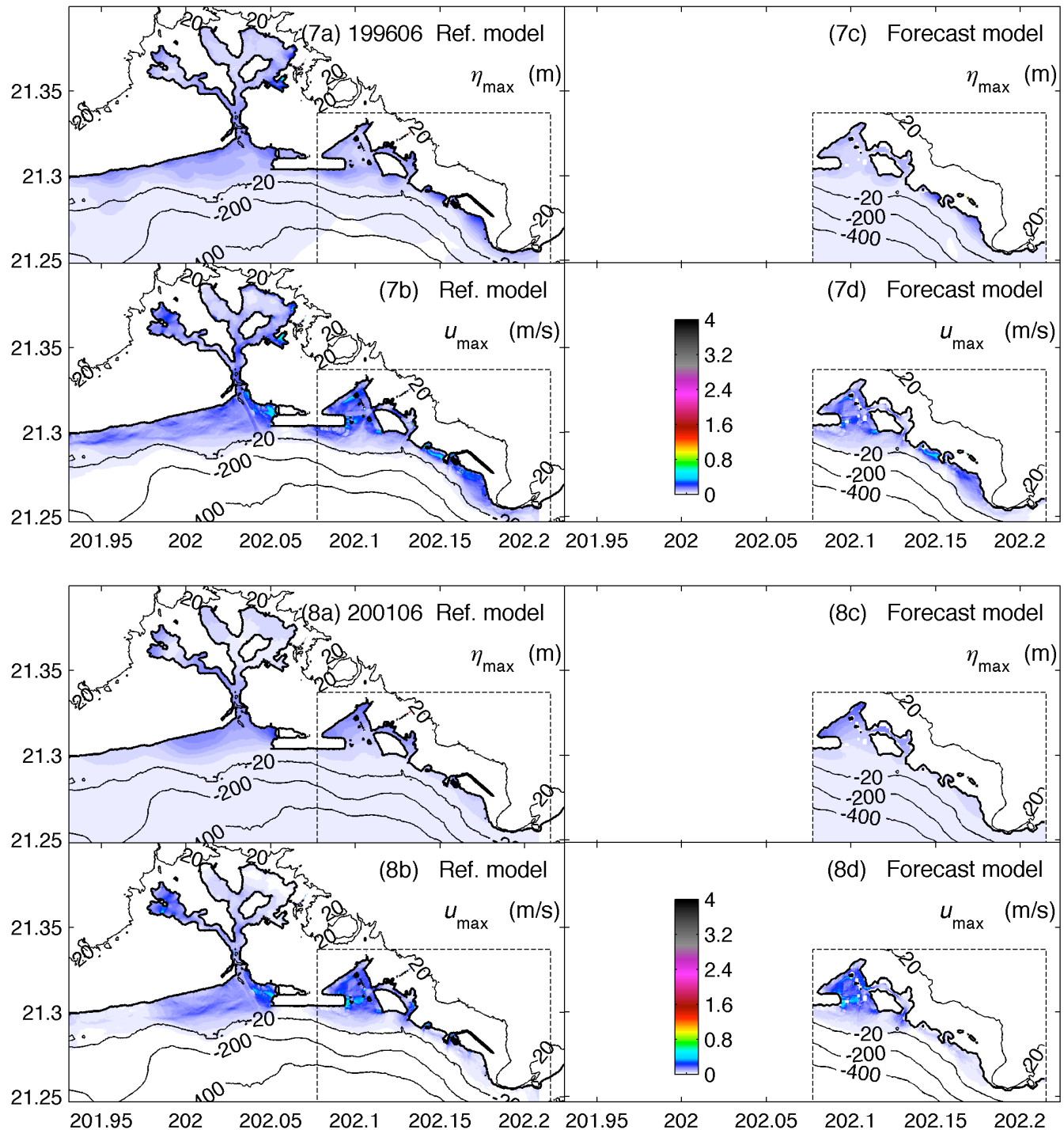


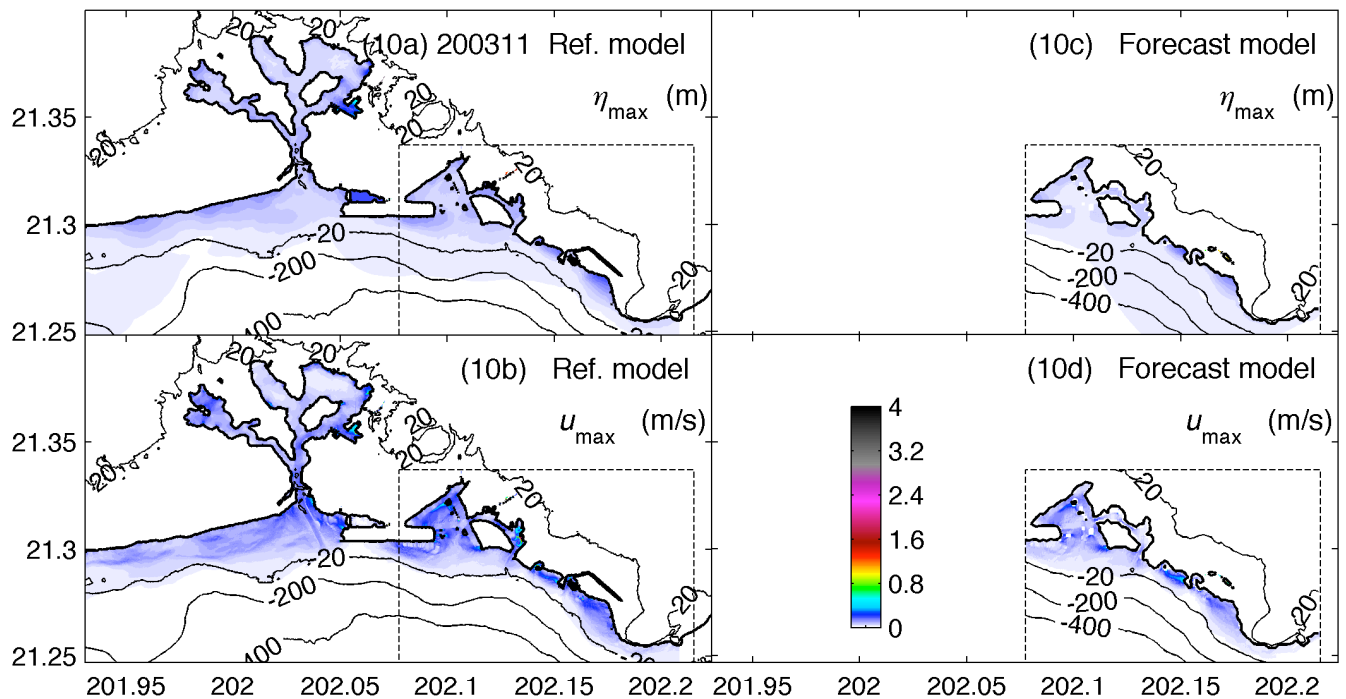
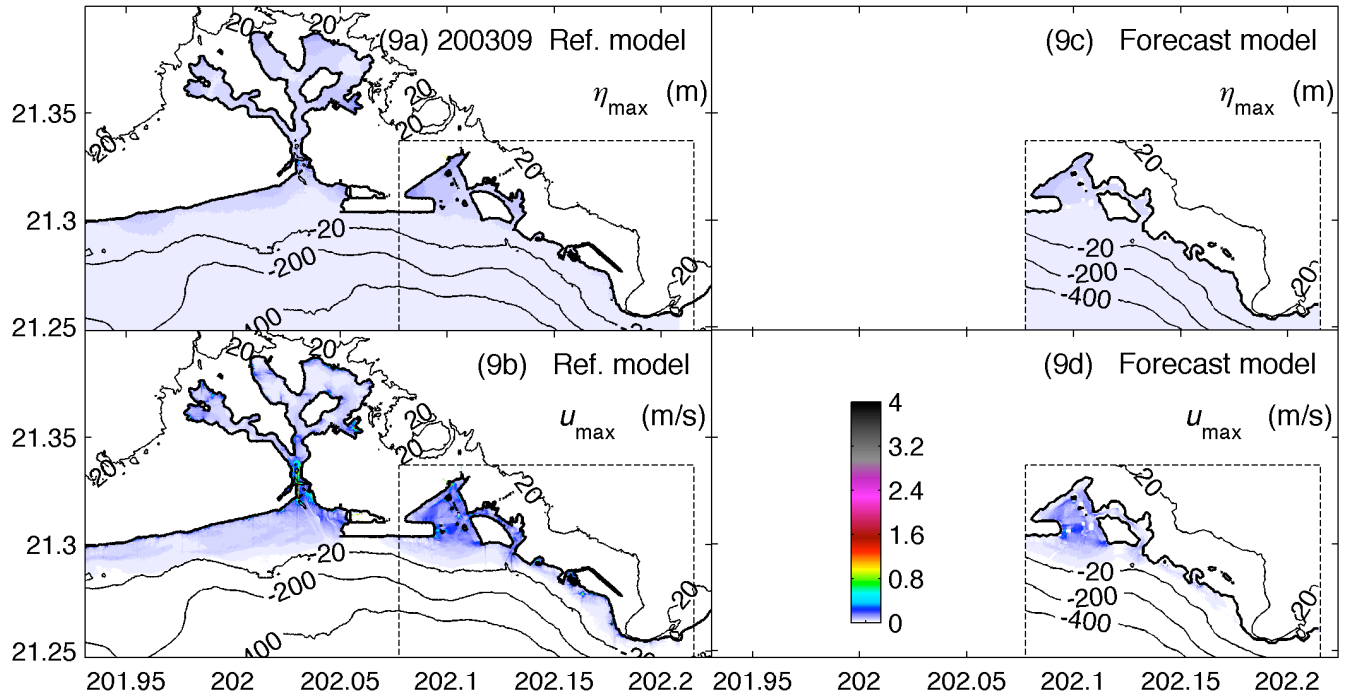
Figure 11 Tsunami time-series of modeled amplitudes at two virtual gages at 2 m water depth for past tsunamis. (a) Gage 1 locates at Ala Moana and (b) Gage 2 is at Waikiki.

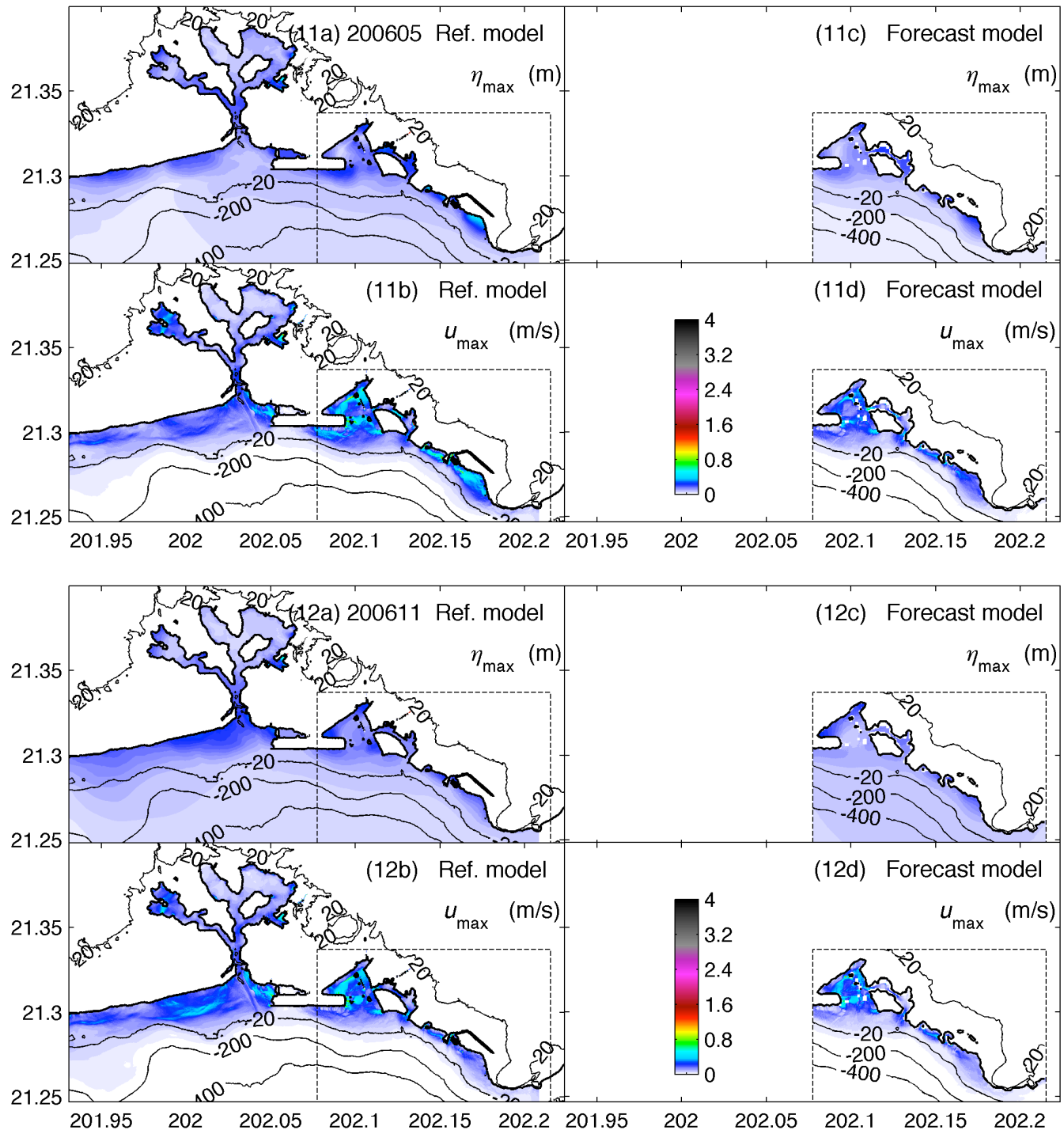


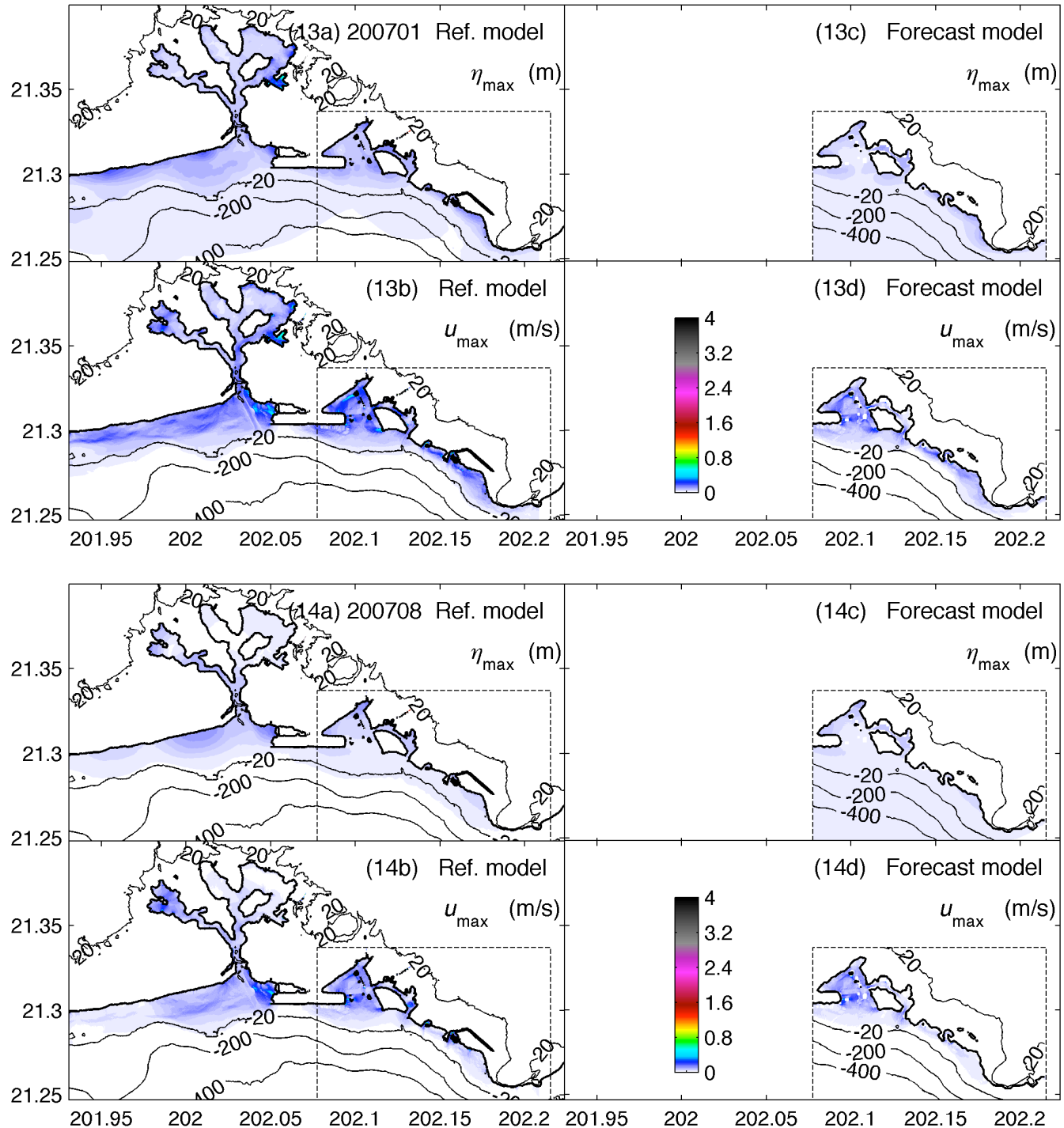


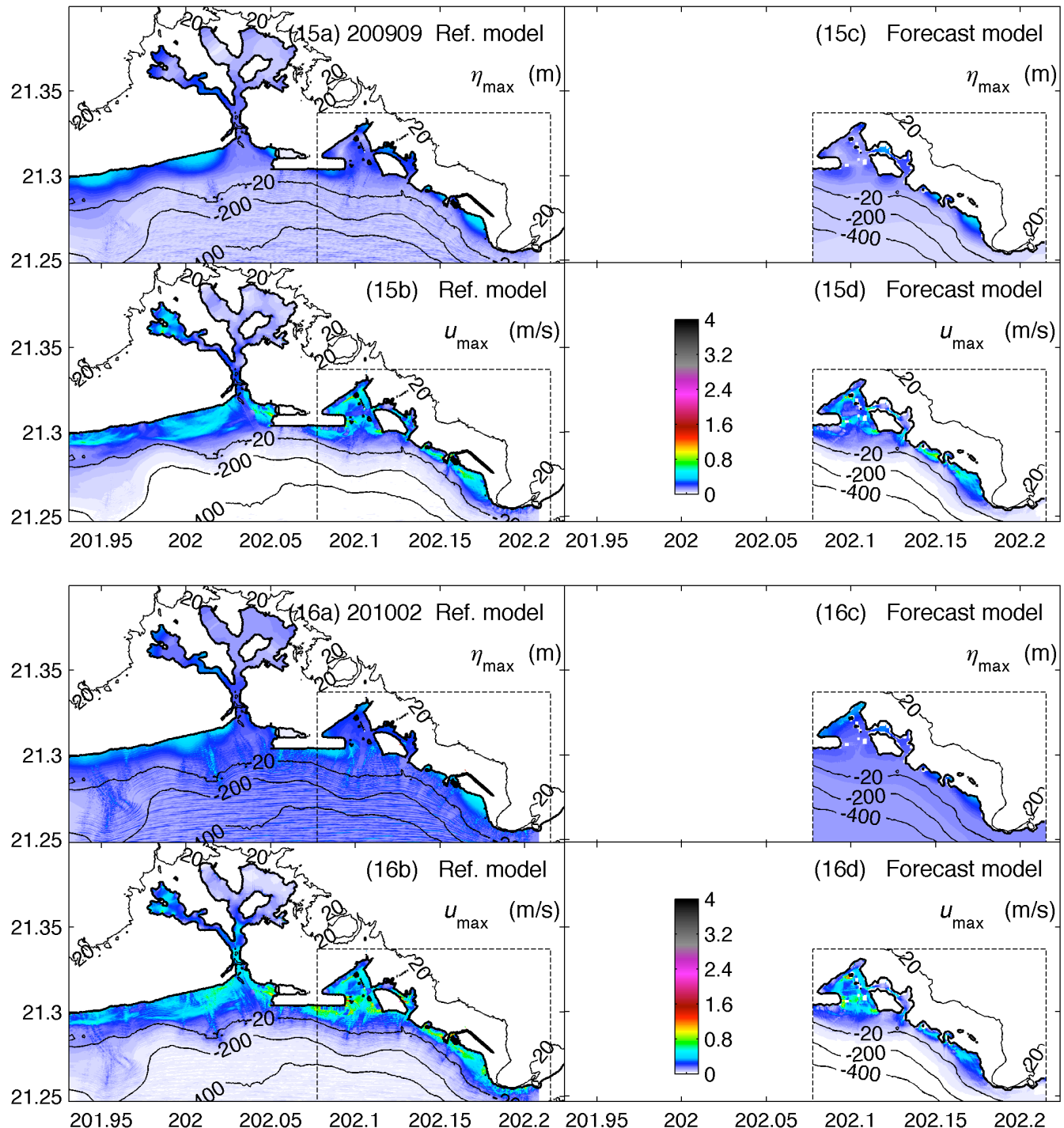












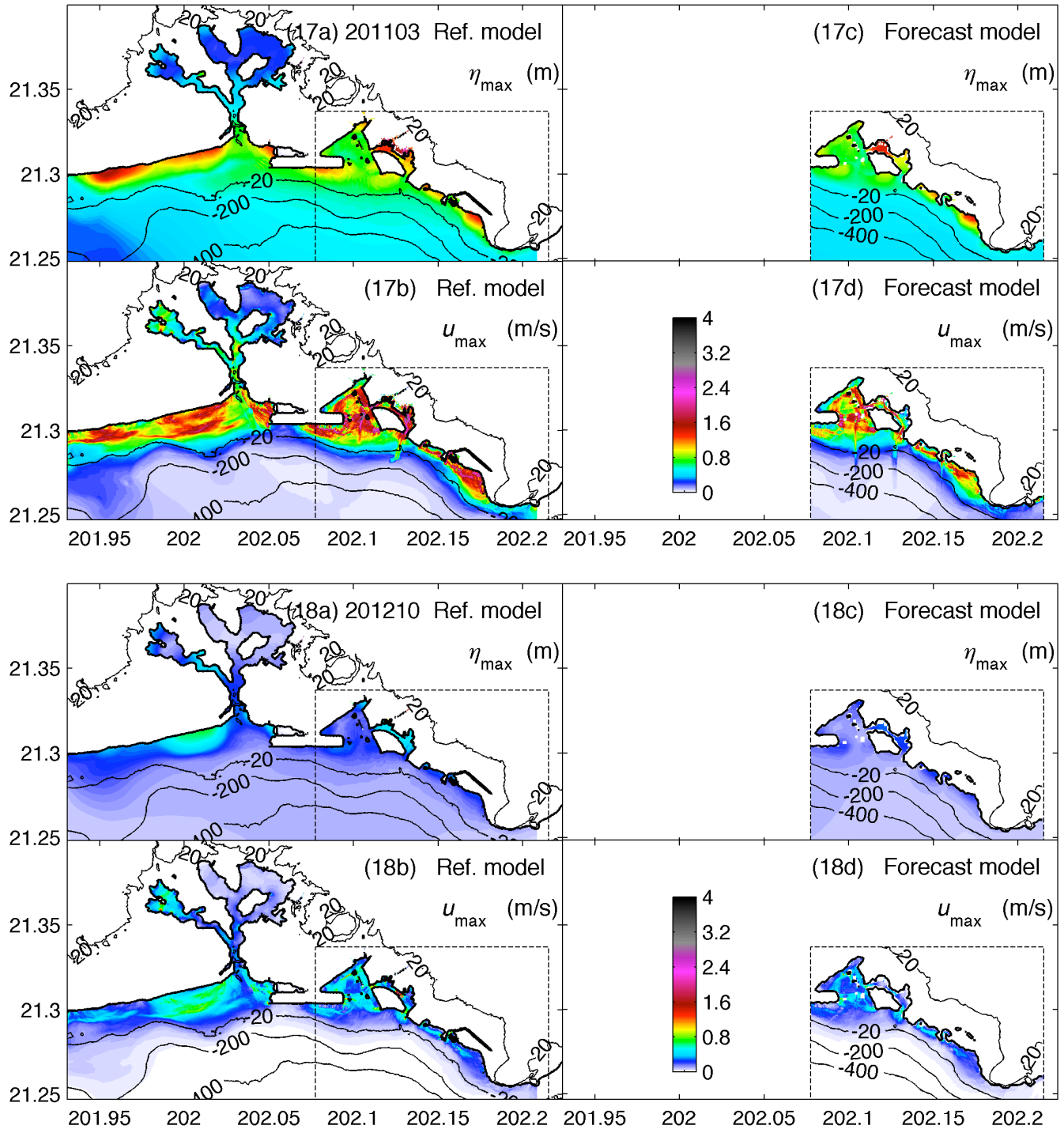
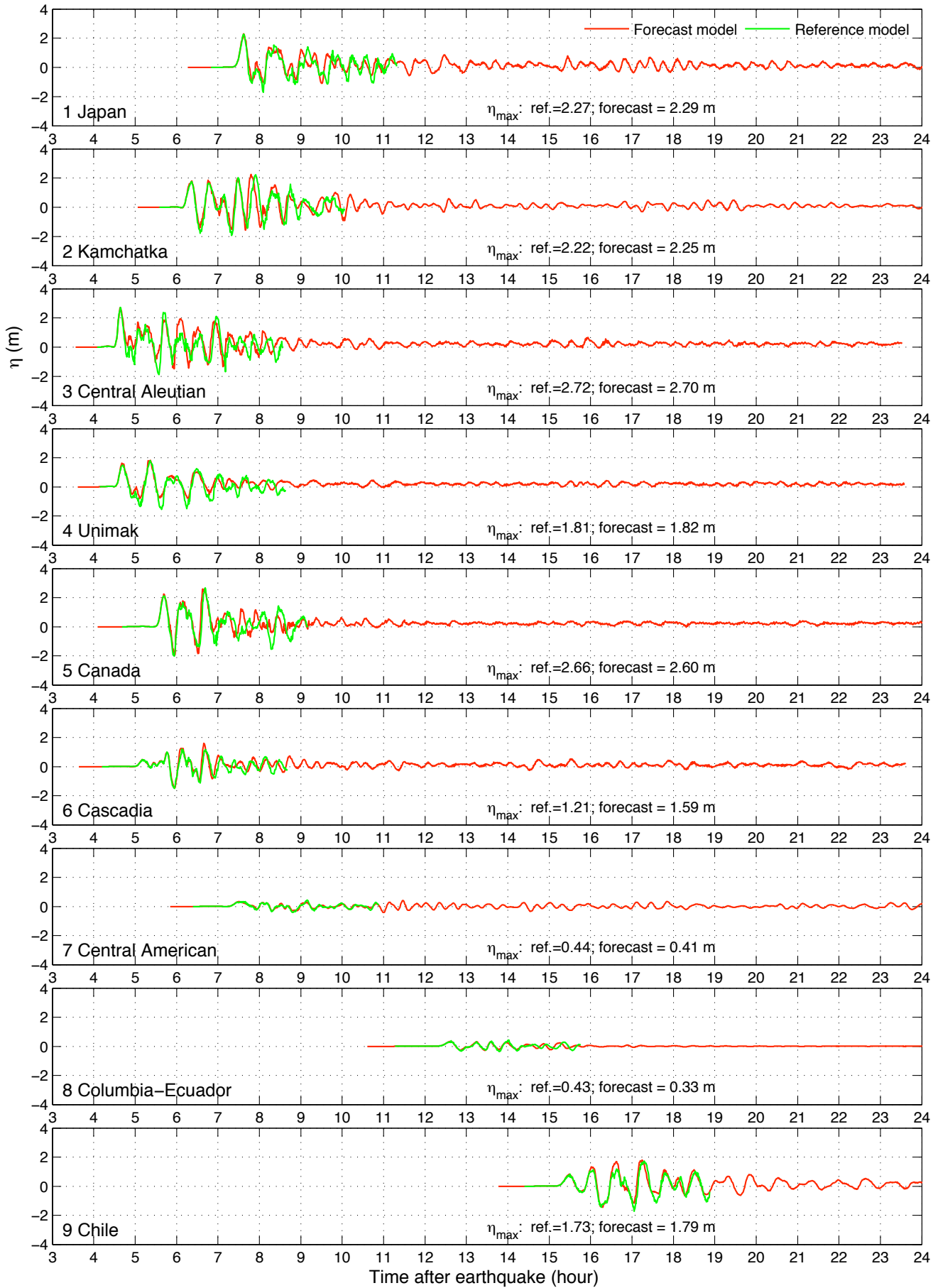


Figure 12 Maximum water elevation and current computed by the Honolulu reference and forecast models for past tsunamis.



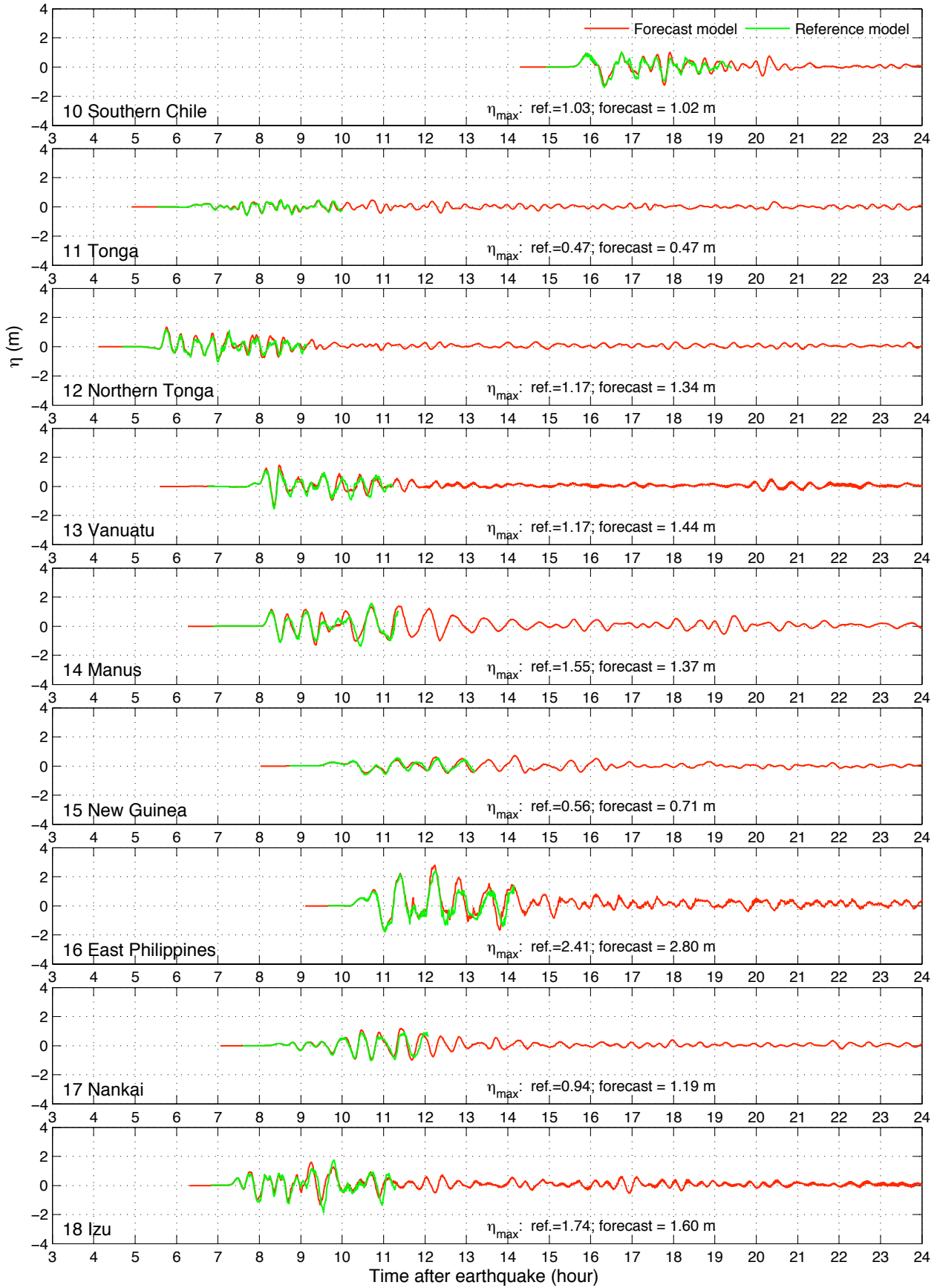
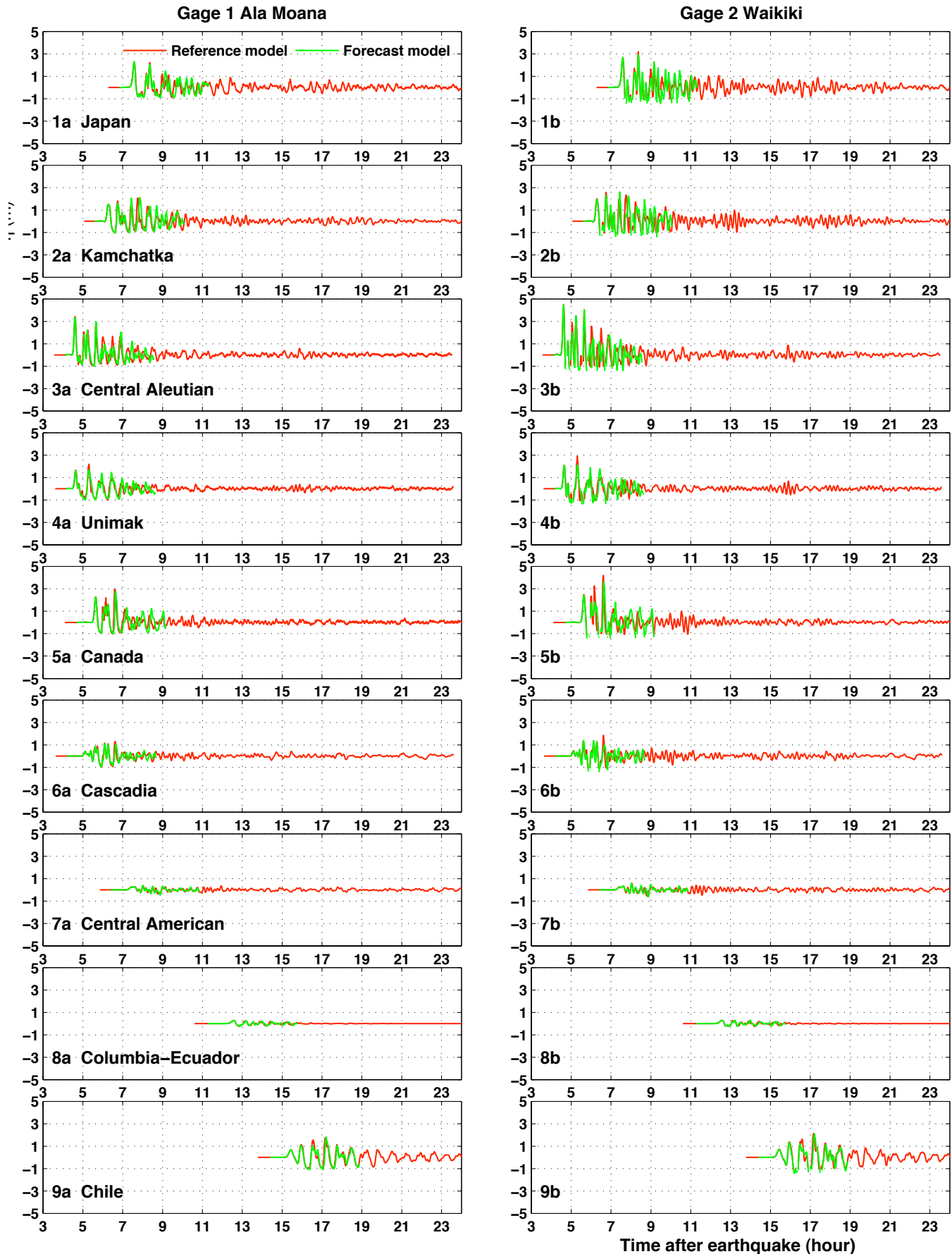


Figure 13 Modeled tsunami time-series for simulated magnitude 9.3 tsunamis.



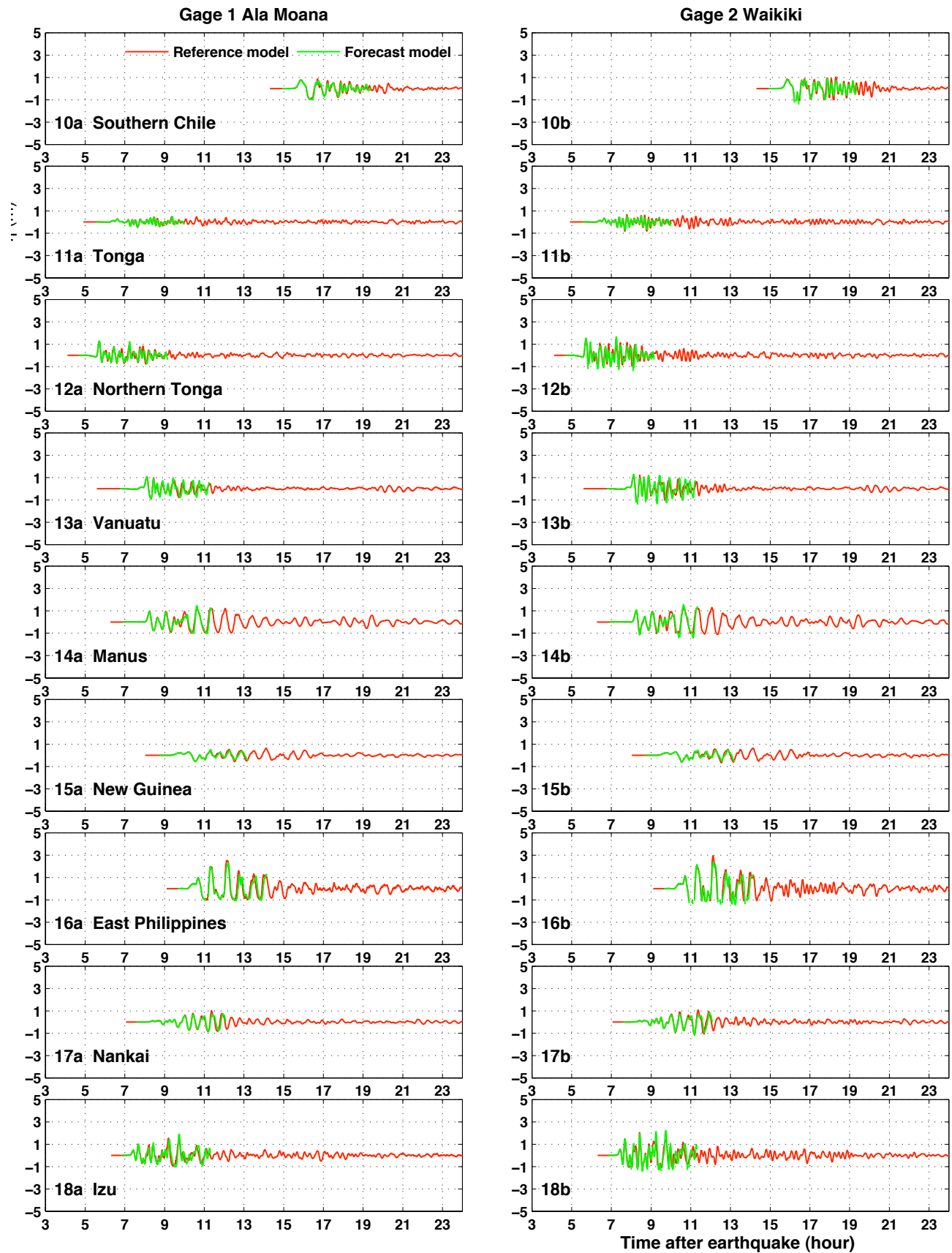
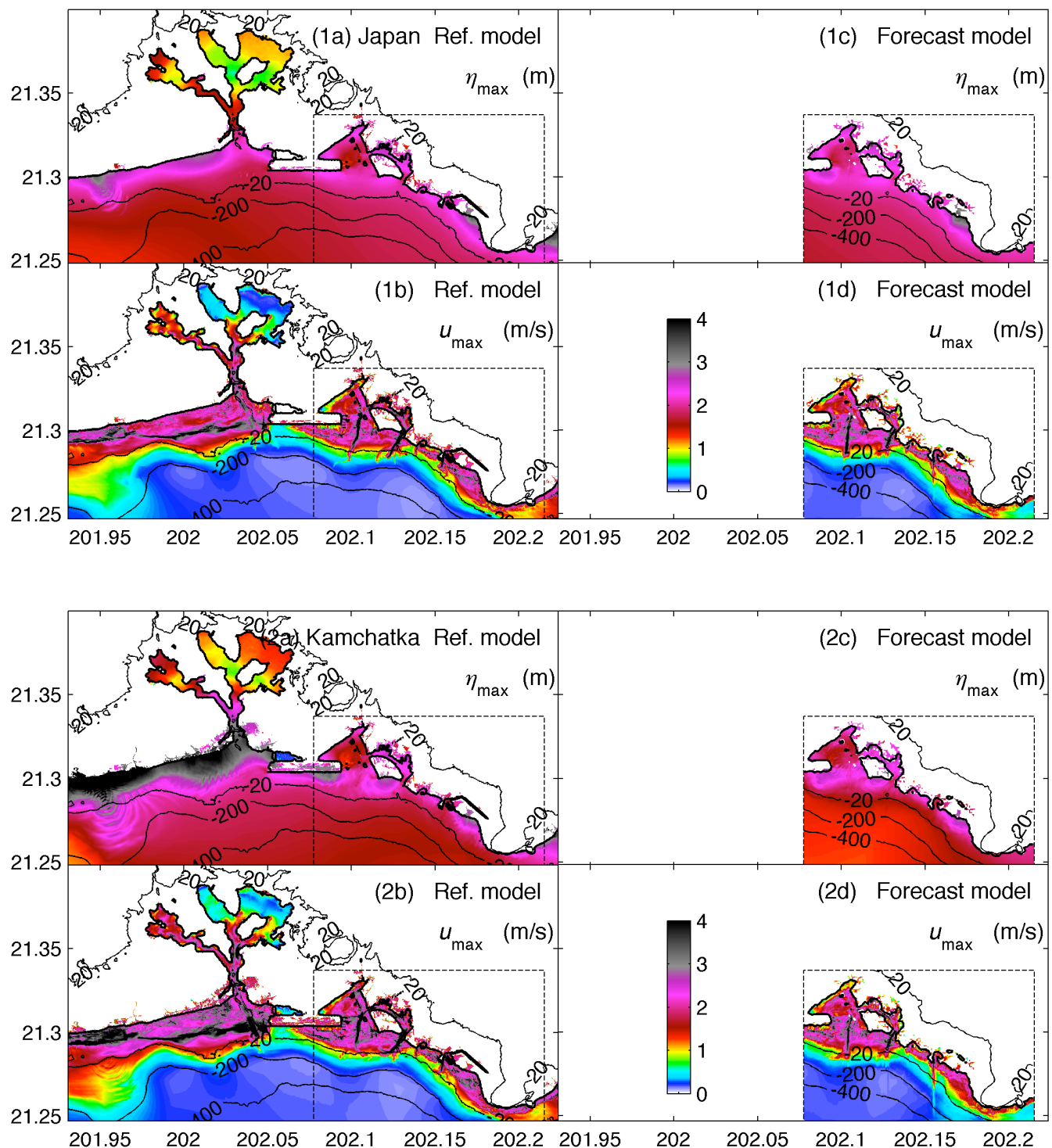
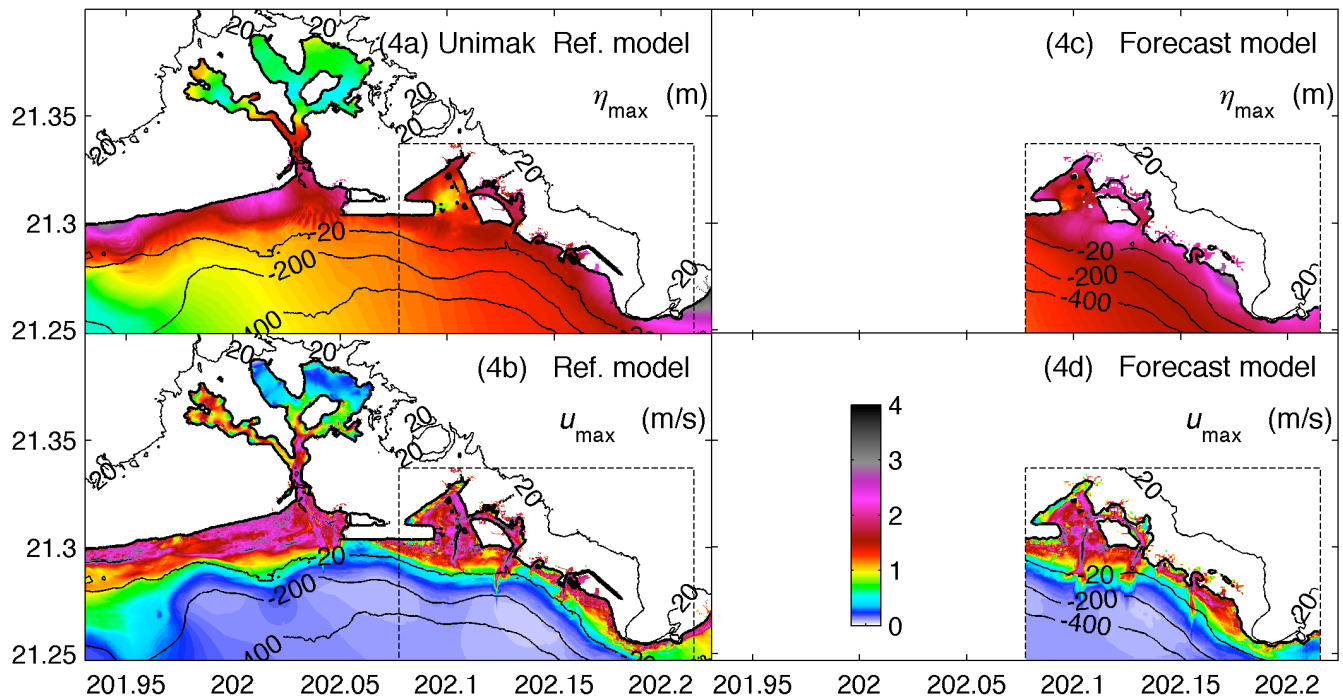
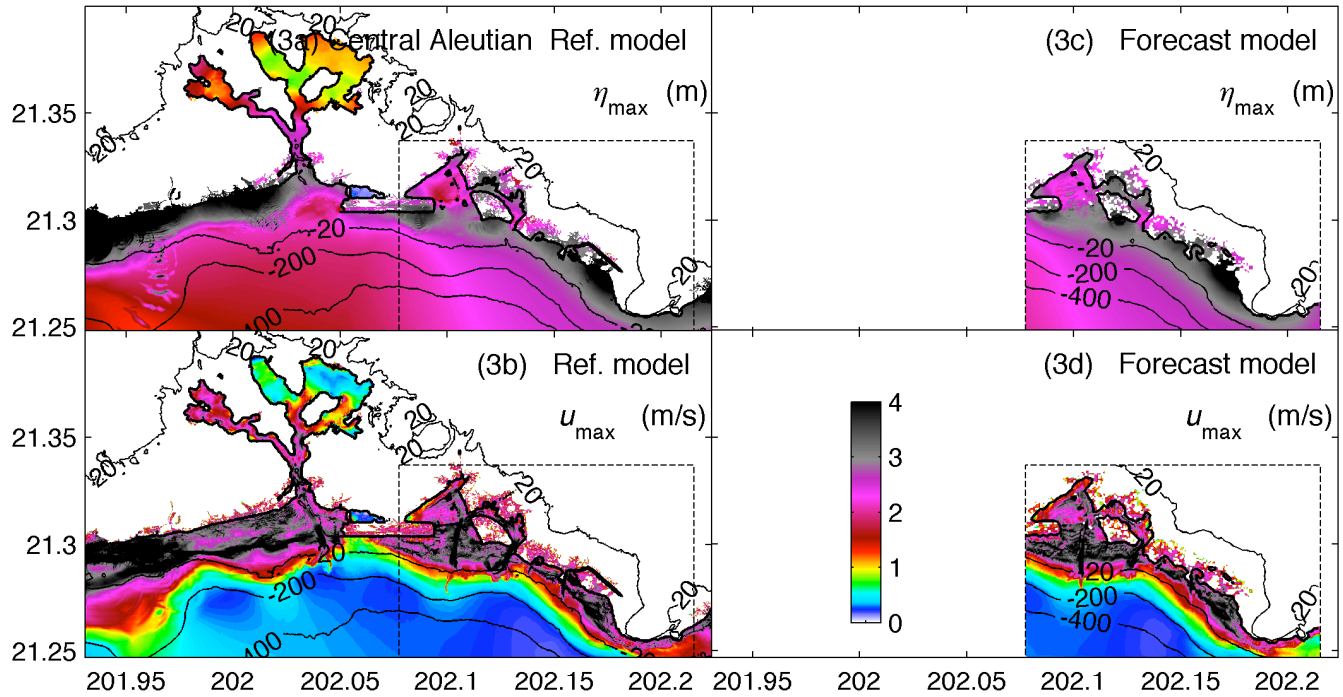
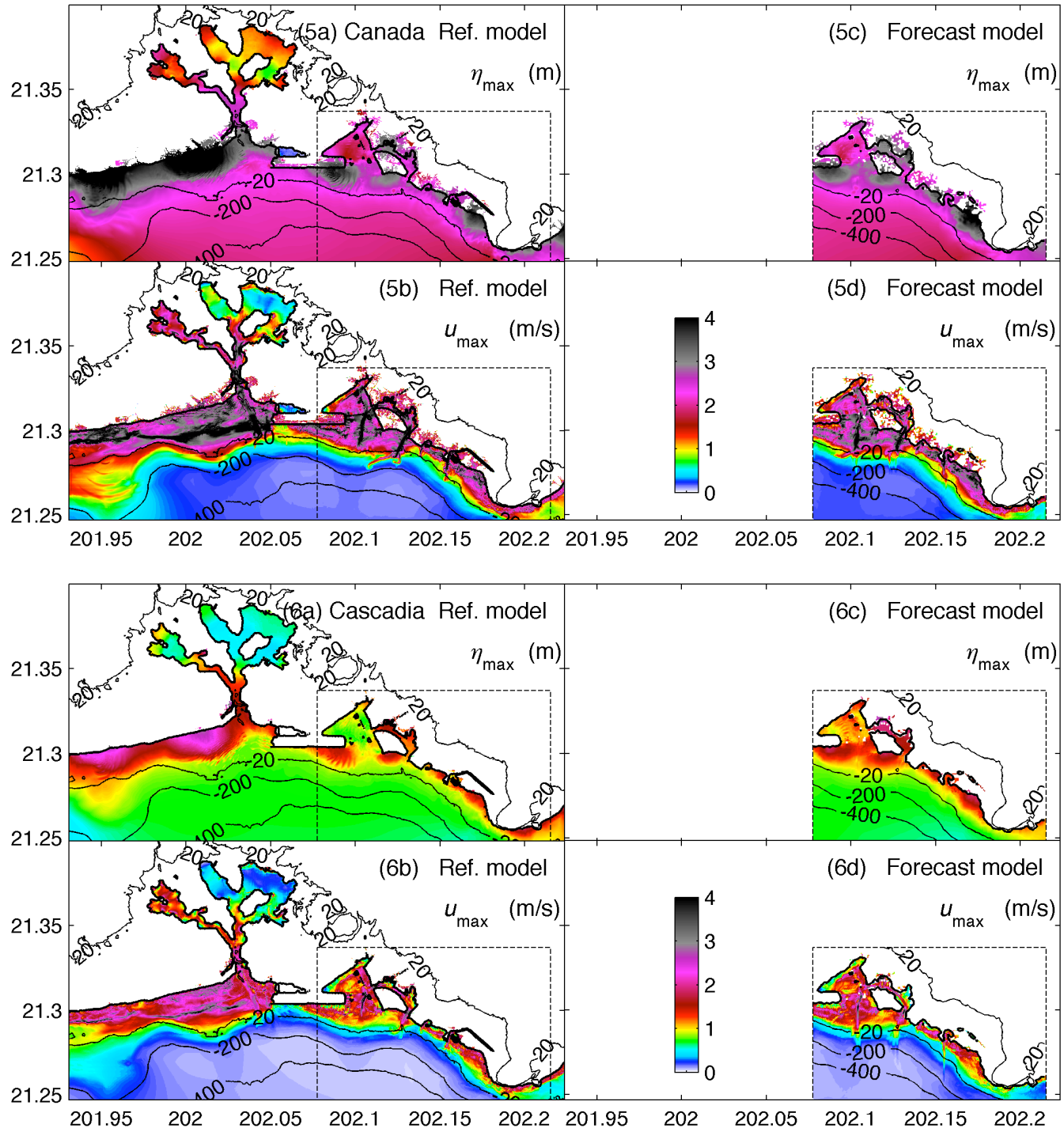
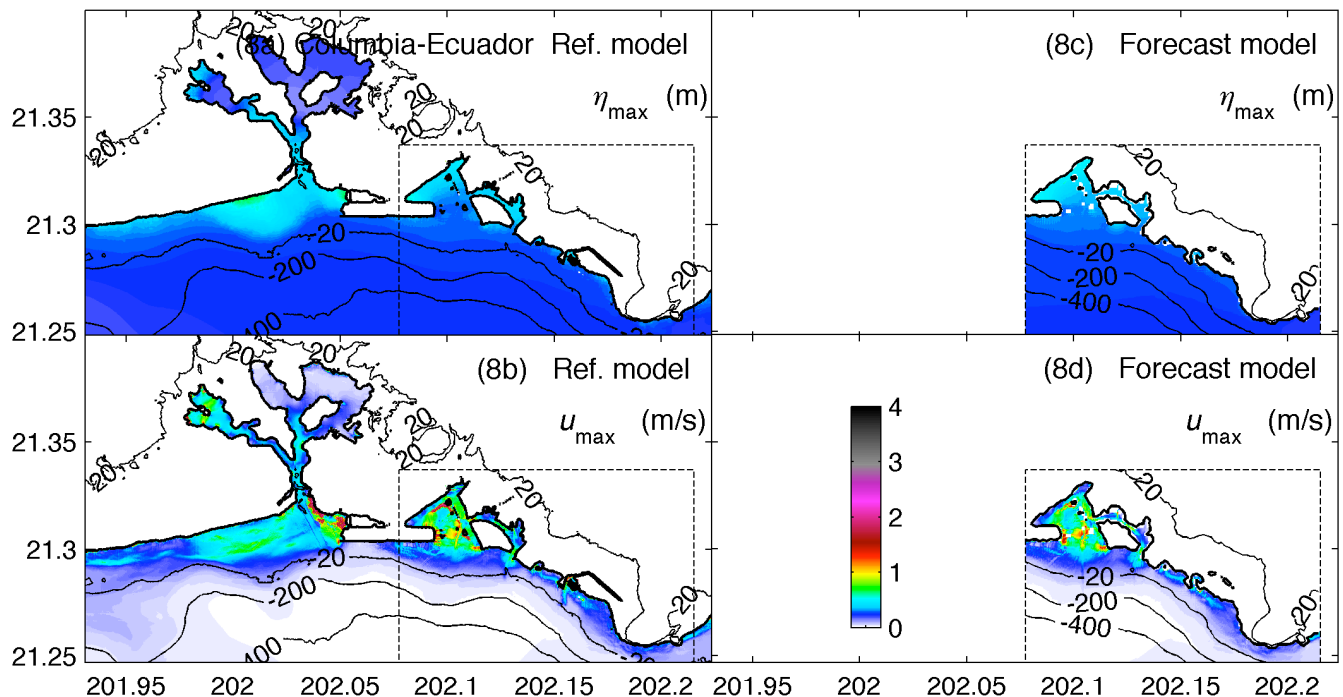
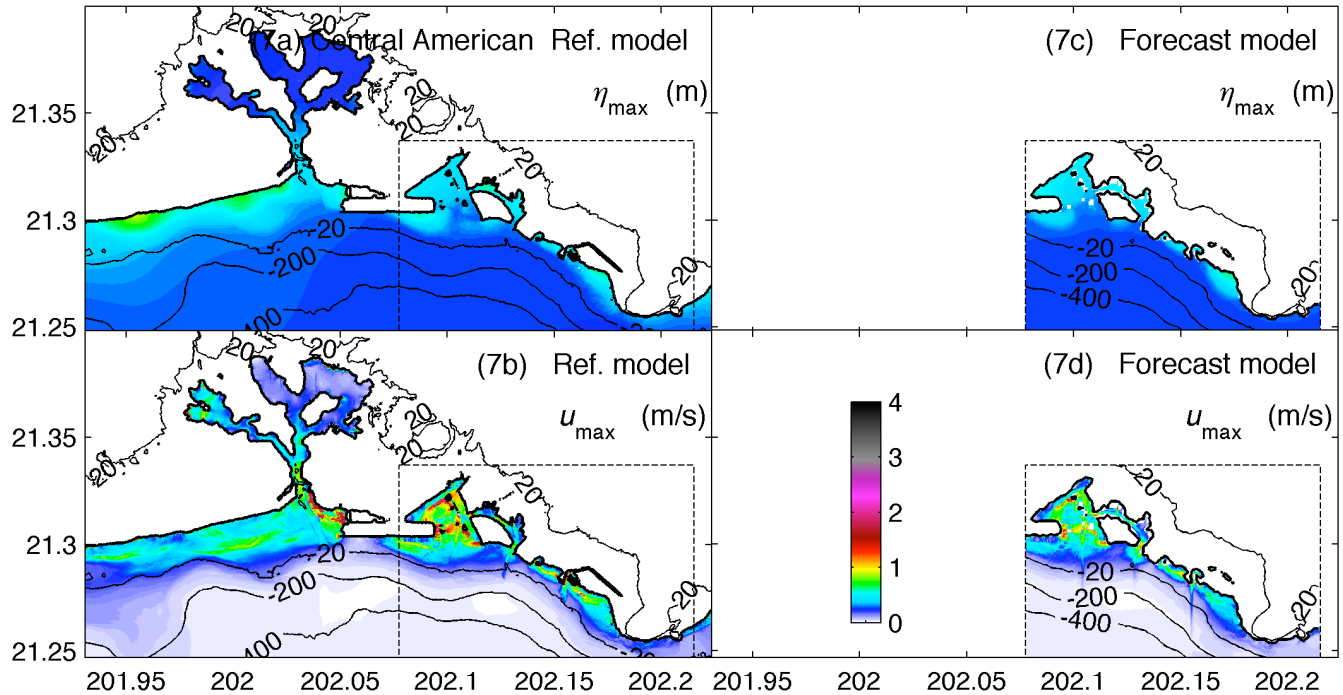


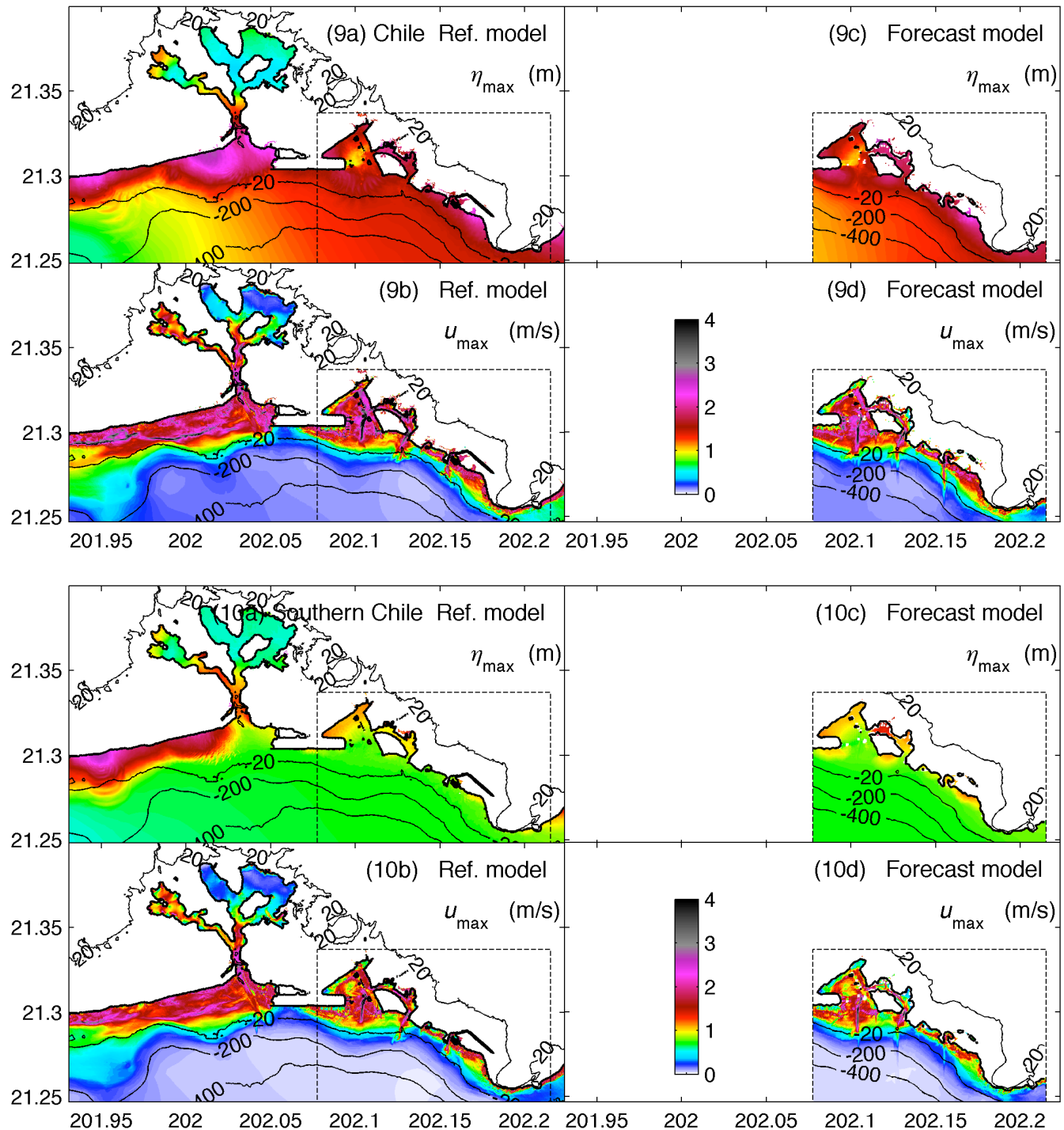
Figure 14 Tsunami time-series of modeled amplitudes at two virtual gages at 2 m water depth for 18 simulated magnitude 9.3 tsunamis. (a) Gage 1 locates at Ala Moana and (b) Gage 2 is at Waikiki.

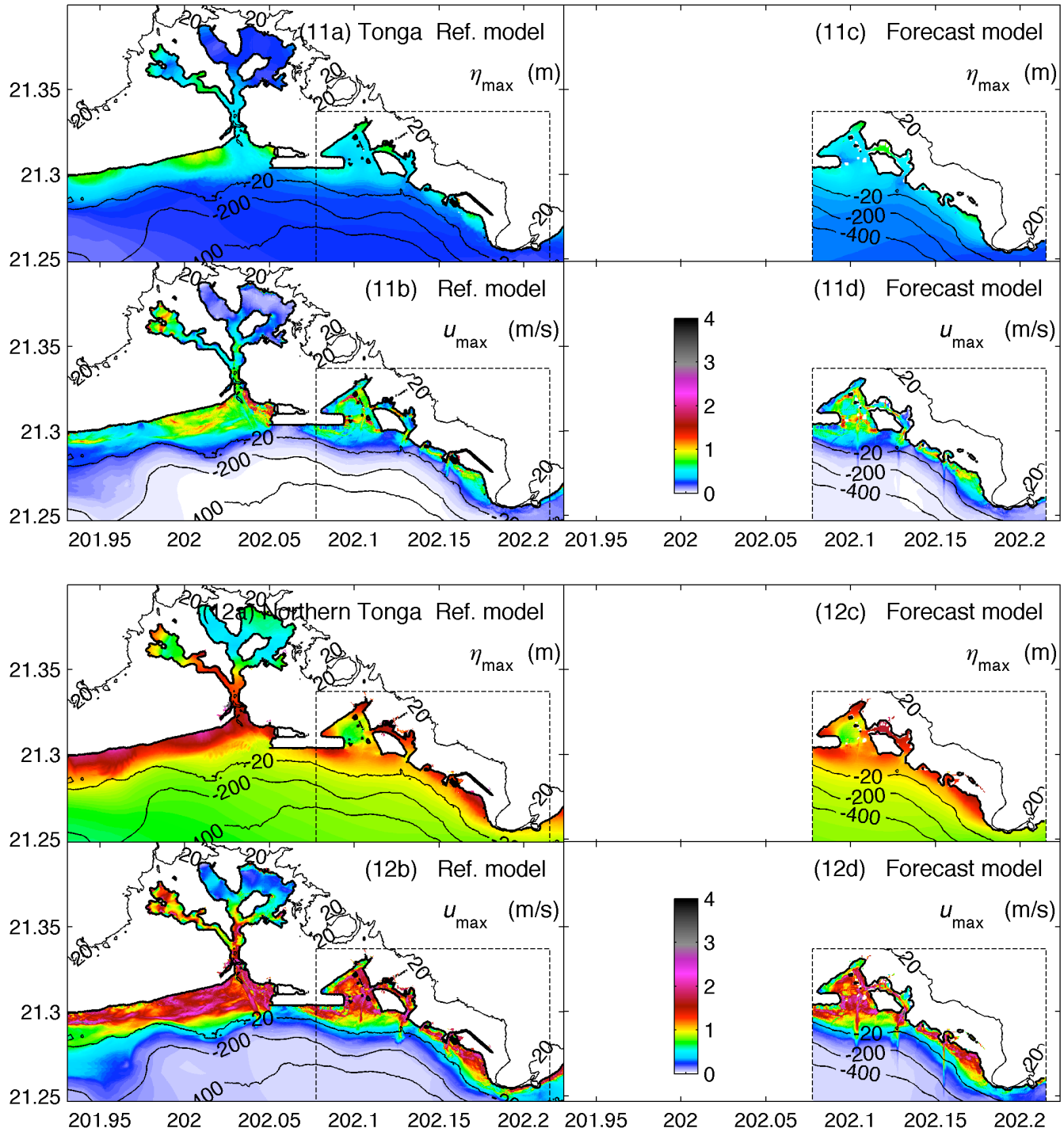


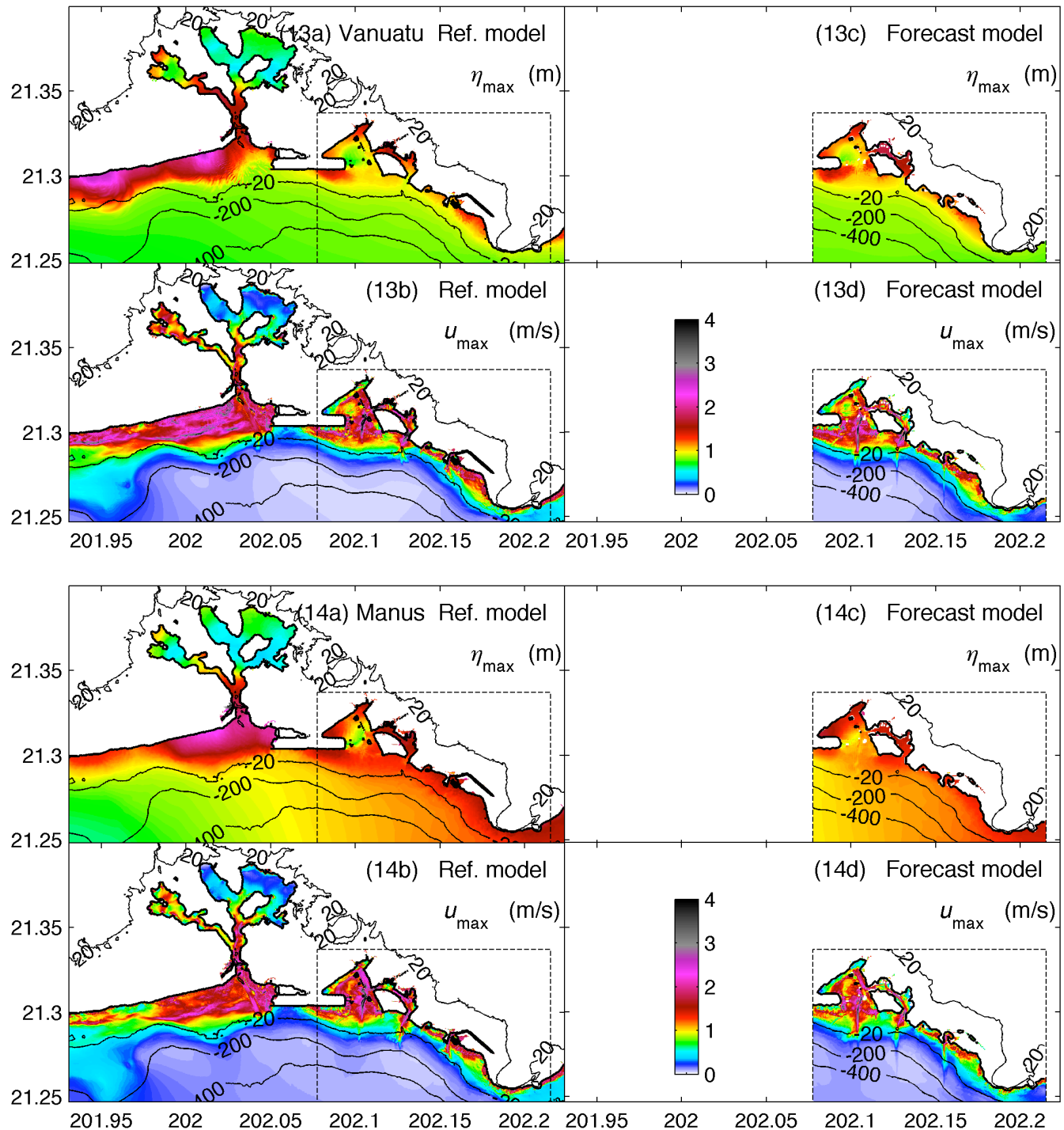


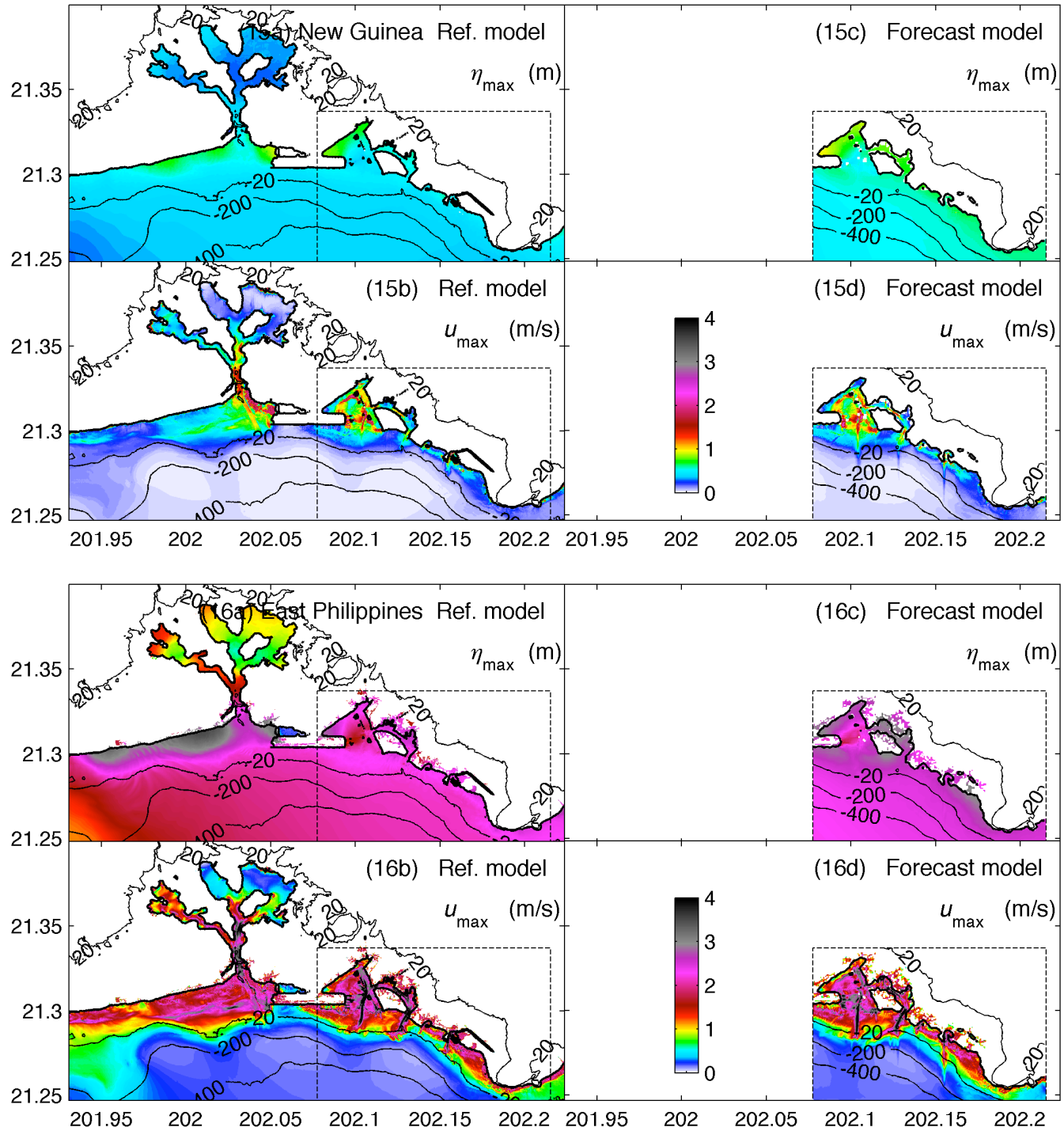












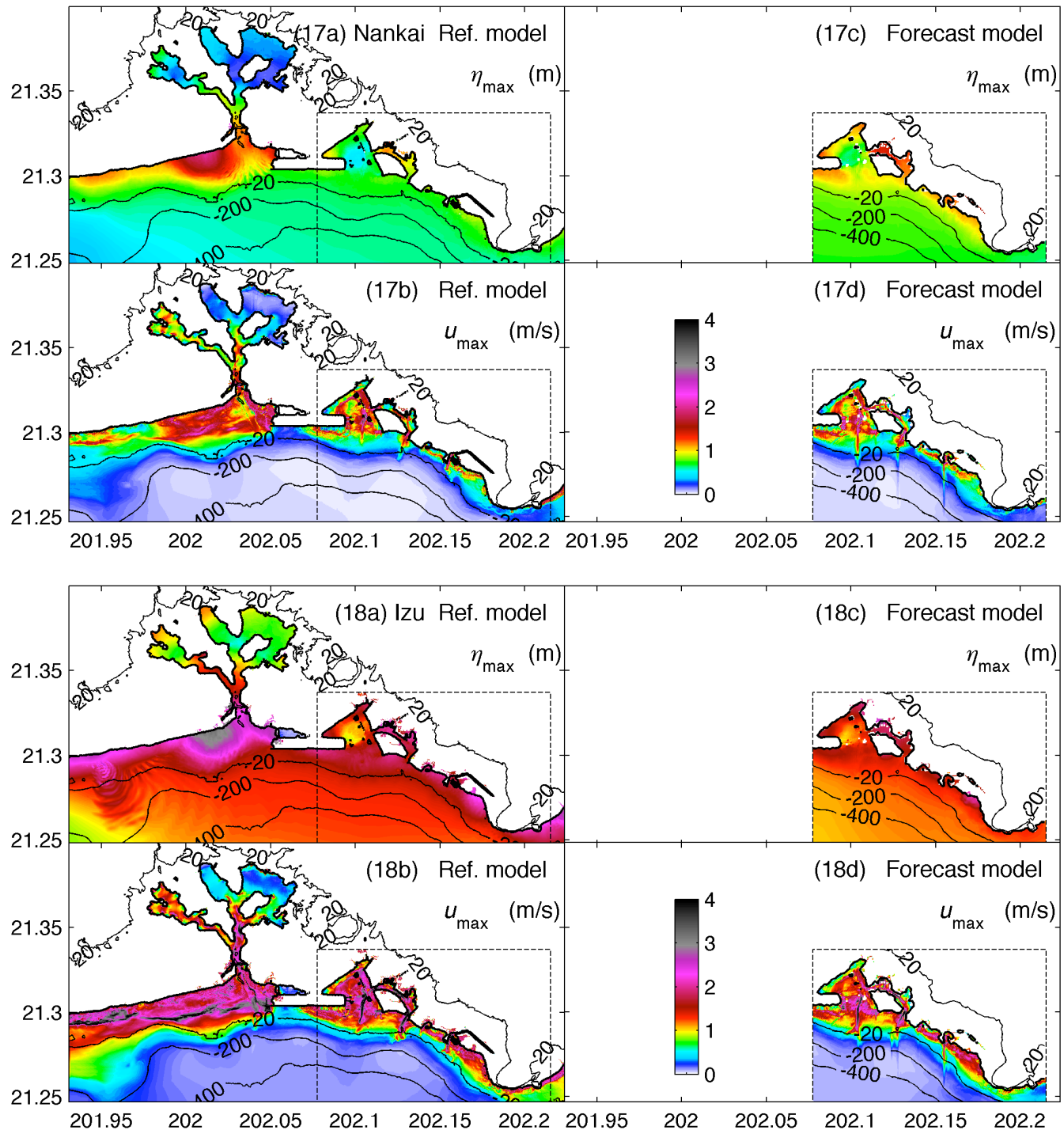
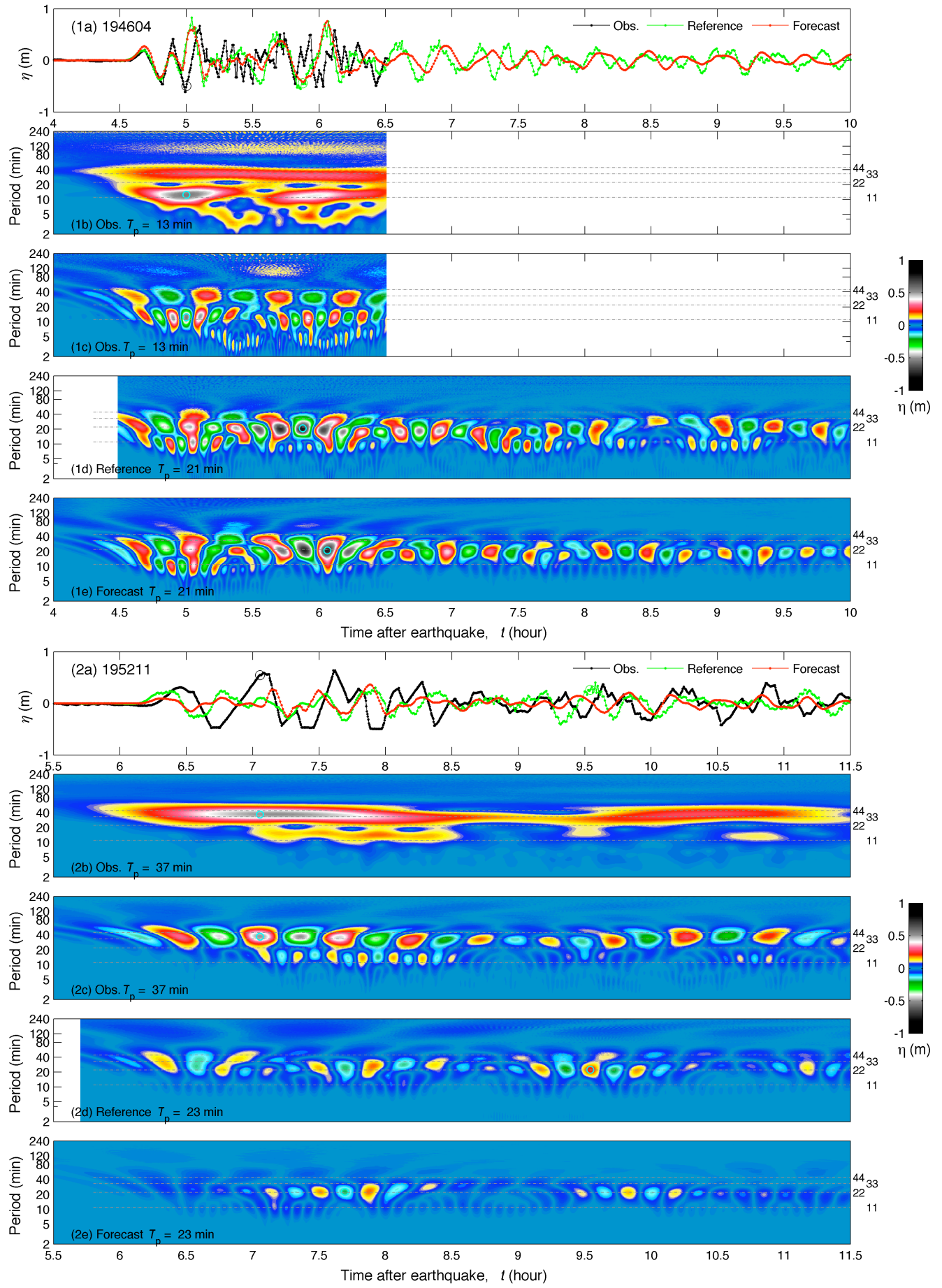
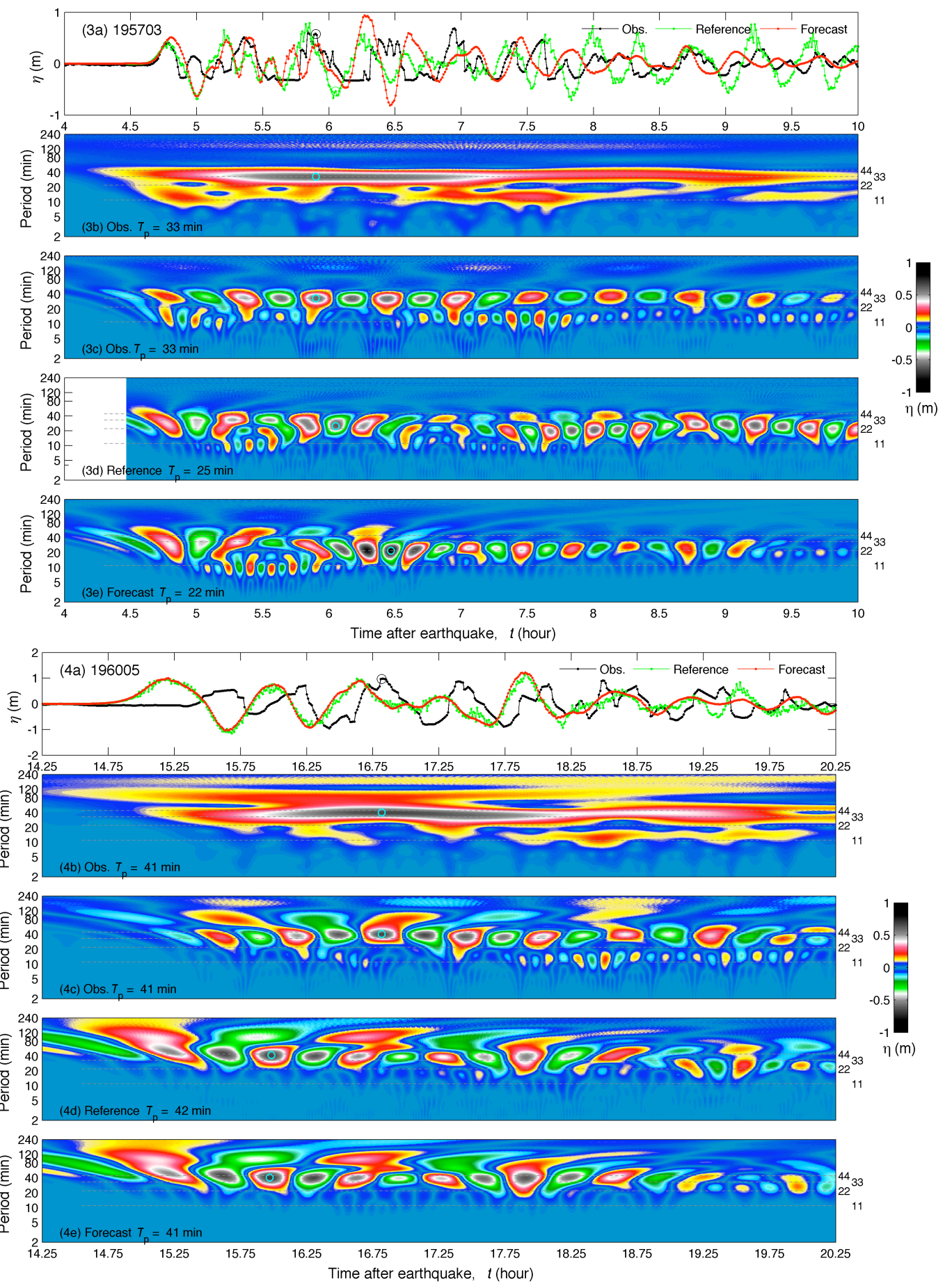
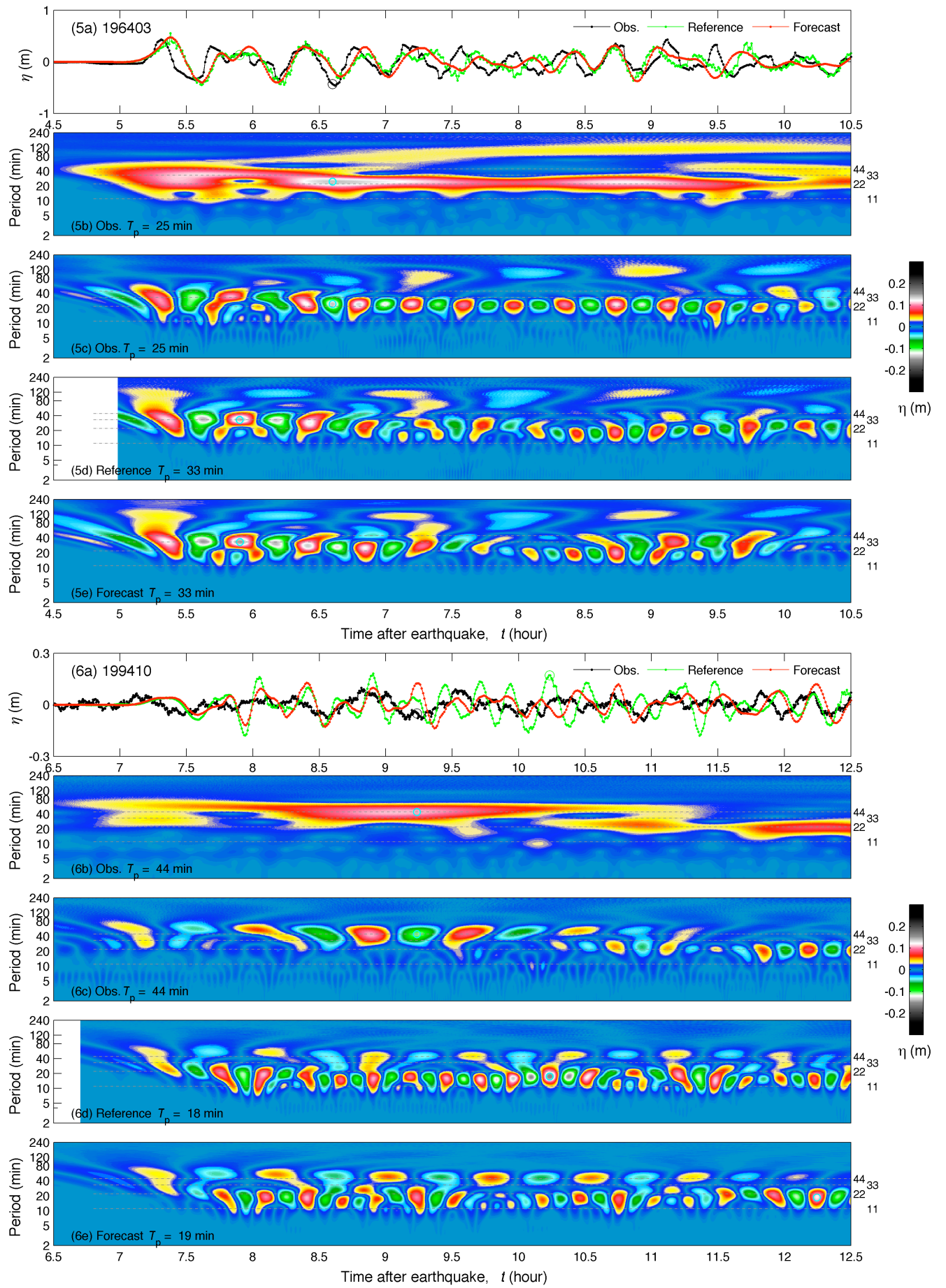
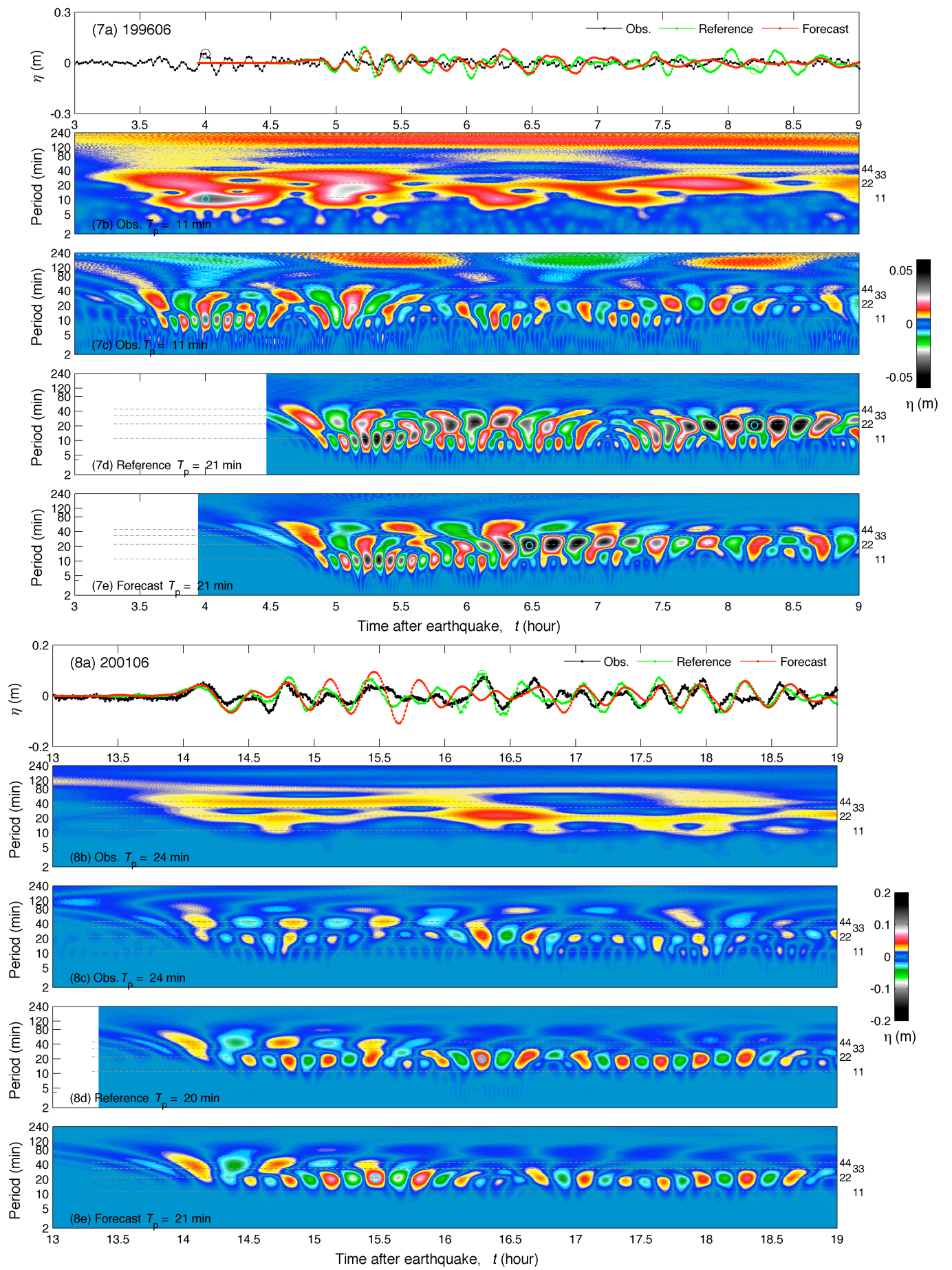


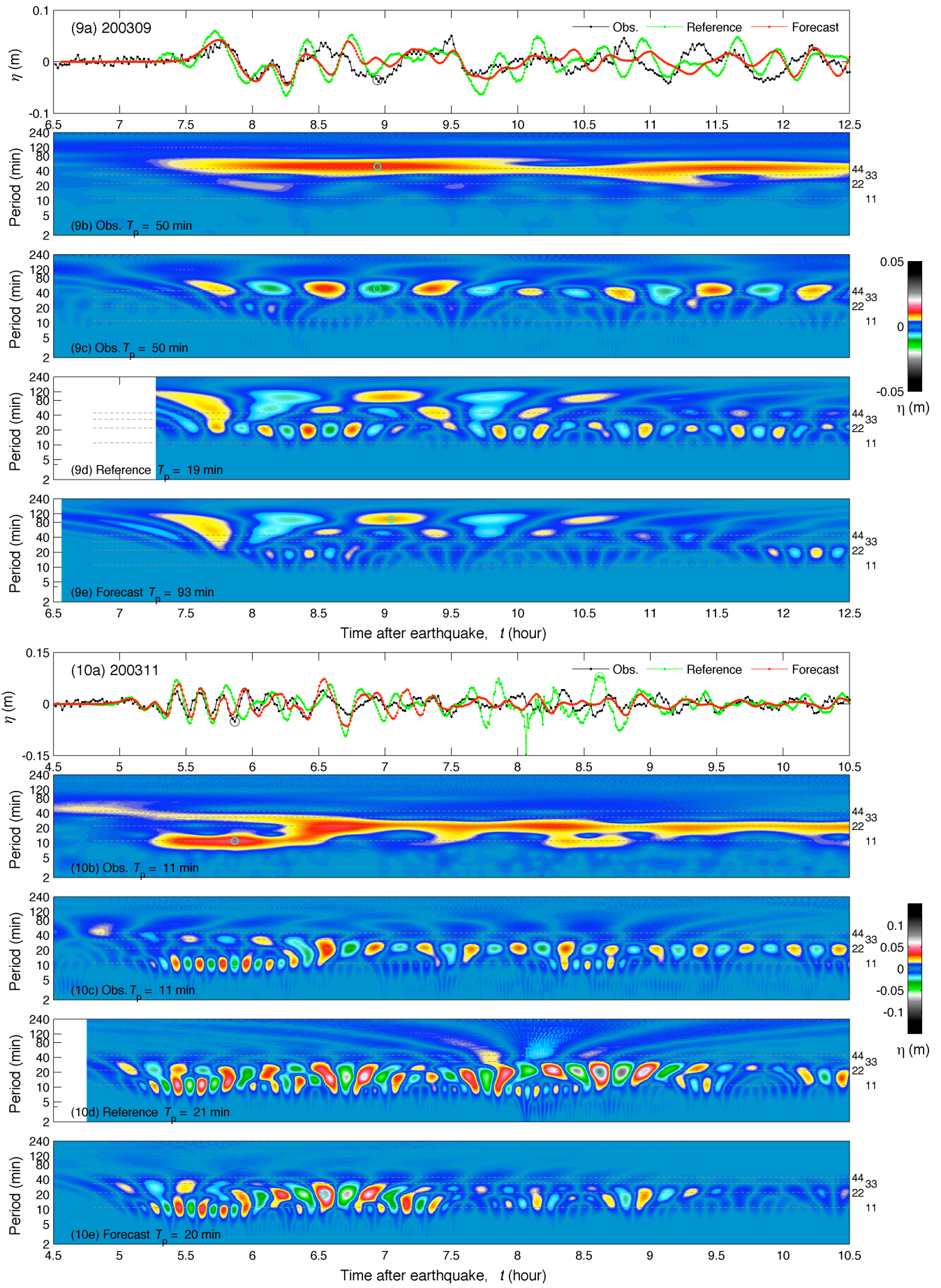
Figure 15 Maximum water elevation and current computed by the Honolulu reference and forecast models for the simulated magnitude 9.3 tsunamis.

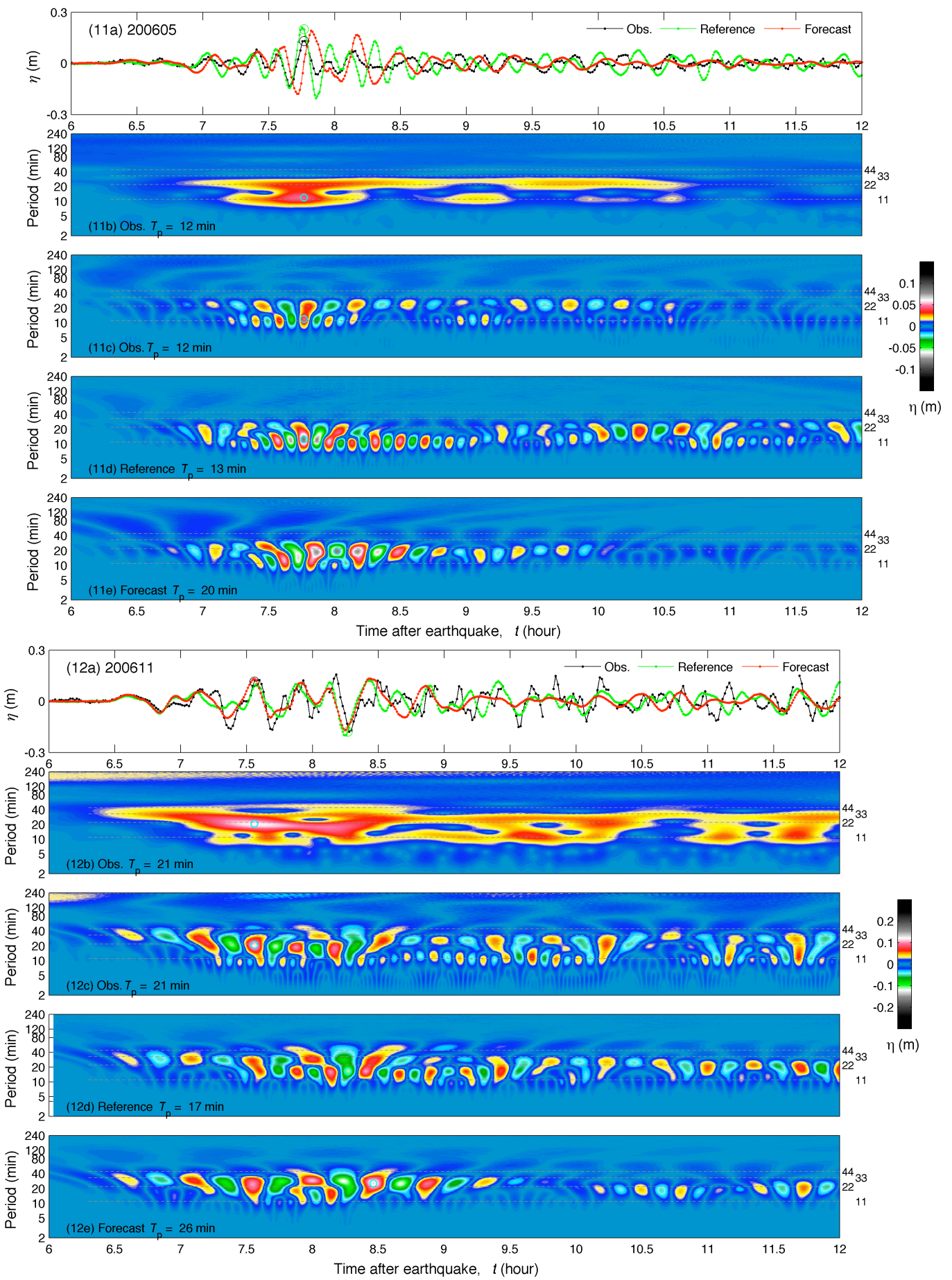


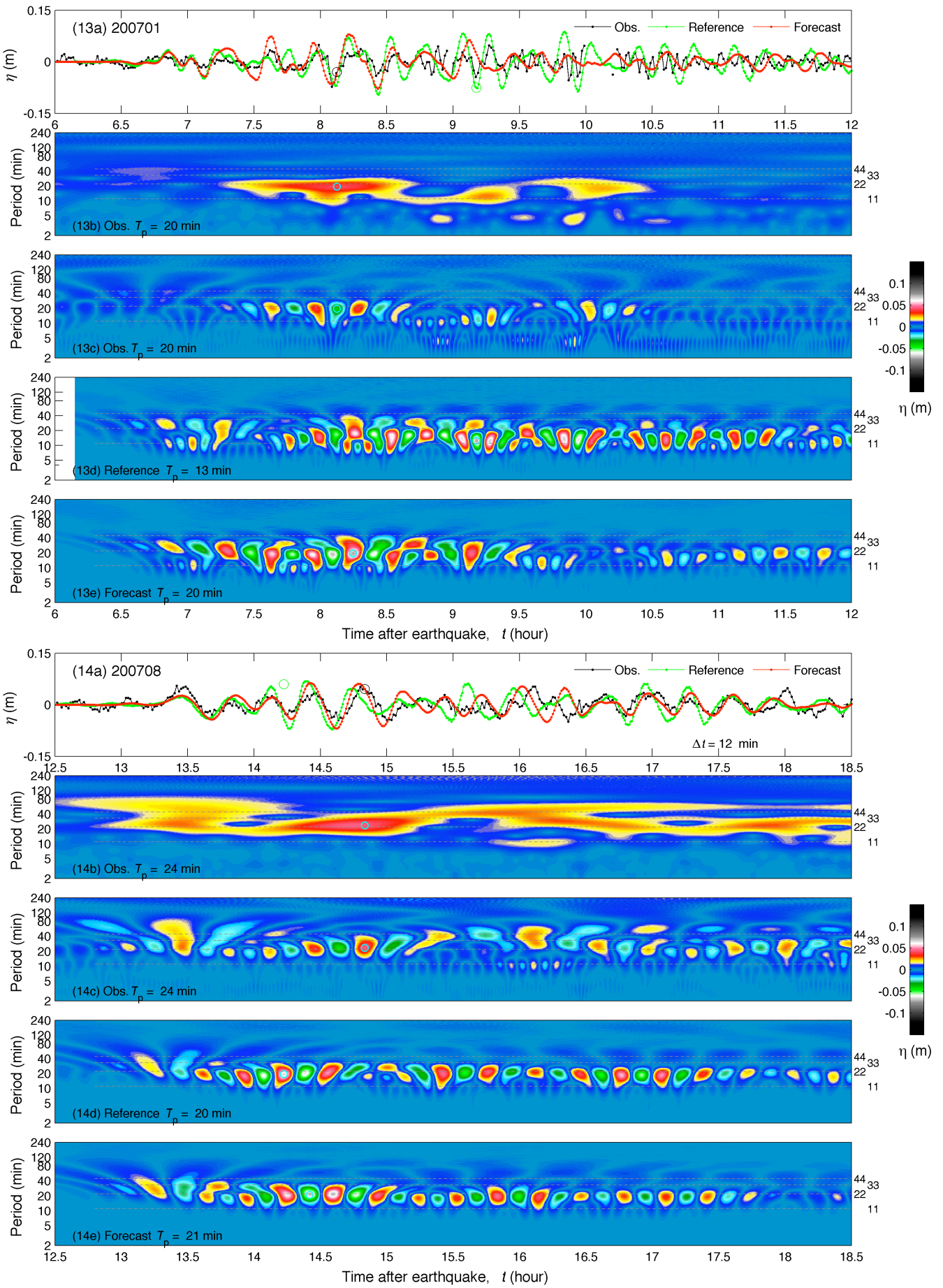


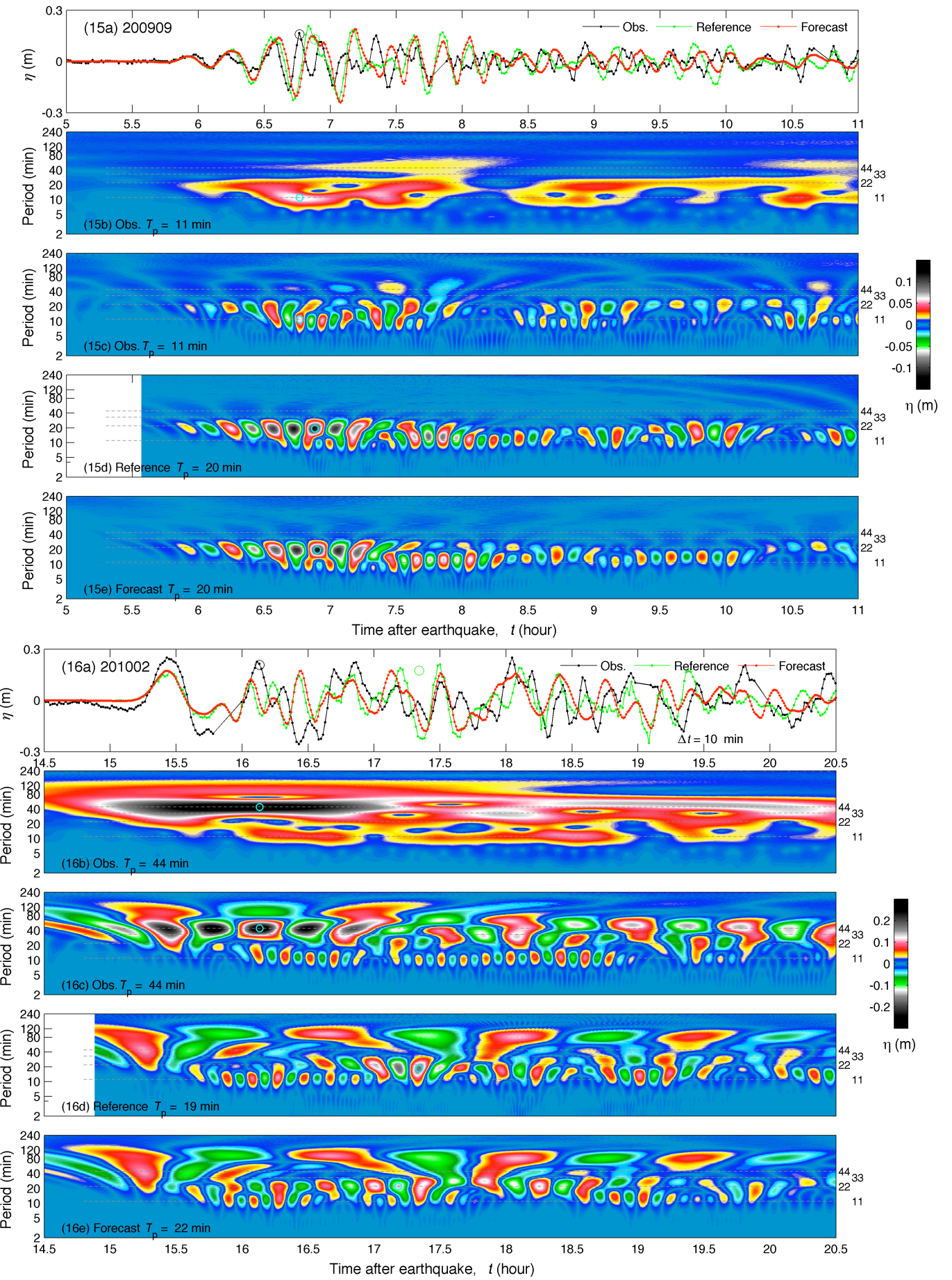












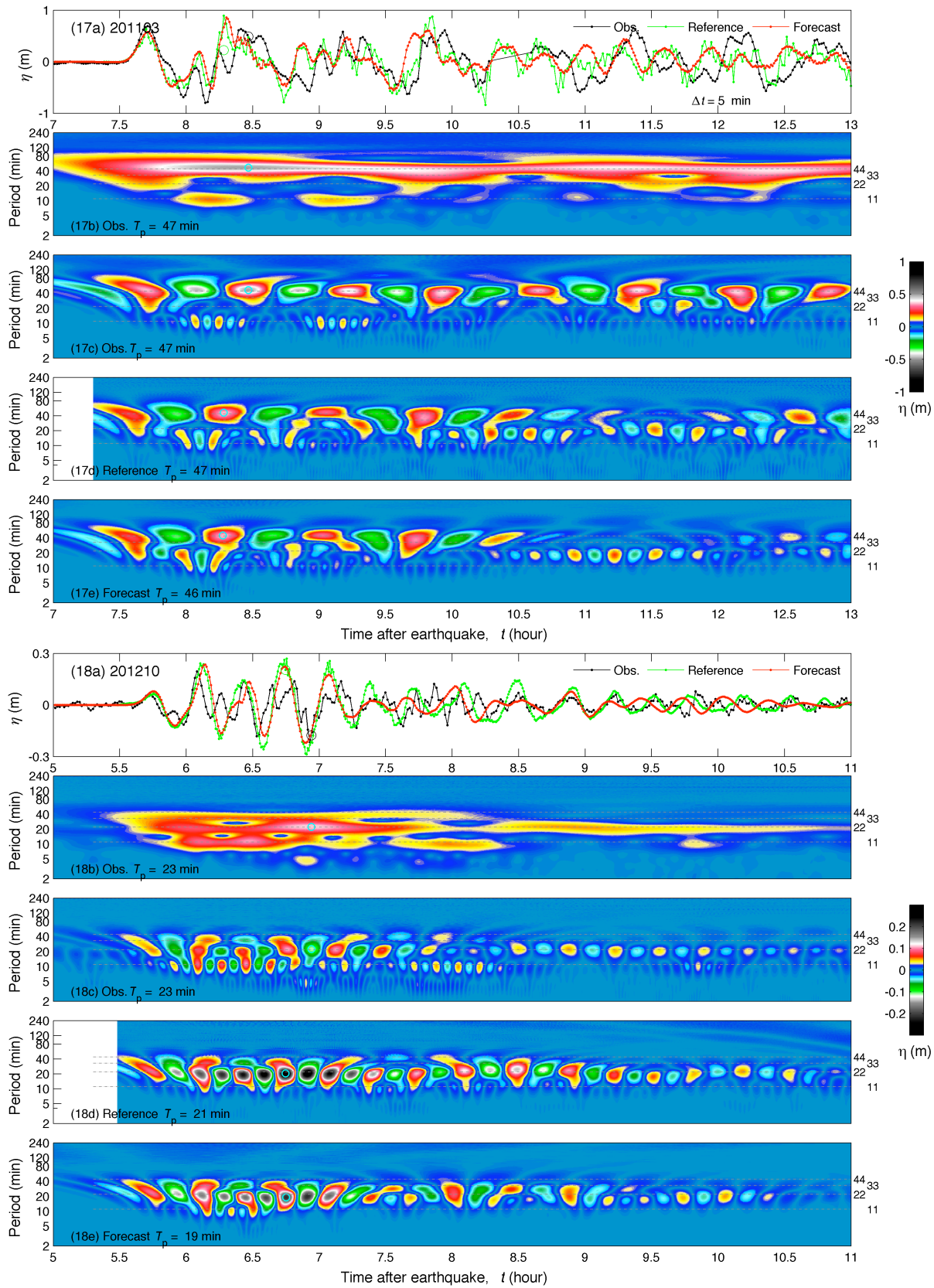
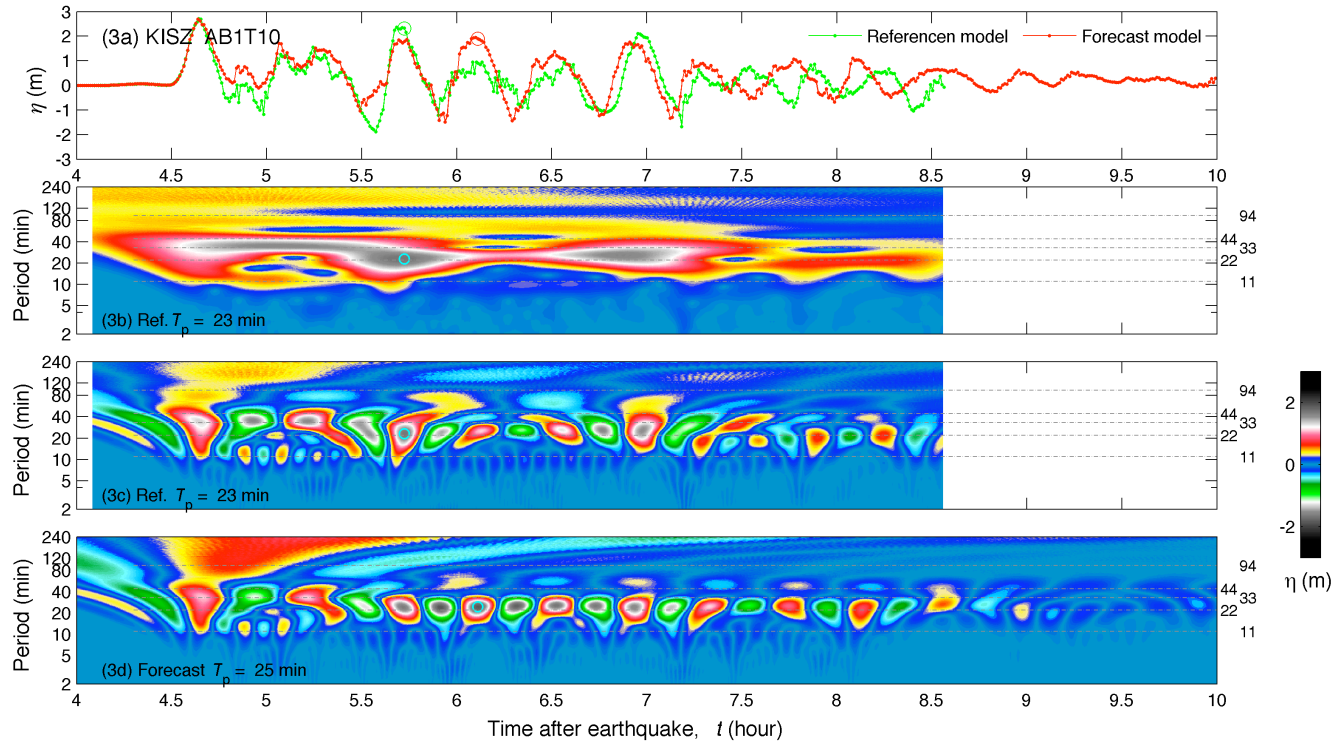
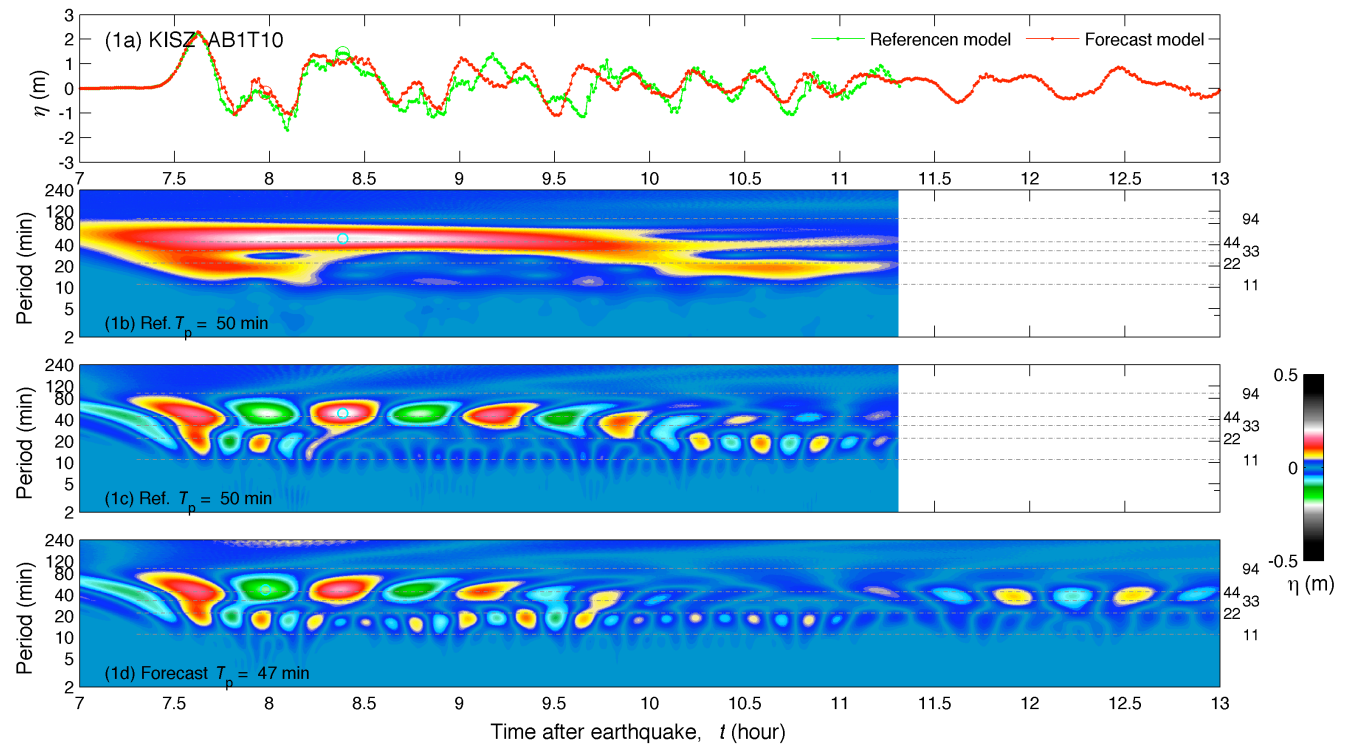
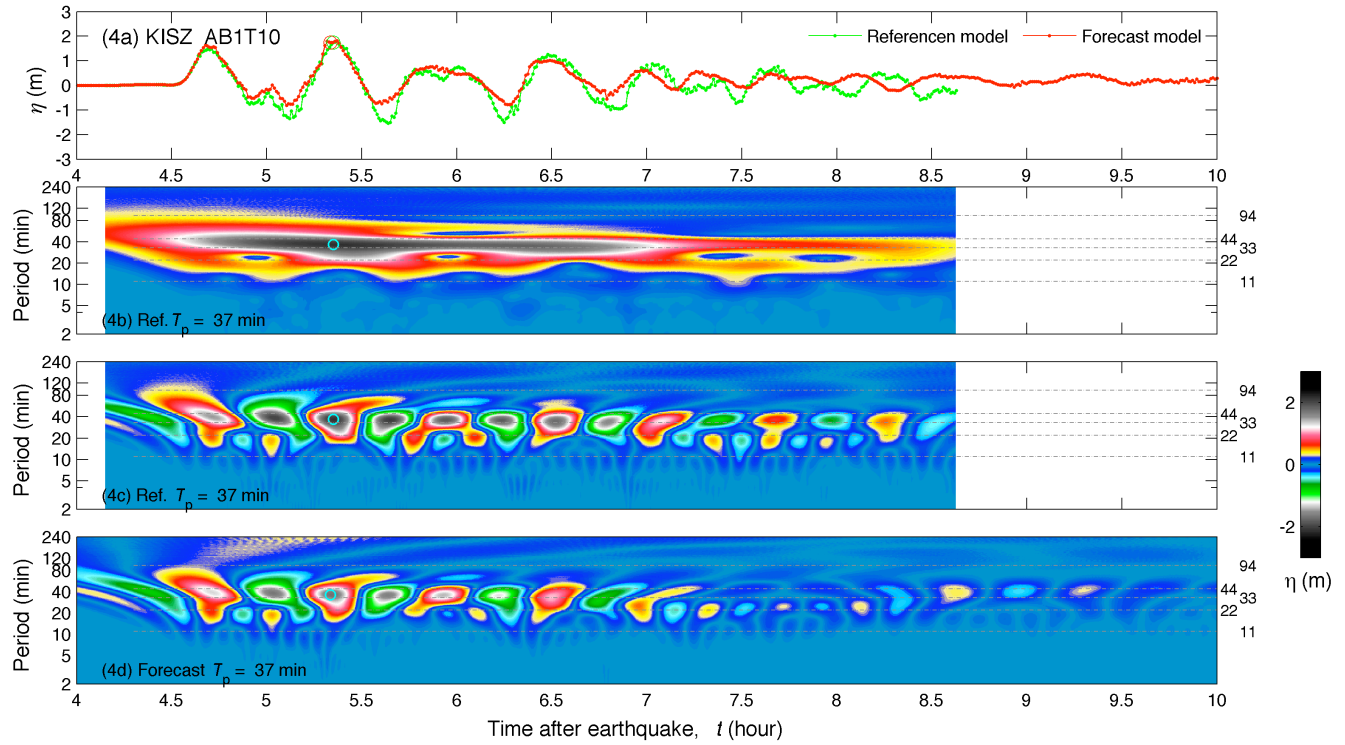
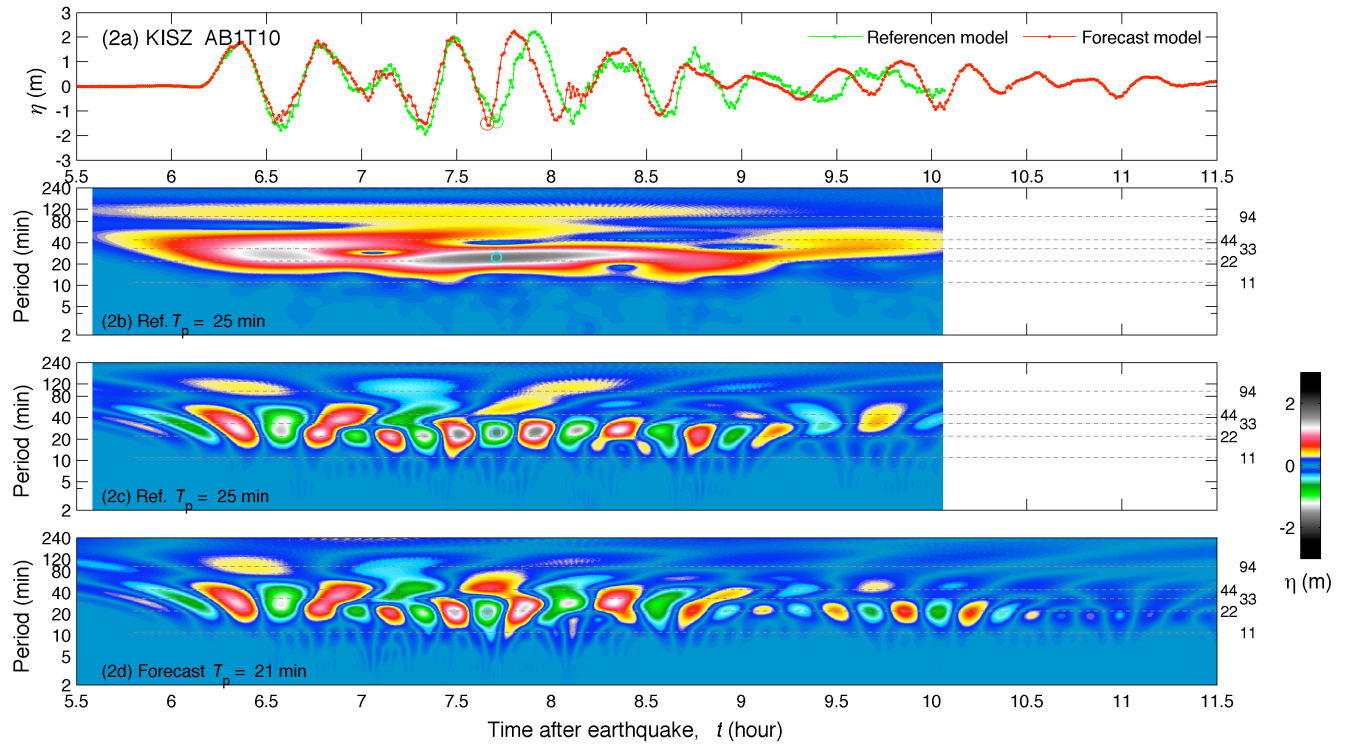
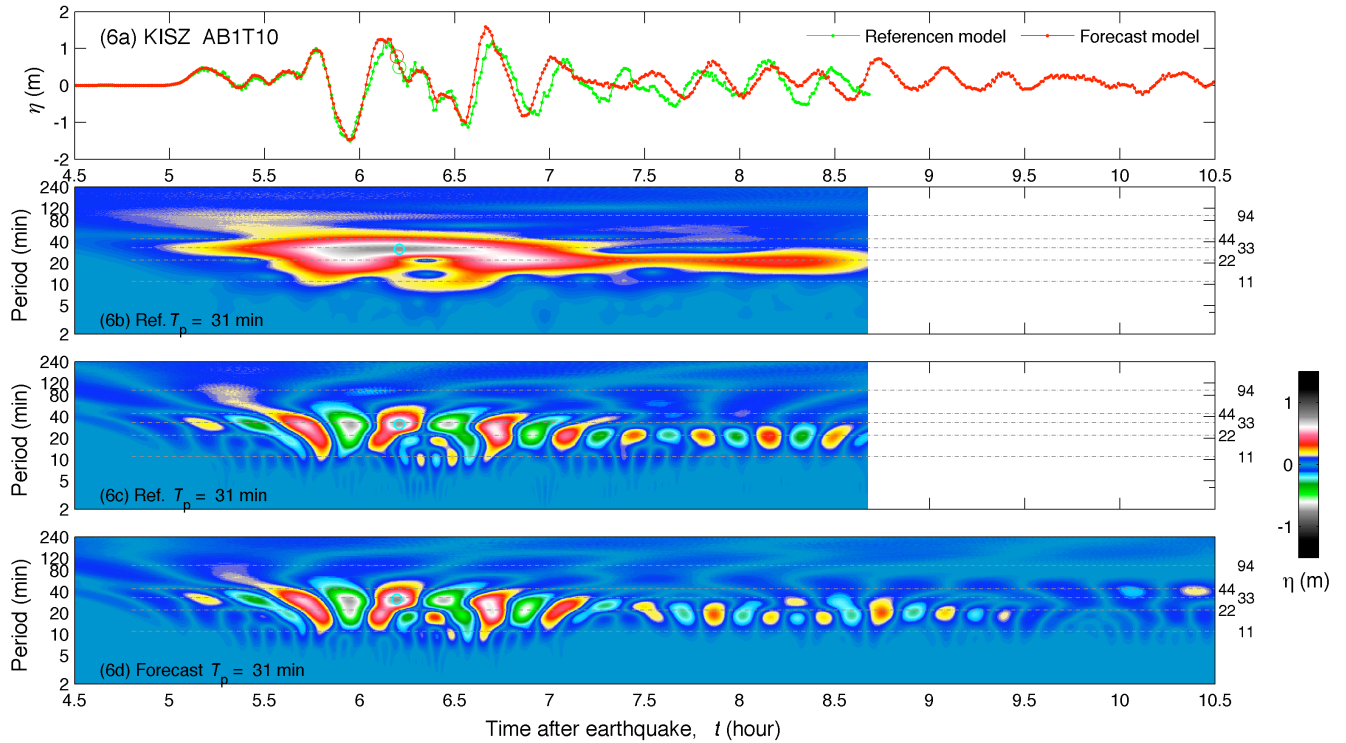
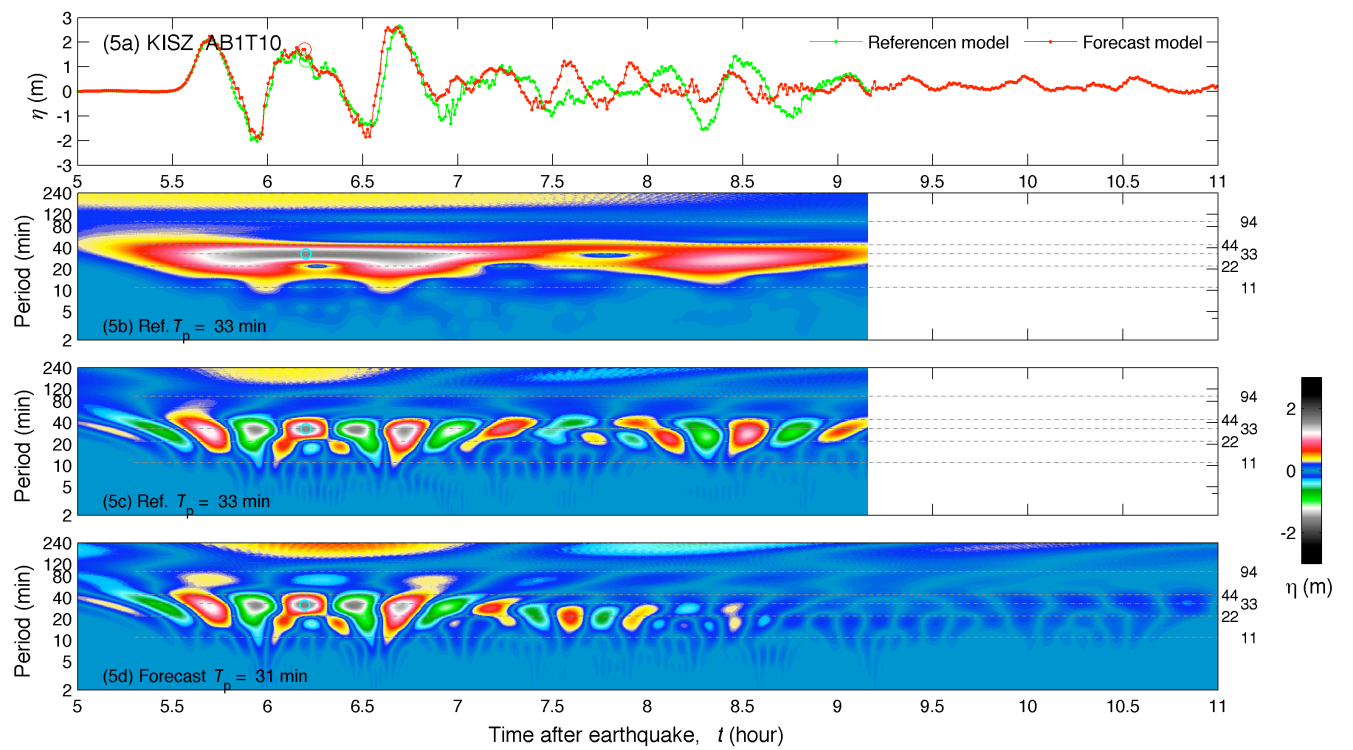
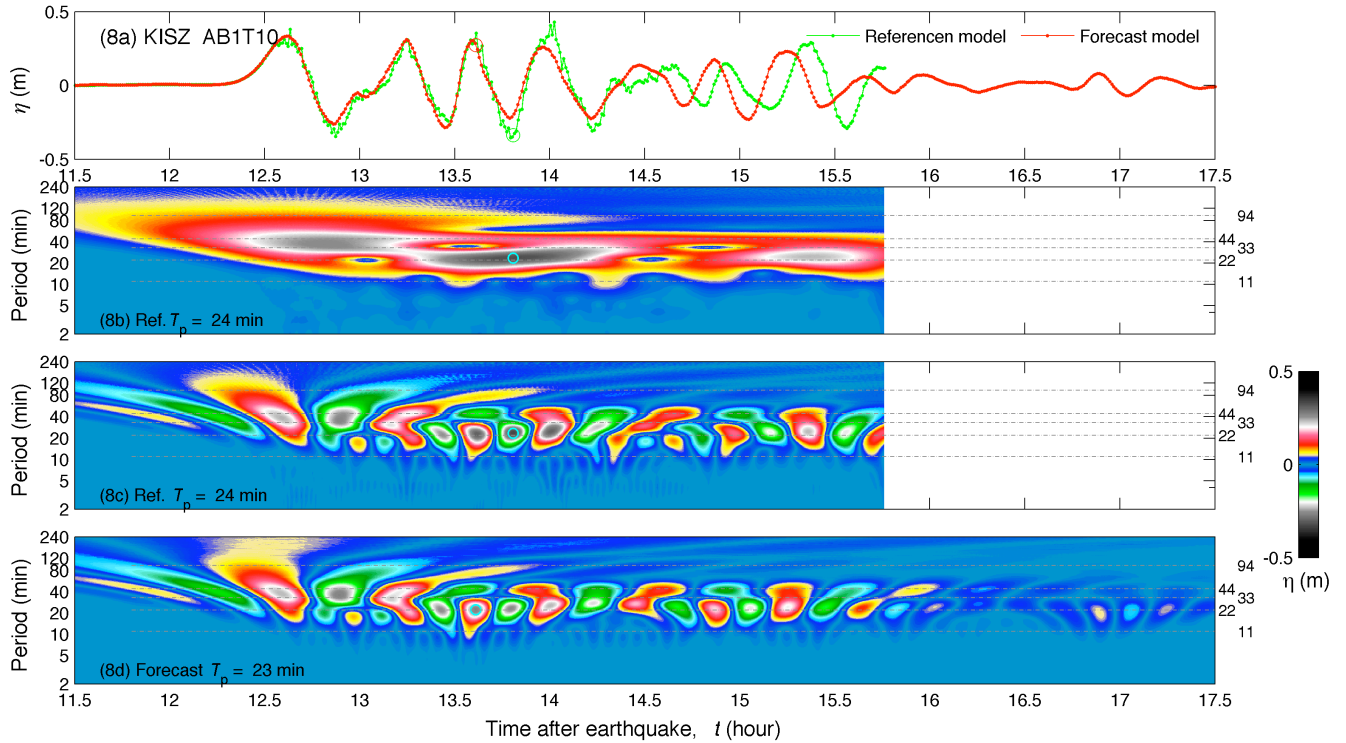
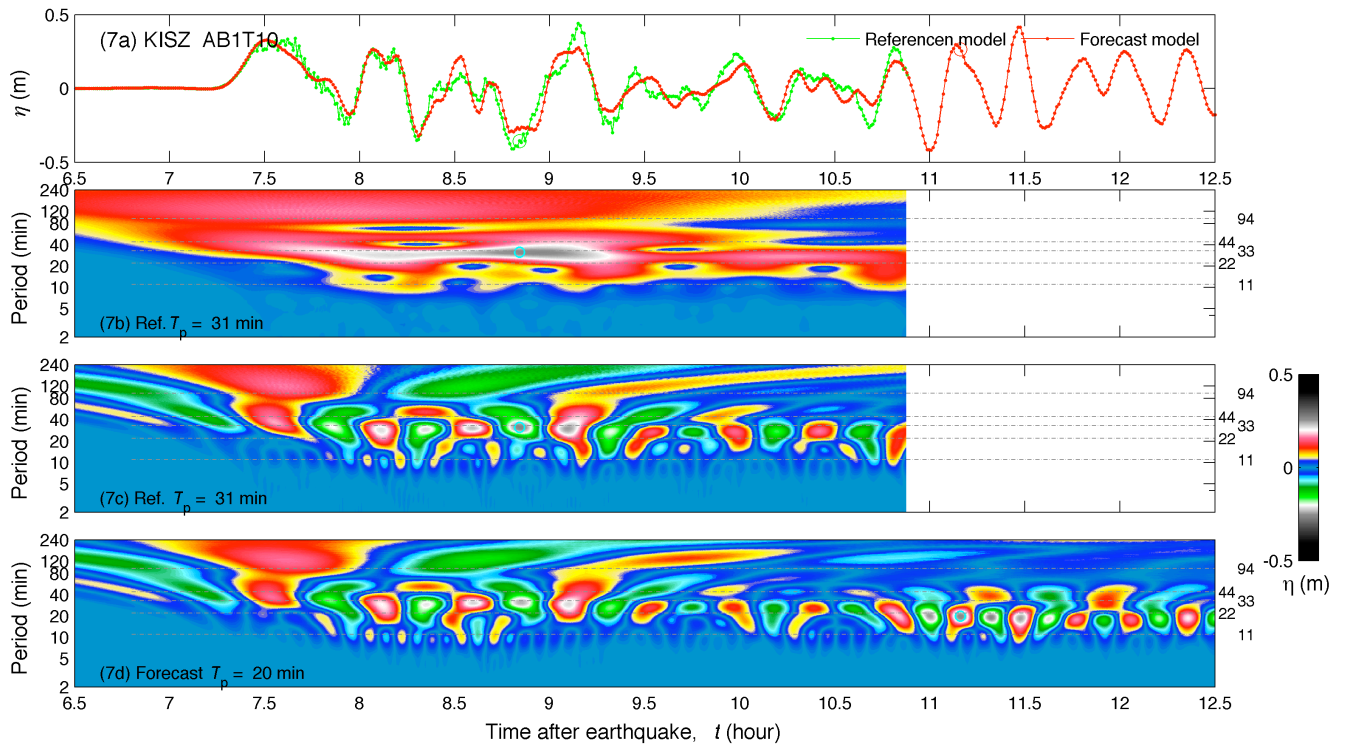


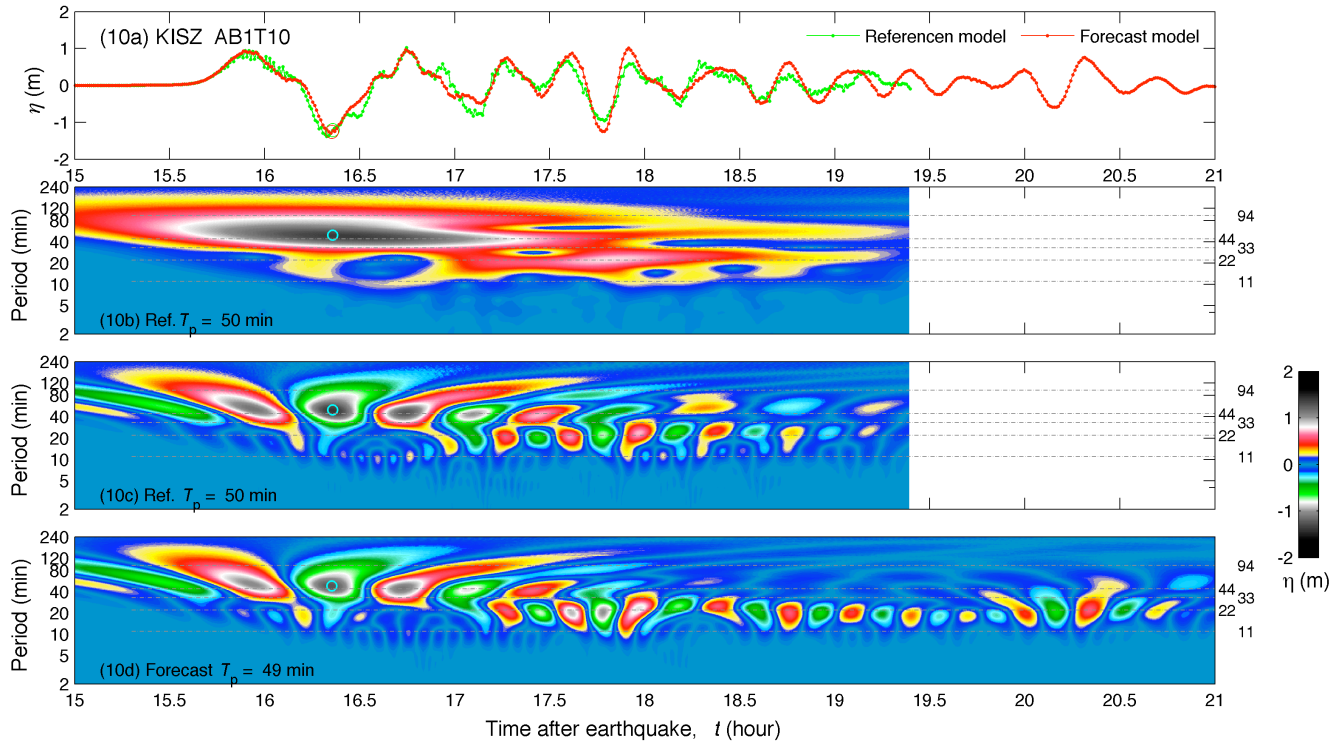
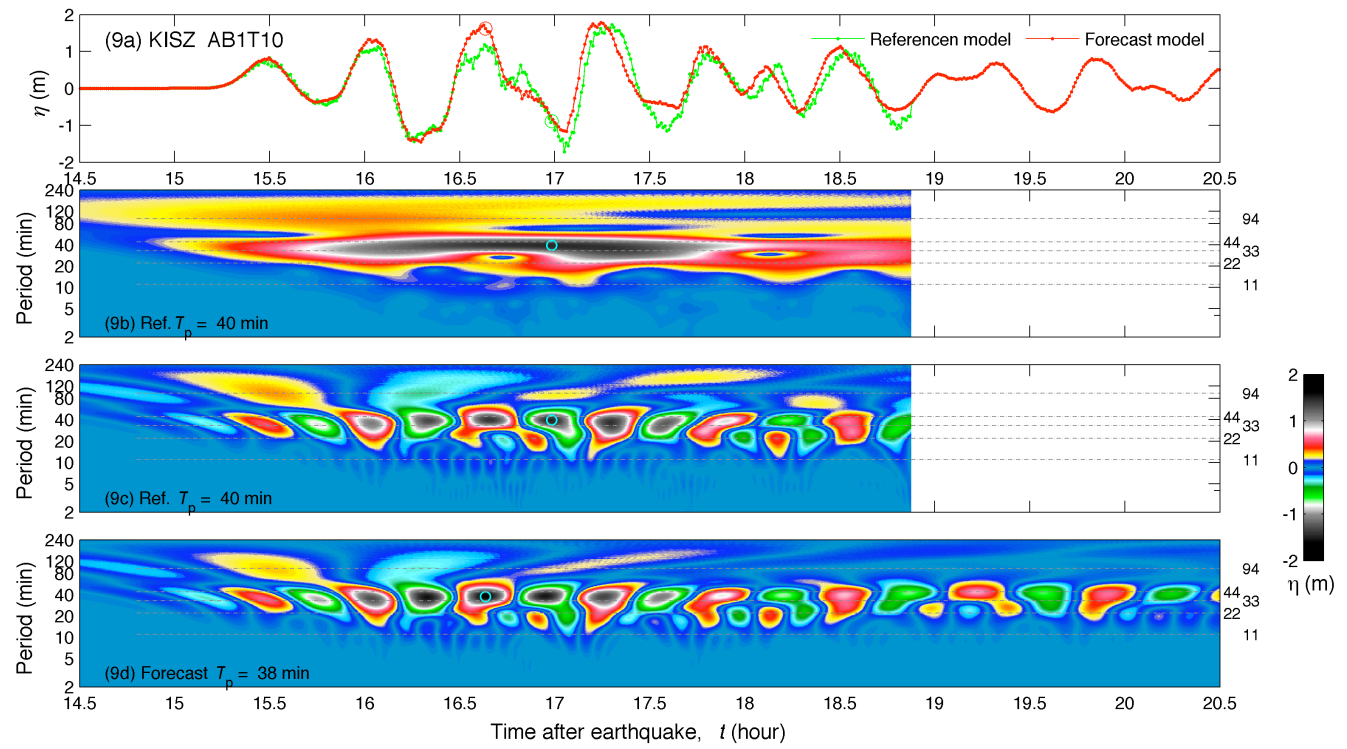
Figure 16 (a) Modeled η time series at Honolulu tide station for the 18 past tsunamis. (b) Wavelet-derived amplitude spectrogram for the observations. Real part of the spectrograms for (c) observations, (d) the reference and (e) the forecast models.

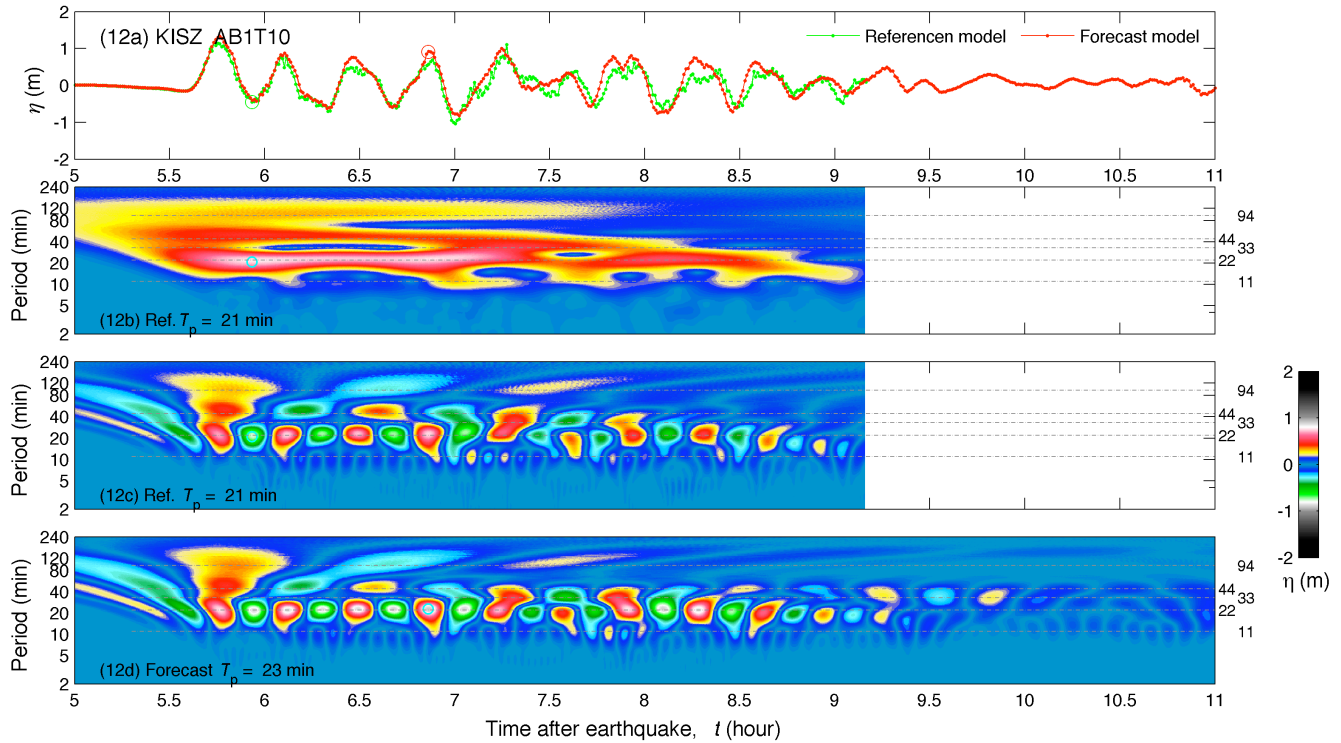
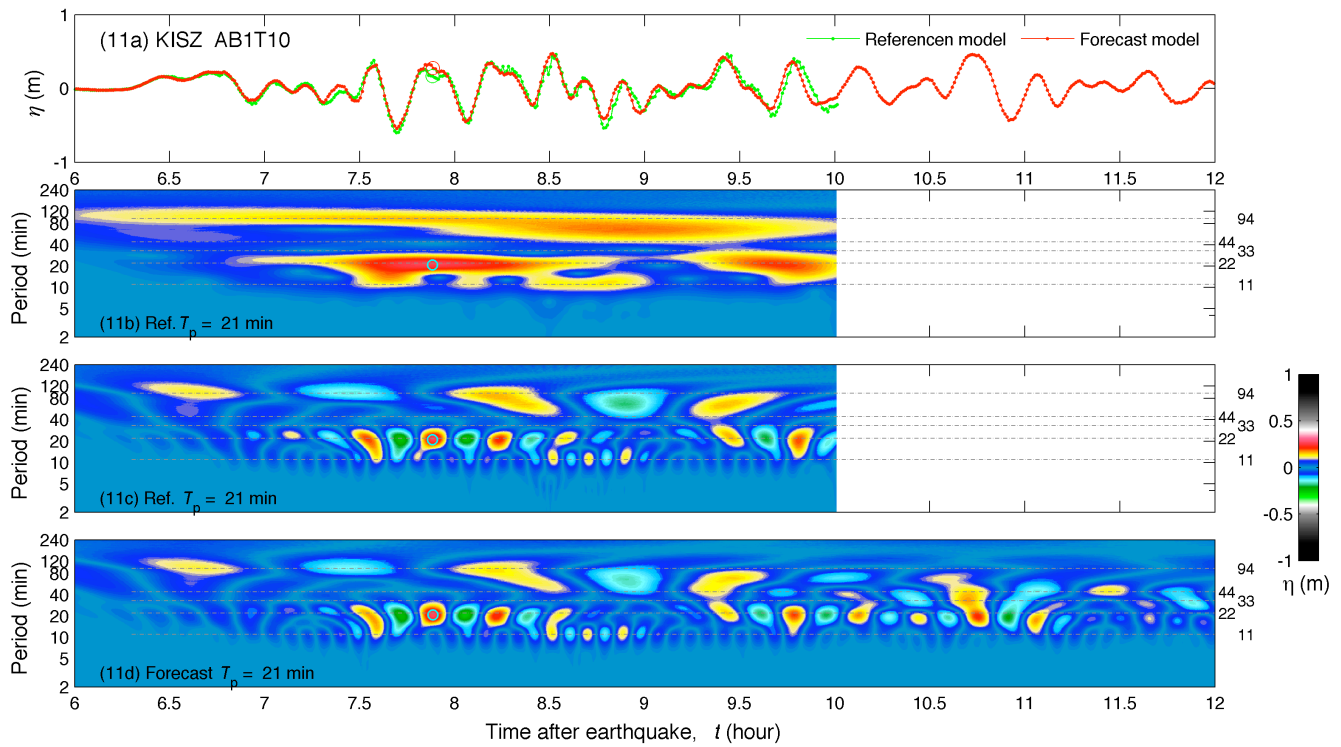


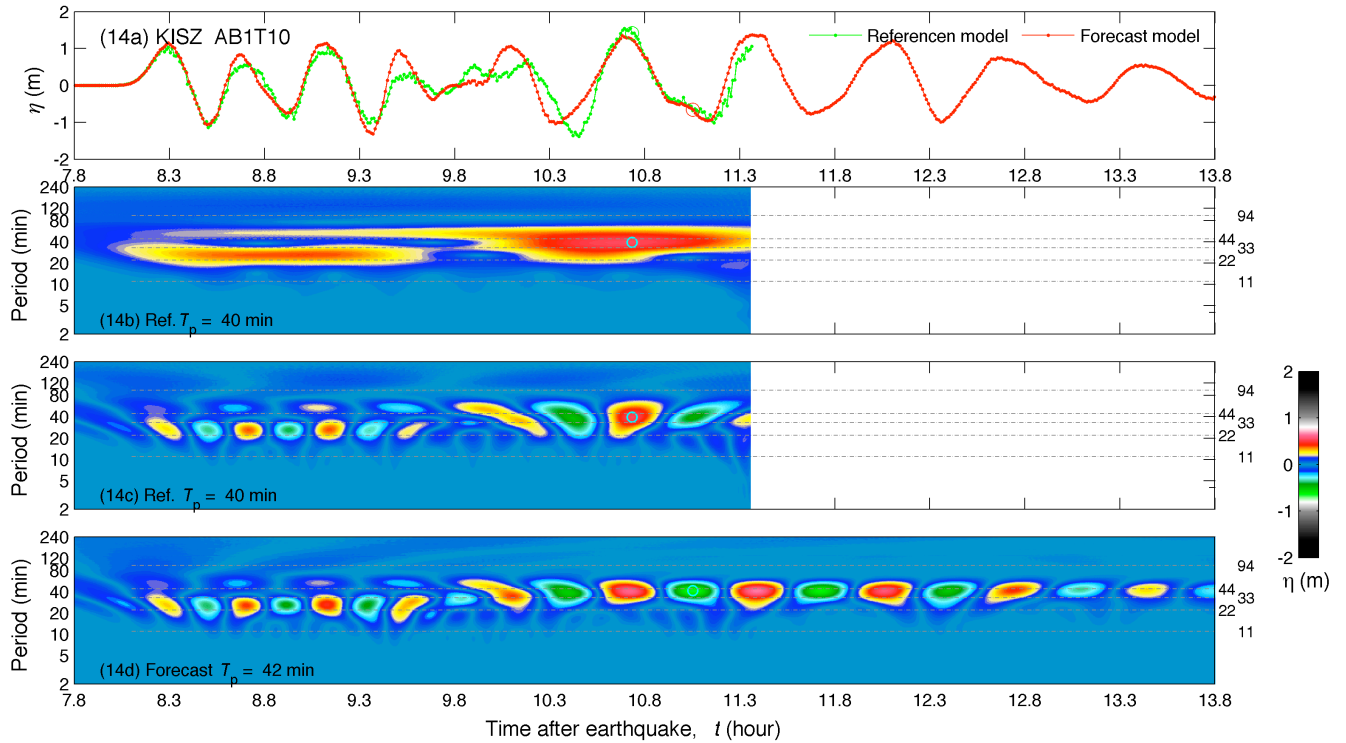
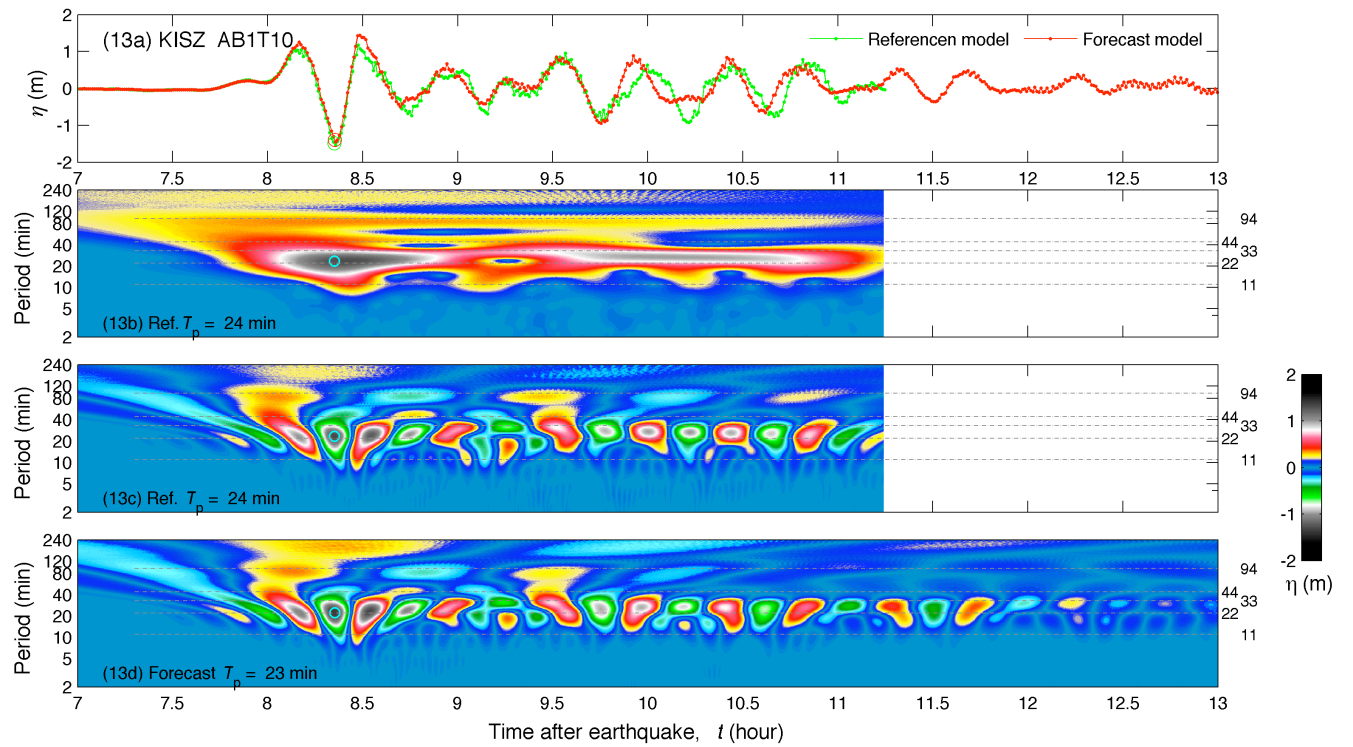


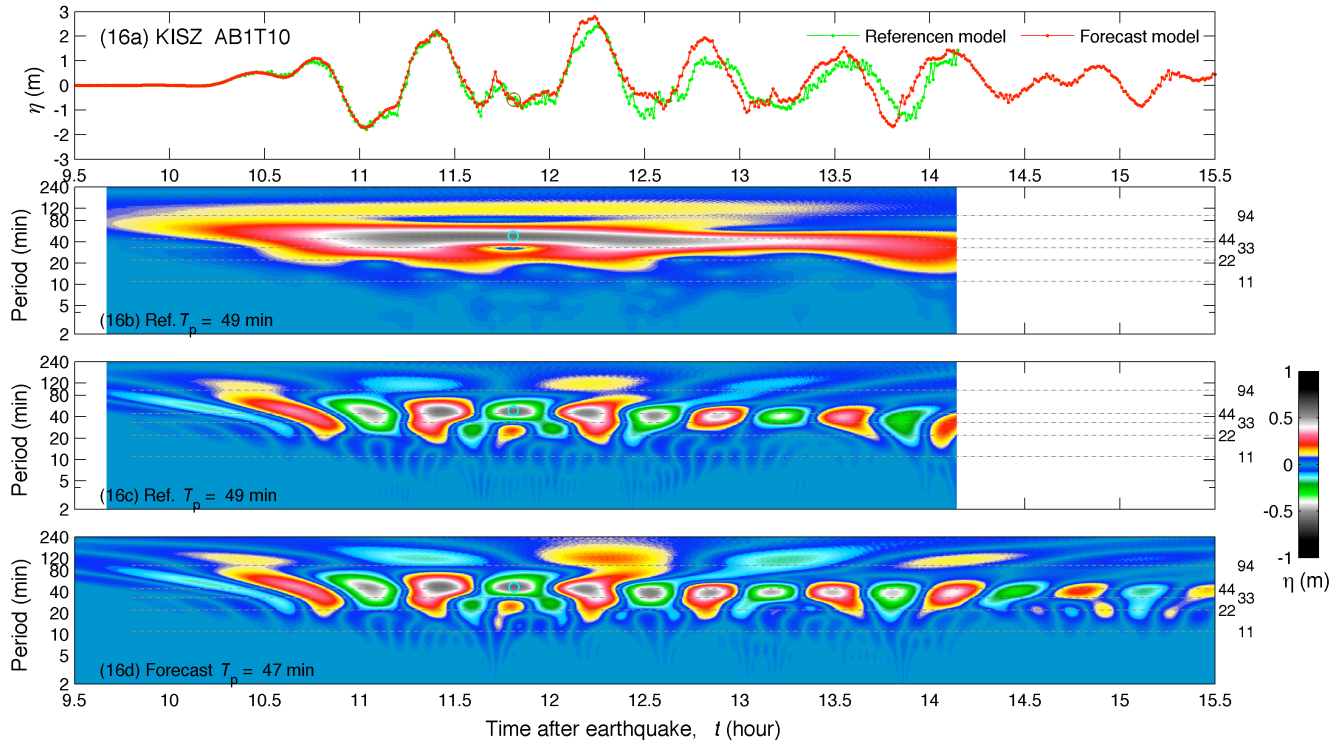
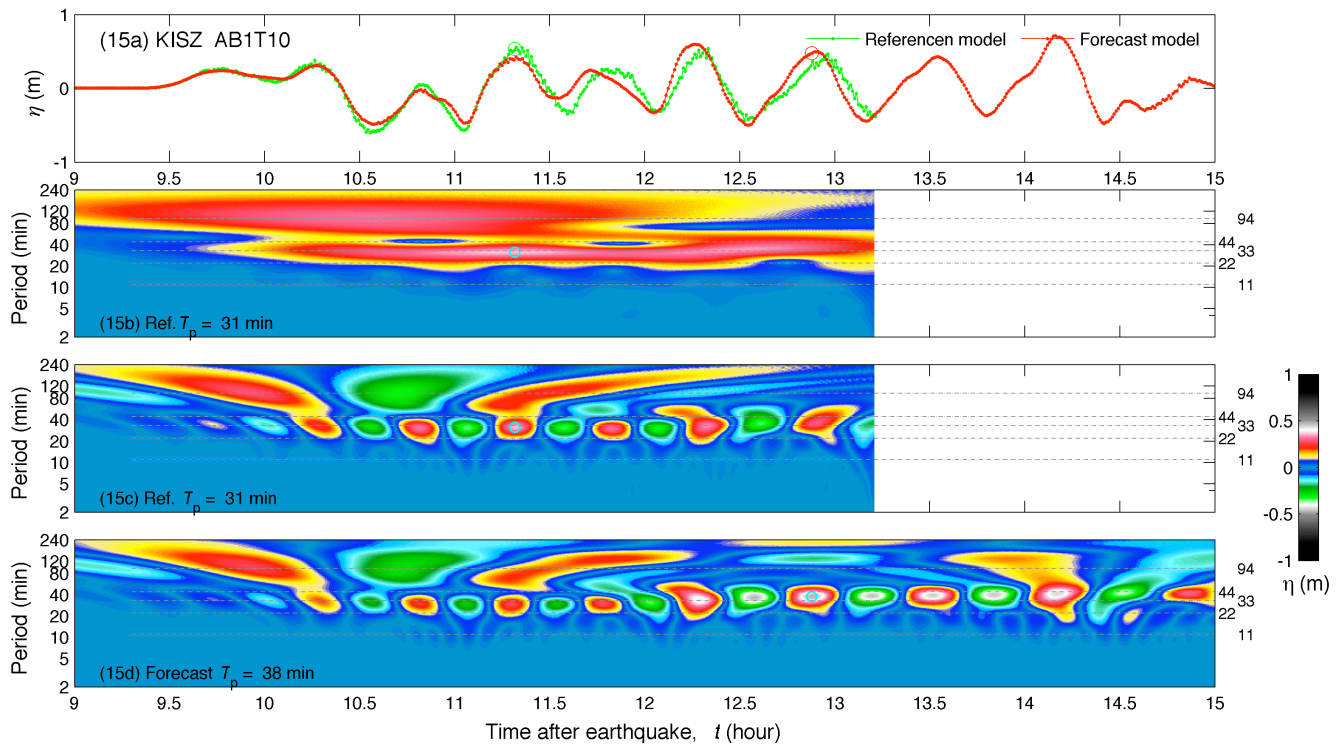












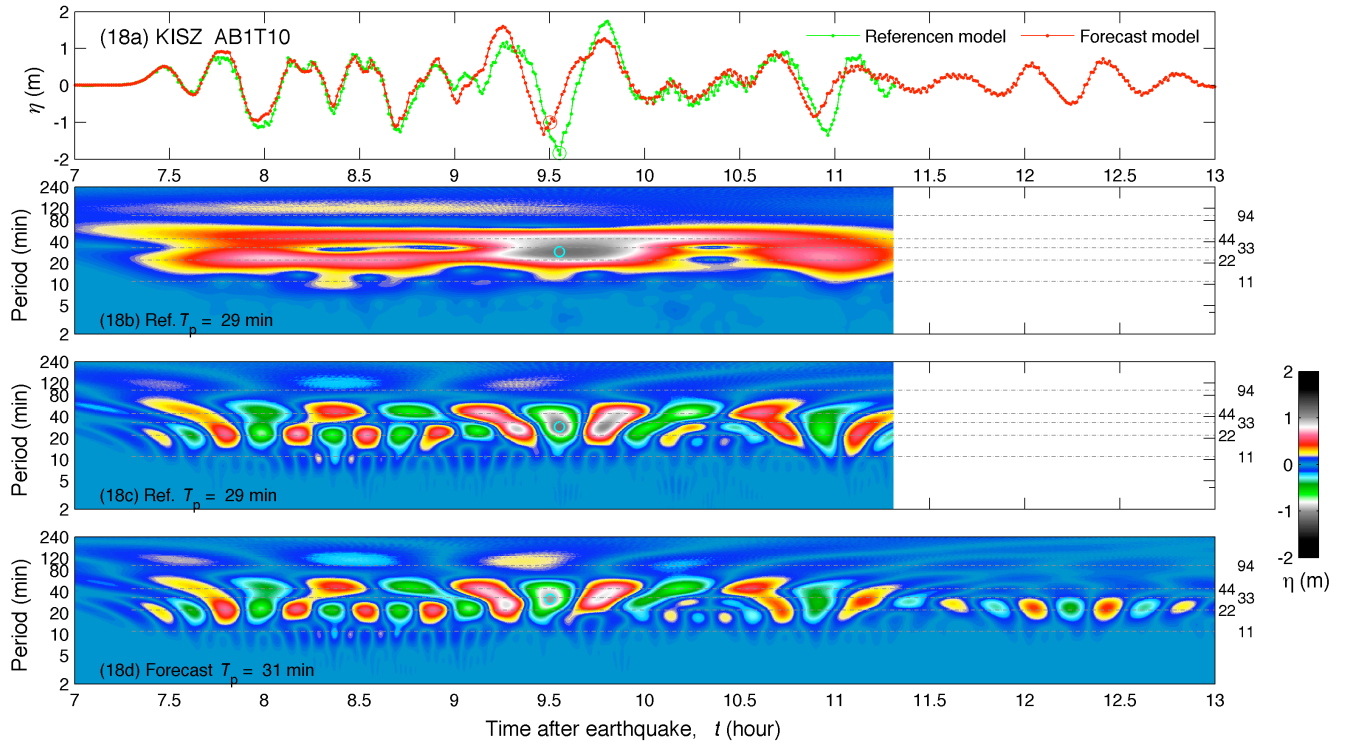
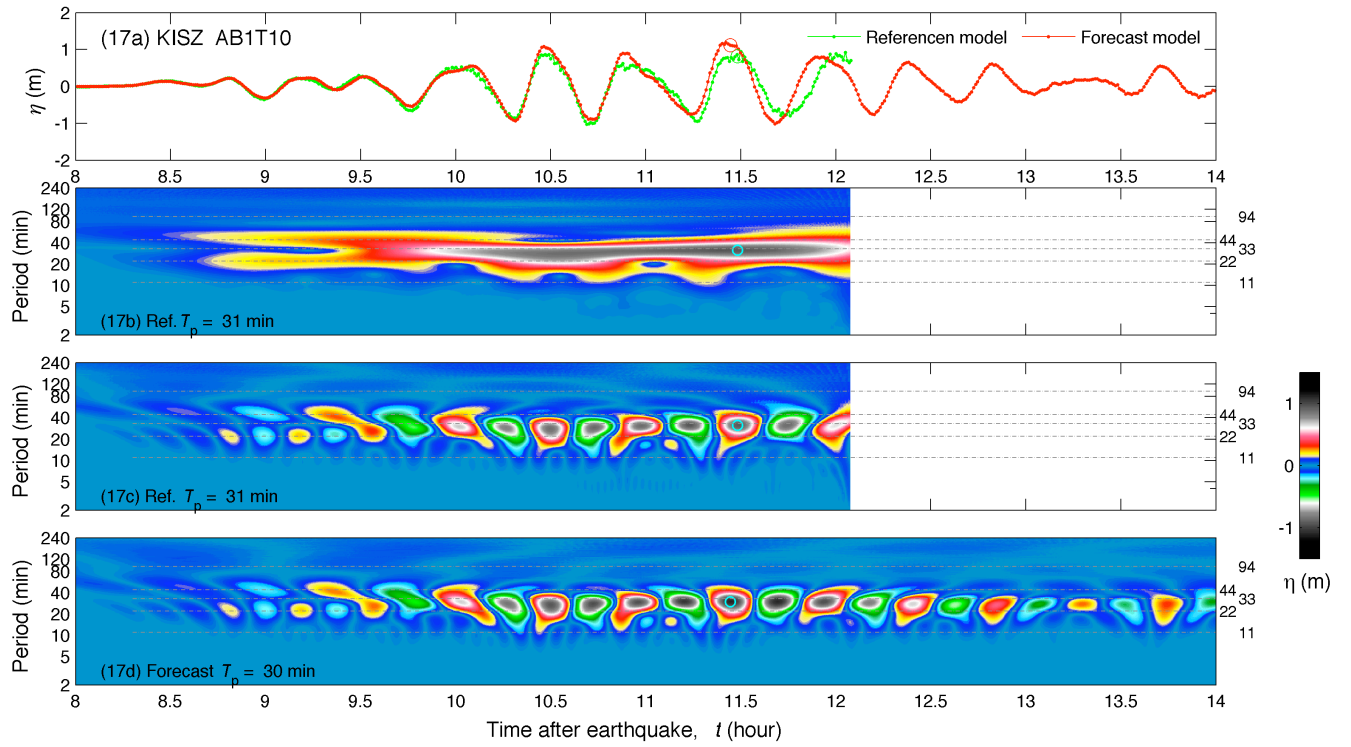


Figure 17 (a) Modeled η time series at Honolulu tide station for the 18 simulated $M_w=9.3$ tsunamis. (b) Wavelet-derived amplitude spectrogram for the reference model. (c and d) Real part of the spectrograms computed by the reference and forecast models.

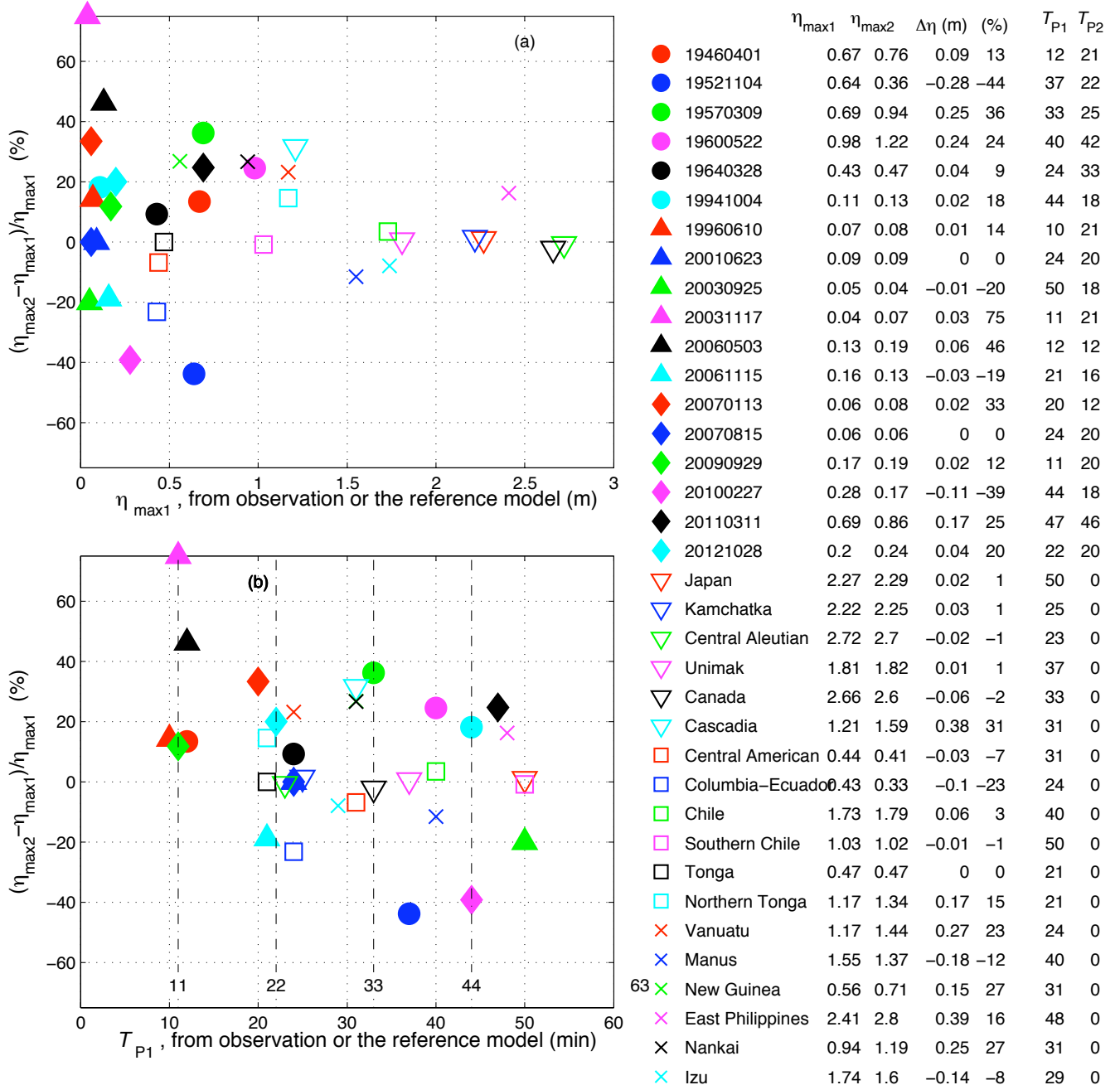
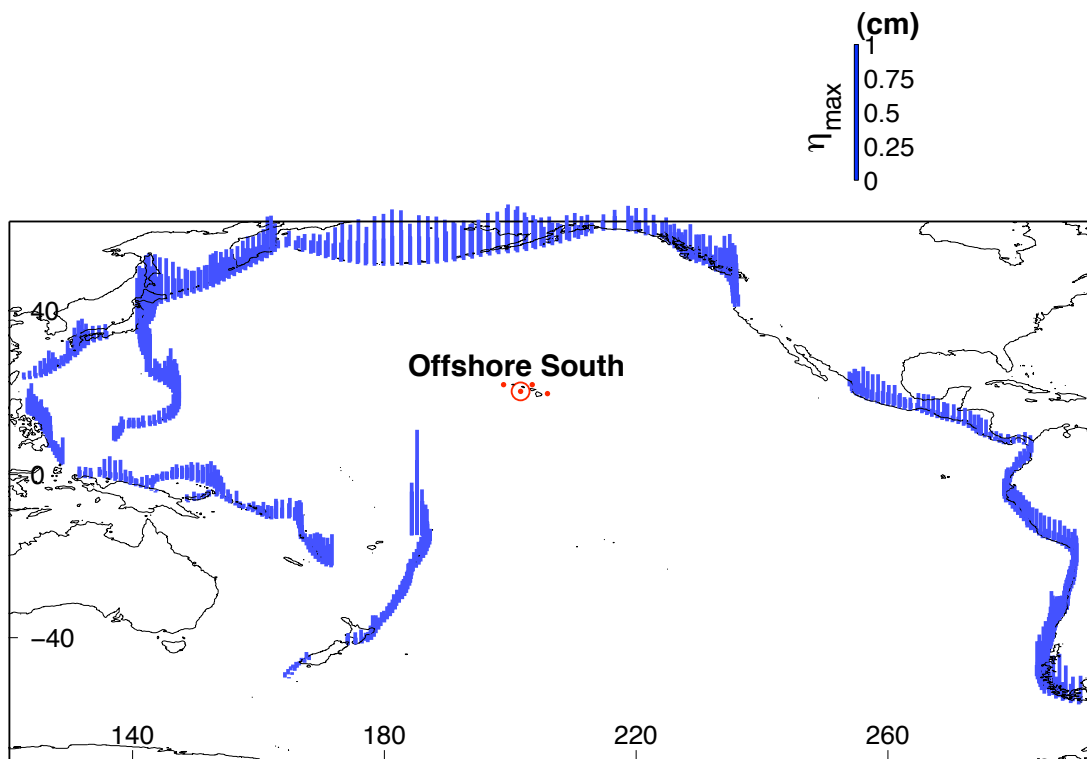
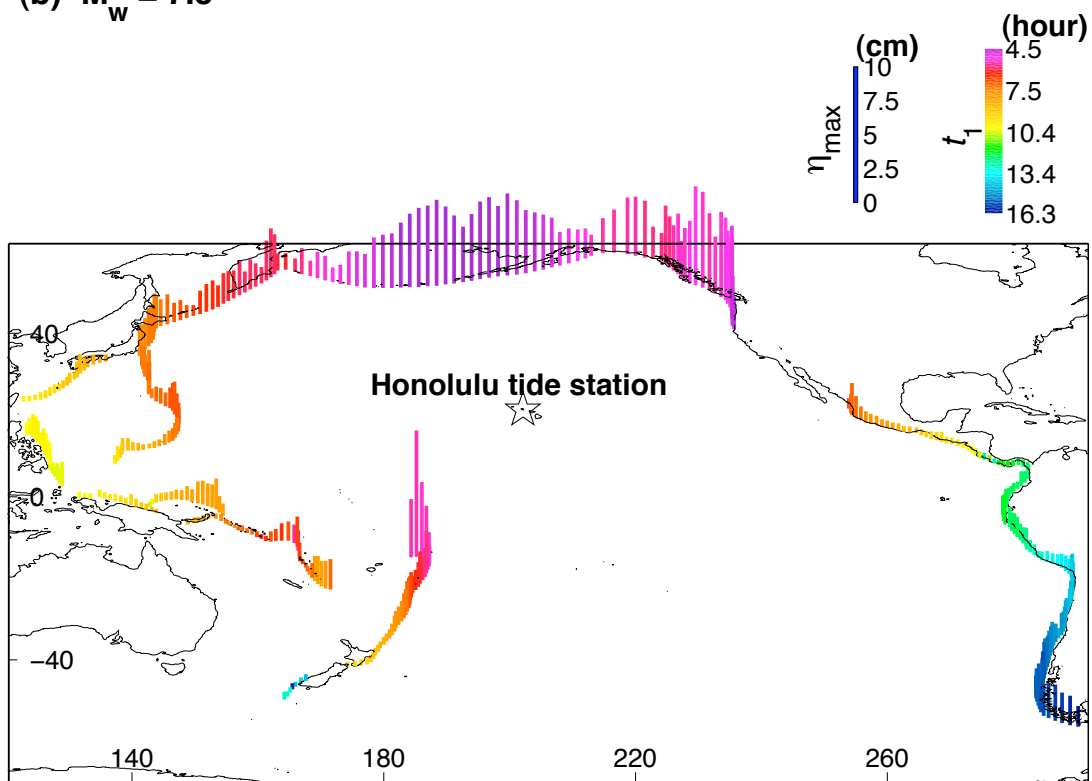
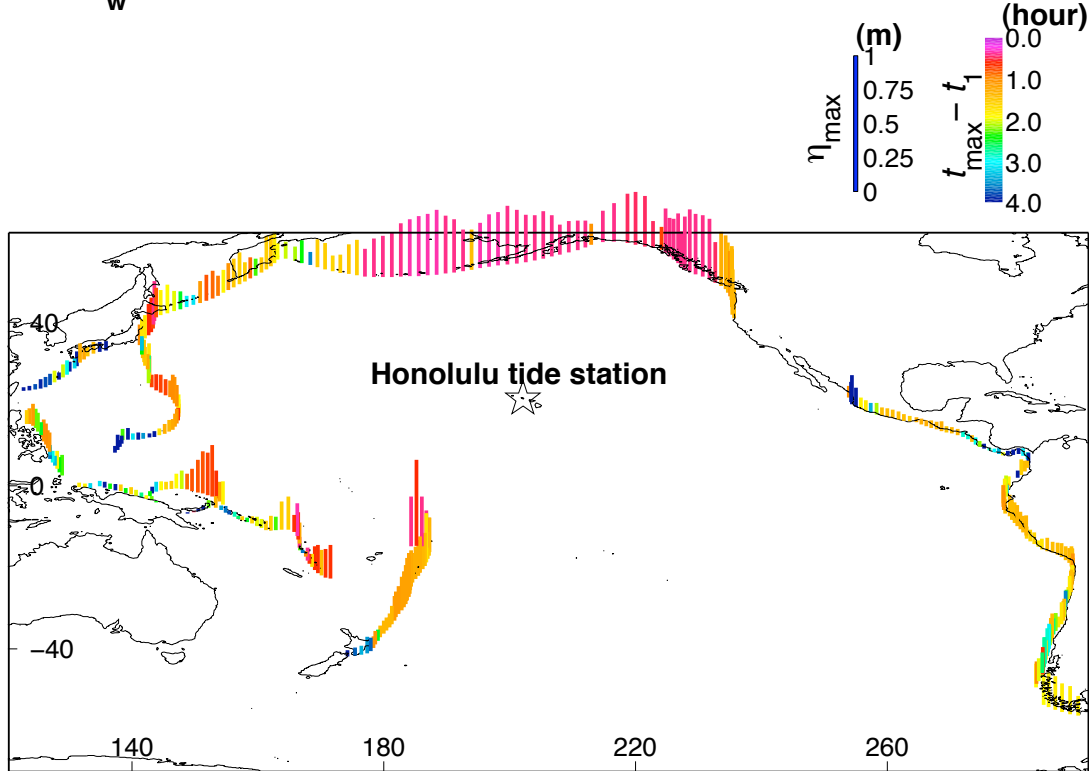
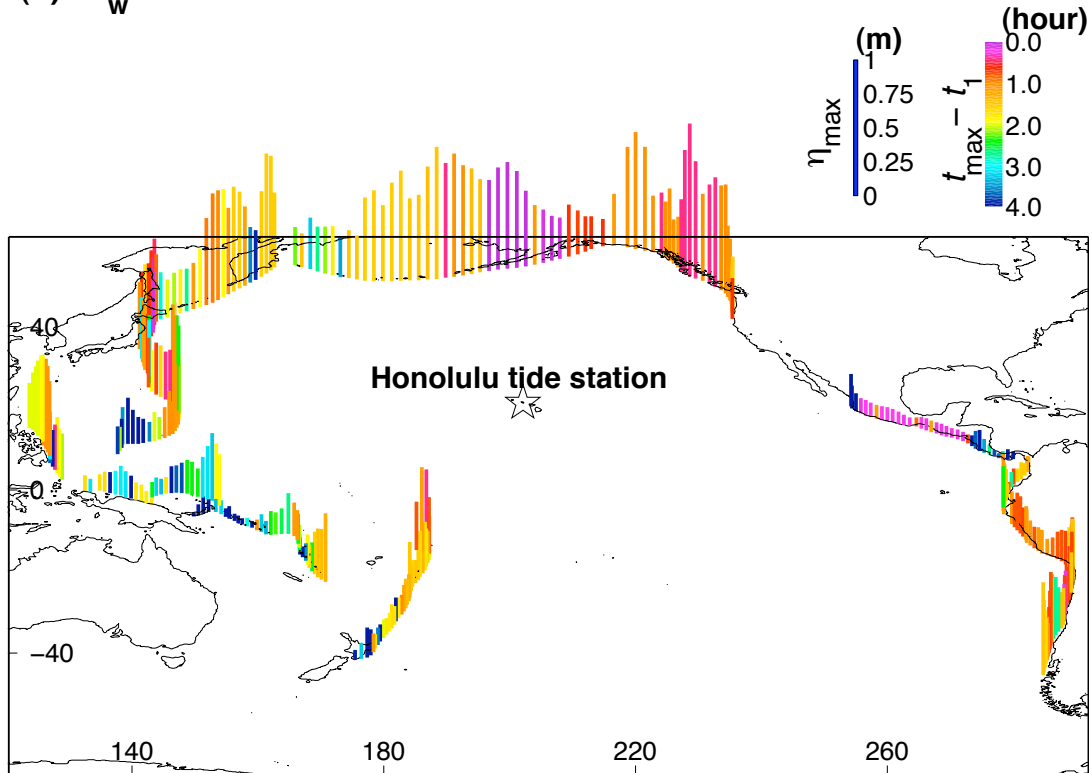


Figure 18 (a) Forecast accuracy and uncertainty in the η_{\max} at Honolulu tide station computed from the forecast model for the 36 scenarios. (b) Uncertainty v.s. peak period. Filled markers, 18 past tsunamis; open markers, 18 simulated $M_w = 9.3$ tsunamis.

(a) $M_w = 7.5$ (b) $M_w = 7.5$ 

(c) $M_w = 8.2$ (d) $M_w = 8.7$ 

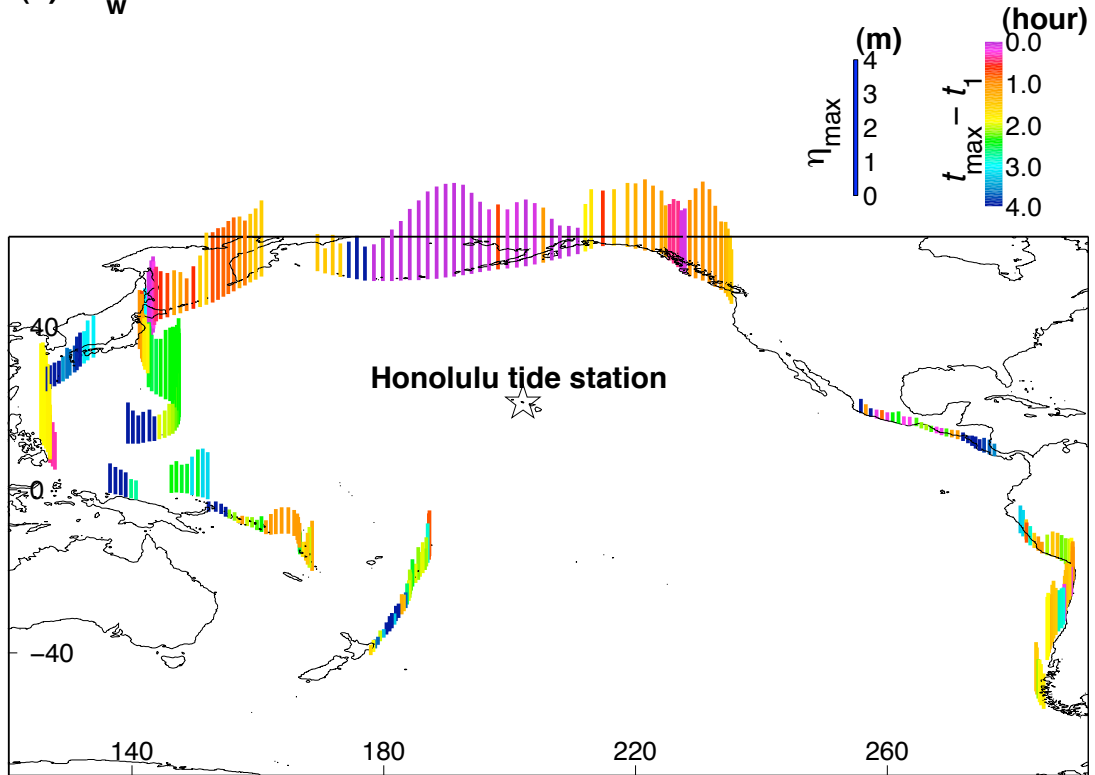
(e) $M_w = 9.3$ 

Figure 19 Maximum water elevation at (a) Honolulu offshore from the propagation database and (b,c, d and e) at Honolulu tide station computed by the Honolulu forecast model for simulated magnitude 7.5, 8.2, 8.7 and 9.3 tsunamis. Colors in (b) represent the first arrival at the station. Colors in (c), (d) and (e) represent the difference in time between the arrival of the maximum elevation and the first arrival.

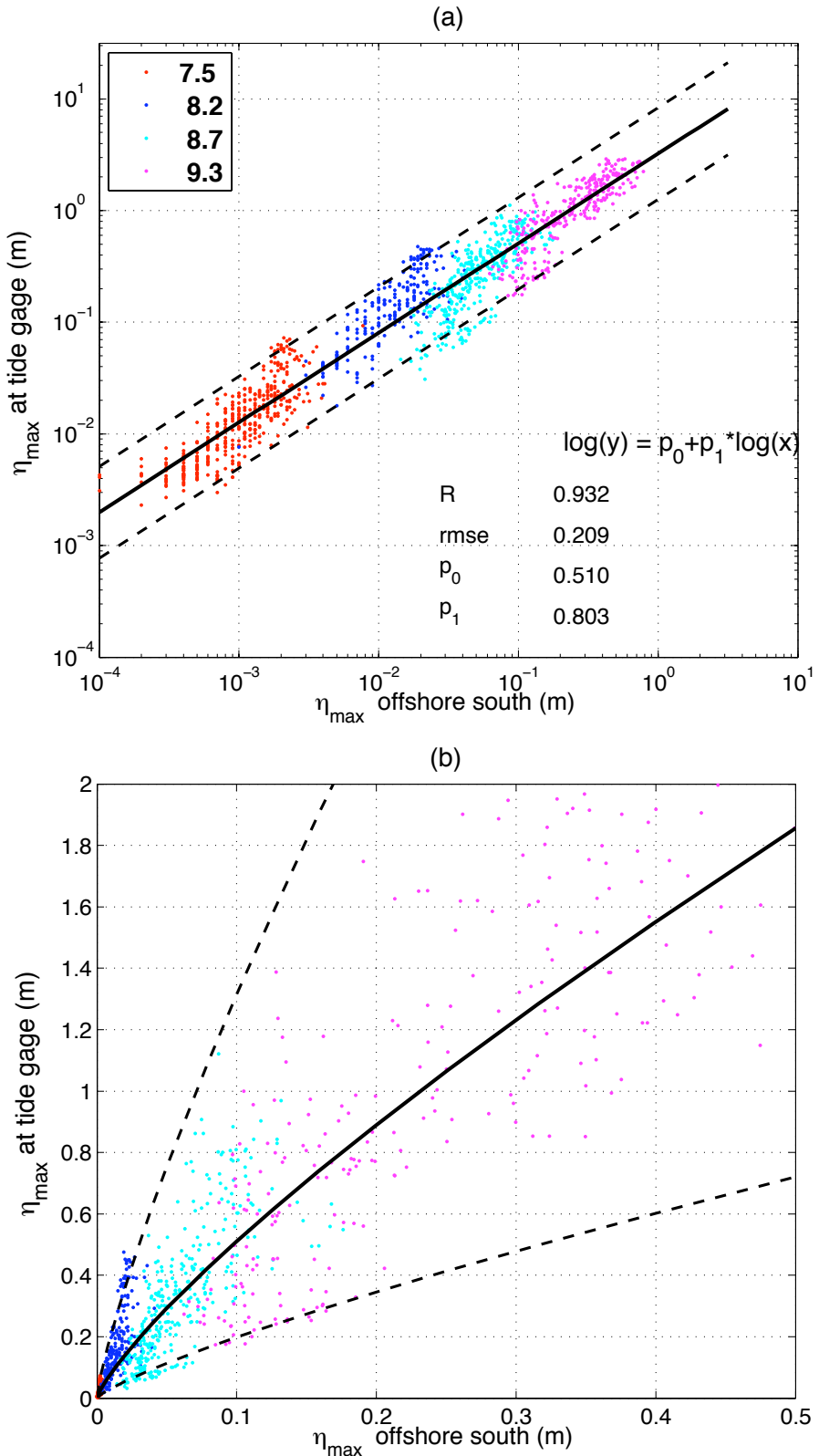


Figure 20 Computed maximum water elevation at offshore deep water (4440 m) and Honolulu tide station (~ 7 m) in (a) logarithmic and (b) Cartesian coordinates. Colors represent tsunami magnitudes. Solid line is the fit by regression analysis in logarithmic scale. Dashed lines are the prediction bounds based on 95% confident level. R, square of the correlation; rmse, root mean squared error; p_0 and p_1 , parameters.

Appendix B

Propagation Database: Pacific Ocean Unit Sources

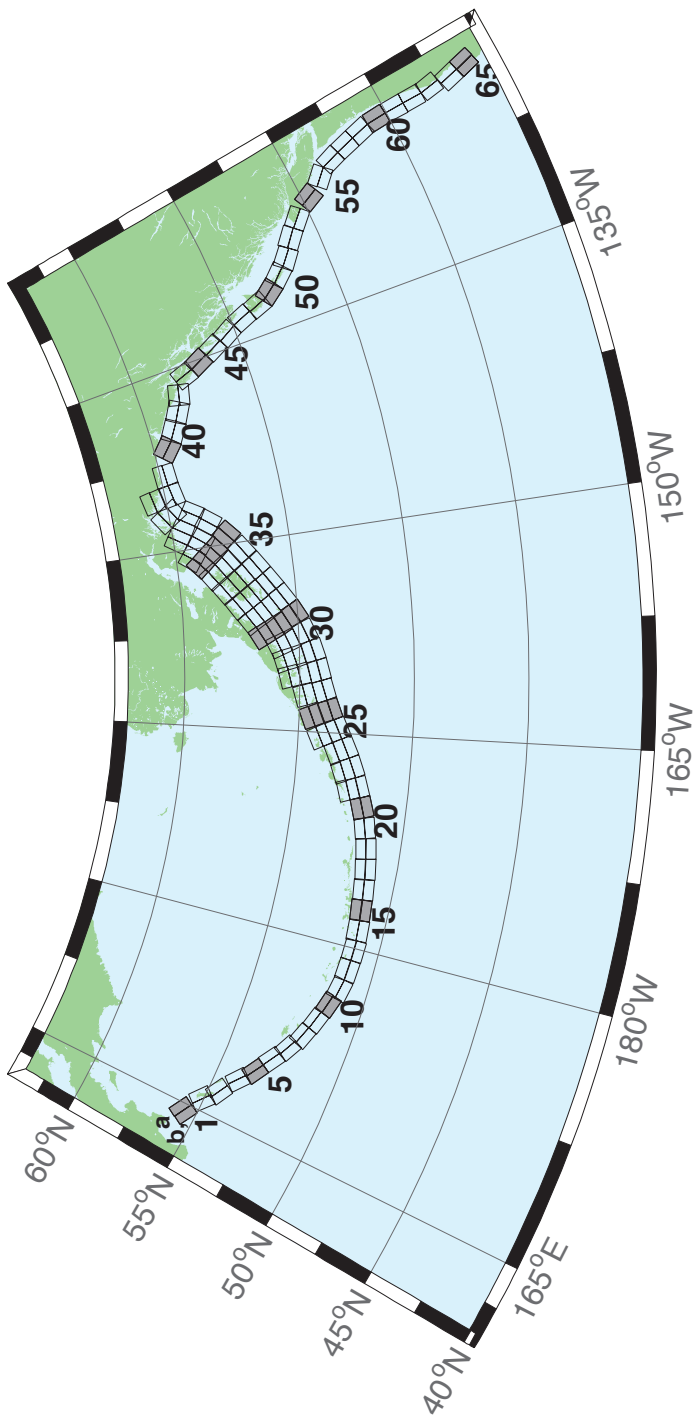


Figure B.1: Aleutian–Alaska–Cascadia Subduction Zone unit sources.

Table B.1: Earthquake parameters for Aleutian–Alaska–Cascadia Subduction Zone unit sources.

Segment	Description	Longitude(°E)	Latitude(°N)	Strike(°)	Dip(°)	Depth (km)
acsz-1a	Aleutian–Alaska–Cascadia	164.7994	55.9606	299	17	19.61
acsz-1b	Aleutian–Alaska–Cascadia	164.4310	55.5849	299	17	5
acsz-2a	Aleutian–Alaska–Cascadia	166.3418	55.4016	310.2	17	19.61
acsz-2b	Aleutian–Alaska–Cascadia	165.8578	55.0734	310.2	17	5
acsz-3a	Aleutian–Alaska–Cascadia	167.2939	54.8919	300.2	23.36	24.82
acsz-3b	Aleutian–Alaska–Cascadia	166.9362	54.5356	300.2	23.36	5
acsz-4a	Aleutian–Alaska–Cascadia	168.7131	54.2852	310.2	38.51	25.33
acsz-4b	Aleutian–Alaska–Cascadia	168.3269	54.0168	310.2	24	5
acsz-5a	Aleutian–Alaska–Cascadia	169.7447	53.7808	302.8	37.02	23.54
acsz-5b	Aleutian–Alaska–Cascadia	169.4185	53.4793	302.8	21.77	5
acsz-6a	Aleutian–Alaska–Cascadia	171.0144	53.3054	303.2	35.31	22.92
acsz-6b	Aleutian–Alaska–Cascadia	170.6813	52.9986	303.2	21	5
acsz-7a	Aleutian–Alaska–Cascadia	172.1500	52.8528	298.2	35.56	20.16
acsz-7b	Aleutian–Alaska–Cascadia	171.8665	52.5307	298.2	17.65	5
acsz-8a	Aleutian–Alaska–Cascadia	173.2726	52.4579	290.8	37.92	20.35
acsz-8b	Aleutian–Alaska–Cascadia	173.0681	52.1266	290.8	17.88	5
acsz-9a	Aleutian–Alaska–Cascadia	174.5866	52.1434	289	39.09	21.05
acsz-9b	Aleutian–Alaska–Cascadia	174.4027	51.8138	289	18.73	5
acsz-10a	Aleutian–Alaska–Cascadia	175.8784	51.8526	286.1	40.51	20.87
acsz-10b	Aleutian–Alaska–Cascadia	175.7265	51.5245	286.1	18.51	5
acsz-11a	Aleutian–Alaska–Cascadia	177.1140	51.6488	280	15	17.94
acsz-11b	Aleutian–Alaska–Cascadia	176.9937	51.2215	280	15	5
acsz-12a	Aleutian–Alaska–Cascadia	178.4500	51.5690	273	15	17.94
acsz-12b	Aleutian–Alaska–Cascadia	178.4130	51.1200	273	15	5
acsz-13a	Aleutian–Alaska–Cascadia	179.8550	51.5340	271	15	17.94
acsz-13b	Aleutian–Alaska–Cascadia	179.8420	51.0850	271	15	5
acsz-14a	Aleutian–Alaska–Cascadia	181.2340	51.5780	267	15	17.94
acsz-14b	Aleutian–Alaska–Cascadia	181.2720	51.1290	267	15	5
acsz-15a	Aleutian–Alaska–Cascadia	182.6380	51.6470	265	15	17.94
acsz-15b	Aleutian–Alaska–Cascadia	182.7000	51.2000	265	15	5
acsz-16a	Aleutian–Alaska–Cascadia	184.0550	51.7250	264	15	17.94
acsz-16b	Aleutian–Alaska–Cascadia	184.1280	51.2780	264	15	5
acsz-17a	Aleutian–Alaska–Cascadia	185.4560	51.8170	262	15	17.94
acsz-17b	Aleutian–Alaska–Cascadia	185.5560	51.3720	262	15	5
acsz-18a	Aleutian–Alaska–Cascadia	186.8680	51.9410	261	15	17.94
acsz-18b	Aleutian–Alaska–Cascadia	186.9810	51.4970	261	15	5
acsz-19a	Aleutian–Alaska–Cascadia	188.2430	52.1280	257	15	17.94
acsz-19b	Aleutian–Alaska–Cascadia	188.4060	51.6900	257	15	5
acsz-20a	Aleutian–Alaska–Cascadia	189.5810	52.3550	251	15	17.94
acsz-20b	Aleutian–Alaska–Cascadia	189.8180	51.9300	251	15	5
acsz-21a	Aleutian–Alaska–Cascadia	190.9570	52.6470	251	15	17.94
acsz-21b	Aleutian–Alaska–Cascadia	191.1960	52.2220	251	15	5
acsz-21z	Aleutian–Alaska–Cascadia	190.7399	53.0443	250.8	15	30.88
acsz-22a	Aleutian–Alaska–Cascadia	192.2940	52.9430	247	15	17.94
acsz-22b	Aleutian–Alaska–Cascadia	192.5820	52.5300	247	15	5
acsz-22z	Aleutian–Alaska–Cascadia	192.0074	53.3347	247.8	15	30.88
acsz-23a	Aleutian–Alaska–Cascadia	193.6270	53.3070	245	15	17.94
acsz-23b	Aleutian–Alaska–Cascadia	193.9410	52.9000	245	15	5
acsz-23z	Aleutian–Alaska–Cascadia	193.2991	53.6768	244.6	15	30.88
acsz-24a	Aleutian–Alaska–Cascadia	194.9740	53.6870	245	15	17.94
acsz-24b	Aleutian–Alaska–Cascadia	195.2910	53.2800	245	15	5
acsz-24y	Aleutian–Alaska–Cascadia	194.3645	54.4604	244.4	15	43.82
acsz-24z	Aleutian–Alaska–Cascadia	194.6793	54.0674	244.6	15	30.88

Continued on next page

Table B.1 – continued

Segment	Description	Longitude(°E)	Latitude(°N)	Strike(°)	Dip(°)	Depth (km)
acsz-25a	Aleutian–Alaska–Cascadia	196.4340	54.0760	250	15	17.94
acsz-25b	Aleutian–Alaska–Cascadia	196.6930	53.6543	250	15	5
acsz-25y	Aleutian–Alaska–Cascadia	195.9009	54.8572	247.9	15	43.82
acsz-25z	Aleutian–Alaska–Cascadia	196.1761	54.4536	248.1	15	30.88
acsz-26a	Aleutian–Alaska–Cascadia	197.8970	54.3600	253	15	17.94
acsz-26b	Aleutian–Alaska–Cascadia	198.1200	53.9300	253	15	5
acsz-26y	Aleutian–Alaska–Cascadia	197.5498	55.1934	253.1	15	43.82
acsz-26z	Aleutian–Alaska–Cascadia	197.7620	54.7770	253.3	15	30.88
acsz-27a	Aleutian–Alaska–Cascadia	199.4340	54.5960	256	15	17.94
acsz-27b	Aleutian–Alaska–Cascadia	199.6200	54.1600	256	15	5
acsz-27x	Aleutian–Alaska–Cascadia	198.9736	55.8631	256.5	15	56.24
acsz-27y	Aleutian–Alaska–Cascadia	199.1454	55.4401	256.6	15	43.82
acsz-27z	Aleutian–Alaska–Cascadia	199.3135	55.0170	256.8	15	30.88
acsz-28a	Aleutian–Alaska–Cascadia	200.8820	54.8300	253	15	17.94
acsz-28b	Aleutian–Alaska–Cascadia	201.1080	54.4000	253	15	5
acsz-28x	Aleutian–Alaska–Cascadia	200.1929	56.0559	252.5	15	56.24
acsz-28y	Aleutian–Alaska–Cascadia	200.4167	55.6406	252.7	15	43.82
acsz-28z	Aleutian–Alaska–Cascadia	200.6360	55.2249	252.9	15	30.88
acsz-29a	Aleutian–Alaska–Cascadia	202.2610	55.1330	247	15	17.94
acsz-29b	Aleutian–Alaska–Cascadia	202.5650	54.7200	247	15	5
acsz-29x	Aleutian–Alaska–Cascadia	201.2606	56.2861	245.7	15	56.24
acsz-29y	Aleutian–Alaska–Cascadia	201.5733	55.8888	246	15	43.82
acsz-29z	Aleutian–Alaska–Cascadia	201.8797	55.4908	246.2	15	30.88
acsz-30a	Aleutian–Alaska–Cascadia	203.6040	55.5090	240	15	17.94
acsz-30b	Aleutian–Alaska–Cascadia	203.9970	55.1200	240	15	5
acsz-30w	Aleutian–Alaska–Cascadia	201.9901	56.9855	239.5	15	69.12
acsz-30x	Aleutian–Alaska–Cascadia	202.3851	56.6094	239.8	15	56.24
acsz-30y	Aleutian–Alaska–Cascadia	202.7724	56.2320	240.2	15	43.82
acsz-30z	Aleutian–Alaska–Cascadia	203.1521	55.8534	240.5	15	30.88
acsz-31a	Aleutian–Alaska–Cascadia	204.8950	55.9700	236	15	17.94
acsz-31b	Aleutian–Alaska–Cascadia	205.3400	55.5980	236	15	5
acsz-31w	Aleutian–Alaska–Cascadia	203.0825	57.3740	234.5	15	69.12
acsz-31x	Aleutian–Alaska–Cascadia	203.5408	57.0182	234.9	15	56.24
acsz-31y	Aleutian–Alaska–Cascadia	203.9904	56.6607	235.3	15	43.82
acsz-31z	Aleutian–Alaska–Cascadia	204.4315	56.3016	235.7	15	30.88
acsz-32a	Aleutian–Alaska–Cascadia	206.2080	56.4730	236	15	17.94
acsz-32b	Aleutian–Alaska–Cascadia	206.6580	56.1000	236	15	5
acsz-32w	Aleutian–Alaska–Cascadia	204.4129	57.8908	234.3	15	69.12
acsz-32x	Aleutian–Alaska–Cascadia	204.8802	57.5358	234.7	15	56.24
acsz-32y	Aleutian–Alaska–Cascadia	205.3385	57.1792	235.1	15	43.82
acsz-32z	Aleutian–Alaska–Cascadia	205.7880	56.8210	235.5	15	30.88
acsz-33a	Aleutian–Alaska–Cascadia	207.5370	56.9750	236	15	17.94
acsz-33b	Aleutian–Alaska–Cascadia	207.9930	56.6030	236	15	5
acsz-33w	Aleutian–Alaska–Cascadia	205.7126	58.3917	234.2	15	69.12
acsz-33x	Aleutian–Alaska–Cascadia	206.1873	58.0371	234.6	15	56.24
acsz-33y	Aleutian–Alaska–Cascadia	206.6527	57.6808	235	15	43.82
acsz-33z	Aleutian–Alaska–Cascadia	207.1091	57.3227	235.4	15	30.88
acsz-34a	Aleutian–Alaska–Cascadia	208.9371	57.5124	236	15	17.94
acsz-34b	Aleutian–Alaska–Cascadia	209.4000	57.1400	236	15	5
acsz-34w	Aleutian–Alaska–Cascadia	206.9772	58.8804	233.5	15	69.12
acsz-34x	Aleutian–Alaska–Cascadia	207.4677	58.5291	233.9	15	56.24
acsz-34y	Aleutian–Alaska–Cascadia	207.9485	58.1760	234.3	15	43.82
acsz-34z	Aleutian–Alaska–Cascadia	208.4198	57.8213	234.7	15	30.88
acsz-35a	Aleutian–Alaska–Cascadia	210.2597	58.0441	230	15	17.94
acsz-35b	Aleutian–Alaska–Cascadia	210.8000	57.7000	230	15	5

Continued on next page

Table B.1 – continued

Segment	Description	Longitude(°E)	Latitude(°N)	Strike(°)	Dip(°)	Depth (km)
acsz-35w	Aleutian–Alaska–Cascadia	208.0204	59.3199	228.8	15	69.12
acsz-35x	Aleutian–Alaska–Cascadia	208.5715	58.9906	229.3	15	56.24
acsz-35y	Aleutian–Alaska–Cascadia	209.1122	58.6590	229.7	15	43.82
acsz-35z	Aleutian–Alaska–Cascadia	209.6425	58.3252	230.2	15	30.88
acsz-36a	Aleutian–Alaska–Cascadia	211.3249	58.6565	218	15	17.94
acsz-36b	Aleutian–Alaska–Cascadia	212.0000	58.3800	218	15	5
acsz-36w	Aleutian–Alaska–Cascadia	208.5003	59.5894	215.6	15	69.12
acsz-36x	Aleutian–Alaska–Cascadia	209.1909	59.3342	216.2	15	56.24
acsz-36y	Aleutian–Alaska–Cascadia	209.8711	59.0753	216.8	15	43.82
acsz-36z	Aleutian–Alaska–Cascadia	210.5412	58.8129	217.3	15	30.88
acsz-37a	Aleutian–Alaska–Cascadia	212.2505	59.2720	213.7	15	17.94
acsz-37b	Aleutian–Alaska–Cascadia	212.9519	59.0312	213.7	15	5
acsz-37x	Aleutian–Alaska–Cascadia	210.1726	60.0644	213	15	56.24
acsz-37y	Aleutian–Alaska–Cascadia	210.8955	59.8251	213.7	15	43.82
acsz-37z	Aleutian–Alaska–Cascadia	211.6079	59.5820	214.3	15	30.88
acsz-38a	Aleutian–Alaska–Cascadia	214.6555	60.1351	260.1	0	15
acsz-38b	Aleutian–Alaska–Cascadia	214.8088	59.6927	260.1	0	15
acsz-38y	Aleutian–Alaska–Cascadia	214.3737	60.9838	259	0	15
acsz-38z	Aleutian–Alaska–Cascadia	214.5362	60.5429	259	0	15
acsz-39a	Aleutian–Alaska–Cascadia	216.5607	60.2480	267	0	15
acsz-39b	Aleutian–Alaska–Cascadia	216.6068	59.7994	267	0	15
acsz-40a	Aleutian–Alaska–Cascadia	219.3069	59.7574	310.9	0	15
acsz-40b	Aleutian–Alaska–Cascadia	218.7288	59.4180	310.9	0	15
acsz-41a	Aleutian–Alaska–Cascadia	220.4832	59.3390	300.7	0	15
acsz-41b	Aleutian–Alaska–Cascadia	220.0382	58.9529	300.7	0	15
acsz-42a	Aleutian–Alaska–Cascadia	221.8835	58.9310	298.9	0	15
acsz-42b	Aleutian–Alaska–Cascadia	221.4671	58.5379	298.9	0	15
acsz-43a	Aleutian–Alaska–Cascadia	222.9711	58.6934	282.3	0	15
acsz-43b	Aleutian–Alaska–Cascadia	222.7887	58.2546	282.3	0	15
acsz-44a	Aleutian–Alaska–Cascadia	224.9379	57.9054	340.9	12	11.09
acsz-44b	Aleutian–Alaska–Cascadia	224.1596	57.7617	340.9	7	5
acsz-45a	Aleutian–Alaska–Cascadia	225.4994	57.1634	334.1	12	11.09
acsz-45b	Aleutian–Alaska–Cascadia	224.7740	56.9718	334.1	7	5
acsz-46a	Aleutian–Alaska–Cascadia	226.1459	56.3552	334.1	12	11.09
acsz-46b	Aleutian–Alaska–Cascadia	225.4358	56.1636	334.1	7	5
acsz-47a	Aleutian–Alaska–Cascadia	226.7731	55.5830	332.3	12	11.09
acsz-47b	Aleutian–Alaska–Cascadia	226.0887	55.3785	332.3	7	5
acsz-48a	Aleutian–Alaska–Cascadia	227.4799	54.6763	339.4	12	11.09
acsz-48b	Aleutian–Alaska–Cascadia	226.7713	54.5217	339.4	7	5
acsz-49a	Aleutian–Alaska–Cascadia	227.9482	53.8155	341.2	12	11.09
acsz-49b	Aleutian–Alaska–Cascadia	227.2462	53.6737	341.2	7	5
acsz-50a	Aleutian–Alaska–Cascadia	228.3970	53.2509	324.5	12	11.09
acsz-50b	Aleutian–Alaska–Cascadia	227.8027	52.9958	324.5	7	5
acsz-51a	Aleutian–Alaska–Cascadia	229.1844	52.6297	318.4	12	11.09
acsz-51b	Aleutian–Alaska–Cascadia	228.6470	52.3378	318.4	7	5
acsz-52a	Aleutian–Alaska–Cascadia	230.0306	52.0768	310.9	12	11.09
acsz-52b	Aleutian–Alaska–Cascadia	229.5665	51.7445	310.9	7	5
acsz-53a	Aleutian–Alaska–Cascadia	231.1735	51.5258	310.9	12	11.09
acsz-53b	Aleutian–Alaska–Cascadia	230.7150	51.1935	310.9	7	5
acsz-54a	Aleutian–Alaska–Cascadia	232.2453	50.8809	314.1	12	11.09
acsz-54b	Aleutian–Alaska–Cascadia	231.7639	50.5655	314.1	7	5
acsz-55a	Aleutian–Alaska–Cascadia	233.3066	49.9032	333.7	12	11.09
acsz-55b	Aleutian–Alaska–Cascadia	232.6975	49.7086	333.7	7	5
acsz-56a	Aleutian–Alaska–Cascadia	234.0588	49.1702	315	11	12.82
acsz-56b	Aleutian–Alaska–Cascadia	233.5849	48.8584	315	9	5

Continued on next page

Table B.1 – continued

Segment	Description	Longitude($^{\circ}$ E)	Latitude($^{\circ}$ N)	Strike($^{\circ}$)	Dip($^{\circ}$)	Depth (km)
acsz-57a	Aleutian–Alaska–Cascadia	234.9041	48.2596	341	11	12.82
acsz-57b	Aleutian–Alaska–Cascadia	234.2797	48.1161	341	9	5
acsz-58a	Aleutian–Alaska–Cascadia	235.3021	47.3812	344	11	12.82
acsz-58b	Aleutian–Alaska–Cascadia	234.6776	47.2597	344	9	5
acsz-59a	Aleutian–Alaska–Cascadia	235.6432	46.5082	345	11	12.82
acsz-59b	Aleutian–Alaska–Cascadia	235.0257	46.3941	345	9	5
acsz-60a	Aleutian–Alaska–Cascadia	235.8640	45.5429	356	11	12.82
acsz-60b	Aleutian–Alaska–Cascadia	235.2363	45.5121	356	9	5
acsz-61a	Aleutian–Alaska–Cascadia	235.9106	44.6227	359	11	12.82
acsz-61b	Aleutian–Alaska–Cascadia	235.2913	44.6150	359	9	5
acsz-62a	Aleutian–Alaska–Cascadia	235.9229	43.7245	359	11	12.82
acsz-62b	Aleutian–Alaska–Cascadia	235.3130	43.7168	359	9	5
acsz-63a	Aleutian–Alaska–Cascadia	236.0220	42.9020	350	11	12.82
acsz-63b	Aleutian–Alaska–Cascadia	235.4300	42.8254	350	9	5
acsz-64a	Aleutian–Alaska–Cascadia	235.9638	41.9818	345	11	12.82
acsz-64b	Aleutian–Alaska–Cascadia	235.3919	41.8677	345	9	5
acsz-65a	Aleutian–Alaska–Cascadia	236.2643	41.1141	345	11	12.82
acsz-65b	Aleutian–Alaska–Cascadia	235.7000	41.0000	345	9	5
acsz-238a	Aleutian–Alaska–Cascadia	213.2878	59.8406	236.8	15	17.94
acsz-238y	Aleutian–Alaska–Cascadia	212.3424	60.5664	236.8	15	43.82
acsz-238z	Aleutian–Alaska–Cascadia	212.8119	60.2035	236.8	15	30.88

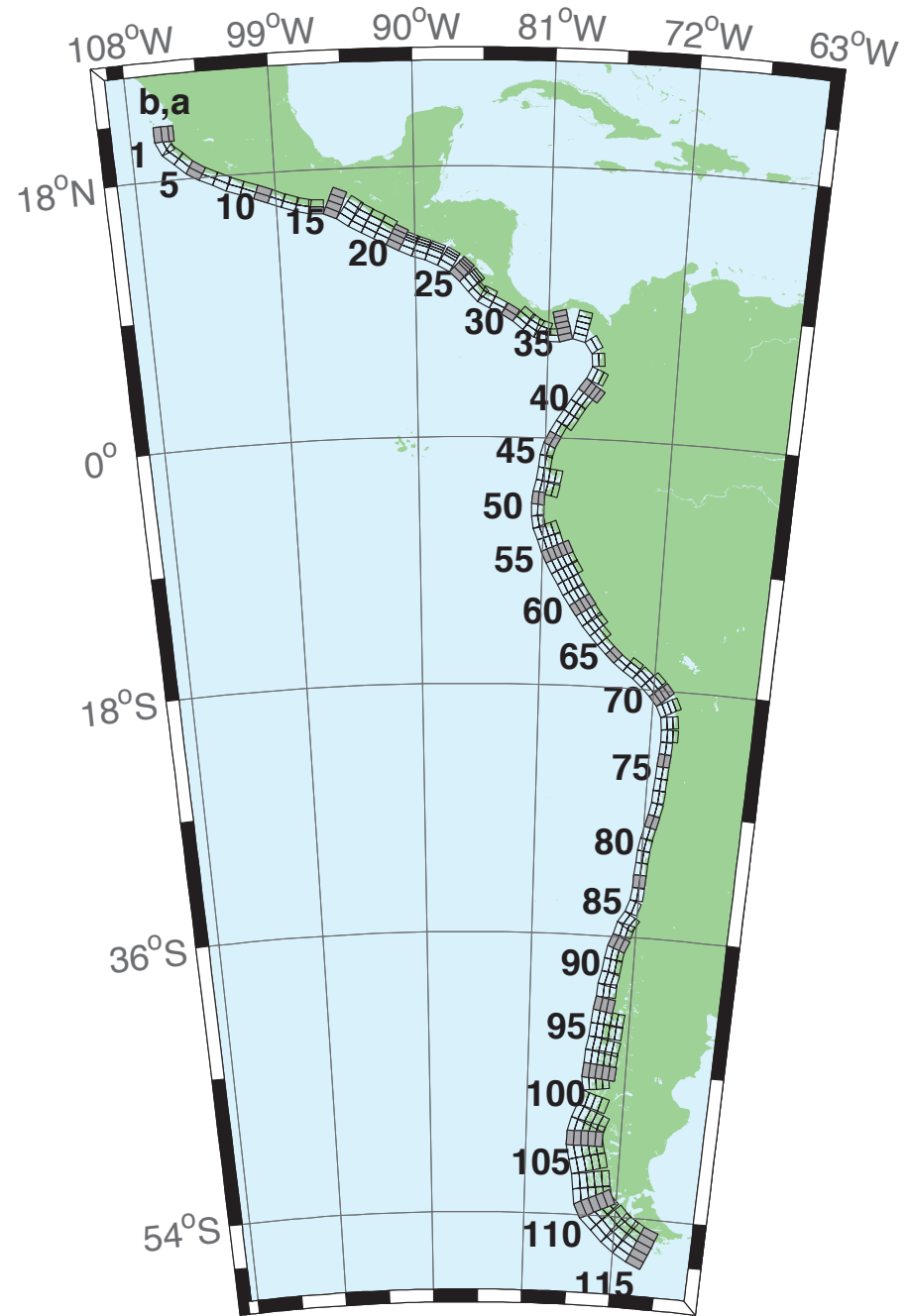


Figure B.2: Central and South America Subduction Zone unit sources.

Table B.2: Earthquake parameters for Central and South America Subduction Zone unit sources.

Segment	Description	Longitude(°E)	Latitude(°N)	Strike(°)	Dip(°)	Depth (km)
cssz-1a	Central and South America	254.4573	20.8170	359	19	15.4
cssz-1b	Central and South America	254.0035	20.8094	359	12	5
cssz-1z	Central and South America	254.7664	20.8222	359	50	31.67
cssz-2a	Central and South America	254.5765	20.2806	336.8	19	15.4
cssz-2b	Central and South America	254.1607	20.1130	336.8	12	5
cssz-3a	Central and South America	254.8789	19.8923	310.6	18.31	15.27
cssz-3b	Central and South America	254.5841	19.5685	310.6	11.85	5
cssz-4a	Central and South America	255.6167	19.2649	313.4	17.62	15.12
cssz-4b	Central and South America	255.3056	18.9537	313.4	11.68	5
cssz-5a	Central and South America	256.2240	18.8148	302.7	16.92	15
cssz-5b	Central and South America	255.9790	18.4532	302.7	11.54	5
cssz-6a	Central and South America	256.9425	18.4383	295.1	16.23	14.87
cssz-6b	Central and South America	256.7495	18.0479	295.1	11.38	5
cssz-7a	Central and South America	257.8137	18.0339	296.9	15.54	14.74
cssz-7b	Central and South America	257.6079	17.6480	296.9	11.23	5
cssz-8a	Central and South America	258.5779	17.7151	290.4	14.85	14.61
cssz-8b	Central and South America	258.4191	17.3082	290.4	11.08	5
cssz-9a	Central and South America	259.4578	17.4024	290.5	14.15	14.47
cssz-9b	Central and South America	259.2983	16.9944	290.5	10.92	5
cssz-10a	Central and South America	260.3385	17.0861	290.8	13.46	14.34
cssz-10b	Central and South America	260.1768	16.6776	290.8	10.77	5
cssz-11a	Central and South America	261.2255	16.7554	291.8	12.77	14.21
cssz-11b	Central and South America	261.0556	16.3487	291.8	10.62	5
cssz-12a	Central and South America	262.0561	16.4603	288.9	12.08	14.08
cssz-12b	Central and South America	261.9082	16.0447	288.9	10.46	5
cssz-13a	Central and South America	262.8638	16.2381	283.2	11.38	13.95
cssz-13b	Central and South America	262.7593	15.8094	283.2	10.31	5
cssz-14a	Central and South America	263.6066	16.1435	272.1	10.69	13.81
cssz-14b	Central and South America	263.5901	15.7024	272.1	10.15	5
cssz-15a	Central and South America	264.8259	15.8829	293	10	13.68
cssz-15b	Central and South America	264.6462	15.4758	293	10	5
cssz-15y	Central and South America	265.1865	16.6971	293	10	31.05
cssz-15z	Central and South America	265.0060	16.2900	293	10	22.36
cssz-16a	Central and South America	265.7928	15.3507	304.9	15	15.82
cssz-16b	Central and South America	265.5353	14.9951	304.9	12.5	5
cssz-16y	Central and South America	266.3092	16.0619	304.9	15	41.7
cssz-16z	Central and South America	266.0508	15.7063	304.9	15	28.76
cssz-17a	Central and South America	266.4947	14.9019	299.5	20	17.94
cssz-17b	Central and South America	266.2797	14.5346	299.5	15	5
cssz-17y	Central and South America	266.9259	15.6365	299.5	20	52.14
cssz-17z	Central and South America	266.7101	15.2692	299.5	20	35.04
cssz-18a	Central and South America	267.2827	14.4768	298	21.5	17.94
cssz-18b	Central and South America	267.0802	14.1078	298	15	5
cssz-18y	Central and South America	267.6888	15.2148	298	21.5	54.59
cssz-18z	Central and South America	267.4856	14.8458	298	21.5	36.27
cssz-19a	Central and South America	268.0919	14.0560	297.6	23	17.94
cssz-19b	Central and South America	267.8943	13.6897	297.6	15	5
cssz-19y	Central and South America	268.4880	14.7886	297.6	23	57.01
cssz-19z	Central and South America	268.2898	14.4223	297.6	23	37.48
cssz-20a	Central and South America	268.8929	13.6558	296.2	24	17.94
cssz-20b	Central and South America	268.7064	13.2877	296.2	15	5
cssz-20y	Central and South America	269.1796	14.2206	296.2	45.5	73.94
cssz-20z	Central and South America	269.0362	13.9382	296.2	45.5	38.28

Continued on next page

Table B.2 – continued

Segment	Description	Longitude($^{\circ}$ E)	Latitude($^{\circ}$ N)	Strike($^{\circ}$)	Dip($^{\circ}$)	Depth (km)
cssz-21a	Central and South America	269.6797	13.3031	292.6	25	17.94
cssz-21b	Central and South America	269.5187	12.9274	292.6	15	5
cssz-21x	Central and South America	269.8797	13.7690	292.6	68	131.8
cssz-21y	Central and South America	269.8130	13.6137	292.6	68	85.43
cssz-21z	Central and South America	269.7463	13.4584	292.6	68	39.07
cssz-22a	Central and South America	270.4823	13.0079	288.6	25	17.94
cssz-22b	Central and South America	270.3492	12.6221	288.6	15	5
cssz-22x	Central and South America	270.6476	13.4864	288.6	68	131.8
cssz-22y	Central and South America	270.5925	13.3269	288.6	68	85.43
cssz-22z	Central and South America	270.5374	13.1674	288.6	68	39.07
cssz-23a	Central and South America	271.3961	12.6734	292.4	25	17.94
cssz-23b	Central and South America	271.2369	12.2972	292.4	15	5
cssz-23x	Central and South America	271.5938	13.1399	292.4	68	131.8
cssz-23y	Central and South America	271.5279	12.9844	292.4	68	85.43
cssz-23z	Central and South America	271.4620	12.8289	292.4	68	39.07
cssz-24a	Central and South America	272.3203	12.2251	300.2	25	17.94
cssz-24b	Central and South America	272.1107	11.8734	300.2	15	5
cssz-24x	Central and South America	272.5917	12.6799	300.2	67	131.1
cssz-24y	Central and South America	272.5012	12.5283	300.2	67	85.1
cssz-24z	Central and South America	272.4107	12.3767	300.2	67	39.07
cssz-25a	Central and South America	273.2075	11.5684	313.8	25	17.94
cssz-25b	Central and South America	272.9200	11.2746	313.8	15	5
cssz-25x	Central and South America	273.5950	11.9641	313.8	66	130.4
cssz-25y	Central and South America	273.4658	11.8322	313.8	66	84.75
cssz-25z	Central and South America	273.3366	11.7003	313.8	66	39.07
cssz-26a	Central and South America	273.8943	10.8402	320.4	25	17.94
cssz-26b	Central and South America	273.5750	10.5808	320.4	15	5
cssz-26x	Central and South America	274.3246	11.1894	320.4	66	130.4
cssz-26y	Central and South America	274.1811	11.0730	320.4	66	84.75
cssz-26z	Central and South America	274.0377	10.9566	320.4	66	39.07
cssz-27a	Central and South America	274.4569	10.2177	316.1	25	17.94
cssz-27b	Central and South America	274.1590	9.9354	316.1	15	5
cssz-27z	Central and South America	274.5907	10.3444	316.1	66	39.07
cssz-28a	Central and South America	274.9586	9.8695	297.1	22	14.54
cssz-28b	Central and South America	274.7661	9.4988	297.1	11	5
cssz-28z	Central and South America	275.1118	10.1643	297.1	42.5	33.27
cssz-29a	Central and South America	275.7686	9.4789	296.6	19	11.09
cssz-29b	Central and South America	275.5759	9.0992	296.6	7	5
cssz-30a	Central and South America	276.6346	8.9973	302.2	19	9.36
cssz-30b	Central and South America	276.4053	8.6381	302.2	5	5
cssz-31a	Central and South America	277.4554	8.4152	309.1	19	7.62
cssz-31b	Central and South America	277.1851	8.0854	309.1	3	5
cssz-31z	Central and South America	277.7260	8.7450	309.1	19	23.9
cssz-32a	Central and South America	278.1112	7.9425	303	18.67	8.49
cssz-32b	Central and South America	277.8775	7.5855	303	4	5
cssz-32z	Central and South America	278.3407	8.2927	303	21.67	24.49
cssz-33a	Central and South America	278.7082	7.6620	287.6	18.33	10.23
cssz-33b	Central and South America	278.5785	7.2555	287.6	6	5
cssz-33z	Central and South America	278.8328	8.0522	287.6	24.33	25.95
cssz-34a	Central and South America	279.3184	7.5592	269.5	18	17.94
cssz-34b	Central and South America	279.3223	7.1320	269.5	15	5
cssz-35a	Central and South America	280.0039	7.6543	255.9	17.67	14.54
cssz-35b	Central and South America	280.1090	7.2392	255.9	11	5
cssz-35x	Central and South America	279.7156	8.7898	255.9	29.67	79.22
cssz-35y	Central and South America	279.8118	8.4113	255.9	29.67	54.47

Continued on next page

Table B.2 – continued

Segment	Description	Longitude(°E)	Latitude(°N)	Strike(°)	Dip(°)	Depth (km)
cssz-35z	Central and South America	279.9079	8.0328	255.9	29.67	29.72
cssz-36a	Central and South America	281.2882	7.6778	282.5	17.33	11.09
cssz-36b	Central and South America	281.1948	7.2592	282.5	7	5
cssz-36x	Central and South America	281.5368	8.7896	282.5	32.33	79.47
cssz-36y	Central and South America	281.4539	8.4190	282.5	32.33	52.73
cssz-36z	Central and South America	281.3710	8.0484	282.5	32.33	25.99
cssz-37a	Central and South America	282.5252	6.8289	326.9	17	10.23
cssz-37b	Central and South America	282.1629	6.5944	326.9	6	5
cssz-38a	Central and South America	282.9469	5.5973	355.4	17	10.23
cssz-38b	Central and South America	282.5167	5.5626	355.4	6	5
cssz-39a	Central and South America	282.7236	4.3108	24.13	17	10.23
cssz-39b	Central and South America	282.3305	4.4864	24.13	6	5
cssz-39z	Central and South America	283.0603	4.1604	24.13	35	24.85
cssz-40a	Central and South America	282.1940	3.3863	35.28	17	10.23
cssz-40b	Central and South America	281.8427	3.6344	35.28	6	5
cssz-40y	Central and South America	282.7956	2.9613	35.28	35	53.52
cssz-40z	Central and South America	282.4948	3.1738	35.28	35	24.85
cssz-41a	Central and South America	281.6890	2.6611	34.27	17	10.23
cssz-41b	Central and South America	281.3336	2.9030	34.27	6	5
cssz-41z	Central and South America	281.9933	2.4539	34.27	35	24.85
cssz-42a	Central and South America	281.2266	1.9444	31.29	17	10.23
cssz-42b	Central and South America	280.8593	2.1675	31.29	6	5
cssz-42z	Central and South America	281.5411	1.7533	31.29	35	24.85
cssz-43a	Central and South America	280.7297	1.1593	33.3	17	10.23
cssz-43b	Central and South America	280.3706	1.3951	33.3	6	5
cssz-43z	Central and South America	281.0373	0.9573	33.3	35	24.85
cssz-44a	Central and South America	280.3018	0.4491	28.8	17	10.23
cssz-44b	Central and South America	279.9254	0.6560	28.8	6	5
cssz-45a	Central and South America	279.9083	-0.3259	26.91	10	8.49
cssz-45b	Central and South America	279.5139	-0.1257	26.91	4	5
cssz-46a	Central and South America	279.6461	-0.9975	15.76	10	8.49
cssz-46b	Central and South America	279.2203	-0.8774	15.76	4	5
cssz-47a	Central and South America	279.4972	-1.7407	6.9	10	8.49
cssz-47b	Central and South America	279.0579	-1.6876	6.9	4	5
cssz-48a	Central and South America	279.3695	-2.6622	8.96	10	8.49
cssz-48b	Central and South America	278.9321	-2.5933	8.96	4	5
cssz-48y	Central and South America	280.2444	-2.8000	8.96	10	25.85
cssz-48z	Central and South America	279.8070	-2.7311	8.96	10	17.17
cssz-49a	Central and South America	279.1852	-3.6070	13.15	10	8.49
cssz-49b	Central and South America	278.7536	-3.5064	13.15	4	5
cssz-49y	Central and South America	280.0486	-3.8082	13.15	10	25.85
cssz-49z	Central and South America	279.6169	-3.7076	13.15	10	17.17
cssz-50a	Central and South America	279.0652	-4.3635	4.78	10.33	9.64
cssz-50b	Central and South America	278.6235	-4.3267	4.78	5.33	5
cssz-51a	Central and South America	279.0349	-5.1773	359.4	10.67	10.81
cssz-51b	Central and South America	278.5915	-5.1817	359.4	6.67	5
cssz-52a	Central and South America	279.1047	-5.9196	349.8	11	11.96
cssz-52b	Central and South America	278.6685	-5.9981	349.8	8	5
cssz-53a	Central and South America	279.3044	-6.6242	339.2	10.25	11.74
cssz-53b	Central and South America	278.8884	-6.7811	339.2	7.75	5
cssz-53y	Central and South America	280.1024	-6.3232	339.2	19.25	37.12
cssz-53z	Central and South America	279.7035	-6.4737	339.2	19.25	20.64
cssz-54a	Central and South America	279.6256	-7.4907	340.8	9.5	11.53
cssz-54b	Central and South America	279.2036	-7.6365	340.8	7.5	5
cssz-54y	Central and South America	280.4267	-7.2137	340.8	20.5	37.29

Continued on next page

Table B.2 – continued

Segment	Description	Longitude(°E)	Latitude(°N)	Strike(°)	Dip(°)	Depth (km)
cssz-54z	Central and South America	280.0262	-7.3522	340.8	20.5	19.78
cssz-55a	Central and South America	279.9348	-8.2452	335.4	8.75	11.74
cssz-55b	Central and South America	279.5269	-8.4301	335.4	7.75	5
cssz-55x	Central and South America	281.0837	-7.7238	335.4	21.75	56.4
cssz-55y	Central and South America	280.7009	-7.8976	335.4	21.75	37.88
cssz-55z	Central and South America	280.3180	-8.0714	335.4	21.75	19.35
cssz-56a	Central and South America	280.3172	-8.9958	331.6	8	11.09
cssz-56b	Central and South America	279.9209	-9.2072	331.6	7	5
cssz-56x	Central and South America	281.4212	-8.4063	331.6	23	57.13
cssz-56y	Central and South America	281.0534	-8.6028	331.6	23	37.59
cssz-56z	Central and South America	280.6854	-8.7993	331.6	23	18.05
cssz-57a	Central and South America	280.7492	-9.7356	328.7	8.6	10.75
cssz-57b	Central and South America	280.3640	-9.9663	328.7	6.6	5
cssz-57x	Central and South America	281.8205	-9.0933	328.7	23.4	57.94
cssz-57y	Central and South America	281.4636	-9.3074	328.7	23.4	38.08
cssz-57z	Central and South America	281.1065	-9.5215	328.7	23.4	18.22
cssz-58a	Central and South America	281.2275	-10.5350	330.5	9.2	10.4
cssz-58b	Central and South America	280.8348	-10.7532	330.5	6.2	5
cssz-58y	Central and South America	281.9548	-10.1306	330.5	23.8	38.57
cssz-58z	Central and South America	281.5913	-10.3328	330.5	23.8	18.39
cssz-59a	Central and South America	281.6735	-11.2430	326.2	9.8	10.05
cssz-59b	Central and South America	281.2982	-11.4890	326.2	5.8	5
cssz-59y	Central and South America	282.3675	-10.7876	326.2	24.2	39.06
cssz-59z	Central and South America	282.0206	-11.0153	326.2	24.2	18.56
cssz-60a	Central and South America	282.1864	-11.9946	326.5	10.4	9.71
cssz-60b	Central and South America	281.8096	-12.2384	326.5	5.4	5
cssz-60y	Central and South America	282.8821	-11.5438	326.5	24.6	39.55
cssz-60z	Central and South America	282.5344	-11.7692	326.5	24.6	18.73
cssz-61a	Central and South America	282.6944	-12.7263	325.5	11	9.36
cssz-61b	Central and South America	282.3218	-12.9762	325.5	5	5
cssz-61y	Central and South America	283.3814	-12.2649	325.5	25	40.03
cssz-61z	Central and South America	283.0381	-12.4956	325.5	25	18.9
cssz-62a	Central and South America	283.1980	-13.3556	319	11	9.79
cssz-62b	Central and South America	282.8560	-13.6451	319	5.5	5
cssz-62y	Central and South America	283.8178	-12.8300	319	27	42.03
cssz-62z	Central and South America	283.5081	-13.0928	319	27	19.33
cssz-63a	Central and South America	283.8032	-14.0147	317.9	11	10.23
cssz-63b	Central and South America	283.4661	-14.3106	317.9	6	5
cssz-63z	Central and South America	284.1032	-13.7511	317.9	29	19.77
cssz-64a	Central and South America	284.4144	-14.6482	315.7	13	11.96
cssz-64b	Central and South America	284.0905	-14.9540	315.7	8	5
cssz-65a	Central and South America	285.0493	-15.2554	313.2	15	13.68
cssz-65b	Central and South America	284.7411	-15.5715	313.2	10	5
cssz-66a	Central and South America	285.6954	-15.7816	307.7	14.5	13.68
cssz-66b	Central and South America	285.4190	-16.1258	307.7	10	5
cssz-67a	Central and South America	286.4127	-16.2781	304.3	14	13.68
cssz-67b	Central and South America	286.1566	-16.6381	304.3	10	5
cssz-67z	Central and South America	286.6552	-15.9365	304.3	23	25.78
cssz-68a	Central and South America	287.2481	-16.9016	311.8	14	13.68
cssz-68b	Central and South America	286.9442	-17.2264	311.8	10	5
cssz-68z	Central and South America	287.5291	-16.6007	311.8	26	25.78
cssz-69a	Central and South America	287.9724	-17.5502	314.9	14	13.68
cssz-69b	Central and South America	287.6496	-17.8590	314.9	10	5
cssz-69y	Central and South America	288.5530	-16.9934	314.9	29	50.02
cssz-69z	Central and South America	288.2629	-17.2718	314.9	29	25.78

Continued on next page

Table B.2 – continued

Segment	Description	Longitude($^{\circ}$ E)	Latitude($^{\circ}$ N)	Strike($^{\circ}$)	Dip($^{\circ}$)	Depth (km)
cssz-70a	Central and South America	288.6731	-18.2747	320.4	14	13.25
cssz-70b	Central and South America	288.3193	-18.5527	320.4	9.5	5
cssz-70y	Central and South America	289.3032	-17.7785	320.4	30	50.35
cssz-70z	Central and South America	288.9884	-18.0266	320.4	30	25.35
cssz-71a	Central and South America	289.3089	-19.1854	333.2	14	12.82
cssz-71b	Central and South America	288.8968	-19.3820	333.2	9	5
cssz-71y	Central and South America	290.0357	-18.8382	333.2	31	50.67
cssz-71z	Central and South America	289.6725	-19.0118	333.2	31	24.92
cssz-72a	Central and South America	289.6857	-20.3117	352.4	14	12.54
cssz-72b	Central and South America	289.2250	-20.3694	352.4	8.67	5
cssz-72z	Central and South America	290.0882	-20.2613	352.4	32	24.63
cssz-73a	Central and South America	289.7731	-21.3061	358.9	14	12.24
cssz-73b	Central and South America	289.3053	-21.3142	358.9	8.33	5
cssz-73z	Central and South America	290.1768	-21.2991	358.9	33	24.34
cssz-74a	Central and South America	289.7610	-22.2671	3.06	14	11.96
cssz-74b	Central and South America	289.2909	-22.2438	3.06	8	5
cssz-75a	Central and South America	289.6982	-23.1903	4.83	14.09	11.96
cssz-75b	Central and South America	289.2261	-23.1536	4.83	8	5
cssz-76a	Central and South America	289.6237	-24.0831	4.67	14.18	11.96
cssz-76b	Central and South America	289.1484	-24.0476	4.67	8	5
cssz-77a	Central and South America	289.5538	-24.9729	4.3	14.27	11.96
cssz-77b	Central and South America	289.0750	-24.9403	4.3	8	5
cssz-78a	Central and South America	289.4904	-25.8621	3.86	14.36	11.96
cssz-78b	Central and South America	289.0081	-25.8328	3.86	8	5
cssz-79a	Central and South America	289.3491	-26.8644	11.34	14.45	11.96
cssz-79b	Central and South America	288.8712	-26.7789	11.34	8	5
cssz-80a	Central and South America	289.1231	-27.7826	14.16	14.54	11.96
cssz-80b	Central and South America	288.6469	-27.6762	14.16	8	5
cssz-81a	Central and South America	288.8943	-28.6409	13.19	14.63	11.96
cssz-81b	Central and South America	288.4124	-28.5417	13.19	8	5
cssz-82a	Central and South America	288.7113	-29.4680	9.68	14.72	11.96
cssz-82b	Central and South America	288.2196	-29.3950	9.68	8	5
cssz-83a	Central and South America	288.5944	-30.2923	5.36	14.81	11.96
cssz-83b	Central and South America	288.0938	-30.2517	5.36	8	5
cssz-84a	Central and South America	288.5223	-31.1639	3.8	14.9	11.96
cssz-84b	Central and South America	288.0163	-31.1351	3.8	8	5
cssz-85a	Central and South America	288.4748	-32.0416	2.55	15	11.96
cssz-85b	Central and South America	287.9635	-32.0223	2.55	8	5
cssz-86a	Central and South America	288.3901	-33.0041	7.01	15	11.96
cssz-86b	Central and South America	287.8768	-32.9512	7.01	8	5
cssz-87a	Central and South America	288.1050	-34.0583	19.4	15	11.96
cssz-87b	Central and South America	287.6115	-33.9142	19.4	8	5
cssz-88a	Central and South America	287.5309	-35.0437	32.81	15	11.96
cssz-88b	Central and South America	287.0862	-34.8086	32.81	8	5
cssz-88z	Central and South America	287.9308	-35.2545	32.81	30	24.9
cssz-89a	Central and South America	287.2380	-35.5993	14.52	16.67	11.96
cssz-89b	Central and South America	286.7261	-35.4914	14.52	8	5
cssz-89z	Central and South America	287.7014	-35.6968	14.52	30	26.3
cssz-90a	Central and South America	286.8442	-36.5645	22.64	18.33	11.96
cssz-90b	Central and South America	286.3548	-36.4004	22.64	8	5
cssz-90z	Central and South America	287.2916	-36.7142	22.64	30	27.68
cssz-91a	Central and South America	286.5925	-37.2488	10.9	20	11.96
cssz-91b	Central and South America	286.0721	-37.1690	10.9	8	5
cssz-91z	Central and South America	287.0726	-37.3224	10.9	30	29.06
cssz-92a	Central and South America	286.4254	-38.0945	8.23	20	11.96

Continued on next page

Table B.2 – continued

Segment	Description	Longitude(°E)	Latitude(°N)	Strike(°)	Dip(°)	Depth (km)
cssz-92b	Central and South America	285.8948	-38.0341	8.23	8	5
cssz-92z	Central and South America	286.9303	-38.1520	8.23	26.67	29.06
cssz-93a	Central and South America	286.2047	-39.0535	13.46	20	11.96
cssz-93b	Central and South America	285.6765	-38.9553	13.46	8	5
cssz-93z	Central and South America	286.7216	-39.1495	13.46	23.33	29.06
cssz-94a	Central and South America	286.0772	-39.7883	3.4	20	11.96
cssz-94b	Central and South America	285.5290	-39.7633	3.4	8	5
cssz-94z	Central and South America	286.6255	-39.8133	3.4	20	29.06
cssz-95a	Central and South America	285.9426	-40.7760	9.84	20	11.96
cssz-95b	Central and South America	285.3937	-40.7039	9.84	8	5
cssz-95z	Central and South America	286.4921	-40.8481	9.84	20	29.06
cssz-96a	Central and South America	285.7839	-41.6303	7.6	20	11.96
cssz-96b	Central and South America	285.2245	-41.5745	7.6	8	5
cssz-96x	Central and South America	287.4652	-41.7977	7.6	20	63.26
cssz-96y	Central and South America	286.9043	-41.7419	7.6	20	46.16
cssz-96z	Central and South America	286.3439	-41.6861	7.6	20	29.06
cssz-97a	Central and South America	285.6695	-42.4882	5.3	20	11.96
cssz-97b	Central and South America	285.0998	-42.4492	5.3	8	5
cssz-97x	Central and South America	287.3809	-42.6052	5.3	20	63.26
cssz-97y	Central and South America	286.8101	-42.5662	5.3	20	46.16
cssz-97z	Central and South America	286.2396	-42.5272	5.3	20	29.06
cssz-98a	Central and South America	285.5035	-43.4553	10.53	20	11.96
cssz-98b	Central and South America	284.9322	-43.3782	10.53	8	5
cssz-98x	Central and South America	287.2218	-43.6866	10.53	20	63.26
cssz-98y	Central and South America	286.6483	-43.6095	10.53	20	46.16
cssz-98z	Central and South America	286.0755	-43.5324	10.53	20	29.06
cssz-99a	Central and South America	285.3700	-44.2595	4.86	20	11.96
cssz-99b	Central and South America	284.7830	-44.2237	4.86	8	5
cssz-99x	Central and South America	287.1332	-44.3669	4.86	20	63.26
cssz-99y	Central and South America	286.5451	-44.3311	4.86	20	46.16
cssz-99z	Central and South America	285.9574	-44.2953	4.86	20	29.06
cssz-100a	Central and South America	285.2713	-45.1664	5.68	20	11.96
cssz-100b	Central and South America	284.6758	-45.1246	5.68	8	5
cssz-100x	Central and South America	287.0603	-45.2918	5.68	20	63.26
cssz-100y	Central and South America	286.4635	-45.2500	5.68	20	46.16
cssz-100z	Central and South America	285.8672	-45.2082	5.68	20	29.06
cssz-101a	Central and South America	285.3080	-45.8607	352.6	20	9.36
cssz-101b	Central and South America	284.7067	-45.9152	352.6	5	5
cssz-101y	Central and South America	286.5089	-45.7517	352.6	20	43.56
cssz-101z	Central and South America	285.9088	-45.8062	352.6	20	26.46
cssz-102a	Central and South America	285.2028	-47.1185	17.72	5	9.36
cssz-102b	Central and South America	284.5772	-46.9823	17.72	5	5
cssz-102y	Central and South America	286.4588	-47.3909	17.72	5	18.07
cssz-102z	Central and South America	285.8300	-47.2547	17.72	5	13.72
cssz-103a	Central and South America	284.7075	-48.0396	23.37	7.5	11.53
cssz-103b	Central and South America	284.0972	-47.8630	23.37	7.5	5
cssz-103x	Central and South America	286.5511	-48.5694	23.37	7.5	31.11
cssz-103y	Central and South America	285.9344	-48.3928	23.37	7.5	24.58
cssz-103z	Central and South America	285.3199	-48.2162	23.37	7.5	18.05
cssz-104a	Central and South America	284.3440	-48.7597	14.87	10	13.68
cssz-104b	Central and South America	283.6962	-48.6462	14.87	10	5
cssz-104x	Central and South America	286.2962	-49.1002	14.87	10	39.73
cssz-104y	Central and South America	285.6440	-48.9867	14.87	10	31.05
cssz-104z	Central and South America	284.9933	-48.8732	14.87	10	22.36
cssz-105a	Central and South America	284.2312	-49.4198	0.25	9.67	13.4

Continued on next page

Table B.2 – continued

Segment	Description	Longitude(°E)	Latitude(°N)	Strike(°)	Dip(°)	Depth (km)
cssz-105b	Central and South America	283.5518	-49.4179	0.25	9.67	5
cssz-105x	Central and South America	286.2718	-49.4255	0.25	9.67	38.59
cssz-105y	Central and South America	285.5908	-49.4236	0.25	9.67	30.2
cssz-105z	Central and South America	284.9114	-49.4217	0.25	9.67	21.8
cssz-106a	Central and South America	284.3730	-50.1117	347.5	9.25	13.04
cssz-106b	Central and South America	283.6974	-50.2077	347.5	9.25	5
cssz-106x	Central and South America	286.3916	-49.8238	347.5	9.25	37.15
cssz-106y	Central and South America	285.7201	-49.9198	347.5	9.25	29.11
cssz-106z	Central and South America	285.0472	-50.0157	347.5	9.25	21.07
cssz-107a	Central and South America	284.7130	-50.9714	346.5	9	12.82
cssz-107b	Central and South America	284.0273	-51.0751	346.5	9	5
cssz-107x	Central and South America	286.7611	-50.6603	346.5	9	36.29
cssz-107y	Central and South America	286.0799	-50.7640	346.5	9	28.47
cssz-107z	Central and South America	285.3972	-50.8677	346.5	9	20.64
cssz-108a	Central and South America	285.0378	-51.9370	352	8.67	12.54
cssz-108b	Central and South America	284.3241	-51.9987	352	8.67	5
cssz-108x	Central and South America	287.1729	-51.7519	352	8.67	35.15
cssz-108y	Central and South America	286.4622	-51.8136	352	8.67	27.61
cssz-108z	Central and South America	285.7505	-51.8753	352	8.67	20.07
cssz-109a	Central and South America	285.2635	-52.8439	353.1	8.33	12.24
cssz-109b	Central and South America	284.5326	-52.8974	353.1	8.33	5
cssz-109x	Central and South America	287.4508	-52.6834	353.1	8.33	33.97
cssz-109y	Central and South America	286.7226	-52.7369	353.1	8.33	26.73
cssz-109z	Central and South America	285.9935	-52.7904	353.1	8.33	19.49
cssz-110a	Central and South America	285.5705	-53.4139	334.2	8	11.96
cssz-110b	Central and South America	284.8972	-53.6076	334.2	8	5
cssz-110x	Central and South America	287.5724	-52.8328	334.2	8	32.83
cssz-110y	Central and South America	286.9081	-53.0265	334.2	8	25.88
cssz-110z	Central and South America	286.2408	-53.2202	334.2	8	18.92
cssz-111a	Central and South America	286.1627	-53.8749	313.8	8	11.96
cssz-111b	Central and South America	285.6382	-54.1958	313.8	8	5
cssz-111x	Central and South America	287.7124	-52.9122	313.8	8	32.83
cssz-111y	Central and South America	287.1997	-53.2331	313.8	8	25.88
cssz-111z	Central and South America	286.6832	-53.5540	313.8	8	18.92
cssz-112a	Central and South America	287.3287	-54.5394	316.4	8	11.96
cssz-112b	Central and South America	286.7715	-54.8462	316.4	8	5
cssz-112x	Central and South America	288.9756	-53.6190	316.4	8	32.83
cssz-112y	Central and South America	288.4307	-53.9258	316.4	8	25.88
cssz-112z	Central and South America	287.8817	-54.2326	316.4	8	18.92
cssz-113a	Central and South America	288.3409	-55.0480	307.6	8	11.96
cssz-113b	Central and South America	287.8647	-55.4002	307.6	8	5
cssz-113x	Central and South America	289.7450	-53.9914	307.6	8	32.83
cssz-113y	Central and South America	289.2810	-54.3436	307.6	8	25.88
cssz-113z	Central and South America	288.8130	-54.6958	307.6	8	18.92
cssz-114a	Central and South America	289.5342	-55.5026	301.5	8	11.96
cssz-114b	Central and South America	289.1221	-55.8819	301.5	8	5
cssz-114x	Central and South America	290.7472	-54.3647	301.5	8	32.83
cssz-114y	Central and South America	290.3467	-54.7440	301.5	8	25.88
cssz-114z	Central and South America	289.9424	-55.1233	301.5	8	18.92
cssz-115a	Central and South America	290.7682	-55.8485	292.7	8	11.96
cssz-115b	Central and South America	290.4608	-56.2588	292.7	8	5
cssz-115x	Central and South America	291.6714	-54.6176	292.7	8	32.83
cssz-115y	Central and South America	291.3734	-55.0279	292.7	8	25.88
cssz-115z	Central and South America	291.0724	-55.4382	292.7	8	18.92

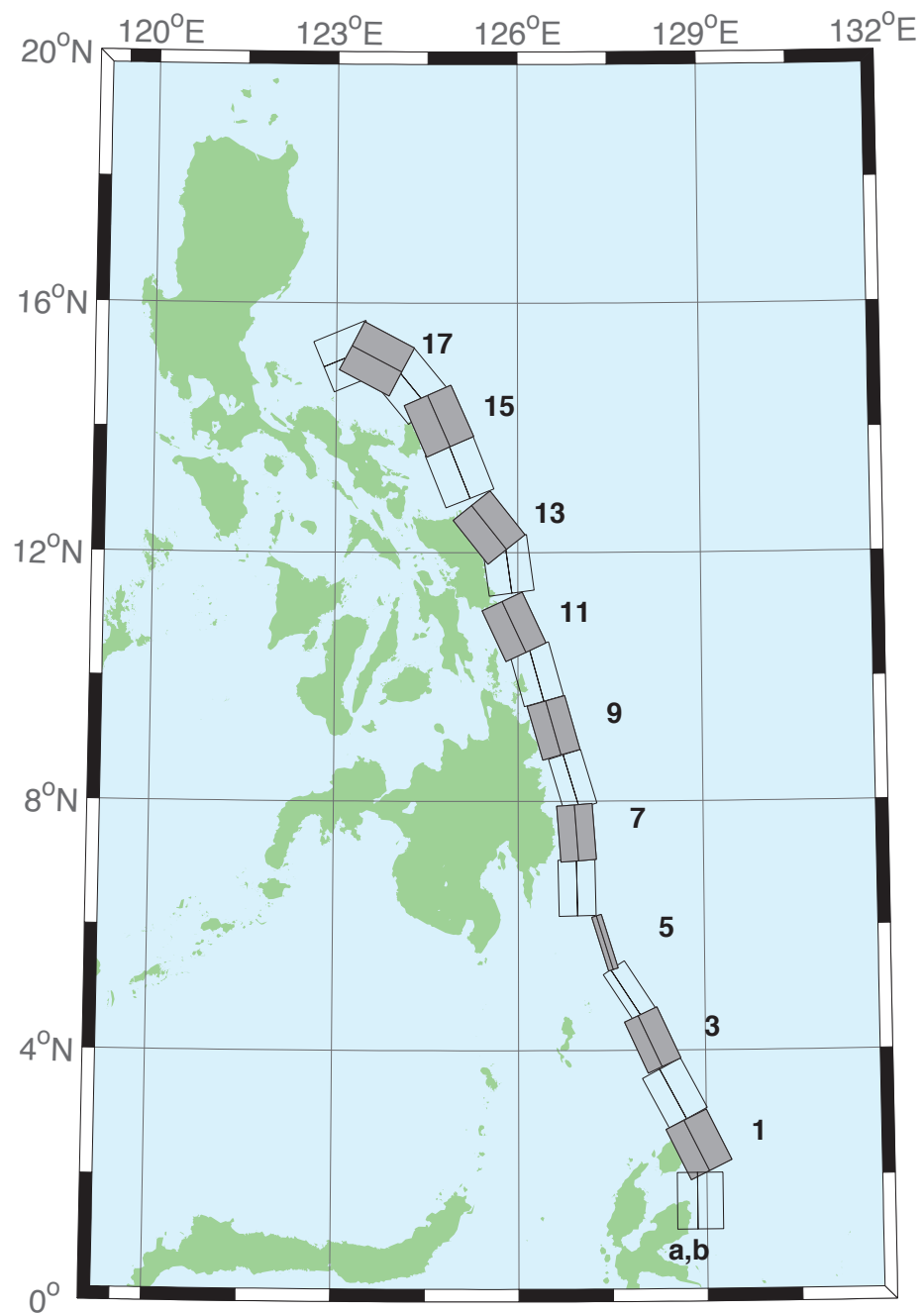


Figure B.3: Eastern Philippines Subduction Zone unit sources.

Table B.3: Earthquake parameters for Eastern Philippines Subduction Zone unit sources.

Segment	Description	Longitude($^{\circ}$ E)	Latitude($^{\circ}$ N)	Strike($^{\circ}$)	Dip($^{\circ}$)	Depth (km)
epsz-1a	Eastern Philippines	128.5521	2.3289	153.6	44.2	27.62
epsz-1b	Eastern Philippines	128.8408	2.4720	153.6	26.9	5
epsz-2a	Eastern Philippines	128.1943	3.1508	151.9	45.9	32.44
epsz-2b	Eastern Philippines	128.4706	3.2979	151.9	32.8	5.35
epsz-3a	Eastern Philippines	127.8899	4.0428	155.2	57.3	40.22
epsz-3b	Eastern Philippines	128.1108	4.1445	155.2	42.7	6.31
epsz-4a	Eastern Philippines	127.6120	4.8371	146.8	71.4	48.25
epsz-4b	Eastern Philippines	127.7324	4.9155	146.8	54.8	7.39
epsz-5a	Eastern Philippines	127.3173	5.7040	162.9	79.9	57.4
epsz-5b	Eastern Philippines	127.3930	5.7272	162.9	79.4	8.25
epsz-6a	Eastern Philippines	126.6488	6.6027	178.9	48.6	45.09
epsz-6b	Eastern Philippines	126.9478	6.6085	178.9	48.6	7.58
epsz-7a	Eastern Philippines	126.6578	7.4711	175.8	50.7	45.52
epsz-7b	Eastern Philippines	126.9439	7.4921	175.8	50.7	6.83
epsz-8a	Eastern Philippines	126.6227	8.2456	163.3	56.7	45.6
epsz-8b	Eastern Philippines	126.8614	8.3164	163.3	48.9	7.92
epsz-9a	Eastern Philippines	126.2751	9.0961	164.1	47	43.59
epsz-9b	Eastern Philippines	126.5735	9.1801	164.1	44.9	8.3
epsz-10a	Eastern Philippines	125.9798	9.9559	164.5	43.1	42.25
epsz-10b	Eastern Philippines	126.3007	10.0438	164.5	43.1	8.09
epsz-11a	Eastern Philippines	125.6079	10.6557	155	37.8	38.29
epsz-11b	Eastern Philippines	125.9353	10.8059	155	37.8	7.64
epsz-12a	Eastern Philippines	125.4697	11.7452	172.1	36	37.01
epsz-12b	Eastern Philippines	125.8374	11.7949	172.1	36	7.62
epsz-13a	Eastern Philippines	125.2238	12.1670	141.5	32.4	33.87
epsz-13b	Eastern Philippines	125.5278	12.4029	141.5	32.4	7.08
epsz-14a	Eastern Philippines	124.6476	13.1365	158.2	23	25.92
epsz-14b	Eastern Philippines	125.0421	13.2898	158.2	23	6.38
epsz-15a	Eastern Philippines	124.3107	13.9453	156.1	24.1	26.51
epsz-15b	Eastern Philippines	124.6973	14.1113	156.1	24.1	6.09
epsz-16a	Eastern Philippines	123.8998	14.4025	140.3	19.5	21.69
epsz-16b	Eastern Philippines	124.2366	14.6728	140.3	19.5	5
epsz-17a	Eastern Philippines	123.4604	14.7222	117.6	15.3	18.19
epsz-17b	Eastern Philippines	123.6682	15.1062	117.6	15.3	5
epsz-18a	Eastern Philippines	123.3946	14.7462	67.4	15	17.94
epsz-18b	Eastern Philippines	123.2219	15.1467	67.4	15	5
epsz-19a	Eastern Philippines	121.3638	15.7400	189.6	15	17.94
epsz-19b	Eastern Philippines	121.8082	15.6674	189.6	15	5
epsz-20a	Eastern Philippines	121.6833	16.7930	203.3	15	17.94
epsz-20b	Eastern Philippines	122.0994	16.6216	203.3	15	5
epsz-21a	Eastern Philippines	121.8279	17.3742	184.2	15	17.94
epsz-21b	Eastern Philippines	122.2814	17.3425	184.2	15	5

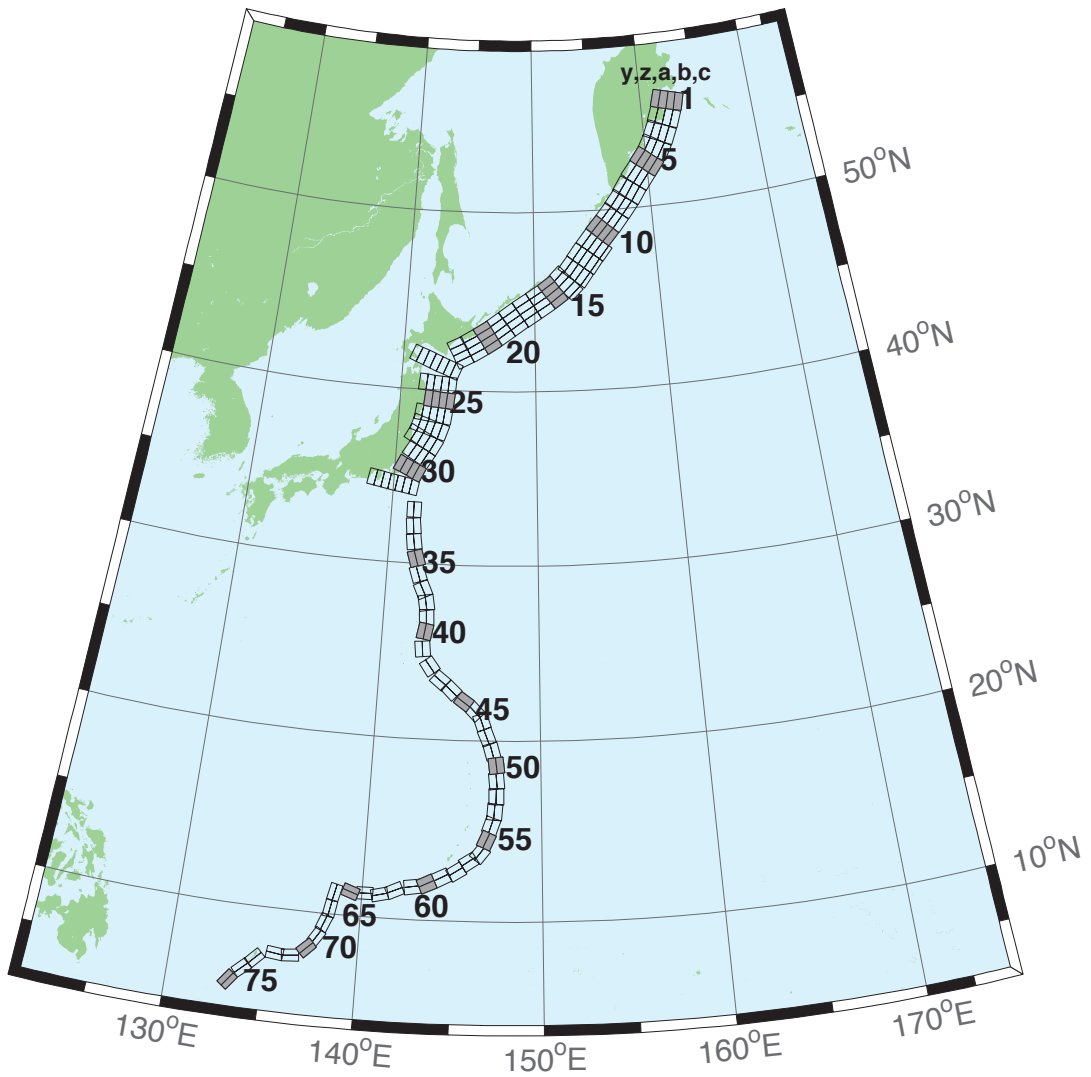


Figure B.4: Kamchatka-Kuril-Japan-Izu-Mariana-Yap Subduction Zone unit sources.

Table B.4: Earthquake parameters for Kamchatka-Kuril-Japan-Izu-Mariana-Yap Subduction Zone unit sources.

Segment	Description	Longitude(°E)	Latitude(°N)	Strike(°)	Dip(°)	Depth (km)
kisz-1a	Kamchatka-Kuril-Japan-Izu-Mariana-Yap	162.4318	55.5017	195	29	26.13
kisz-1b	Kamchatka-Kuril-Japan-Izu-Mariana-Yap	163.1000	55.4000	195	25	5
kisz-1y	Kamchatka-Kuril-Japan-Izu-Mariana-Yap	161.0884	55.7050	195	29	74.61
kisz-1z	Kamchatka-Kuril-Japan-Izu-Mariana-Yap	161.7610	55.6033	195	29	50.37
kisz-2a	Kamchatka-Kuril-Japan-Izu-Mariana-Yap	161.9883	54.6784	200	29	26.13
kisz-2b	Kamchatka-Kuril-Japan-Izu-Mariana-Yap	162.6247	54.5440	200	25	5
kisz-2y	Kamchatka-Kuril-Japan-Izu-Mariana-Yap	160.7072	54.9471	200	29	74.61
kisz-2z	Kamchatka-Kuril-Japan-Izu-Mariana-Yap	161.3488	54.8127	200	29	50.37
kisz-3a	Kamchatka-Kuril-Japan-Izu-Mariana-Yap	161.4385	53.8714	204	29	26.13
kisz-3b	Kamchatka-Kuril-Japan-Izu-Mariana-Yap	162.0449	53.7116	204	25	5
kisz-3y	Kamchatka-Kuril-Japan-Izu-Mariana-Yap	160.2164	54.1910	204	29	74.61
kisz-3z	Kamchatka-Kuril-Japan-Izu-Mariana-Yap	160.8286	54.0312	204	29	50.37
kisz-4a	Kamchatka-Kuril-Japan-Izu-Mariana-Yap	160.7926	53.1087	210	29	26.13
kisz-4b	Kamchatka-Kuril-Japan-Izu-Mariana-Yap	161.3568	52.9123	210	25	5
kisz-4y	Kamchatka-Kuril-Japan-Izu-Mariana-Yap	159.6539	53.5015	210	29	74.61
kisz-4z	Kamchatka-Kuril-Japan-Izu-Mariana-Yap	160.2246	53.3051	210	29	50.37
kisz-5a	Kamchatka-Kuril-Japan-Izu-Mariana-Yap	160.0211	52.4113	218	29	26.13
kisz-5b	Kamchatka-Kuril-Japan-Izu-Mariana-Yap	160.5258	52.1694	218	25	5
kisz-5y	Kamchatka-Kuril-Japan-Izu-Mariana-Yap	159.0005	52.8950	218	29	74.61
kisz-5z	Kamchatka-Kuril-Japan-Izu-Mariana-Yap	159.5122	52.6531	218	29	50.37
kisz-6a	Kamchatka-Kuril-Japan-Izu-Mariana-Yap	159.1272	51.7034	218	29	26.13
kisz-6b	Kamchatka-Kuril-Japan-Izu-Mariana-Yap	159.6241	51.4615	218	25	5
kisz-6y	Kamchatka-Kuril-Japan-Izu-Mariana-Yap	158.1228	52.1871	218	29	74.61
kisz-6z	Kamchatka-Kuril-Japan-Izu-Mariana-Yap	158.6263	51.9452	218	29	50.37
kisz-7a	Kamchatka-Kuril-Japan-Izu-Mariana-Yap	158.2625	50.9549	214	29	26.13
kisz-7b	Kamchatka-Kuril-Japan-Izu-Mariana-Yap	158.7771	50.7352	214	25	5
kisz-7y	Kamchatka-Kuril-Japan-Izu-Mariana-Yap	157.2236	51.3942	214	29	74.61
kisz-7z	Kamchatka-Kuril-Japan-Izu-Mariana-Yap	157.7443	51.1745	214	29	50.37
kisz-8a	Kamchatka-Kuril-Japan-Izu-Mariana-Yap	157.4712	50.2459	218	31	27.7
kisz-8b	Kamchatka-Kuril-Japan-Izu-Mariana-Yap	157.9433	50.0089	218	27	5
kisz-8y	Kamchatka-Kuril-Japan-Izu-Mariana-Yap	156.5176	50.7199	218	31	79.2
kisz-8z	Kamchatka-Kuril-Japan-Izu-Mariana-Yap	156.9956	50.4829	218	31	53.45
kisz-9a	Kamchatka-Kuril-Japan-Izu-Mariana-Yap	156.6114	49.5583	220	31	27.7
kisz-9b	Kamchatka-Kuril-Japan-Izu-Mariana-Yap	157.0638	49.3109	220	27	5
kisz-9y	Kamchatka-Kuril-Japan-Izu-Mariana-Yap	155.6974	50.0533	220	31	79.2
kisz-9z	Kamchatka-Kuril-Japan-Izu-Mariana-Yap	156.1556	49.8058	220	31	53.45
kisz-10a	Kamchatka-Kuril-Japan-Izu-Mariana-Yap	155.7294	48.8804	221	31	27.7
kisz-10b	Kamchatka-Kuril-Japan-Izu-Mariana-Yap	156.1690	48.6278	221	27	5
kisz-10y	Kamchatka-Kuril-Japan-Izu-Mariana-Yap	154.8413	49.3856	221	31	79.2
kisz-10z	Kamchatka-Kuril-Japan-Izu-Mariana-Yap	155.2865	49.1330	221	31	53.45
kisz-11a	Kamchatka-Kuril-Japan-Izu-Mariana-Yap	154.8489	48.1821	219	31	27.7
kisz-11b	Kamchatka-Kuril-Japan-Izu-Mariana-Yap	155.2955	47.9398	219	27	5
kisz-11y	Kamchatka-Kuril-Japan-Izu-Mariana-Yap	153.9472	48.6667	219	31	79.2
kisz-11z	Kamchatka-Kuril-Japan-Izu-Mariana-Yap	154.3991	48.4244	219	31	53.45
kisz-11c	Kamchatka-Kuril-Japan-Izu-Mariana-Yap	156.0358	47.5374	39	57.89	4.602
kisz-12a	Kamchatka-Kuril-Japan-Izu-Mariana-Yap	153.9994	47.4729	217	31	27.7
kisz-12b	Kamchatka-Kuril-Japan-Izu-Mariana-Yap	154.4701	47.2320	217	27	5
kisz-12y	Kamchatka-Kuril-Japan-Izu-Mariana-Yap	153.0856	47.9363	217	31	79.2
kisz-12z	Kamchatka-Kuril-Japan-Izu-Mariana-Yap	153.5435	47.7046	217	31	53.45
kisz-12c	Kamchatka-Kuril-Japan-Izu-Mariana-Yap	155.2208	46.8473	37	57.89	4.602
kisz-13a	Kamchatka-Kuril-Japan-Izu-Mariana-Yap	153.2239	46.7564	218	31	27.7
kisz-13b	Kamchatka-Kuril-Japan-Izu-Mariana-Yap	153.6648	46.5194	218	27	5

Continued on next page

Table B.4 – continued

Segment	Description	Longitude($^{\circ}$ E)	Latitude($^{\circ}$ N)	Strike($^{\circ}$)	Dip($^{\circ}$)	Depth (km)
kisz-13y	Kamchatka-Kuril-Japan-Izu-Mariana-Yap	152.3343	47.2304	218	31	79.2
kisz-13z	Kamchatka-Kuril-Japan-Izu-Mariana-Yap	152.7801	46.9934	218	31	53.45
kisz-13c	Kamchatka-Kuril-Japan-Izu-Mariana-Yap	154.3957	46.1257	38	57.89	4.602
kisz-14a	Kamchatka-Kuril-Japan-Izu-Mariana-Yap	152.3657	46.1514	225	23	24.54
kisz-14b	Kamchatka-Kuril-Japan-Izu-Mariana-Yap	152.7855	45.8591	225	23	5
kisz-14y	Kamchatka-Kuril-Japan-Izu-Mariana-Yap	151.5172	46.7362	225	23	63.62
kisz-14z	Kamchatka-Kuril-Japan-Izu-Mariana-Yap	151.9426	46.4438	225	23	44.08
kisz-14c	Kamchatka-Kuril-Japan-Izu-Mariana-Yap	153.4468	45.3976	45	57.89	4.602
kisz-15a	Kamchatka-Kuril-Japan-Izu-Mariana-Yap	151.4663	45.5963	233	25	23.73
kisz-15b	Kamchatka-Kuril-Japan-Izu-Mariana-Yap	151.8144	45.2712	233	22	5
kisz-15y	Kamchatka-Kuril-Japan-Izu-Mariana-Yap	150.7619	46.2465	233	25	65.99
kisz-15z	Kamchatka-Kuril-Japan-Izu-Mariana-Yap	151.1151	45.9214	233	25	44.86
kisz-16a	Kamchatka-Kuril-Japan-Izu-Mariana-Yap	150.4572	45.0977	237	25	23.73
kisz-16b	Kamchatka-Kuril-Japan-Izu-Mariana-Yap	150.7694	44.7563	237	22	5
kisz-16y	Kamchatka-Kuril-Japan-Izu-Mariana-Yap	149.8253	45.7804	237	25	65.99
kisz-16z	Kamchatka-Kuril-Japan-Izu-Mariana-Yap	150.1422	45.4390	237	25	44.86
kisz-17a	Kamchatka-Kuril-Japan-Izu-Mariana-Yap	149.3989	44.6084	237	25	23.73
kisz-17b	Kamchatka-Kuril-Japan-Izu-Mariana-Yap	149.7085	44.2670	237	22	5
kisz-17y	Kamchatka-Kuril-Japan-Izu-Mariana-Yap	148.7723	45.2912	237	25	65.99
kisz-17z	Kamchatka-Kuril-Japan-Izu-Mariana-Yap	149.0865	44.9498	237	25	44.86
kisz-18a	Kamchatka-Kuril-Japan-Izu-Mariana-Yap	148.3454	44.0982	235	25	23.73
kisz-18b	Kamchatka-Kuril-Japan-Izu-Mariana-Yap	148.6687	43.7647	235	22	5
kisz-18y	Kamchatka-Kuril-Japan-Izu-Mariana-Yap	147.6915	44.7651	235	25	65.99
kisz-18z	Kamchatka-Kuril-Japan-Izu-Mariana-Yap	148.0194	44.4316	235	25	44.86
kisz-19a	Kamchatka-Kuril-Japan-Izu-Mariana-Yap	147.3262	43.5619	233	25	23.73
kisz-19b	Kamchatka-Kuril-Japan-Izu-Mariana-Yap	147.6625	43.2368	233	22	5
kisz-19y	Kamchatka-Kuril-Japan-Izu-Mariana-Yap	146.6463	44.2121	233	25	65.99
kisz-19z	Kamchatka-Kuril-Japan-Izu-Mariana-Yap	146.9872	43.8870	233	25	44.86
kisz-20a	Kamchatka-Kuril-Japan-Izu-Mariana-Yap	146.3513	43.0633	237	25	23.73
kisz-20b	Kamchatka-Kuril-Japan-Izu-Mariana-Yap	146.6531	42.7219	237	22	5
kisz-20y	Kamchatka-Kuril-Japan-Izu-Mariana-Yap	145.7410	43.7461	237	25	65.99
kisz-20z	Kamchatka-Kuril-Japan-Izu-Mariana-Yap	146.0470	43.4047	237	25	44.86
kisz-21a	Kamchatka-Kuril-Japan-Izu-Mariana-Yap	145.3331	42.5948	239	25	23.73
kisz-21b	Kamchatka-Kuril-Japan-Izu-Mariana-Yap	145.6163	42.2459	239	22	5
kisz-21y	Kamchatka-Kuril-Japan-Izu-Mariana-Yap	144.7603	43.2927	239	25	65.99
kisz-21z	Kamchatka-Kuril-Japan-Izu-Mariana-Yap	145.0475	42.9438	239	25	44.86
kisz-22a	Kamchatka-Kuril-Japan-Izu-Mariana-Yap	144.3041	42.1631	242	25	23.73
kisz-22b	Kamchatka-Kuril-Japan-Izu-Mariana-Yap	144.5605	41.8037	242	22	5
kisz-22y	Kamchatka-Kuril-Japan-Izu-Mariana-Yap	143.7854	42.8819	242	25	65.99
kisz-22z	Kamchatka-Kuril-Japan-Izu-Mariana-Yap	144.0455	42.5225	242	25	44.86
kisz-23a	Kamchatka-Kuril-Japan-Izu-Mariana-Yap	143.2863	41.3335	202	21	21.28
kisz-23b	Kamchatka-Kuril-Japan-Izu-Mariana-Yap	143.8028	41.1764	202	19	5
kisz-23v	Kamchatka-Kuril-Japan-Izu-Mariana-Yap	140.6816	42.1189	202	21	110.9
kisz-23w	Kamchatka-Kuril-Japan-Izu-Mariana-Yap	141.2050	41.9618	202	21	92.95
kisz-23x	Kamchatka-Kuril-Japan-Izu-Mariana-Yap	141.7273	41.8047	202	21	75.04
kisz-23y	Kamchatka-Kuril-Japan-Izu-Mariana-Yap	142.2482	41.6476	202	21	57.12
kisz-23z	Kamchatka-Kuril-Japan-Izu-Mariana-Yap	142.7679	41.4905	202	21	39.2
kisz-24a	Kamchatka-Kuril-Japan-Izu-Mariana-Yap	142.9795	40.3490	185	21	21.28
kisz-24b	Kamchatka-Kuril-Japan-Izu-Mariana-Yap	143.5273	40.3125	185	19	5
kisz-24x	Kamchatka-Kuril-Japan-Izu-Mariana-Yap	141.3339	40.4587	185	21	75.04
kisz-24y	Kamchatka-Kuril-Japan-Izu-Mariana-Yap	141.8827	40.4221	185	21	57.12
kisz-24z	Kamchatka-Kuril-Japan-Izu-Mariana-Yap	142.4312	40.3856	185	21	39.2
kisz-25a	Kamchatka-Kuril-Japan-Izu-Mariana-Yap	142.8839	39.4541	185	21	21.28
kisz-25b	Kamchatka-Kuril-Japan-Izu-Mariana-Yap	143.4246	39.4176	185	19	5
kisz-25y	Kamchatka-Kuril-Japan-Izu-Mariana-Yap	141.8012	39.5272	185	21	57.12

Continued on next page

Table B.4 – continued

Segment	Description	Longitude(°E)	Latitude(°N)	Strike(°)	Dip(°)	Depth (km)
kisz-25z	Kamchatka-Kuril-Japan-Izu-Mariana-Yap	142.3426	39.4907	185	21	39.2
kisz-26a	Kamchatka-Kuril-Japan-Izu-Mariana-Yap	142.7622	38.5837	188	21	21.28
kisz-26b	Kamchatka-Kuril-Japan-Izu-Mariana-Yap	143.2930	38.5254	188	19	5
kisz-26x	Kamchatka-Kuril-Japan-Izu-Mariana-Yap	141.1667	38.7588	188	21	75.04
kisz-26y	Kamchatka-Kuril-Japan-Izu-Mariana-Yap	141.6990	38.7004	188	21	57.12
kisz-26z	Kamchatka-Kuril-Japan-Izu-Mariana-Yap	142.2308	38.6421	188	21	39.2
kisz-27a	Kamchatka-Kuril-Japan-Izu-Mariana-Yap	142.5320	37.7830	198	21	21.28
kisz-27b	Kamchatka-Kuril-Japan-Izu-Mariana-Yap	143.0357	37.6534	198	19	5
kisz-27x	Kamchatka-Kuril-Japan-Izu-Mariana-Yap	141.0142	38.1717	198	21	75.04
kisz-27y	Kamchatka-Kuril-Japan-Izu-Mariana-Yap	141.5210	38.0421	198	21	57.12
kisz-27z	Kamchatka-Kuril-Japan-Izu-Mariana-Yap	142.0269	37.9126	198	21	39.2
kisz-28a	Kamchatka-Kuril-Japan-Izu-Mariana-Yap	142.1315	37.0265	208	21	21.28
kisz-28b	Kamchatka-Kuril-Japan-Izu-Mariana-Yap	142.5941	36.8297	208	19	5
kisz-28x	Kamchatka-Kuril-Japan-Izu-Mariana-Yap	140.7348	37.6171	208	21	75.04
kisz-28y	Kamchatka-Kuril-Japan-Izu-Mariana-Yap	141.2016	37.4202	208	21	57.12
kisz-28z	Kamchatka-Kuril-Japan-Izu-Mariana-Yap	141.6671	37.2234	208	21	39.2
kisz-29a	Kamchatka-Kuril-Japan-Izu-Mariana-Yap	141.5970	36.2640	211	21	21.28
kisz-29b	Kamchatka-Kuril-Japan-Izu-Mariana-Yap	142.0416	36.0481	211	19	5
kisz-29y	Kamchatka-Kuril-Japan-Izu-Mariana-Yap	140.7029	36.6960	211	21	57.12
kisz-29z	Kamchatka-Kuril-Japan-Izu-Mariana-Yap	141.1506	36.4800	211	21	39.2
kisz-30a	Kamchatka-Kuril-Japan-Izu-Mariana-Yap	141.0553	35.4332	205	21	21.28
kisz-30b	Kamchatka-Kuril-Japan-Izu-Mariana-Yap	141.5207	35.2560	205	19	5
kisz-30y	Kamchatka-Kuril-Japan-Izu-Mariana-Yap	140.1204	35.7876	205	21	57.12
kisz-30z	Kamchatka-Kuril-Japan-Izu-Mariana-Yap	140.5883	35.6104	205	21	39.2
kisz-31a	Kamchatka-Kuril-Japan-Izu-Mariana-Yap	140.6956	34.4789	190	22	22.1
kisz-31b	Kamchatka-Kuril-Japan-Izu-Mariana-Yap	141.1927	34.4066	190	20	5
kisz-31v	Kamchatka-Kuril-Japan-Izu-Mariana-Yap	138.2025	34.8405	190	22	115.8
kisz-31w	Kamchatka-Kuril-Japan-Izu-Mariana-Yap	138.7021	34.7682	190	22	97.02
kisz-31x	Kamchatka-Kuril-Japan-Izu-Mariana-Yap	139.2012	34.6958	190	22	78.29
kisz-31y	Kamchatka-Kuril-Japan-Izu-Mariana-Yap	139.6997	34.6235	190	22	59.56
kisz-31z	Kamchatka-Kuril-Japan-Izu-Mariana-Yap	140.1979	34.5512	190	22	40.83
kisz-32a	Kamchatka-Kuril-Japan-Izu-Mariana-Yap	141.0551	33.0921	180	32	23.48
kisz-32b	Kamchatka-Kuril-Japan-Izu-Mariana-Yap	141.5098	33.0921	180	21.69	5
kisz-33a	Kamchatka-Kuril-Japan-Izu-Mariana-Yap	141.0924	32.1047	173.8	27.65	20.67
kisz-33b	Kamchatka-Kuril-Japan-Izu-Mariana-Yap	141.5596	32.1473	173.8	18.27	5
kisz-34a	Kamchatka-Kuril-Japan-Izu-Mariana-Yap	141.1869	31.1851	172.1	25	18.26
kisz-34b	Kamchatka-Kuril-Japan-Izu-Mariana-Yap	141.6585	31.2408	172.1	15.38	5
kisz-35a	Kamchatka-Kuril-Japan-Izu-Mariana-Yap	141.4154	30.1707	163	25	17.12
kisz-35b	Kamchatka-Kuril-Japan-Izu-Mariana-Yap	141.8662	30.2899	163	14.03	5
kisz-36a	Kamchatka-Kuril-Japan-Izu-Mariana-Yap	141.6261	29.2740	161.7	25.73	18.71
kisz-36b	Kamchatka-Kuril-Japan-Izu-Mariana-Yap	142.0670	29.4012	161.7	15.91	5
kisz-37a	Kamchatka-Kuril-Japan-Izu-Mariana-Yap	142.0120	28.3322	154.7	20	14.54
kisz-37b	Kamchatka-Kuril-Japan-Izu-Mariana-Yap	142.4463	28.5124	154.7	11	5
kisz-38a	Kamchatka-Kuril-Japan-Izu-Mariana-Yap	142.2254	27.6946	170.3	20	14.54
kisz-38b	Kamchatka-Kuril-Japan-Izu-Mariana-Yap	142.6955	27.7659	170.3	11	5
kisz-39a	Kamchatka-Kuril-Japan-Izu-Mariana-Yap	142.3085	26.9127	177.2	24.23	17.42
kisz-39b	Kamchatka-Kuril-Japan-Izu-Mariana-Yap	142.7674	26.9325	177.2	14.38	5
kisz-40a	Kamchatka-Kuril-Japan-Izu-Mariana-Yap	142.2673	26.1923	189.4	26.49	22.26
kisz-40b	Kamchatka-Kuril-Japan-Izu-Mariana-Yap	142.7090	26.1264	189.4	20.2	5
kisz-41a	Kamchatka-Kuril-Japan-Izu-Mariana-Yap	142.1595	25.0729	173.7	22.07	19.08
kisz-41b	Kamchatka-Kuril-Japan-Izu-Mariana-Yap	142.6165	25.1184	173.7	16.36	5
kisz-42a	Kamchatka-Kuril-Japan-Izu-Mariana-Yap	142.7641	23.8947	143.5	21.54	18.4
kisz-42b	Kamchatka-Kuril-Japan-Izu-Mariana-Yap	143.1321	24.1432	143.5	15.54	5
kisz-43a	Kamchatka-Kuril-Japan-Izu-Mariana-Yap	143.5281	23.0423	129.2	23.02	18.77
kisz-43b	Kamchatka-Kuril-Japan-Izu-Mariana-Yap	143.8128	23.3626	129.2	15.99	5

Continued on next page

Table B.4 – continued

Segment	Description	Longitude($^{\circ}$ E)	Latitude($^{\circ}$ N)	Strike($^{\circ}$)	Dip($^{\circ}$)	Depth (km)
kisz-44a	Kamchatka-Kuril-Japan-Izu-Mariana-Yap	144.2230	22.5240	134.6	28.24	18.56
kisz-44b	Kamchatka-Kuril-Japan-Izu-Mariana-Yap	144.5246	22.8056	134.6	15.74	5
kisz-45a	Kamchatka-Kuril-Japan-Izu-Mariana-Yap	145.0895	21.8866	125.8	36.73	22.79
kisz-45b	Kamchatka-Kuril-Japan-Izu-Mariana-Yap	145.3171	22.1785	125.8	20.84	5
kisz-46a	Kamchatka-Kuril-Japan-Izu-Mariana-Yap	145.6972	21.3783	135.9	30.75	20.63
kisz-46b	Kamchatka-Kuril-Japan-Izu-Mariana-Yap	145.9954	21.6469	135.9	18.22	5
kisz-47a	Kamchatka-Kuril-Japan-Izu-Mariana-Yap	146.0406	20.9341	160.1	29.87	19.62
kisz-47b	Kamchatka-Kuril-Japan-Izu-Mariana-Yap	146.4330	21.0669	160.1	17	5
kisz-48a	Kamchatka-Kuril-Japan-Izu-Mariana-Yap	146.3836	20.0690	158	32.75	19.68
kisz-48b	Kamchatka-Kuril-Japan-Izu-Mariana-Yap	146.7567	20.2108	158	17.07	5
kisz-49a	Kamchatka-Kuril-Japan-Izu-Mariana-Yap	146.6689	19.3123	164.5	25.07	21.41
kisz-49b	Kamchatka-Kuril-Japan-Izu-Mariana-Yap	147.0846	19.4212	164.5	19.16	5
kisz-50a	Kamchatka-Kuril-Japan-Izu-Mariana-Yap	146.9297	18.5663	172.1	22	22.1
kisz-50b	Kamchatka-Kuril-Japan-Izu-Mariana-Yap	147.3650	18.6238	172.1	20	5
kisz-51a	Kamchatka-Kuril-Japan-Izu-Mariana-Yap	146.9495	17.7148	175.1	22.06	22.04
kisz-51b	Kamchatka-Kuril-Japan-Izu-Mariana-Yap	147.3850	17.7503	175.1	19.93	5
kisz-52a	Kamchatka-Kuril-Japan-Izu-Mariana-Yap	146.9447	16.8869	180	25.51	18.61
kisz-52b	Kamchatka-Kuril-Japan-Izu-Mariana-Yap	147.3683	16.8869	180	15.79	5
kisz-53a	Kamchatka-Kuril-Japan-Izu-Mariana-Yap	146.8626	16.0669	185.2	27.39	18.41
kisz-53b	Kamchatka-Kuril-Japan-Izu-Mariana-Yap	147.2758	16.0309	185.2	15.56	5
kisz-54a	Kamchatka-Kuril-Japan-Izu-Mariana-Yap	146.7068	15.3883	199.1	28.12	20.91
kisz-54b	Kamchatka-Kuril-Japan-Izu-Mariana-Yap	147.0949	15.2590	199.1	18.56	5
kisz-55a	Kamchatka-Kuril-Japan-Izu-Mariana-Yap	146.4717	14.6025	204.3	29.6	26.27
kisz-55b	Kamchatka-Kuril-Japan-Izu-Mariana-Yap	146.8391	14.4415	204.3	25.18	5
kisz-56a	Kamchatka-Kuril-Japan-Izu-Mariana-Yap	146.1678	13.9485	217.4	32.04	26.79
kisz-56b	Kamchatka-Kuril-Japan-Izu-Mariana-Yap	146.4789	13.7170	217.4	25.84	5
kisz-57a	Kamchatka-Kuril-Japan-Izu-Mariana-Yap	145.6515	13.5576	235.8	37	24.54
kisz-57b	Kamchatka-Kuril-Japan-Izu-Mariana-Yap	145.8586	13.2609	235.8	23	5
kisz-58a	Kamchatka-Kuril-Japan-Izu-Mariana-Yap	144.9648	12.9990	237.8	37.72	24.54
kisz-58b	Kamchatka-Kuril-Japan-Izu-Mariana-Yap	145.1589	12.6984	237.8	23	5
kisz-59a	Kamchatka-Kuril-Japan-Izu-Mariana-Yap	144.1799	12.6914	242.9	34.33	22.31
kisz-59b	Kamchatka-Kuril-Japan-Izu-Mariana-Yap	144.3531	12.3613	242.9	20.25	5
kisz-60a	Kamchatka-Kuril-Japan-Izu-Mariana-Yap	143.3687	12.3280	244.9	30.9	20.62
kisz-60b	Kamchatka-Kuril-Japan-Izu-Mariana-Yap	143.5355	11.9788	244.9	18.2	5
kisz-61a	Kamchatka-Kuril-Japan-Izu-Mariana-Yap	142.7051	12.1507	261.8	35.41	25.51
kisz-61b	Kamchatka-Kuril-Japan-Izu-Mariana-Yap	142.7582	11.7883	261.8	24.22	5
kisz-62a	Kamchatka-Kuril-Japan-Izu-Mariana-Yap	141.6301	11.8447	245.7	39.86	34.35
kisz-62b	Kamchatka-Kuril-Japan-Izu-Mariana-Yap	141.7750	11.5305	245.7	35.94	5
kisz-63a	Kamchatka-Kuril-Japan-Izu-Mariana-Yap	140.8923	11.5740	256.2	42	38.46
kisz-63b	Kamchatka-Kuril-Japan-Izu-Mariana-Yap	140.9735	11.2498	256.2	42	5
kisz-64a	Kamchatka-Kuril-Japan-Izu-Mariana-Yap	140.1387	11.6028	269.6	42.48	38.77
kisz-64b	Kamchatka-Kuril-Japan-Izu-Mariana-Yap	140.1410	11.2716	269.6	42.48	5
kisz-65a	Kamchatka-Kuril-Japan-Izu-Mariana-Yap	139.4595	11.5883	288.7	44.16	39.83
kisz-65b	Kamchatka-Kuril-Japan-Izu-Mariana-Yap	139.3541	11.2831	288.7	44.16	5
kisz-66a	Kamchatka-Kuril-Japan-Izu-Mariana-Yap	138.1823	11.2648	193.1	45	40.36
kisz-66b	Kamchatka-Kuril-Japan-Izu-Mariana-Yap	138.4977	11.1929	193.1	45	5
kisz-67a	Kamchatka-Kuril-Japan-Izu-Mariana-Yap	137.9923	10.3398	189.8	45	40.36
kisz-67b	Kamchatka-Kuril-Japan-Izu-Mariana-Yap	138.3104	10.2856	189.8	45	5
kisz-68a	Kamchatka-Kuril-Japan-Izu-Mariana-Yap	137.7607	9.6136	201.7	45	40.36
kisz-68b	Kamchatka-Kuril-Japan-Izu-Mariana-Yap	138.0599	9.4963	201.7	45	5
kisz-69a	Kamchatka-Kuril-Japan-Izu-Mariana-Yap	137.4537	8.8996	213.5	45	40.36
kisz-69b	Kamchatka-Kuril-Japan-Izu-Mariana-Yap	137.7215	8.7241	213.5	45	5
kisz-70a	Kamchatka-Kuril-Japan-Izu-Mariana-Yap	137.0191	8.2872	226.5	45	40.36
kisz-70b	Kamchatka-Kuril-Japan-Izu-Mariana-Yap	137.2400	8.0569	226.5	45	5
kisz-71a	Kamchatka-Kuril-Japan-Izu-Mariana-Yap	136.3863	7.9078	263.9	45	40.36

Continued on next page

Table B.4 – continued

Segment	Description	Longitude($^{\circ}$ E)	Latitude($^{\circ}$ N)	Strike($^{\circ}$)	Dip($^{\circ}$)	Depth (km)
kisz-71b	Kamchatka-Kuril-Japan-Izu-Mariana-Yap	136.4202	7.5920	263.9	45	5
kisz-72a	Kamchatka-Kuril-Japan-Izu-Mariana-Yap	135.6310	7.9130	276.9	45	40.36
kisz-72b	Kamchatka-Kuril-Japan-Izu-Mariana-Yap	135.5926	7.5977	276.9	45	5
kisz-73a	Kamchatka-Kuril-Japan-Izu-Mariana-Yap	134.3296	7.4541	224	45	40.36
kisz-73b	Kamchatka-Kuril-Japan-Izu-Mariana-Yap	134.5600	7.2335	224	45	5
kisz-74a	Kamchatka-Kuril-Japan-Izu-Mariana-Yap	133.7125	6.8621	228.1	45	40.36
kisz-74b	Kamchatka-Kuril-Japan-Izu-Mariana-Yap	133.9263	6.6258	228.1	45	5
kisz-75a	Kamchatka-Kuril-Japan-Izu-Mariana-Yap	133.0224	6.1221	217.7	45	40.36
kisz-75b	Kamchatka-Kuril-Japan-Izu-Mariana-Yap	133.2751	5.9280	217.7	45	5

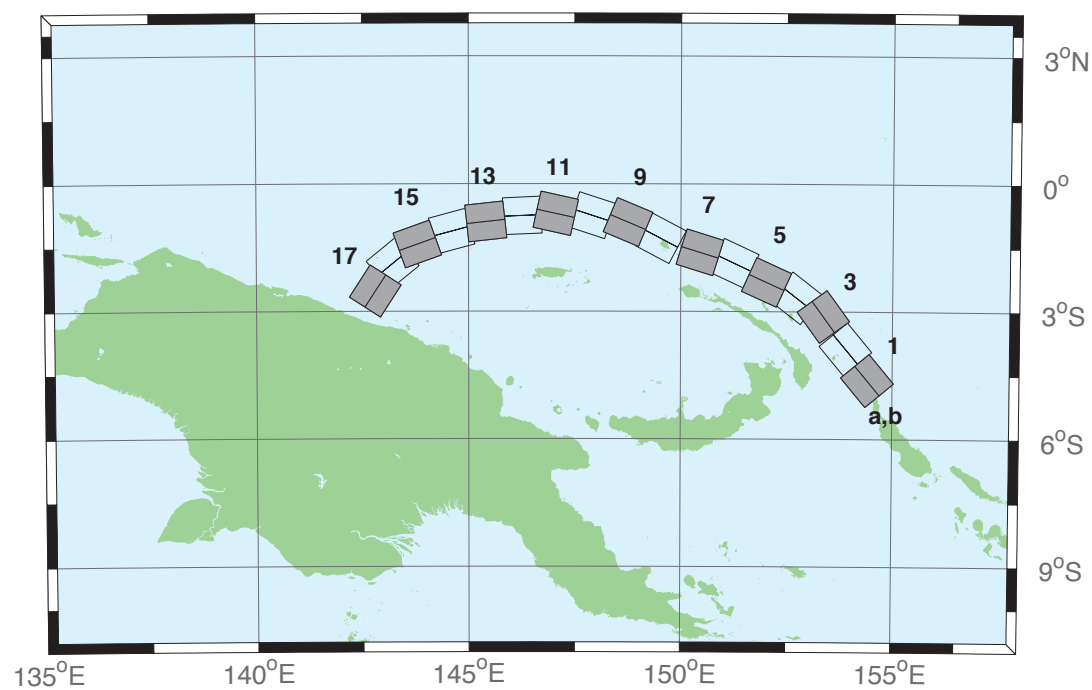


Figure B.5: Manus–Oceanic Convergent Boundary Subduction Zone unit sources.

Table B.5: Earthquake parameters for Manus–Oceanic Convergent Boundary Subduction Zone unit sources.

Segment	Description	Longitude(°E)	Latitude(°N)	Strike(°)	Dip(°)	Depth (km)
mosz-1a	Manus	154.0737	-4.8960	140.2	15	15.88
mosz-1b	Manus	154.4082	-4.6185	140.2	15	2.94
mosz-2a	Manus	153.5589	-4.1575	140.2	15	15.91
mosz-2b	Manus	153.8931	-3.8800	140.2	15	2.97
mosz-3a	Manus	153.0151	-3.3716	143.9	15	16.64
mosz-3b	Manus	153.3662	-3.1160	143.9	15	3.7
mosz-4a	Manus	152.4667	-3.0241	127.7	15	17.32
mosz-4b	Manus	152.7321	-2.6806	127.7	15	4.38
mosz-5a	Manus	151.8447	-2.7066	114.3	15	17.57
mosz-5b	Manus	152.0235	-2.3112	114.3	15	4.63
mosz-6a	Manus	151.0679	-2.2550	115	15	17.66
mosz-6b	Manus	151.2513	-1.8618	115	15	4.72
mosz-7a	Manus	150.3210	-2.0236	107.2	15	17.73
mosz-7b	Manus	150.4493	-1.6092	107.2	15	4.79
mosz-8a	Manus	149.3226	-1.6666	117.8	15	17.83
mosz-8b	Manus	149.5251	-1.2829	117.8	15	4.89
mosz-9a	Manus	148.5865	-1.3017	112.7	15	17.84
mosz-9b	Manus	148.7540	-0.9015	112.7	15	4.9
mosz-10a	Manus	147.7760	-1.1560	108	15	17.78
mosz-10b	Manus	147.9102	-0.7434	108	15	4.84
mosz-11a	Manus	146.9596	-1.1226	102.5	15	17.54
mosz-11b	Manus	147.0531	-0.6990	102.5	15	4.6
mosz-12a	Manus	146.2858	-1.1820	87.48	15	17.29
mosz-12b	Manus	146.2667	-0.7486	87.48	15	4.35
mosz-13a	Manus	145.4540	-1.3214	83.75	15	17.34
mosz-13b	Manus	145.4068	-0.8901	83.75	15	4.4
mosz-14a	Manus	144.7151	-1.5346	75.09	15	17.21
mosz-14b	Manus	144.6035	-1.1154	75.09	15	4.27
mosz-15a	Manus	143.9394	-1.8278	70.43	15	16.52
mosz-15b	Manus	143.7940	-1.4190	70.43	15	3.58
mosz-16a	Manus	143.4850	-2.2118	50.79	15	15.86
mosz-16b	Manus	143.2106	-1.8756	50.79	15	2.92
mosz-17a	Manus	143.1655	-2.7580	33	15	16.64
mosz-17b	Manus	142.8013	-2.5217	33	15	3.7

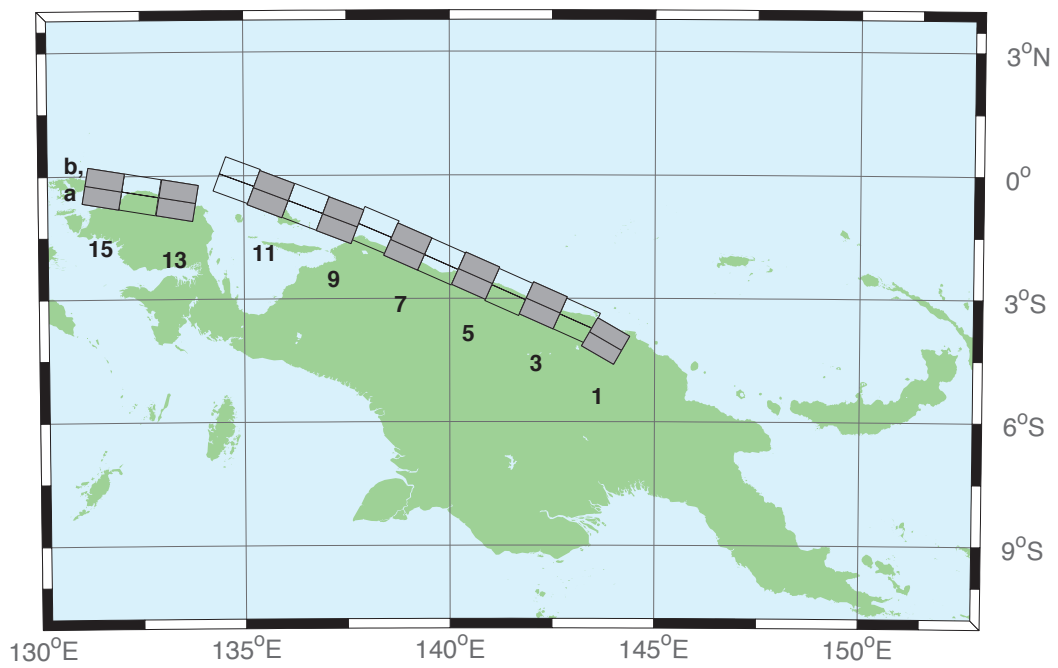


Figure B.6: New Guinea Subduction Zone unit sources.

Table B.6: Earthquake parameters for New Guinea Subduction Zone unit sources.

Segment	Description	Longitude($^{\circ}$ E)	Latitude($^{\circ}$ N)	Strike($^{\circ}$)	Dip($^{\circ}$)	Depth (km)
ngsz-1a	New Guinea	143.6063	-4.3804	120	29	25.64
ngsz-1b	New Guinea	143.8032	-4.0402	120	29	1.4
ngsz-2a	New Guinea	142.9310	-3.9263	114	27.63	20.1
ngsz-2b	New Guinea	143.0932	-3.5628	114	21.72	1.6
ngsz-3a	New Guinea	142.1076	-3.5632	114	20.06	18.73
ngsz-3b	New Guinea	142.2795	-3.1778	114	15.94	5
ngsz-4a	New Guinea	141.2681	-3.2376	114	21	17.76
ngsz-4b	New Guinea	141.4389	-2.8545	114	14.79	5
ngsz-5a	New Guinea	140.4592	-2.8429	114	21.26	16.14
ngsz-5b	New Guinea	140.6296	-2.4605	114	12.87	5
ngsz-6a	New Guinea	139.6288	-2.4960	114	22.72	15.4
ngsz-6b	New Guinea	139.7974	-2.1175	114	12	5
ngsz-7a	New Guinea	138.8074	-2.1312	114	21.39	15.4
ngsz-7b	New Guinea	138.9776	-1.7491	114	12	5
ngsz-8a	New Guinea	138.0185	-1.7353	113.1	18.79	15.14
ngsz-8b	New Guinea	138.1853	-1.3441	113.1	11.7	5
ngsz-9a	New Guinea	137.1805	-1.5037	111	15.24	13.23
ngsz-9b	New Guinea	137.3358	-1.0991	111	9.47	5
ngsz-10a	New Guinea	136.3418	-1.1774	111	13.51	11.09
ngsz-10b	New Guinea	136.4983	-0.7697	111	7	5
ngsz-11a	New Guinea	135.4984	-0.8641	111	11.38	12.49
ngsz-11b	New Guinea	135.6562	-0.4530	111	8.62	5
ngsz-12a	New Guinea	134.6759	-0.5216	110.5	10	13.68
ngsz-12b	New Guinea	134.8307	-0.1072	110.5	10	5
ngsz-13a	New Guinea	133.3065	-1.0298	99.5	10	13.68
ngsz-13b	New Guinea	133.3795	-0.5935	99.5	10	5
ngsz-14a	New Guinea	132.4048	-0.8816	99.5	10	13.68
ngsz-14b	New Guinea	132.4778	-0.4453	99.5	10	5
ngsz-15a	New Guinea	131.5141	-0.7353	99.5	10	13.68
ngsz-15b	New Guinea	131.5871	-0.2990	99.5	10	5

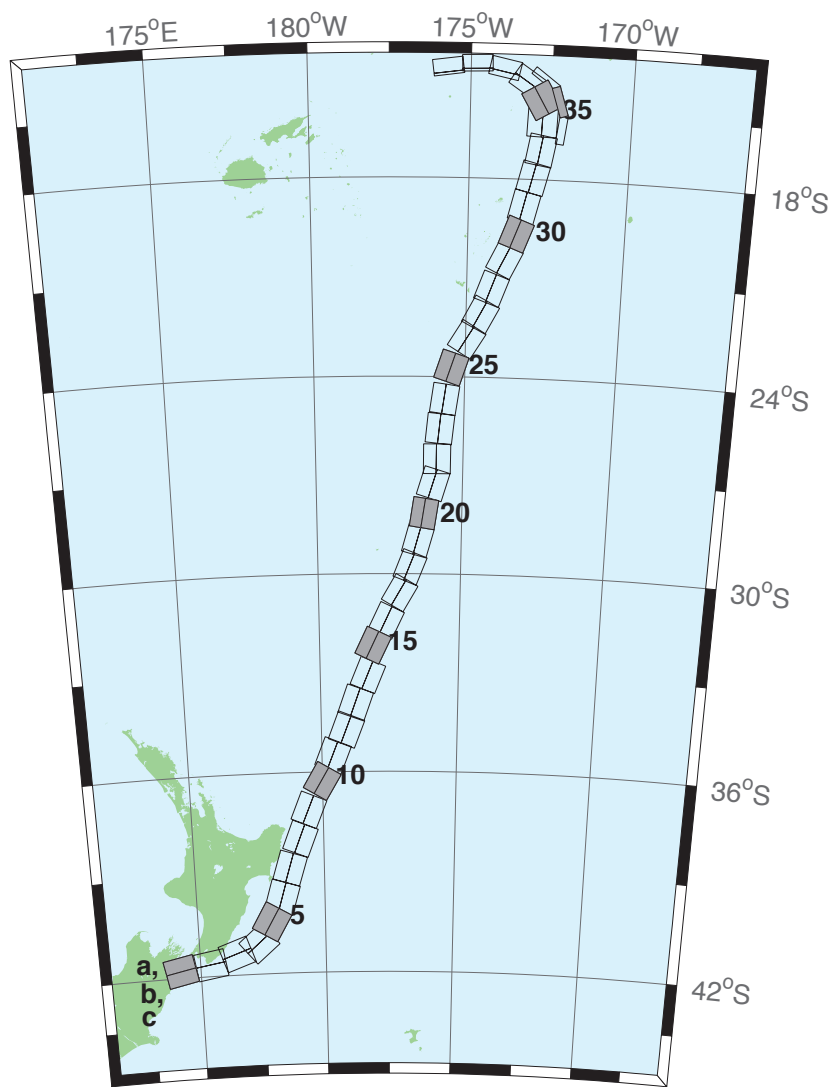


Figure B.7: New Zealand–Kermadec–Tonga Subduction Zone unit sources.

Table B.7: Earthquake parameters for New Zealand–Kermadec–Tonga Subduction Zone unit sources.

Segment	Description	Longitude($^{\circ}$ E)	Latitude($^{\circ}$ N)	Strike($^{\circ}$)	Dip($^{\circ}$)	Depth (km)
ntsz-1a	New Zealand–Tonga	174.0985	-41.3951	258.6	24	25.34
ntsz-1b	New Zealand–Tonga	174.2076	-41.7973	258.6	24	5
ntsz-2a	New Zealand–Tonga	175.3289	-41.2592	260.6	29.38	23.17
ntsz-2b	New Zealand–Tonga	175.4142	-41.6454	260.6	21.31	5
ntsz-3a	New Zealand–Tonga	176.2855	-40.9950	250.7	29.54	21.74
ntsz-3b	New Zealand–Tonga	176.4580	-41.3637	250.7	19.56	5
ntsz-4a	New Zealand–Tonga	177.0023	-40.7679	229.4	24.43	18.87
ntsz-4b	New Zealand–Tonga	177.3552	-41.0785	229.4	16.1	5
ntsz-5a	New Zealand–Tonga	177.4114	-40.2396	210	18.8	19.29
ntsz-5b	New Zealand–Tonga	177.8951	-40.4525	210	16.61	5
ntsz-6a	New Zealand–Tonga	177.8036	-39.6085	196.7	18.17	15.8
ntsz-6b	New Zealand–Tonga	178.3352	-39.7310	196.7	12.48	5
ntsz-7a	New Zealand–Tonga	178.1676	-38.7480	197	28.1	17.85
ntsz-7b	New Zealand–Tonga	178.6541	-38.8640	197	14.89	5
ntsz-8a	New Zealand–Tonga	178.6263	-37.8501	201.4	31.47	18.78
ntsz-8b	New Zealand–Tonga	179.0788	-37.9899	201.4	16	5
ntsz-9a	New Zealand–Tonga	178.9833	-36.9770	202.2	29.58	20.02
ntsz-9b	New Zealand–Tonga	179.4369	-37.1245	202.2	17.48	5
ntsz-10a	New Zealand–Tonga	179.5534	-36.0655	210.6	32.1	20.72
ntsz-10b	New Zealand–Tonga	179.9595	-36.2593	210.6	18.32	5
ntsz-11a	New Zealand–Tonga	179.9267	-35.3538	201.7	25	16.09
ntsz-11b	New Zealand–Tonga	180.3915	-35.5040	201.7	12.81	5
ntsz-12a	New Zealand–Tonga	180.4433	-34.5759	201.2	25	15.46
ntsz-12b	New Zealand–Tonga	180.9051	-34.7230	201.2	12.08	5
ntsz-13a	New Zealand–Tonga	180.7990	-33.7707	199.8	25.87	19.06
ntsz-13b	New Zealand–Tonga	181.2573	-33.9073	199.8	16.33	5
ntsz-14a	New Zealand–Tonga	181.2828	-32.9288	202.4	31.28	22.73
ntsz-14b	New Zealand–Tonga	181.7063	-33.0751	202.4	20.77	5
ntsz-15a	New Zealand–Tonga	181.4918	-32.0035	205.4	32.33	22.64
ntsz-15b	New Zealand–Tonga	181.8967	-32.1665	205.4	20.66	5
ntsz-16a	New Zealand–Tonga	181.9781	-31.2535	205.5	34.29	23.59
ntsz-16b	New Zealand–Tonga	182.3706	-31.4131	205.5	21.83	5
ntsz-17a	New Zealand–Tonga	182.4819	-30.3859	210.3	37.6	25.58
ntsz-17b	New Zealand–Tonga	182.8387	-30.5655	210.3	24.3	5
ntsz-18a	New Zealand–Tonga	182.8176	-29.6545	201.6	37.65	26.13
ntsz-18b	New Zealand–Tonga	183.1985	-29.7856	201.6	25	5
ntsz-19a	New Zealand–Tonga	183.0622	-28.8739	195.7	34.41	26.13
ntsz-19b	New Zealand–Tonga	183.4700	-28.9742	195.7	25	5
ntsz-20a	New Zealand–Tonga	183.2724	-28.0967	188.8	38	26.13
ntsz-20b	New Zealand–Tonga	183.6691	-28.1508	188.8	25	5
ntsz-21a	New Zealand–Tonga	183.5747	-27.1402	197.1	32.29	24.83
ntsz-21b	New Zealand–Tonga	183.9829	-27.2518	197.1	23.37	5
ntsz-22a	New Zealand–Tonga	183.6608	-26.4975	180	29.56	18.63
ntsz-22b	New Zealand–Tonga	184.0974	-26.4975	180	15.82	5
ntsz-23a	New Zealand–Tonga	183.7599	-25.5371	185.8	32.42	20.56
ntsz-23b	New Zealand–Tonga	184.1781	-25.5752	185.8	18.13	5
ntsz-24a	New Zealand–Tonga	183.9139	-24.6201	188.2	33.31	23.73
ntsz-24b	New Zealand–Tonga	184.3228	-24.6734	188.2	22	5
ntsz-25a	New Zealand–Tonga	184.1266	-23.5922	198.5	29.34	19.64
ntsz-25b	New Zealand–Tonga	184.5322	-23.7163	198.5	17.03	5
ntsz-26a	New Zealand–Tonga	184.6613	-22.6460	211.7	30.26	19.43
ntsz-26b	New Zealand–Tonga	185.0196	-22.8497	211.7	16.78	5
ntsz-27a	New Zealand–Tonga	185.0879	-21.9139	207.9	31.73	20.67

Continued on next page

Table B.7 – continued

Segment	Description	Longitude($^{\circ}$ E)	Latitude($^{\circ}$ N)	Strike($^{\circ}$)	Dip($^{\circ}$)	Depth (km)
ntszz-27b	New Zealand–Tonga	185.4522	-22.0928	207.9	18.27	5
ntszz-28a	New Zealand–Tonga	185.4037	-21.1758	200.5	32.44	21.76
ntszz-28b	New Zealand–Tonga	185.7849	-21.3084	200.5	19.58	5
ntszz-29a	New Zealand–Tonga	185.8087	-20.2629	206.4	32.47	20.4
ntszz-29b	New Zealand–Tonga	186.1710	-20.4312	206.4	17.94	5
ntszz-30a	New Zealand–Tonga	186.1499	-19.5087	200.9	32.98	22.46
ntszz-30b	New Zealand–Tonga	186.5236	-19.6432	200.9	20.44	5
ntszz-31a	New Zealand–Tonga	186.3538	-18.7332	193.9	34.41	21.19
ntszz-31b	New Zealand–Tonga	186.7339	-18.8221	193.9	18.89	5
ntszz-32a	New Zealand–Tonga	186.5949	-17.8587	194.1	30	19.12
ntszz-32b	New Zealand–Tonga	186.9914	-17.9536	194.1	16.4	5
ntszz-33a	New Zealand–Tonga	186.8172	-17.0581	190	33.15	23.34
ntszz-33b	New Zealand–Tonga	187.2047	-17.1237	190	21.52	5
ntszz-34a	New Zealand–Tonga	186.7814	-16.2598	182.1	15	13.41
ntszz-34b	New Zealand–Tonga	187.2330	-16.2759	182.1	9.68	5
ntszz-34c	New Zealand–Tonga	187.9697	-16.4956	7.62	57.06	6.571
ntszz-35a	New Zealand–Tonga	186.8000	-15.8563	149.8	15	12.17
ntszz-35b	New Zealand–Tonga	187.1896	-15.6384	149.8	8.24	5
ntszz-35c	New Zealand–Tonga	187.8776	-15.6325	342.4	57.06	6.571
ntszz-36a	New Zealand–Tonga	186.5406	-15.3862	123.9	40.44	36.72
ntszz-36b	New Zealand–Tonga	186.7381	-15.1025	123.9	39.38	5
ntszz-36c	New Zealand–Tonga	187.3791	-14.9234	307	57.06	6.571
ntszz-37a	New Zealand–Tonga	185.9883	-14.9861	102	68.94	30.99
ntszz-37b	New Zealand–Tonga	186.0229	-14.8282	102	31.32	5
ntszz-38a	New Zealand–Tonga	185.2067	-14.8259	88.4	80	26.13
ntszz-38b	New Zealand–Tonga	185.2044	-14.7479	88.4	25	5
ntszz-39a	New Zealand–Tonga	184.3412	-14.9409	82.55	80	26.13
ntszz-39b	New Zealand–Tonga	184.3307	-14.8636	82.55	25	5

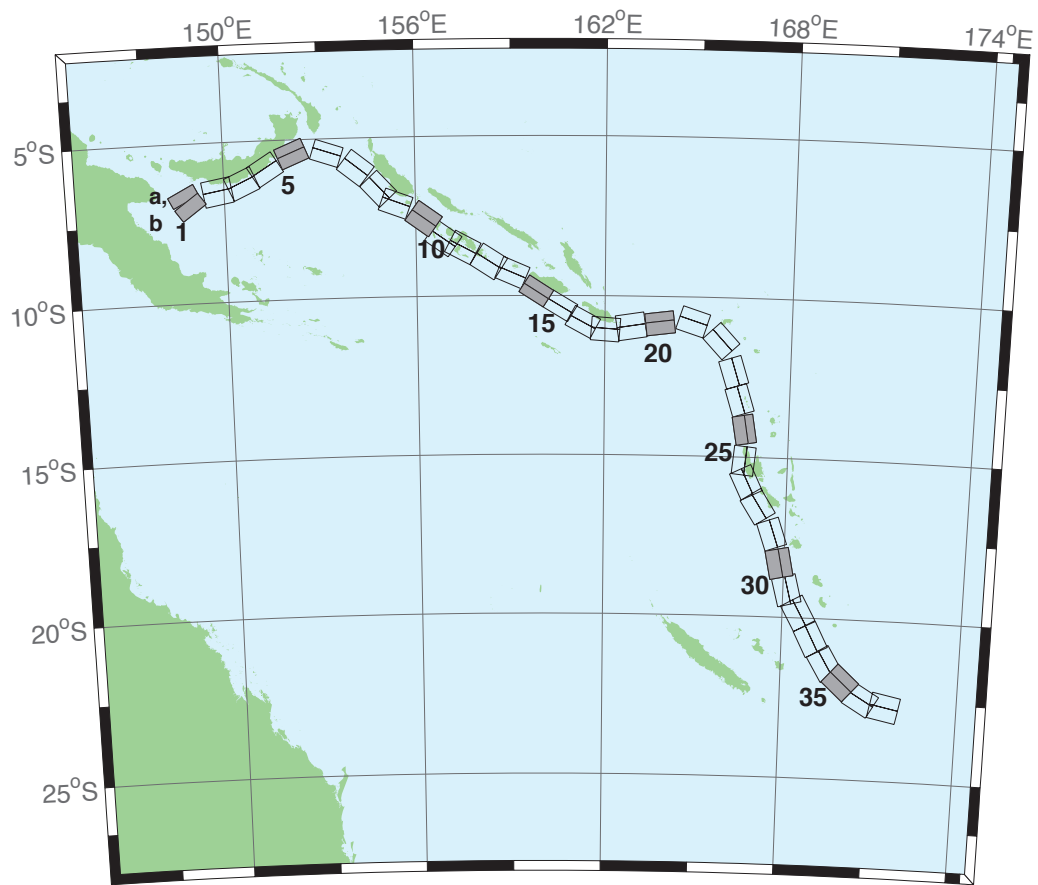


Figure B.8: New Britain–Solomons–Vanuatu Zone unit sources.

Table B.8: Earthquake parameters for New Britain–Solomons–Vanuatu Subduction Zone unit sources.

Segment	Description	Longitude($^{\circ}$ E)	Latitude($^{\circ}$ N)	Strike($^{\circ}$)	Dip($^{\circ}$)	Depth (km)
nvsz-1a	New Britain–Vanuatu	148.6217	-6.4616	243.2	32.34	15.69
nvsz-1b	New Britain–Vanuatu	148.7943	-6.8002	234.2	12.34	5
nvsz-2a	New Britain–Vanuatu	149.7218	-6.1459	260.1	35.1	16.36
nvsz-2b	New Britain–Vanuatu	149.7856	-6.5079	260.1	13.13	5
nvsz-3a	New Britain–Vanuatu	150.4075	-5.9659	245.7	42.35	18.59
nvsz-3b	New Britain–Vanuatu	150.5450	-6.2684	245.7	15.77	5
nvsz-4a	New Britain–Vanuatu	151.1095	-5.5820	238.2	42.41	23.63
nvsz-4b	New Britain–Vanuatu	151.2851	-5.8639	238.2	21.88	5
nvsz-5a	New Britain–Vanuatu	152.0205	-5.1305	247.7	49.22	32.39
nvsz-5b	New Britain–Vanuatu	152.1322	-5.4020	247.7	33.22	5
nvsz-6a	New Britain–Vanuatu	153.3450	-5.1558	288.6	53.53	33.59
nvsz-6b	New Britain–Vanuatu	153.2595	-5.4089	288.6	34.87	5
nvsz-7a	New Britain–Vanuatu	154.3814	-5.6308	308.3	39.72	19.18
nvsz-7b	New Britain–Vanuatu	154.1658	-5.9017	308.3	16.48	5
nvsz-8a	New Britain–Vanuatu	155.1097	-6.3511	317.2	45.33	22.92
nvsz-8b	New Britain–Vanuatu	154.8764	-6.5656	317.2	21	5
nvsz-9a	New Britain–Vanuatu	155.5027	-6.7430	290.5	48.75	22.92
nvsz-9b	New Britain–Vanuatu	155.3981	-7.0204	290.5	21	5
nvsz-10a	New Britain–Vanuatu	156.4742	-7.2515	305.9	36.88	27.62
nvsz-10b	New Britain–Vanuatu	156.2619	-7.5427	305.9	26.9	5
nvsz-11a	New Britain–Vanuatu	157.0830	-7.8830	305.4	32.97	29.72
nvsz-11b	New Britain–Vanuatu	156.8627	-8.1903	305.4	29.63	5
nvsz-12a	New Britain–Vanuatu	157.6537	-8.1483	297.9	37.53	28.57
nvsz-12b	New Britain–Vanuatu	157.4850	-8.4630	297.9	28.13	5
nvsz-13a	New Britain–Vanuatu	158.5089	-8.5953	302.7	33.62	23.02
nvsz-13b	New Britain–Vanuatu	158.3042	-8.9099	302.7	21.12	5
nvsz-14a	New Britain–Vanuatu	159.1872	-8.9516	293.3	38.44	34.06
nvsz-14b	New Britain–Vanuatu	159.0461	-9.2747	293.3	35.54	5
nvsz-15a	New Britain–Vanuatu	159.9736	-9.5993	302.8	46.69	41.38
nvsz-15b	New Britain–Vanuatu	159.8044	-9.8584	302.8	46.69	5
nvsz-16a	New Britain–Vanuatu	160.7343	-10.0574	301	46.05	41
nvsz-16b	New Britain–Vanuatu	160.5712	-10.3246	301	46.05	5
nvsz-17a	New Britain–Vanuatu	161.4562	-10.5241	298.4	40.12	37.22
nvsz-17b	New Britain–Vanuatu	161.2900	-10.8263	298.4	40.12	5
nvsz-18a	New Britain–Vanuatu	162.0467	-10.6823	274.1	40.33	29.03
nvsz-18b	New Britain–Vanuatu	162.0219	-11.0238	274.1	28.72	5
nvsz-19a	New Britain–Vanuatu	162.7818	-10.5645	261.3	34.25	24.14
nvsz-19b	New Britain–Vanuatu	162.8392	-10.9315	261.3	22.51	5
nvsz-20a	New Britain–Vanuatu	163.7222	-10.5014	262.9	50.35	26.3
nvsz-20b	New Britain–Vanuatu	163.7581	-10.7858	262.9	25.22	5
nvsz-21a	New Britain–Vanuatu	164.9445	-10.4183	287.9	40.31	23.3
nvsz-21b	New Britain–Vanuatu	164.8374	-10.7442	287.9	21.47	5
nvsz-22a	New Britain–Vanuatu	166.0261	-11.1069	317.1	42.39	20.78
nvsz-22b	New Britain–Vanuatu	165.7783	-11.3328	317.1	18.4	5
nvsz-23a	New Britain–Vanuatu	166.5179	-12.2260	342.4	47.95	22.43
nvsz-23b	New Britain–Vanuatu	166.2244	-12.3171	342.4	20.4	5
nvsz-24a	New Britain–Vanuatu	166.7236	-13.1065	342.6	47.13	28.52
nvsz-24b	New Britain–Vanuatu	166.4241	-13.1979	342.6	28.06	5
nvsz-25a	New Britain–Vanuatu	166.8914	-14.0785	350.3	54.1	31.16
nvsz-25b	New Britain–Vanuatu	166.6237	-14.1230	350.3	31.55	5
nvsz-26a	New Britain–Vanuatu	166.9200	-15.1450	365.6	50.46	29.05
nvsz-26b	New Britain–Vanuatu	166.6252	-15.1170	365.6	28.75	5
nvsz-27a	New Britain–Vanuatu	167.0053	-15.6308	334.2	44.74	25.46

Continued on next page

Table B.8 – continued

Segment	Description	Longitude($^{\circ}$ E)	Latitude($^{\circ}$ N)	Strike($^{\circ}$)	Dip($^{\circ}$)	Depth (km)
nvsz-27b	New Britain–Vanuatu	166.7068	-15.7695	334.2	24.15	5
nvsz-28a	New Britain–Vanuatu	167.4074	-16.3455	327.5	41.53	22.44
nvsz-28b	New Britain–Vanuatu	167.1117	-16.5264	327.5	20.42	5
nvsz-29a	New Britain–Vanuatu	167.9145	-17.2807	341.2	49.1	24.12
nvsz-29b	New Britain–Vanuatu	167.6229	-17.3757	341.2	22.48	5
nvsz-30a	New Britain–Vanuatu	168.2220	-18.2353	348.6	44.19	23.99
nvsz-30b	New Britain–Vanuatu	167.8895	-18.2991	348.6	22.32	5
nvsz-31a	New Britain–Vanuatu	168.5022	-19.0510	345.6	42.2	22.26
nvsz-31b	New Britain–Vanuatu	168.1611	-19.1338	345.6	20.2	5
nvsz-32a	New Britain–Vanuatu	168.8775	-19.6724	331.1	42.03	21.68
nvsz-32b	New Britain–Vanuatu	168.5671	-19.8338	331.1	19.49	5
nvsz-33a	New Britain–Vanuatu	169.3422	-20.4892	332.9	40.25	22.4
nvsz-33b	New Britain–Vanuatu	169.0161	-20.6453	332.9	20.37	5
nvsz-34a	New Britain–Vanuatu	169.8304	-21.2121	329.1	39	22.73
nvsz-34b	New Britain–Vanuatu	169.5086	-21.3911	329.1	20.77	5
nvsz-35a	New Britain–Vanuatu	170.3119	-21.6945	311.9	39	22.13
nvsz-35b	New Britain–Vanuatu	170.0606	-21.9543	311.9	20.03	5
nvsz-36a	New Britain–Vanuatu	170.9487	-22.1585	300.4	39.42	23.5
nvsz-36b	New Britain–Vanuatu	170.7585	-22.4577	300.4	21.71	5
nvsz-37a	New Britain–Vanuatu	171.6335	-22.3087	281.3	30	22.1
nvsz-37b	New Britain–Vanuatu	171.5512	-22.6902	281.3	20	5

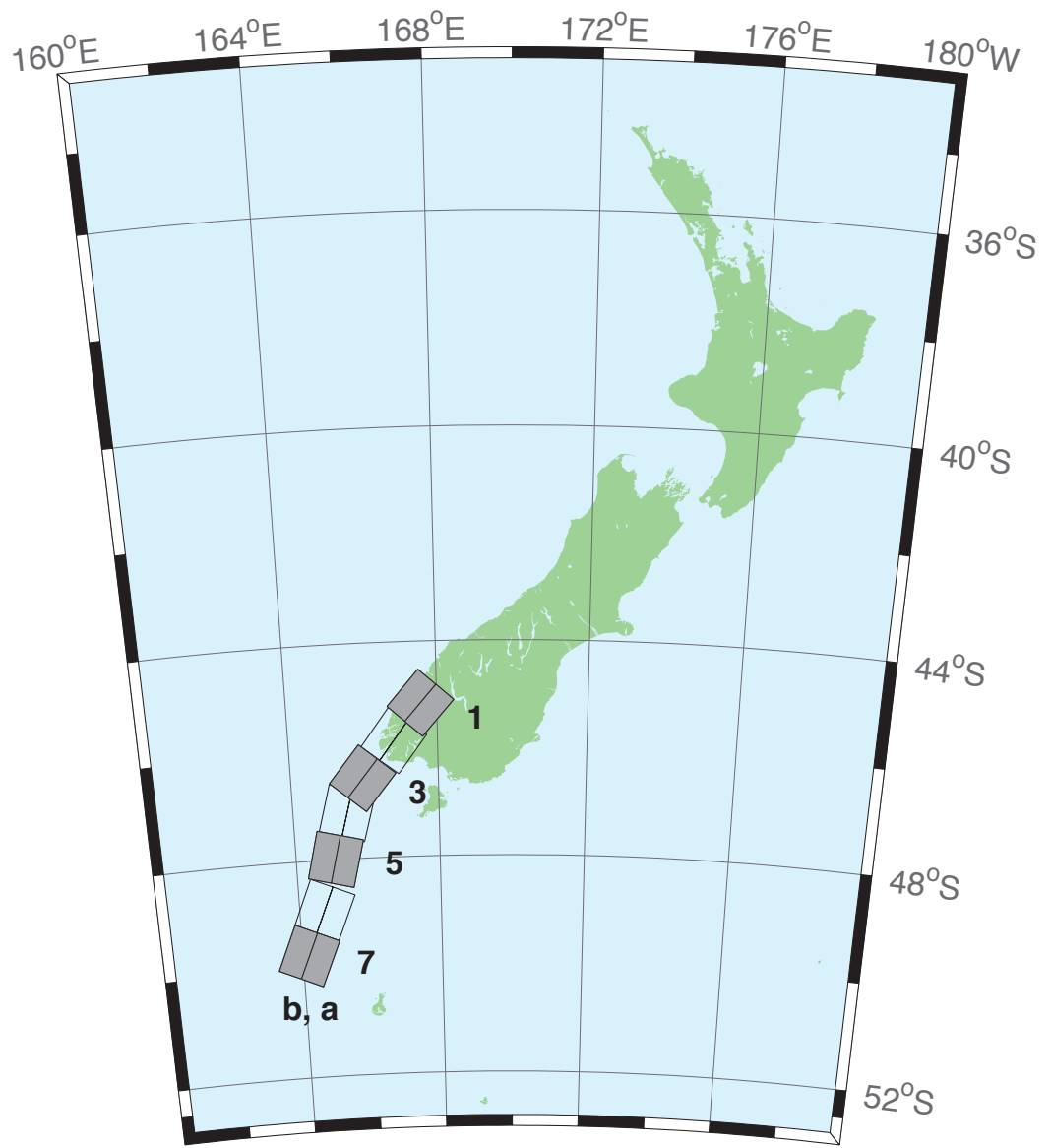


Figure B.9: New Zealand–Puysegur Zone unit sources.

Table B.9: Earthquake parameters for New Zealand–Puysegur Subduction Zone unit sources.

Segment	Description	Longitude($^{\circ}$ E)	Latitude($^{\circ}$ N)	Strike($^{\circ}$)	Dip($^{\circ}$)	Depth (km)
nzs–1a	New Zealand–Puysegur	168.0294	-45.4368	41.5	15	17.94
nzs–1b	New Zealand–Puysegur	167.5675	-45.1493	41.5	15	5
nzs–2a	New Zealand–Puysegur	167.3256	-46.0984	37.14	15	17.94
nzs–2b	New Zealand–Puysegur	166.8280	-45.8365	37.14	15	5
nzs–3a	New Zealand–Puysegur	166.4351	-46.7897	39.53	15	17.94
nzs–3b	New Zealand–Puysegur	165.9476	-46.5136	39.53	15	5
nzs–4a	New Zealand–Puysegur	166.0968	-47.2583	15.38	15	17.94
nzs–4b	New Zealand–Puysegur	165.4810	-47.1432	15.38	15	5
nzs–5a	New Zealand–Puysegur	165.7270	-48.0951	13.94	15	17.94
nzs–5b	New Zealand–Puysegur	165.0971	-47.9906	13.94	15	5
nzs–6a	New Zealand–Puysegur	165.3168	-49.0829	22.71	15	17.94
nzs–6b	New Zealand–Puysegur	164.7067	-48.9154	22.71	15	5
nzs–7a	New Zealand–Puysegur	164.8017	-49.9193	23.25	15	17.94
nzs–7b	New Zealand–Puysegur	164.1836	-49.7480	23.25	15	5

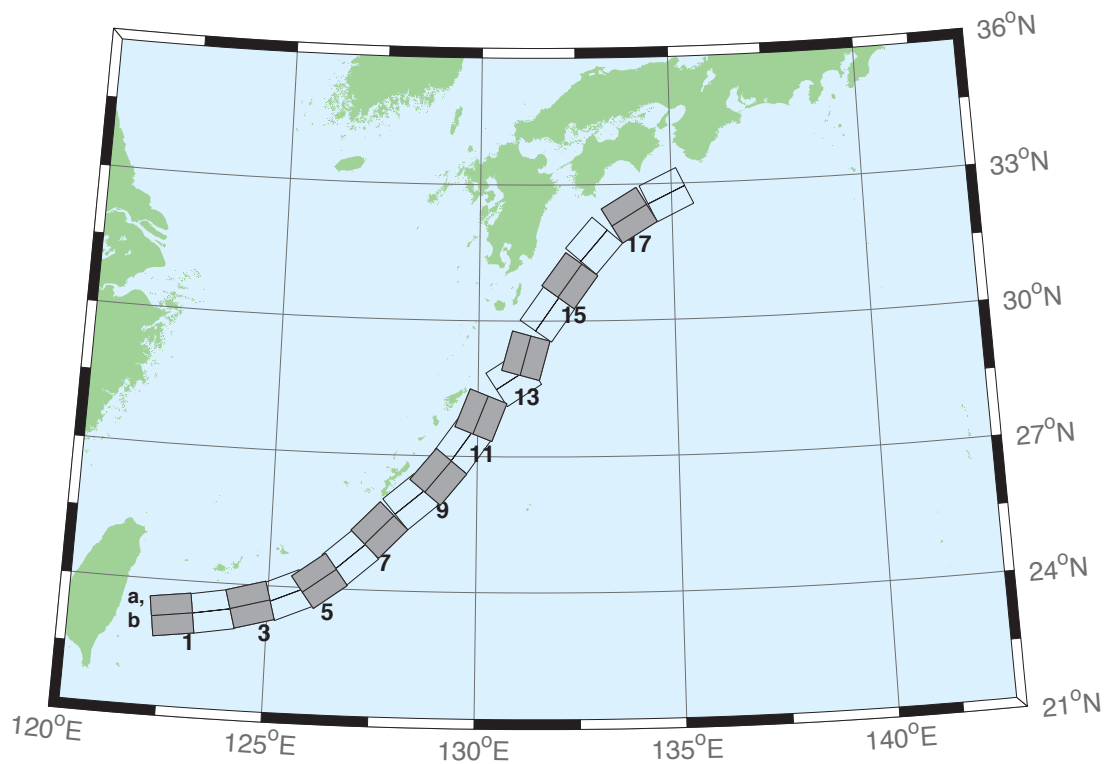


Figure B.10: Ryukyu–Kyushu–Nankai Zone unit sources.

Table B.10: Earthquake parameters for Ryukyu–Kyushu–Nankai Subduction Zone unit sources.

Segment	Description	Longitude($^{\circ}$ E)	Latitude($^{\circ}$ N)	Strike($^{\circ}$)	Dip($^{\circ}$)	Depth (km)
rnsz–1a	Ryukyu–Nankai	122.6672	23.6696	262	14	11.88
rnsz–1b	Ryukyu–Nankai	122.7332	23.2380	262	10	3.2
rnsz–2a	Ryukyu–Nankai	123.5939	23.7929	259.9	18.11	12.28
rnsz–2b	Ryukyu–Nankai	123.6751	23.3725	259.9	10	3.6
rnsz–3a	Ryukyu–Nankai	124.4604	23.9777	254.6	19.27	14.65
rnsz–3b	Ryukyu–Nankai	124.5830	23.5689	254.6	12.18	4.1
rnsz–4a	Ryukyu–Nankai	125.2720	24.2102	246.8	18	20.38
rnsz–4b	Ryukyu–Nankai	125.4563	23.8177	246.8	16	6.6
rnsz–5a	Ryukyu–Nankai	125.9465	24.5085	233.6	18	20.21
rnsz–5b	Ryukyu–Nankai	126.2241	24.1645	233.6	16	6.43
rnsz–6a	Ryukyu–Nankai	126.6349	25.0402	228.7	17.16	19.55
rnsz–6b	Ryukyu–Nankai	126.9465	24.7176	228.7	15.16	6.47
rnsz–7a	Ryukyu–Nankai	127.2867	25.6343	224	15.85	17.98
rnsz–7b	Ryukyu–Nankai	127.6303	25.3339	224	13.56	6.26
rnsz–8a	Ryukyu–Nankai	128.0725	26.3146	229.7	14.55	14.31
rnsz–8b	Ryukyu–Nankai	128.3854	25.9831	229.7	9.64	5.94
rnsz–9a	Ryukyu–Nankai	128.6642	26.8177	219.2	15.4	12.62
rnsz–9b	Ryukyu–Nankai	129.0391	26.5438	219.2	8	5.66
rnsz–10a	Ryukyu–Nankai	129.2286	27.4879	215.2	17	12.55
rnsz–10b	Ryukyu–Nankai	129.6233	27.2402	215.2	8.16	5.45
rnsz–11a	Ryukyu–Nankai	129.6169	28.0741	201.3	17	12.91
rnsz–11b	Ryukyu–Nankai	130.0698	27.9181	201.3	8.8	5.26
rnsz–12a	Ryukyu–Nankai	130.6175	29.0900	236.7	16.42	13.05
rnsz–12b	Ryukyu–Nankai	130.8873	28.7299	236.7	9.57	4.74
rnsz–13a	Ryukyu–Nankai	130.7223	29.3465	195.2	20.25	15.89
rnsz–13b	Ryukyu–Nankai	131.1884	29.2362	195.2	12.98	4.66
rnsz–14a	Ryukyu–Nankai	131.3467	30.3899	215.1	22.16	19.73
rnsz–14b	Ryukyu–Nankai	131.7402	30.1507	215.1	17.48	4.71
rnsz–15a	Ryukyu–Nankai	131.9149	31.1450	216	15.11	16.12
rnsz–15b	Ryukyu–Nankai	132.3235	30.8899	216	13.46	4.48
rnsz–16a	Ryukyu–Nankai	132.5628	31.9468	220.9	10.81	10.88
rnsz–16b	Ryukyu–Nankai	132.9546	31.6579	220.9	7.19	4.62
rnsz–17a	Ryukyu–Nankai	133.6125	32.6956	239	10.14	12.01
rnsz–17b	Ryukyu–Nankai	133.8823	32.3168	239	8.41	4.7
rnsz–18a	Ryukyu–Nankai	134.6416	33.1488	244.7	10.99	14.21
rnsz–18b	Ryukyu–Nankai	134.8656	32.7502	244.5	10.97	4.7
rnsz–19a	Ryukyu–Nankai	135.6450	33.5008	246.5	14.49	14.72
rnsz–19b	Ryukyu–Nankai	135.8523	33.1021	246.5	11.87	4.44
rnsz–20a	Ryukyu–Nankai	136.5962	33.8506	244.8	15	14.38
rnsz–20b	Ryukyu–Nankai	136.8179	33.4581	244.8	12	3.98
rnsz–21a	Ryukyu–Nankai	137.2252	34.3094	231.9	15	15.4
rnsz–21b	Ryukyu–Nankai	137.5480	33.9680	231.9	12	5
rnsz–22a	Ryukyu–Nankai	137.4161	34.5249	192.3	15	15.4
rnsz–22b	Ryukyu–Nankai	137.9301	34.4327	192.3	12	5

Appendix C SIFT Testing Report

Honolulu, Hawaii

Jean C. Newman

1.0 PURPOSE

Forecast models are tested with synthetic tsunami events covering a range of tsunami source locations. Testing is also done with selected historical tsunami events when available.

The purpose of forecast model testing is three-fold. The first objective is to assure that the results obtained with NOAA's tsunami forecast system, which has been released to the Tsunami Warning Centers for operational use, are identical or close to those obtained by the researcher during the development of the forecast model. The second objective is to test the forecast model for consistency, accuracy, time efficiency, and quality of results over a range of possible tsunami locations and magnitudes. The third objective is to identify bugs and issues in need of resolution by the researcher who developed the Forecast Model or by the forecast software development team before the next version release to NOAA's two Tsunami Warning Centers.

Local hardware and software applications, and tools familiar to the researcher(s), are used to run the Method of Splitting Tsunamis (MOST) model during the forecast model development. The test results presented in this report lend confidence that the model performs as developed and produces the same results when initiated within the forecast application in an operational setting as those produced by the researcher during the forecast model development. The test results assure those who rely on the Honolulu tsunami forecast model that consistent results are produced irrespective of system.

2.0 TESTING PROCEDURE

The general procedure for forecast model testing is to run a set of synthetic tsunami scenarios and a selected set of historical tsunami events through the forecast system application and compare the results with those obtained by the researcher during the forecast model development and presented in the Tsunami Forecast Model Report. Specific steps taken to test the model include:

1. Identification of testing scenarios, including the standard set of synthetic events, appropriate historical events, and customized synthetic scenarios that may have been used by the researcher(s) in developing the forecast model.
 2. Creation of new events to represent customized synthetic scenarios used by the researcher(s) in developing the forecast model, if any.
 3. Submission of test model runs with the forecast system, and export of the results from A, B, and C grids, along with time series.
 4. Recording applicable metadata, including the specific version of the forecast system used for testing.
 5. Examination of forecast model results from the forecast system for instabilities in both time series and plot results.
 6. Comparison of forecast model results obtained through the forecast system with those obtained during the forecast model development.
 7. Summarization of results with specific mention of quality, consistency, and time efficiency.
 8. Reporting of issues identified to modeler and forecast software development team.
9. Retesting the forecast models in the forecast system when reported issues have been addressed or explained.

Synthetic model runs were tested on a DELL PowerEdge R510 computer equipped with two Xeon E5670 processors at 2.93 Ghz, each with 12 MBytes of cache and 32GB memory. The processors are hex core and support hyperthreading, resulting in the computer performing as a 24 processor core machine. Additionally, the testing computer supports 10 Gigabit Ethernet for fast network connections. This computer configuration is similar or the same as the configurations of the computers installed at the Tsunami Warning Centers so the compute times should only vary slightly.

Results

The Honolulu forecast model was tested with NOAA's tsunami forecast system version 3.2.

The Honolulu, Hawaii forecast model was tested with four synthetic scenarios and one historical tsunami event. Test results from the forecast system and comparisons with the results obtained during the forecast model development are shown numerically in Table C1 and graphically in Figures C1 to C5. The results show that the forecast model is stable and robust, with consistent and high quality results across geographically distributed tsunami sources and mega-event tsunami magnitudes. The model run time (wall clock time) was under 12 minutes for 8 hours of simulation time, and under 6 minutes for 4 hours. This run time is under the 10 minute run time for 4 hours of simulation time and satisfies time efficiency requirements.

Four synthetic events were run on the Honolulu forecast model (the sources used in the report have been update). The modeled scenarios were stable for all cases tested, with no instabilities or ringing. Results show that the largest modeled height was 218 cm and originated in the Kamchatka-Yap-Mariana-Izu-Bonin (KISZ 22-31) source. Amplitudes greater than 100 cm were recorded for 4 out of 4 test sources. The smallest signal of 135.4 cm was recorded at the Aleutian-Alaska-Cascadia (ACSZ 56-65) source. Direct comparisons, of output from the forecast tool with results of both the historical event (Tohoku 2011) and available development synthetic events, demonstrated that the wave pattern were similar in shape, pattern and amplitude but not the same (the Tohoku 2011 event is very close). Maximum amplitudes differ by up to 24 cm. It should be noted the propagation database used during the development is dated in 2007. The difference database may cause the differences in the maximum waves for the synthetic scenarios.

Table C1. Table of maximum and minimum amplitudes (cm) at the Honolulu, Hawaii warning point for synthetic and historical events tested using SIFT 3.2 and obtained during development.

Scenario Name	Source Zone	Tsunami Source	α [m]	SIFT Max (cm)	Development Max (cm)	SIFT Min (cm)	Development Min (cm)
Mega-tsunami Scenarios							
KISZ 22-31	Kamchatka-Yap-Mariana-Izu-Bonin	A22-A31, B22-B31	29	218.0	225	-156.2	n/a
ASCZ 56-65	Aleutian-Alaska-Cascadia	A56-A65, B56-B65	29	135.4	159	-149.6	n/a
CSSZ 89-98	Central and South America	A89-A98, B89-B98	29	139.5	n/a	-128.3	n/a
NTSZ 30-39	New Zealand-Kermadec-Tonga	A30-A39, B30-B39	29	156.9	134	-70.8	n/a
Historical Events							
Tohoku 2011	Kamchatka-Yap-Mariana-Izu-Bonin	4.66 b24 + 12.23 b25+26.31 a26+21.27 b26+22.75 a27 +4.98 b27		85.6	86	-57.3	n/a

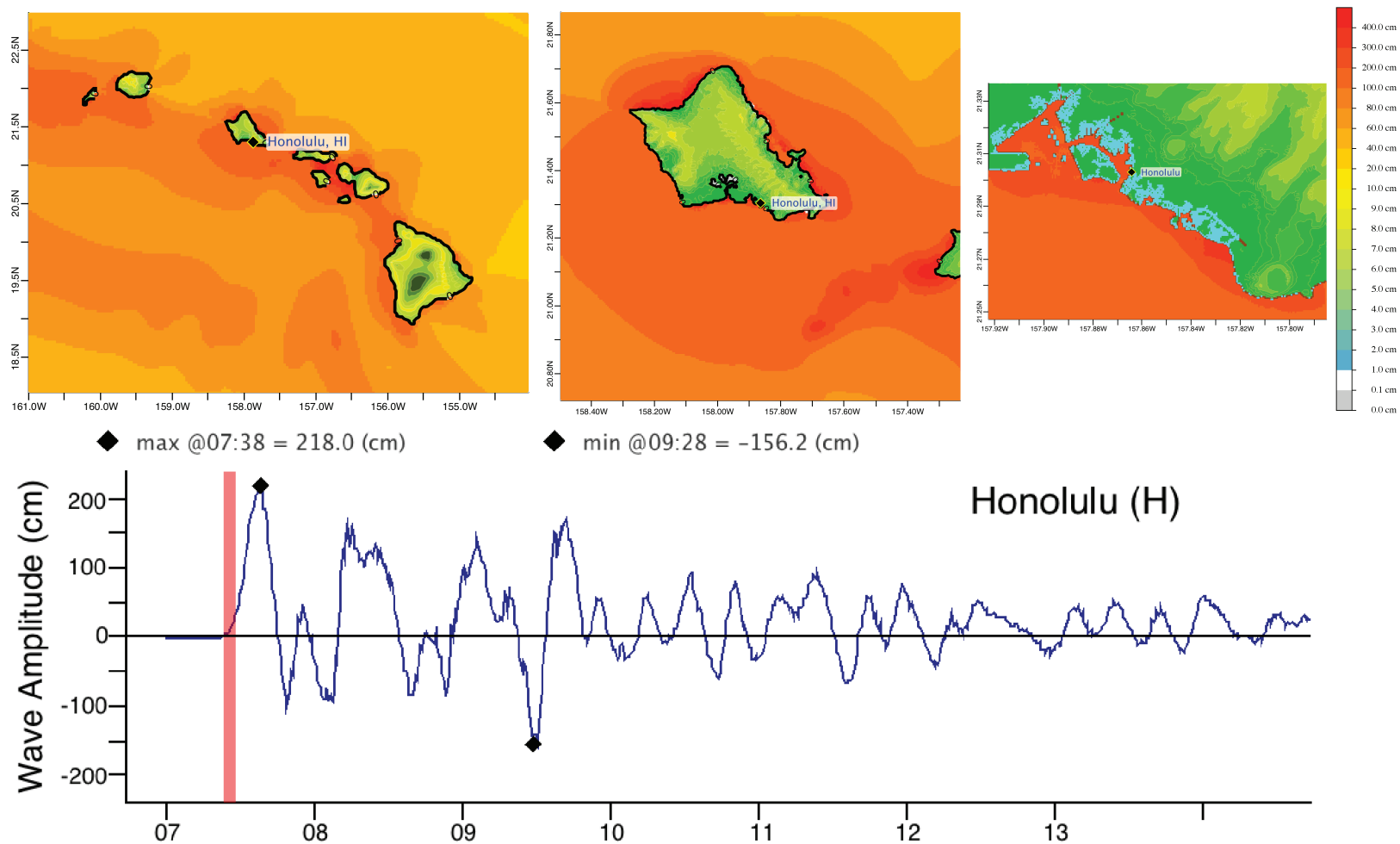


Figure C1: Response of the Honolulu forecast model to synthetic scenario KISZ 22-31 ($\alpha=29$). Maximum sea surface elevation for (a) A-grid, b) B-grid, c) C-grid. Sea surface elevation time series at the C-grid warning point (d).

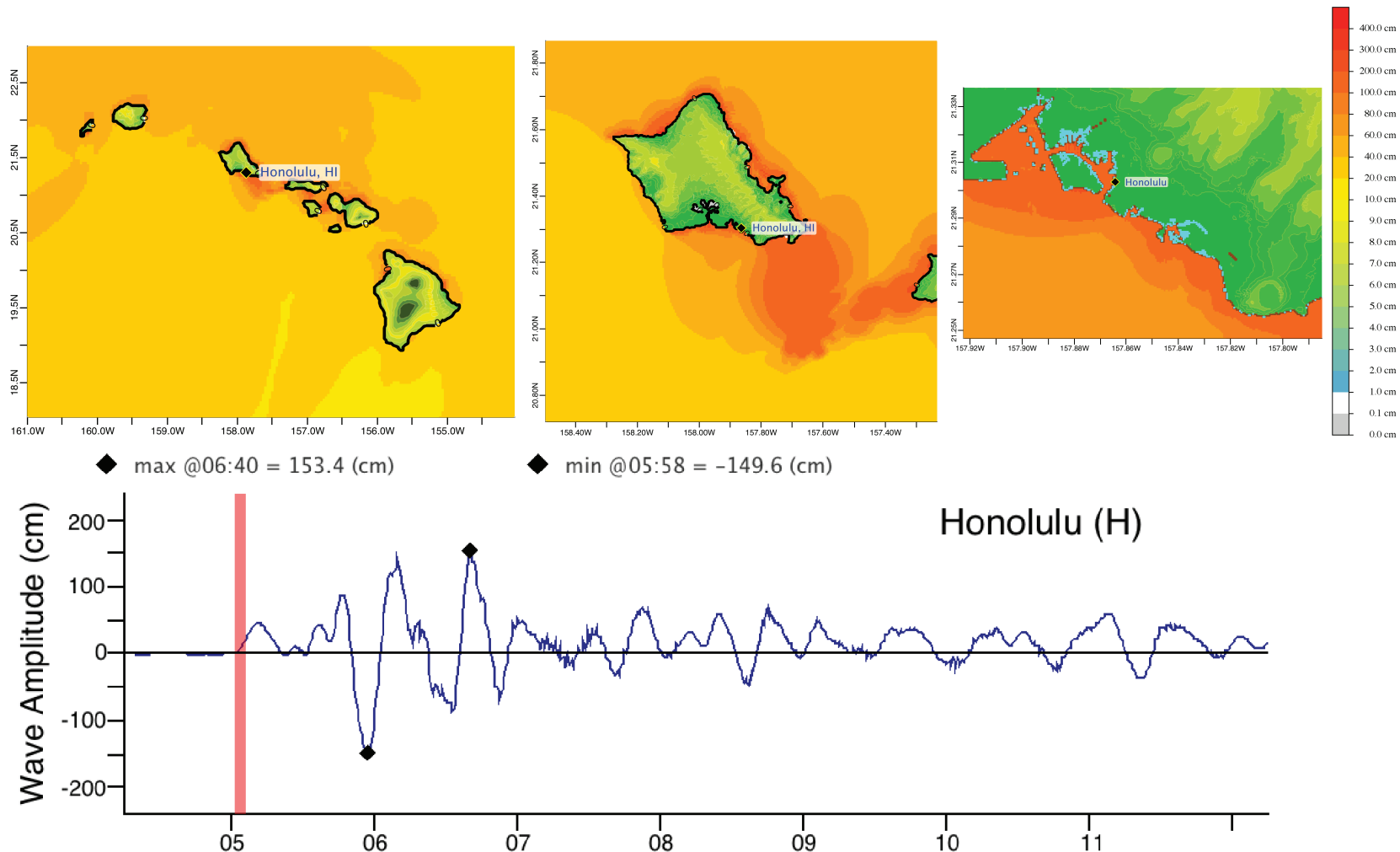


Figure C2: Response of the Honolulu forecast model to synthetic scenario ACSZ 56-65 ($\alpha=29$). Maximum sea surface elevation for (a) A-grid, b) B-grid, c) C-grid. Sea surface elevation time series at the C-grid warning point (d).

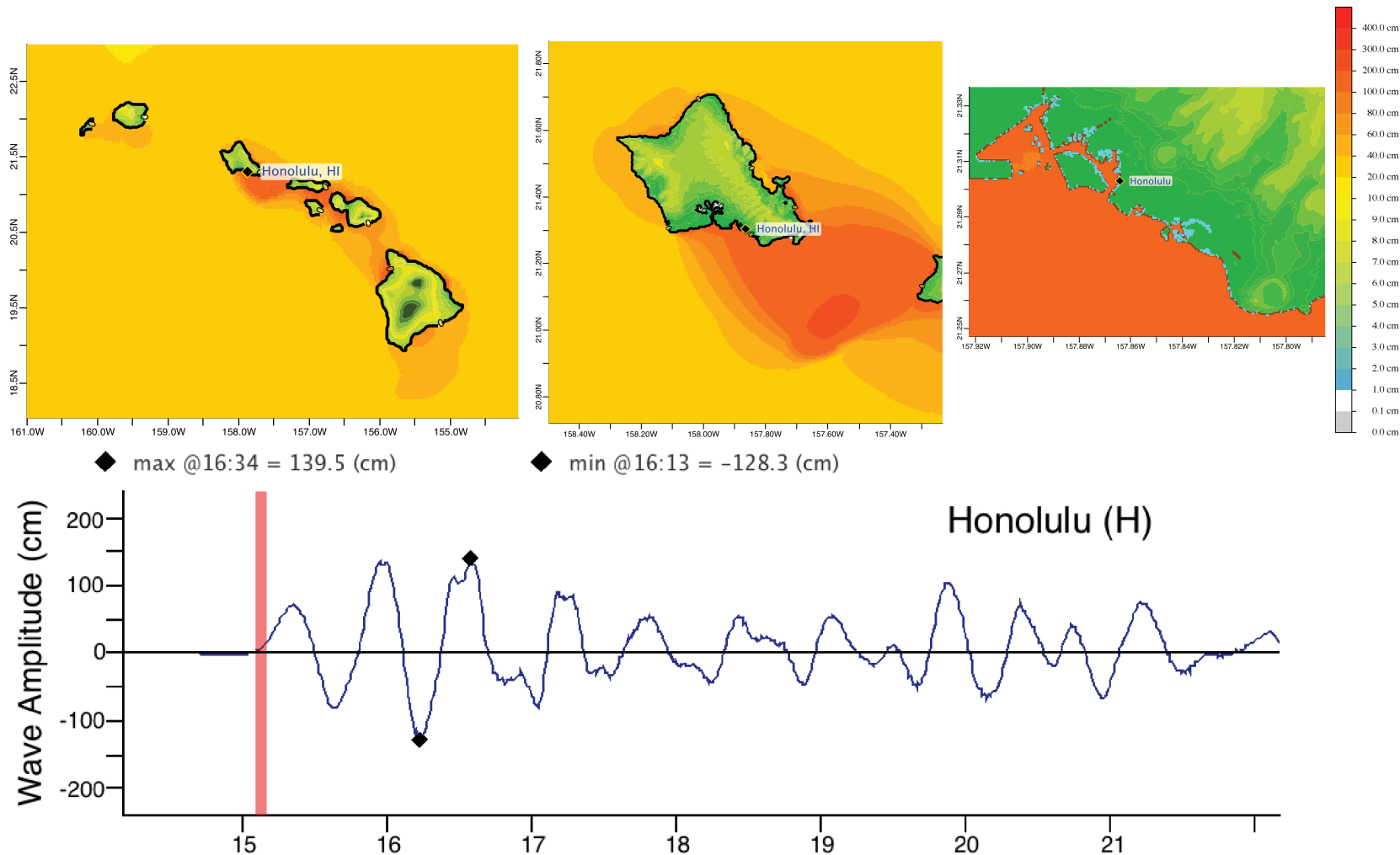


Figure C3: Response of the Honolulu forecast model to synthetic scenario CSSZ 86-95 ($\alpha=29$). Maximum sea surface elevation for (a) A-grid, b) B-grid, c) C-grid. Sea surface elevation time series at the C-grid warning point (d).

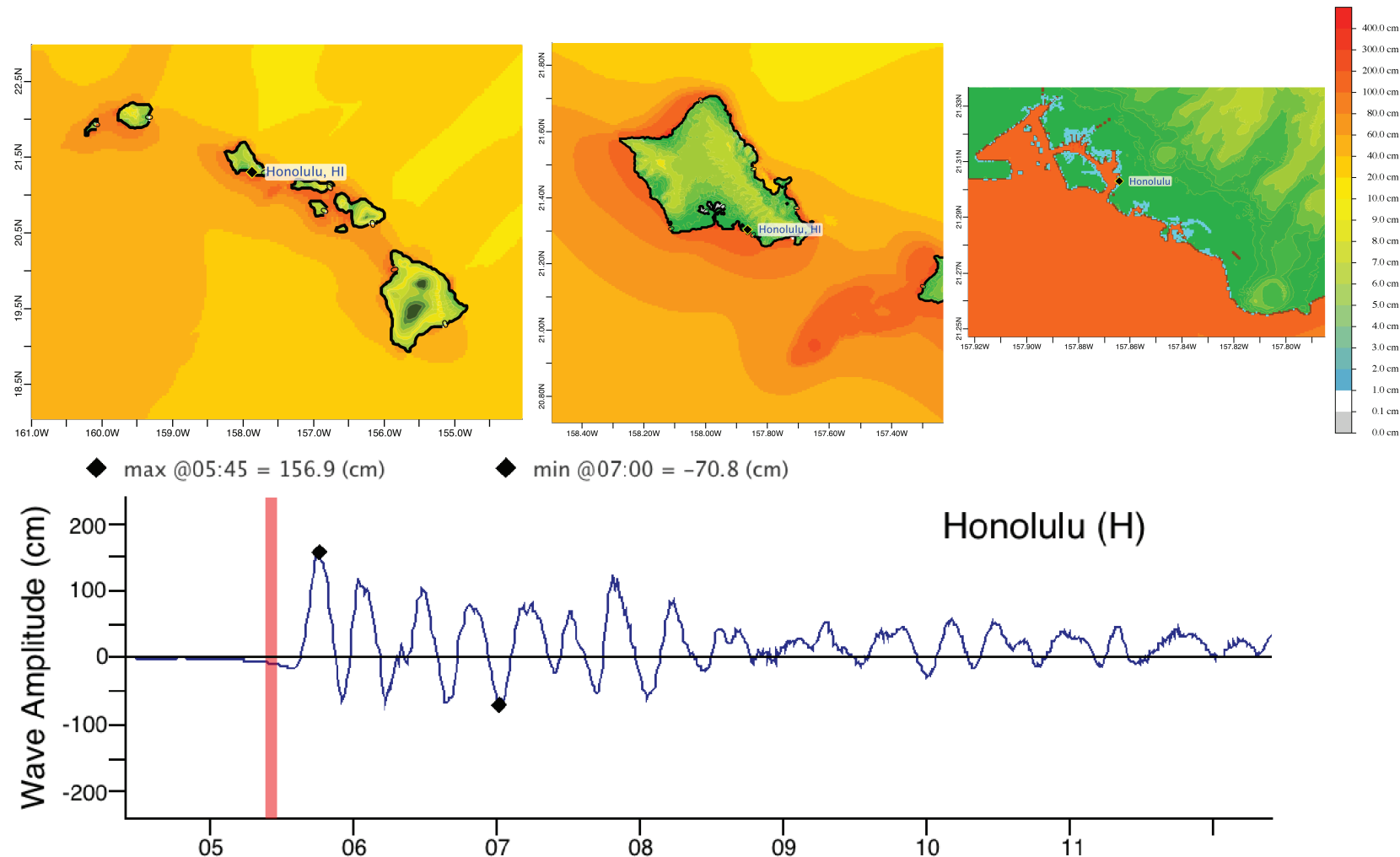


Figure C4: Response of the Honolulu forecast model to synthetic scenario NTSZ 30-39 ($\alpha=29$). Maximum sea surface elevation for (a) A-grid, b) B-grid, c) C-grid. Sea surface elevation time series at the C-grid warning point (d).

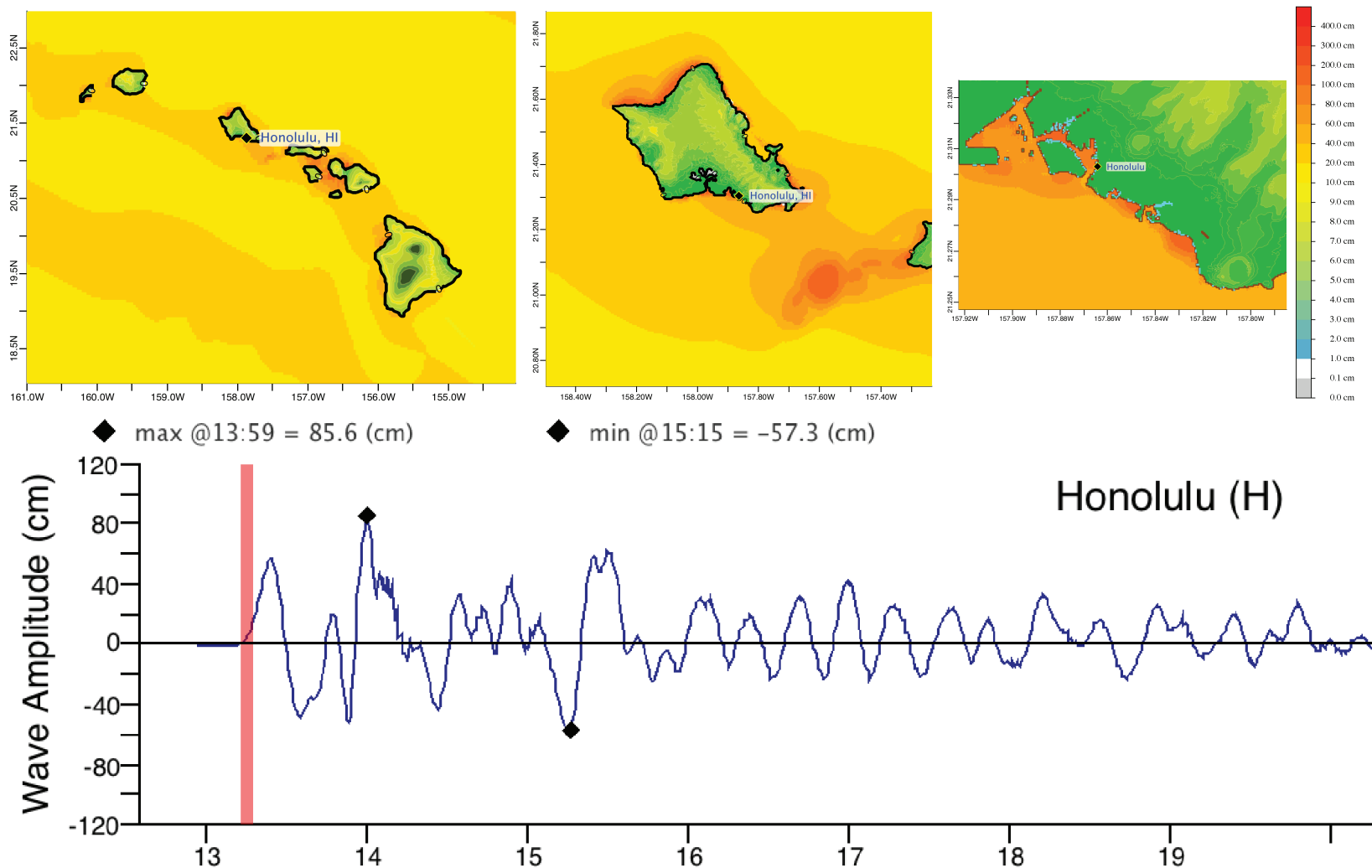


Figure C5: Response of the Honolulu forecast model to the 2011 Tohoku tsunami. Maximum sea surface elevation for (a) A-grid, b) B-grid, c) C-grid. Sea surface elevation time series at the C-grid warning point (d).